

Role of vegetation on river bank accretion

Vargas Luna, Andres

DOI

[10.4233/uuid:286c36e8-3cac-403c-9d0a-72a5232c5093](https://doi.org/10.4233/uuid:286c36e8-3cac-403c-9d0a-72a5232c5093)

Publication date

2016

Document Version

Final published version

Citation (APA)

Vargas Luna, A. (2016). *Role of vegetation on river bank accretion*. [Dissertation (TU Delft), Delft University of Technology]. <https://doi.org/10.4233/uuid:286c36e8-3cac-403c-9d0a-72a5232c5093>

Important note

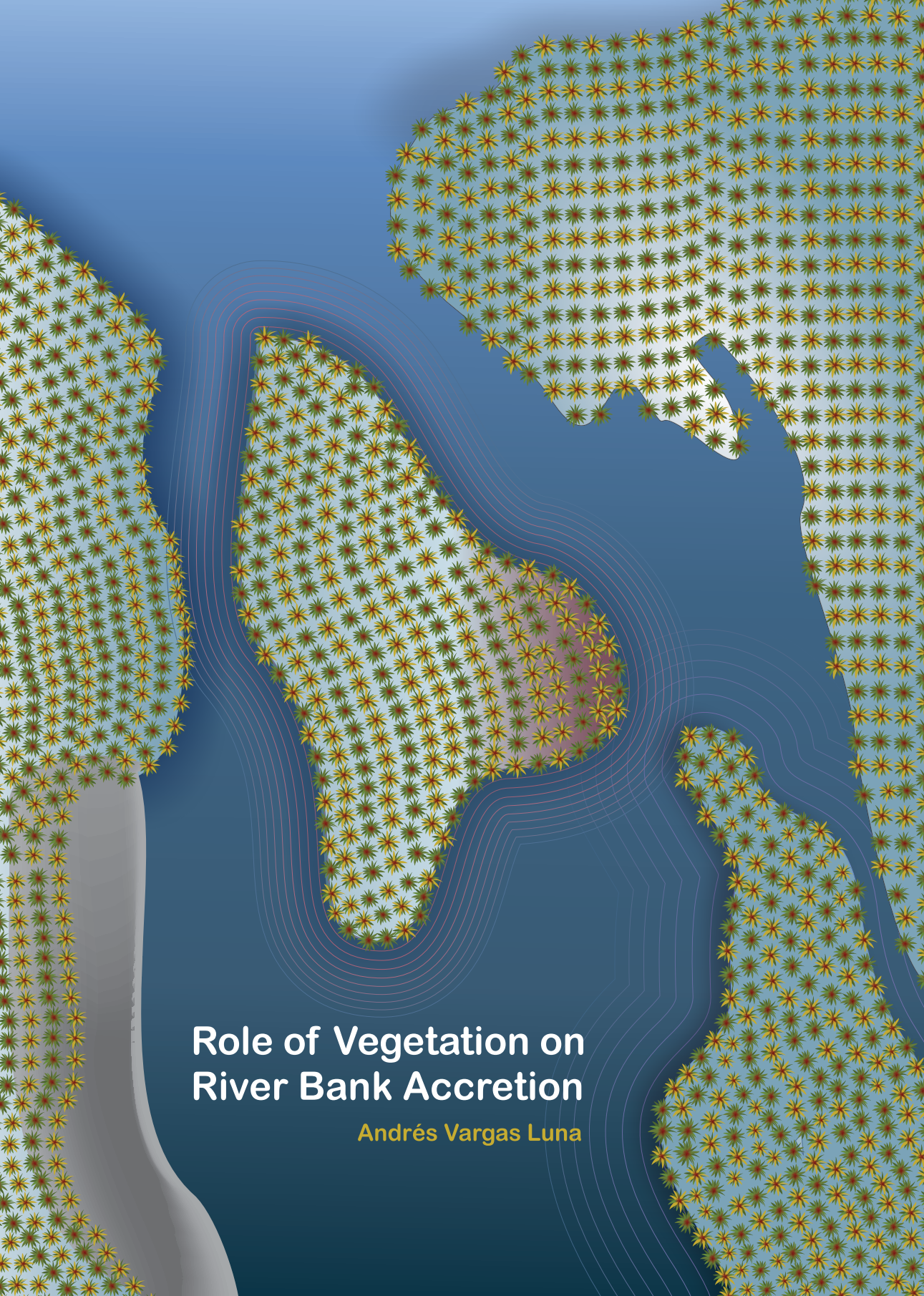
To cite this publication, please use the final published version (if applicable).
Please check the document version above.

Copyright

Other than for strictly personal use, it is not permitted to download, forward or distribute the text or part of it, without the consent of the author(s) and/or copyright holder(s), unless the work is under an open content license such as Creative Commons.

Takedown policy

Please contact us and provide details if you believe this document breaches copyrights.
We will remove access to the work immediately and investigate your claim.



Role of Vegetation on River Bank Accretion

Andrés Vargas Luna

ROLE OF VEGETATION ON RIVER BANK ACCRETION

ROLE OF VEGETATION ON RIVER BANK ACCRETION

Proefschrift

ter verkrijging van de graad van doctor
aan de Technische Universiteit Delft,
op gezag van de Rector Magnificus prof. ir. K. C. A. M. Luyben,
voorzitter van het College voor Promoties,
in het openbaar te verdedigen op woensdag 16 november 2016 om 10:00 uur

door

Andrés VARGAS LUNA

Ingeniero Civil y Master en Ingeniería - Recursos Hidráulicos,
Universidad Nacional de Colombia, Bogotá, Colombia,
geboren te Bogota, Colombia.

This dissertation has been approved by the:

promotor: Prof. dr. ir. W.S.J. Uijttewaal
copromotor: Dr. ir. A. Crosato

Composition of the doctoral committee:

Rector Magnificus,	chairman
Prof. dr. ir. W. S. J. Uijttewaal	Delft University of Technology, promotor
Dr. ir. A. Crosato	UNESCO-IHE, copromotor

Independent members:

Prof. dr. A. Armanini	University of Trento, Italy
Prof. dr. P. Perona	University of Edinburgh, UK
Prof. dr. F. Klijn	Delft University of Technology
Dr. ir. A. J. F. Hoitink	Wageningen University
Prof. dr. ir. A. E. Mynett	Delft University of Technology/ UNESCO-IHE

This research was funded by Delft University of Technology, COLCIENCIAS (Administrative Department of Science, Technology and Innovation, Grant No. 512 of 2010), and the Pontificia Universidad Javeriana.



Keywords: River morphodynamics, Bank accretion, Vegetation modelling

Printed by: Gildeprint Drukkerijen - The Netherlands

Cover design: Iván Dávila.

Copyright © 2016 by A. Vargas Luna

Typeset by MiKTeX

ISBN: 978-94-6233-438-0

An electronic version of this dissertation is available at
<http://repository.tudelft.nl/>.

*To my family,
and to my **Bonita***
with all my love

LIST OF FIGURES

1.1	Casanare River. Photo taken in Hato Corozal, Casanare, Colombia. Source: Claudia Jara.	21
1.2	(a) Aerial view of the Yopal river, Colombia. Source: Claudia Jara; (b) Schematic representation of the bank erosion and accretion sequences in the bend shown in (a).	22
1.3	Examples of river planform styles: a) Braided system (Waimakariri river, New Zealand); b) Meandering river (Agan river, Russia); and c) Anabranching river (Negro river, Brazil). Source: Google Earth.	23
1.4	Facilities at the Environmental Fluid Mechanics Laboratory of Delft University of Technology.	27
2.1	Schematic distribution of accretionary deposits on meandering floodplain formation (source: Page et al., 2003).	29
2.2	Point bar stabilized in the Nakashibetsu River, Hokkaido (Japan) by vegetation growth and fine sediment capture, a) November 2003, b) August 2006 (adapted from: Parker et al., 2011).	31
2.3	Bank erosion and accretion in the Ningxia-Inner Mongolia reach. Flow is from left to right. Displacements observed in a) Left bank, and b) Right bank (source: Yao et al., 2011).	32
2.4	Schematic representation of Tsujimoto's model (source: Tsujimoto, 1999).	38
2.5	Schematization for bank erosion and accretion processes (source: Mosselman et al., 2000).	39
2.6	Land accreting process in Asahi et al. (2013)'s model (source: Asahi et al., 2013).	39
2.7	Bank migration phases proposed in Eke et al. (2014)'s model (source: Eke et al., 2014a).	40
2.8	Results obtained with Bertoldi et al.'s (2014) model for the case of the Magra river (Italy) (source: Bertoldi et al., 2014).	41
3.1	Artificial plants used in flume experiments to test the effects of different types of vegetation on flow resistance.	43
3.2	Floodplain forming processes according to Nanson and Croke (1992): (a) lateral accretion, (b) vertical accretion in a partly confined valley, and (c) vertical accretion across a wide plain. Adapted from Brierley and Fryirs (2013).	45
3.3	Schematic vertical profiles of flow velocity (left) and shear stress (right) for the flow in un-vegetated channels.	47

3.4	Schematic vertical profiles of flow velocity and Reynolds shear stress for channels with emergent: (a) Rigid plants, and (b) Flexible plants.	48
3.5	Schematic vertical profiles of flow velocity and Reynolds shear stress for channels with submerged: (a) Rigid plants, and (b) Flexible plants. (c) Special behaviour of submerged plants: vegetation with coherent waving motion and prone vegetation.	50
4.1	Schematic representation of different stages of vegetation development (Source: www.pinterest.com).	57
4.2	Scheme for seeds: (a) dispersal, (b) germination and growth, and (c) establishment, proposed by Bradley and Smith (1986). Adapted from Camporeale et al. (2013).	60
4.3	Flow variability and its relationship with pioneer trees recruitment: (a) absent, (b) on the former channel, (c) on point bars, and (d) at high elevations. Adapted from Friedman and Auble (2000).	60
4.4	Schematic cross-section showing ideal location for germination and survival of cottonwood seedlings (after Mahoney and Rood, 1998).	61
4.5	The influence of the flood pulse within the river-floodplain complex for yearly fluctuations. (Source: Large and Prach, 1999)	61
4.6	Schematic representation of vegetation development by using the flood-pulse concept (After Bayley (1995); Source: FISRWG (1998)).	62
4.7	Plant species distribution in Southern California as a function of unit stream power and height above the water table (After Bendix and Hupp (2000))	63
4.8	Application of the recruitment box model of Mahoney and Rood (1998) adapted by Camporeale et al. (2013).	64
4.9	Vegetation colonization in Kim et al.(2014)'s model (source: Kim et al., 2014).	65
4.10	River planforms and corresponding vegetation patterns for three (a to c) biomass transversal distributions (Perucca et al., 2007) considering the Camporeale and Ridolfi's (2006) model shown schematically in (d).	66
4.11	Vegetation model considering linear vegetation growth by Takebayashi et al. (2006)'s model (source: Takebayashi et al., 2006).	67
4.12	<i>Chara aspera</i> population densities from 1993 to 1997: (a) measured, (b) simulated with a daily coupling, and (c) simulated with a coupling of 6 hours. Population density is classified from low to high into Class 0 to Class 7. Adapted from Ye (2012).	68
4.13	Differences in river planform obtained by using vegetation with (a) static characteristics, and (b) dynamic characteristics. Adapted from: van Oorschot et al. (2016).	68
4.14	Vegetation spatial distribution modelled for the Gongreung river: (a) Initial condition, (b) 1 year after dam removal, and (c) 5 years after dam removal. Adapted from Kim et al. (2014).	69
4.15	Stand-density management diagrams for pines based on Reineke's relation (Left) and on the $-3/2$ power law (Right) (Modified from Newton, 1997)	71

4.16 Example of the use of chronosequences for establishing succession time scales on North Carolina Piedmont, after: Goudie (1989) (modified from Johnson and Miyanishi, 2008)	72
4.17 Two-dimensional scheme of spatiotemporal scales of vegetation dynamics	73
5.1 Scheme of the geometric properties for real vegetation (left) rigid-cylinder analogy (right).	75
5.2 Main characteristics of rigid and flexible vegetation in open channels. Left: side view of emergent vegetation (above) and submerged vegetation (below) [Adapted from: Wu and He (2009)]. Right: plan view of staggered and parallel patterns.	79
5.3 Submerged artificial vegetation: measured against estimated global flow resistance for: (a) Klopstra et al. (1997), (b) Stone and Shen (2002), (c) Van Velzen et al. (2003), (d) Baptist (2005), (e) Huthoff (2007), (f) Yang and Choi (2010), and (g) Cheng (2011)	86
5.4 Emergent artificial vegetation: measured against estimated global flow resistance for: (a) Petryk and Bosmajian (1975), (b) Stone and Shen (2002), (c) Ishikawa et al. (2003), (d) James et al. (2004), (e) Hoffmann (2004), (f) Baptist (2005), and (g) Cheng (2011).	88
5.5 Real vegetation: measured against estimated global flow resistance for: (a) Baptist (2005), and (b) Stone and Shen (2002). The conditions considered were: <i>E</i> = Emergent; <i>S</i> = Submerged; <i>NL</i> = No leaves; <i>LL</i> = Low concentration of leaves; and <i>HL</i> = High concentration of leaves. The ellipses define groups with different characteristics with respect to vegetation properties, see the text.	89
5.6 Global flow resistance coefficient as a function of the degree of submergence according to Stone and Shen (2002) and Baptist (2005) for a plant area per unit of volume, <i>a</i> , of (a) $1.0\ m^{-1}$ and (b) $3.0\ m^{-1}$. Two heights of the vegetated layer were considered: $0.05\ m$ and $0.25\ m$	90
5.7 Submerged vegetation: measured against estimated vertical velocity profiles according to Klopstra et al. (1997) and Yang and Choi (2010). Datasets: (a) Velasco et al. (2008) (Test T3-3), (b) Shimizu et al. (1991) (Test A31), (c) Ghisalberti and Nepf (2004) (Test H), (d) Nezu and Sanjou (2008) (Test A-10), (e) Carollo et al. (2002) (Test 1), and (f) Tinoco Lopez (2011) (Test M4). Degree of discontinuity, ξ , defined in Eqs. 5.9, 5.10 and the Appendix A . .	91
5.8 Emergent artificial vegetation: Comparison between the bed-shear stresses measured in vegetated flumes and the estimated values by (a) Barfield et al. (1979), (b) Raupach (1992), (c) Stone and Shen (2002), (d) Ishikawa et al. (2003), (e) Baptist (2005), and (f) Kothyari et al. (2009a).	94
5.9 Emergent artificial vegetation: ratio between bed-shear stress and total shear stress for vegetated beds as a function of ah_v . Measured values against estimated by Baptist (2005) (Continuous line), and Ishikawa et al. (2003) (Dashed line).	95

5.10	Ratio between bed-shear stress and total shear stress for vegetated beds as a function of the degree of submergence for: (a) Barfield et al. (1979), (b) Stone and Shen (2002), and (c) Baptist (2005).	96
5.11	Apparent drag coefficient as a function of the element Reynolds number reported in previous studies. Vegetation condition: <i>S</i> =Submerged, <i>E</i> =Emergent, <i>F</i> =Foliated, and <i>D</i> =Defoliated.	97
5.12	Comparison between measured and predicted sediment transport rates per unit width using the estimations of (a) Barfield et al. (1979), (b) Stone and Shen (2002), and (c) Baptist (2005). Markers in black: computed by applying Engelund and Hansen (1967). Markers in white: computed by applying van Rijn (1984a).	98
6.1	Comparison of geometric characteristics of plants: (a) Uniform, cylindrical and leafless; and (b) Irregular, with high variability in density and foliage. Photo taken at Plitvice, Croatia.	103
6.2	Main characteristics of rigid and flexible vegetation in open channels. Left: side view of emergent vegetation (above) and submerged vegetation (below), Adapted from: Wu and He [10]. Right: plan view of staggered and parallel patterns. Variables and units shown in the notation section.	107
6.3	Experimental set-up for Flume No. 1. (a) and vegetation arrays used: (b) Rigid (Wooden) sticks [Test W11], (c) Artificial Grass [Test G2], (d) Artificial with Leaves (<i>Egeria densa</i>) [Test ED3], (e) Real (<i>Peperomia rotundifolia</i>) [Test R2]. Vegetation properties are presented in Table 6.1.	110
6.4	Sediments used in the laboratory experiments.	111
6.5	Experimental set-up for Flume No. 2. (a) Plan view, (b) Vegetation distribution on the floodplains, (c) Typical cross-section, and (d) Hydrographs used in the experiments. Initial bed slope = 0.01 <i>m/m</i>	113
6.6	Experimental set-up for Flume No. 3. (a) Plan view, (b) Typical cross-section, and (c) Hydrographs used in the experiments. Initial bed slope = 0.01 <i>m/m</i>	114
6.7	Friction coefficient (C_f) as a function of the element Reynolds number (Re_D) for: (a) Real plants [h/h_p : 2.0 - 3.6], (b) Plastic grass [h/h_p : 4.7 - 8.7], (c) Plastic <i>Egeria Densa</i> [h/h_p : 1.8 - 8.8], and (d) Wooden sticks [h/h_p : 1.5 - 7.8] and cylindrical rods by Cheng (2011) [h/h_p : 1.3 - 2.0]. Vegetation properties are listed in Table 6.1.	116
6.8	Channel-width (B) variation with time in the experiments carried out in Flume No. 2 for: (a) Constant discharge, (b) Hydrograph 1, and (c) Hydrograph 2. The vegetation properties are summarized in Table 6.2 and the hydrographs are shown in Figure 6.5d.	118
6.9	Equilibrium channel width (Be) for the experiments carried out in Flume No. 2 for: (a) Constant discharge, (b) Hydrograph 1, and (c) Hydrograph 2. The vegetation properties used are summarized in Table 6.2 and the hydrographs are shown in Figure 6.5d.	119

6.10 Channel sinuosity (I_S) variation with time for the experiments carried out in Flume No. 3. The letter C indicates the experiment that was performed with constant discharge. The vegetation properties used are summarized in Table 6.3 and the hydrographs are shown in Figure 6.6c.	120
6.11 Common initial configuration (a) and channel planform after 240 minutes for the experiments in Flume No. 3: (b) Test P-NV (constant discharge); (c) Test P-NV (variable discharge); (d) Test P-V1; (e) Test P-V2; (f) Test P-V3; (g) Test P-V4. Vegetation properties are listed in Table 6.3.	121
6.12 Processes observed in the experiments carried out in Flume No. 3: (a) bank failure (view from upstream); (b) large wood deposition (view from above), and (c) Scroll bars formation (view from above).	123
6.13 Measured and estimated Chézy coefficient and mean flow velocity for real and artificial plants at submerged conditions: (a) Chézy coefficient, and (b) mean flow velocity. Vegetation properties are listed in Table 6.1.	125
6.14 Measured and estimated Chézy coefficient and mean flow velocity for submerged rigid cylinders with different densities. Left panels: Chézy coefficient; right panels: mean flow velocity. Larger marker sizes indicate larger submergence ratios.	126
7.1 The Lunterse Beek stream, Renswoude, The Netherlands.	133
7.2 Study area. (a) Localization and boundary conditions of the reconstructed channel, and (b) Sketch of the stream employed in this study	136
7.3 Box and whisker plot of the monthly hydrological variables recorded at the Veenkampen station for the period 1971-2015 of: (a) Mean air temperature (°C), and (b) Precipitation (mm).	143
7.4 Time series of the information available after stream restoration: discharge (m^3/s), mean air temperature (°C), morphological campaigns and aerial photos. Information about the morphological campaigns and aerial photos can be found in Tables 7.3 and 7.4, respectively.	144
7.5 Evolution of the Lunterse Beek from (a) January 2012 to (b) September 2015. Left panel: Aerial pictures, Right panel: DEMs with legend indicating the bed level (masl), the initially reconstructed channel is shown in dashed lines. (c) Difference between the two campaigns, erosion is indicated in blue and sedimentation in red. The cross-section is indicated in (c) is used further analyses. Monitoring area enclosed with a black contour.	145
7.6 Temporal evolution of reach averaged: (a) channel slope (%), (b) channel width (m), (c) elevation of bed channel and floodplains (masl), and (d) bankfull water depth (m), as well as (e) discharge (m^3/s) in the Lunterse Beek after restoration (Day 0).	146

7.7	DEMs of difference (DoDs) in bed topography occurred in: (a) Spring 2012, (b) Summer 2012, (c) Autumn 2012, (d) Winter 2012, (e) Spring 2013, (f) Summer 2013, (g) Autumn 2013, (h) Winter 2013, (i) Spring 2014, (j) Summer 2014, (k) Autumn 2014 (After vegetation cut on left floodplain), (l) Winter 2014, (m) Spring 2015, (n) Summer 2015, (o) Autumn 2015 (After vegetation cut on right floodplain), (p) Winter 2015, and (q) Spring 2016. The solid black line indicates the monitored area (See Figure 7.2b). Erosion is indicated in blue and deposition in red.	147
7.8	Seasonal variation observed on cross-section C, see Figure 7.2.	148
7.9	Seasonal variation observed on cross-section E, see Figure 7.2.	149
7.10	(a-d) Aerial photographs and vegetation classification maps of the Lunterse Beek in the summers and (e) spatial distribution in percentage. Information about the aerial photos is presented in Table 7.4.	150
7.11	(a-d) Aerial photographs and vegetation classification maps of the Lunterse Beek in the winters and (e) spatial distribution in percentage. Information about the aerial photos is presented in Table 7.4.	151
7.12	(a-d) Aerial photographs and vegetation classification maps of the Lunterse Beek for the vegetation growth and decay observed in 2015 and (e) spatial distribution in percentage. Information about the aerial photos is presented in Table 7.4.	152
7.13	Terrestrial photographs highlighting vegetation succession. (a) Scheme indicating the position and direction of the photographs, Vegetation stages from (b) to (g) explained in the text.	153
7.14	DEMs of difference (DoDs) in bed topography at the end of the study between the estimations with the model and the observations for: (a) Scenario 1, (b) Scenario 2, (c) Scenario 3, and (d) Scenario 4.	154
7.15	Comparison between the initial conditions, and the observed and modelled bed levels at the end of the study for the cross-section indicated in Figure 7.4 for: a) Scenario 1, b) Scenario 2, c) Scenario 3, and d) Scenario 4.	155
8.1	Large-scale laboratory flume for studying bank accretion at Delft University of Technology.	157
8.2	Meandering planforms obtained in laboratory experiments without vegetation. Flow direction as indicated. (a) Friedkin (1945), (b) Schumm and Khan (1972), (c) Smith (1998), (d) Peakall et al. (2007), (e) van Dijk et al. (2012).	160
8.3	Laboratory experiments with vegetation. Flow from top to bottom. (a) Gran and Paola (2001), (b) Tal and Paola (2007), (c) Coulthard (2005), (d) Braudrick et al. (2009).	163
8.4	Experimental set-up of the mobile-bed flume: (a) Planview, (b) Initial cross-section A-A (Vertically distorted 1V:2H); and Initial (c) and final (d) planforms obtained for Test 3. All dimensions in metres.	164
8.5	Grain size distribution of the sediment used in the laboratory experiments.	164
8.6	Vegetation used in the laboratory experiments: (a) Seeding process, (b) A plant unit, (c) Seeded floodplain.	166

8.7	Discharge hydrograph indicating the vegetation colonization moments.	166
8.8	Measured bed-levels and planview of the channel for: (a) Initial condition for all the scenarios; and bar pattern after 31 hours for: (b) Scenario 1, (c) Scenario 2, and (d) Scenario 3. Indicated cross-sections are shown in Figure 8.9. Flow from left to right.	168
8.9	Cross-sections comparison between the starting condition and the bar development after 31 hours for the considered scenarios. Localization of the cross-sections shown in Figure 8.8.	169
8.10	Rendered point clouds of the mobile-bed flume. Bed topography of: (a) Initial condition for all the scenarios (0 hours), and after 86 hours for (b) Scenario 1, (c) Scenario 2, (d) Scenario 3.	169
8.11	Temporal evolution of reach averaged: (a) Water depth, h , and (b) Wet channel width, B , during the experimental tests	170
8.12	Measured bed-levels and planview of the channel for: (a) Initial condition for all the scenarios; after 86 hours for: (b) scenario 1, (c) scenario 2, and (d) scenario 3; after 97 hours for: (e) scenario 2, (f) scenario 3. Indicated cross-sections are shown in Figure 8.13. Flow from left to right.	171
8.13	Cross-sections comparison between the starting condition and the final configuration of a bar (after 86 hours) for the considered scenarios. Localization of the cross-sections shown in Figure 8.12.	171
9.1	PhD project word cloud (Created with Wordle: http://www.wordle.net/)	173

LIST OF TABLES

2.1	Spatiotemporal scales of the river bank accretion and related processes. . .	36
5.1	Summary of experiments and their vegetation configuration considering artificial vegetation gathered for the present study.	77
5.2	Summary of measurements using real vegetation gathered for the present study.	78
5.3	Summary of methods considered in the analysis carried out.	83
5.4	Experiments used for the analysis of vertical velocity profiles.	84
5.5	Summary of bed-shear stress and sediment transport measurements gathered for the present study.	84
5.6	Submerged artificial vegetation: statistical estimators obtained by comparing measurements with estimations.	87
5.7	Emergent artificial vegetation: statistical estimators obtained by comparing measurements with estimations.	87
5.8	Velocity in the vegetation layer: statistical estimators obtained by comparing measurements with estimations.	93
6.1	Vegetation arrays considered in the experiments in Flume No. 1.	112
6.2	Vegetation arrays considered in the experiments in Flume No. 2 (for the spatial distribution see Figure 6.5).	112
6.3	Vegetation arrays considered in the experiments in Flume No. 3 (for the spatial distribution see Figures 6.5 and 6.6).	115
6.4	Characteristics of vegetation adopted by: Baptist and de Jong (2005) (1); Facchini et al. (2009) (2); Montes Arboleda et al. (2010) (3).	128
7.1	Catchment characteristics in the study area for the Lunterse Beek.	137
7.2	Summary of the field campaigns carried out.	138
7.3	Summary of the constructed DODs.	139
7.4	Summary of the aerial photographs used in the study.	139
7.5	Classification rules for the extraction of vegetation classes from the UAV imagery.	140
7.6	Measured erosion and accretion rates between spring seasons. The localization of the selected cross-sections can be seen in Figure 7.2.	146
8.1	Main characteristics of previous laboratory experiments on river planforms.	162
8.2	Reach-averaged channel characteristics for the considered scenarios at different times.	170

CONTENTS

List of Figures	1
List of Tables	9
Summary	15
Samenvatting	17
Resumen	19
1 Introduction	21
1.1 Background of the study	22
1.2 Research aims.	24
1.3 General approach.	26
1.4 Structure of the thesis.	27
2 River bank accretion	29
2.1 General description.	30
2.2 Role of discharge regime	31
2.3 Role of sediment transport	33
2.4 Role of riparian vegetation	33
2.5 Role of opposite bank dynamics	34
2.6 Role of climate	34
2.7 Role of soil consolidation	35
2.8 Spatiotemporal scales.	35
2.9 Modelling attempts	37
2.10 Discussion	40
3 Interaction between vegetation and river dynamics	43
3.1 The need for a bio-geomorphological approach to describe river dynamics	44
3.2 Effects of vegetation on river dynamics	45
3.2.1 Effects on flow resistance	46
3.2.2 Effects on sediment transport	51
3.2.3 Effects on bank dynamics	52
3.2.4 Effects on river bed dynamics	52
3.3 Effects of river and sediment fluxes on vegetation.	53
3.3.1 Effects of water flow	54
3.3.2 Effects of floods	54
3.3.3 Effects of river bed dynamics.	54
3.4 Modelling the effects of vegetation on river dynamics.	54
3.5 Discussion	55

4	Riparian vegetation dynamics and its modelling	57
4.1	Vegetation dynamics	58
4.1.1	Seed dispersal	58
4.1.2	Colonization	58
4.1.3	Plant growth and vegetation succession	59
4.2	Vegetation dynamics modelling	63
4.2.1	Colonization modelling	63
4.2.2	Plant growth modelling	65
4.2.3	Vegetation succession modelling	69
4.3	Interaction between plant populations	70
4.4	Spatiotemporal scales	71
4.5	Discussion	73
5	Models predicting the effects of vegetation on flow and sediment fluxes	75
5.1	Introduction	76
5.1.1	Outline	76
5.1.2	Theoretical background	78
5.2	Materials and methods	82
5.2.1	Accuracy	82
5.2.2	Global flow resistance	83
5.2.3	Vertical velocity profiles	83
5.2.4	Bed-shear stress	84
5.2.5	Apparent drag coefficient	84
5.2.6	Sediment transport	85
5.3	Results	85
5.3.1	Global flow resistance	85
5.3.2	Vertical flow velocity profile with submerged vegetation	89
5.3.3	Bed-shear stress	92
5.3.4	Apparent drag coefficient	93
5.3.5	Sediment transport	97
5.4	Discussion and conclusions	99
5.4.1	Model evaluation	99
5.4.2	Research needs	100
6	Representing plants as rigid cylinders in experiments and models	103
6.1	Introduction	104
6.2	Theoretical background: Baptist's model	106
6.3	Materials and methods: laboratory experiments	109
6.3.1	Representation of vegetated flows using rigid cylinders	109
6.3.2	Representation of the channel-width formation using rigid cylinders	111
6.3.3	Representation of bank dynamics using rigid cylinders	113

6.4	Results of laboratory experiments.	115
6.4.1	Representation of vegetated flows using rigid cylinders	115
6.4.2	Representation of the channel-width formation using rigid cylinders	117
6.4.3	Representation of bank dynamics using rigid cylinders	119
6.5	Representation of rivers processes adopting Baptist's method	122
6.5.1	Reproduction of the morphological effects of vegetation observed in experiments by Baptist's method	124
6.5.2	Reproduction of the effects of floodplain vegetation on river morphology with Baptist's method	125
6.5.3	Reproduction of sedimentation rates on vegetated floodplains with Baptist's method	129
6.6	Conclusions.	130
7	Morphological effects of riparian vegetation growth after stream restoration	133
7.1	Introduction	134
7.2	Study area description	136
7.3	Materials and methods	137
7.3.1	Data sources, data collection and processing	137
7.3.2	Morphodynamic modelling	140
7.3.3	Model set-up and calibration	141
7.4	Results of data analysis	142
7.4.1	Seasonal variations	142
7.4.2	Morphological evolution.	142
7.4.3	Evolution of vegetation	150
7.5	Results of numerical modelling	152
7.6	Conclusions.	154
8	Morphological effects of plant colonization and bank accretion	157
8.1	Introduction	158
8.2	Literature review	158
8.2.1	Bar formation	158
8.2.2	Laboratory investigations without vegetation	159
8.2.3	Laboratory investigations with vegetation	161
8.3	Experimental set-up	163
8.3.1	Design	163
8.3.2	Flume	163
8.3.3	Vegetation characteristics	165
8.3.4	Tests	165
8.4	Results	168
8.4.1	Effects of vegetation colonization on floodplains	168
8.4.2	Effects of vegetation colonization on bars	170
8.5	Discussion and conclusions.	172

9	Conclusions and recommendations	173
9.1	Main conclusions	174
9.2	General conclusions	178
9.3	Recommendations	179
	Appendices	181
A	List of models predicting the effects of vegetation	183
A.1	Models applicable to emergent conditions	184
A.1.1	Petryk and Bosmajian (1975) [P&B]	184
A.1.2	Raupach (1992) [R]	184
A.1.3	Ishikawa et al. (2003) [I]	184
A.1.4	James et al. (2004) [J]	185
A.1.5	Hoffmann (2004) [Hof]	185
A.1.6	Kothyari et al. (2009) [Ko]	185
A.2	Models applicable to submerged conditions	185
A.2.1	Klopstra et al. (1997) [K]	185
A.2.2	van Velzen et al. (2003) [vV]	187
A.2.3	Huthoff et al. (2007) [H]	188
A.2.4	Yang and Choi (2010) [Y&C]	188
A.3	Models applicable to both emergent and submerged conditions	188
A.3.1	Barfield et al. (1979) [Bf]	188
A.3.2	Stone and Shen (2002) [S&S]	189
A.3.3	Baptist (2005) [B]	190
A.3.4	Cheng (2011) [Ch]	190
	References	193
	List of main symbols	233
	Acknowledgements	235
	List of Publications	237
	Curriculum Vitae	241

SUMMARY

THERE is rising awareness of the need to include the effects of vegetation in studies dealing with the morphological response of rivers. By increasing the local hydraulic roughness and the soil resistance against erosion, riparian vegetation affects water depth, flow velocity, sediment processes and soil erodibility. As a result, vegetation growth on river banks and floodplains alters the river bed topography, reduces the bank erosion rates and enhances the development of new floodplains through river bank accretion.

This thesis examines the role of riparian vegetation on river morphology, with particular attention to its effects on bank accretion, focusing on lowland streams in temperate climates. The work is based on the combination of extensive literature review, laboratory experiments, field observations and numerical simulations to overcome the shortcomings of single approaches. A thorough quantitative analysis of state-of-the-art methods assessing the effects of vegetation on flow resistance and sediment transport is carried out in the initial phase of the work. This method review allowed: identifying the dominant processes responsible for river bank accretion, determining the consequences of using simplified methods to represent vegetation in experiments and models, selecting the most promising method, establishing the recommendations for its proper use, and defining its applicability ranges.

A series of laboratory investigations was performed to establish the effects of vegetation colonization on rivers with alternate bars. Considering the problems related to the upscaling of experimental results to real rivers, the experiments were carried out in a newly-constructed large flume. This allowed obtaining realistic flow conditions and bank characteristics. Several small-scale experiments were also carried out in order to set up the large-scale investigations, establishing, for instance, the differences on the behaviour of plants with contrasting characteristics and the performance of different types of sediment.

Systematic field observations were conducted to study the accretion processes at the real river scale. The selected case study is the Lunterse Beek, a small lowland stream in the Netherlands. The field measurements covered a period of five years after river restoration, which allowed studying the river dynamics with and without riparian vegetation and assessing the effects of seasonal variations. Numerical simulations allowed quantitatively analysing the role of these different factors on the morphological evolution of the monitored stream.

The results of the unique large-scale laboratory experiments and the field observations demonstrated that vegetation is essential for the accretion of river banks in non-clay-dominated environments. These results highlighted the role of colonization of new deposits by plants, which is strongly influenced by the alternation of high and low flows, and dominated by their intensity and duration. Vegetation establishment plays a key

role on the stabilization of the channel-width and on the vertical accretion of both levees and floodplains. The vertical accretion and channel incision induced by colonizing plants observed in the large-scale experiments showed that vegetation colonization increases the amplitude and length of the bars in the main river channel, affecting the final river planform. Lateral bank accretion was found to be strongly dependent on water level variability. These outcomes highlight the relevance of considering the effects of vegetation on the river management and on the designing, planning and maintenance programs of restoration projects.

The field observations showed that the plant root system plays an important role on the soil reinforcement in lowland streams. The simulations performed with Delft3D for the field study case showed the potential of this model in reproducing the effects of vegetation and the observed morphological changes. However, model limitations were identified in the simplified description of bank erosion and the lack of a quantitative estimation of the soil reinforcement by plants. The model investigation allowed to identify that including the seasonal variations of vegetation is only relevant for short-term predictions, whereas, the assumption of a constant vegetation coverage dominated by herbaceous plants can reflect the long-term behaviour of changing vegetation. These aspects contribute in defining recommendations for modelling purposes of this type of streams.

This work comprises the first attempt towards a physics-based description of river bank accretion by combining experimental and field observations with numerical simulations. However, more efforts in establishing the role of root systems and fine sediments on the reinforcement and consolidation processes of soils are required to advance in the understanding of the dynamics of river banks.

SAMENVATTING

ER is een toenemend bewustzijn dat in studies betreffende de morfologische respons van rivieren de effecten van vegetatie moeten worden meegenomen. Oevervegetatie beïnvloedt waterdiepte en stroomsnelheid als ook de erodeerbaarheid van de bodem doordat het de lokale hydraulische weerstand verhoogt en de bodem minder erodeerbaar maakt. Het resultaat hiervan is dat begroeiing op de oevers en in de uiterwaarden de ligging van de rivierbodem verandert, oever erosie vermindert en bijdraagt aan vorming van nieuwe uiterwaarden door aangroei van de rivieroever.

Dit proefschrift beschrijft een studie naar de rol van oevervegetatie bij riviermorfologische processen, met speciale aandacht voor de effecten op oeveraangroei bij laaglandrivieren in gematigd klimaat. Het onderzoek is gebaseerd op de combinatie van uitgebreide analyse van bestaande literatuur, laboratorium experimenten, veldwaarnemingen en numerieke simulaties, dit om de beperkingen van een enkele benadering te omzeilen. Een grondige kwantitatieve analyse van 'state of the art' methoden om de effecten van vegetatie op stromingsweerstand en sediment transport vast te stellen, uitgevoerd in het beginstadium van het onderzoek, heeft de mogelijkheid geboden om: de dominante processen die verantwoordelijk zijn voor oeveraangroei te identificeren, de consequenties in te schatten van het gebruik van versimpelde methoden waarmee vegetatie in experimenten en rekenmodellen wordt weergegeven, de meest veelbelovende methode te selecteren en de toepasbaarheid ervan te bepalen. De resultaten laten duidelijk de rol zien van de kolonisatie door planten van nieuw-afgezet sediment, wat sterk beïnvloed wordt door de afwisseling van sterke en zwakke stromingen en gedomineerd wordt door intensiteit en duur ervan.

Een reeks laboratoriumexperimenten is uitgevoerd om de effecten van kolonisatie door vegetatie van rivieren met alternerende banken vast te stellen. Met inachtneming van de moeilijkheid om experimentele resultaten verkregen op kleine schaal te vertalen naar de werkelijke schaal van laagland rivieren, zijn de experimenten uitgevoerd in een nieuw-gebouwde grote stroomgoot. Hiermee kon een realistische stroming en dito oeverkarakteristieken verkregen worden. Voorafgaand hieraan is een aantal experimenten op kleinere schaal uitgevoerd, bijvoorbeeld om vast te stellen welke kunstmatige planten en welke verschillende soorten van sediment goed werkten.

Er zijn systematisch veldwaarnemingen gedaan om oeveraangroei-processen op de schaal van een echte rivier te bestuderen. De geselecteerde casus betreft de Lunterse Beek, een klein laagland riviertje in Nederland. De veldwaarnemingen besloegen een periode van 5 jaren volgend op een rivierrestauratie, zodat de dynamica van de rivier met en zonder vegetatie bestudeerd kon worden, als ook de effecten van de seizoenen. Numerieke modellering maakte het mogelijk de gevolgen van verschillende factoren voor de morfologische veranderingen in de gemonitorde beek kwantitatief te analyseren.

De resultaten van de unieke grootschalige laboratoriumexperiment en de veldwaarnemingen hebben het belang aangetoond van begroeiing voor de stabilisatie van de breedte van de stroomgeul en voor de verticale aangroei van oevers en uiterwaarden. De aangroei van oevers in dwarsrichting bleek sterk samen te hangen met de variabiliteit van het waterniveau. De stabilisatie van de geulbreedte en aanzanding als gevolg van kolonisatie door vegetatie zoals waargenomen in de grootschalige goot- experimenten lieten zien dat de planten de karakteristieken van zandbanken beïnvloeden en daarmee ook het patroon van de rivier. Deze resultaten tonen aan dat het van belang is de invloed van vegetatie mee te nemen in het rivierbeheer en bij ontwerp, planning en onderhouds-programma's van rivier-restauratie-projecten.

De waarnemingen in het veld lieten zien dat de wortelstelsels van planten een belangrijke rol spelen bij het versterken van grond en oevers in een laagland rivier. De simulaties van de veldstudie met behulp van het rekenprogramma Delft3D, hebben de potentie van dit model aangetoond voor het reproduceren van de effecten van vegetatie en de geobserveerde morfologische veranderingen. Er zijn echter beperkingen van het model geïdentificeerd die vooral betrekking hebben op de gesimplificeerde beschrijving van oevererosie en het gebrek aan een kwantitatieve schatting van de bodemversterking door planten. De studie met het rekenmodel liet zien dat het meenemen van seizoensvariëaties alleen relevant is voor korte-termijn voorspellingen, terwijl de aanname van een constante bedekking door vegetatie die gedomineerd wordt door kruidachtige planten het lange-termijn gedrag van veranderende vegetatie weer kan geven. Deze aspecten dragen bij aan het definiëren van aanbevelingen voor het modelleren van dergelijke rivieren.

Dit werk omvat een eerste poging richting een op de fysica gebaseerde beschrijving van rivier-oever-aangroei, door middel van het combineren van waarnemingen in het laboratorium en het veld met numerieke simulaties. Om beter begrip te krijgen van de dynamica van rivieroevers is er meer inspanning nodig ter vaststelling van de rol van wortels en fijn sediment in het consolidatieproces en het versterken van bodem en oever.

RESUMEN

EXISTE un aumento en la conciencia de la necesidad de incluir los efectos de la vegetación en estudios relacionados con la respuesta morfológica de los ríos. Por medio del incremento de la rugosidad hidráulica local y de la resistencia del suelo ante la erosión, la vegetación riparia afecta la profundidad hidráulica, la velocidad del flujo, los procesos de sedimentos y la erodibilidad del suelo. Como resultado, el crecimiento de la vegetación en las bancas de los ríos y en las planicies de inundación altera la topografía del lecho del cauce, reduce las tasas de erosión de las bancas y favorece el desarrollo de nuevas planicies de inundación a través de la acreción de las bancas de río.

Esta tesis examina el rol de la vegetación riparia en la morfología fluvial, con interés particular en los efectos de ésta en la acreción de bancas, enfocado en corrientes de tierras bajas localizadas en climas templados. El trabajo está basado en la combinación de una extensa revisión de literatura, experimentos de laboratorio, observaciones de campo y simulaciones numéricas con el fin de superar las deficiencias del empleo de metodologías únicas. Un exhaustivo análisis cuantitativo de métodos modernos que consideran los efectos de la vegetación en la resistencia al flujo y en el transporte de sedimentos se lleva a cabo en la fase inicial del trabajo. Ésta revisión de métodos permitió: identificar los procesos dominantes que son responsables de la acreción de bancas de río, determinar las consecuencias de utilizar métodos simplificados para representar la vegetación en experimentos y modelos, seleccionar el método más promisorio, establecer las recomendaciones para su uso apropiado y definir sus rangos de aplicación.

Una serie de investigaciones de laboratorio se desarrolló para establecer los efectos de la colonización de la vegetación en ríos con barras de sedimento alternadas. Considerando los problemas relacionados con la amplificación de la escala de los resultados de laboratorio a la escala de río real, los experimentos fueron realizados en un canal de laboratorio de gran escala recientemente construido. Esto permitió obtener condiciones de flujo y características de las bancas más reales. Varios experimentos de pequeña escala fueron también realizados para preparar las investigaciones de gran escala, estableciendo, por ejemplo, los diferentes comportamientos de plantas con características contrastantes y el desempeño de diferentes tipos de sedimento.

Observaciones de campo fueron realizadas de manera sistemática para estudiar los procesos de acreción a la escala de río real. El caso de estudio seleccionado es el del Lunterse Beek, una pequeña corriente de tierra baja localizada en los países bajos. Las mediciones de campo cubrieron un período de cinco años después de la restauración del río, lo cual permitió el estudio de la dinámica del cauce sin y con la presencia de vegetación riparia y la evaluación de los efectos de las variaciones estacionales. La modelación numérica permitió analizar el rol de estos diferentes factores en la evolución morfológica de ésta corriente.

Los resultados de los experimentos a gran escala (únicos en su tipo) y de las observaciones de campo demostraron que la vegetación es esencial para la acreción de bancas de río en ambientes que no están dominados por suelos arcillosos. Estos resultados destacan el rol de la colonización de las plantas en nuevos depósitos, la cual está fuertemente influenciada por la alternación de caudales altos y bajos, y dominado por la intensidad y duración de los mismos. El establecimiento de la vegetación desempeña un importante papel en la estabilización del ancho del cauce y en la acreción vertical observada en las planicies de inundación y en los diques naturales que se forman en las márgenes. La acreción vertical y la incisión del canal inducidas por la colonización de las plantas observada en los experimentos de laboratorio de gran escala mostró que la colonización de la vegetación incrementa la amplitud y longitud de las barras de sedimento en el cauce principal del río, afectando su forma final en planta. Se encontró que la acreción lateral de bancas depende fuertemente de la variabilidad de los niveles de agua. Estos resultados resaltan la relevancia de considerar los efectos de la vegetación tanto en el manejo de ríos como en el diseño, planeación y programas de mantenimiento de proyectos de restauración.

Las observaciones de campo mostraron que el sistema de raíces de las plantas desempeña un importante rol en el refuerzo del suelo de las corrientes de tierras bajas. Las simulaciones realizadas con Delft3D para el caso de estudio mostraron el potencial de este modelo en la reproducción de los efectos de la vegetación y de los cambios morfológicos observados. Sin embargo, limitaciones en el modelo fueron encontradas en la descripción simplificada de la erosión de bancas y en la inexistencia de una estimación cuantitativa del refuerzo del suelo debido a las plantas. La investigación numérica permitió identificar que la inclusión de las variaciones estacionales de la vegetación solo es relevante para las predicciones a corto plazo, mientras que asumir una cobertura vegetal constante dominada por plantas de tipo herbáceo puede reflejar el comportamiento a largo plazo de la vegetación cambiante. Estos aspectos contribuyen en la definición de recomendaciones útiles en la modelación de este tipo de corrientes.

Este trabajo consiste en el primer intento hacia la descripción basada en la física de la acreción de bancas por medio de la combinación de observaciones de campo y experimentales con simulaciones numéricas. Sin embargo, más esfuerzos en el establecimiento del rol de los sistemas de raíces y sedimentos finos en los procesos de refuerzo y consolidación de suelos son requeridos para avanzar en el entendimiento de la dinámica de bancas de río.

1

INTRODUCTION

"A good river is nature's life work in song."

Mark Helprin, Freddy and Fredericka



Figure 1.1: Casanare River. Photo taken in Hato Corozal, Casanare, Colombia. Source: Claudia Jara.

In this first chapter the background, aim and approach of this PhD dissertation are explained. General comments about the structure of the document are also included here.

1.1. BACKGROUND OF THE STUDY

PREDICTING the response of rivers to natural and anthropic changes has been a challenging task for researchers from several disciplines during the last decades (Church and Ferguson, 2015). The morphology of an alluvial river is the result of the interaction between vegetation, flow discharge and sediment dynamics, through entrainment, transport and deposition of bed material. Morphological changes include bed-shape evolution, river-width adjustment and lateral channel migration arising from a combination of erosion and accretion processes which, in turn, modify the flow characteristics.

Width adjustment and lateral channel migration are the result of the joint action of opposite river banks (Blench, 1969; Parker, 1978a; Mosselman, 1992). In particular, banks can retreat (bank erosion) from the river channel or advance (bank accretion) into the river channel, resulting in width adaptation and transverse channel shift, see Figure 1.2. Only by studying separately the phenomena of bank accretion and opposite bank erosion it is possible to predict river width adjustment and lateral channel migration (Allmendinger et al., 2005; Crosato, 2008; Parker et al., 2011).

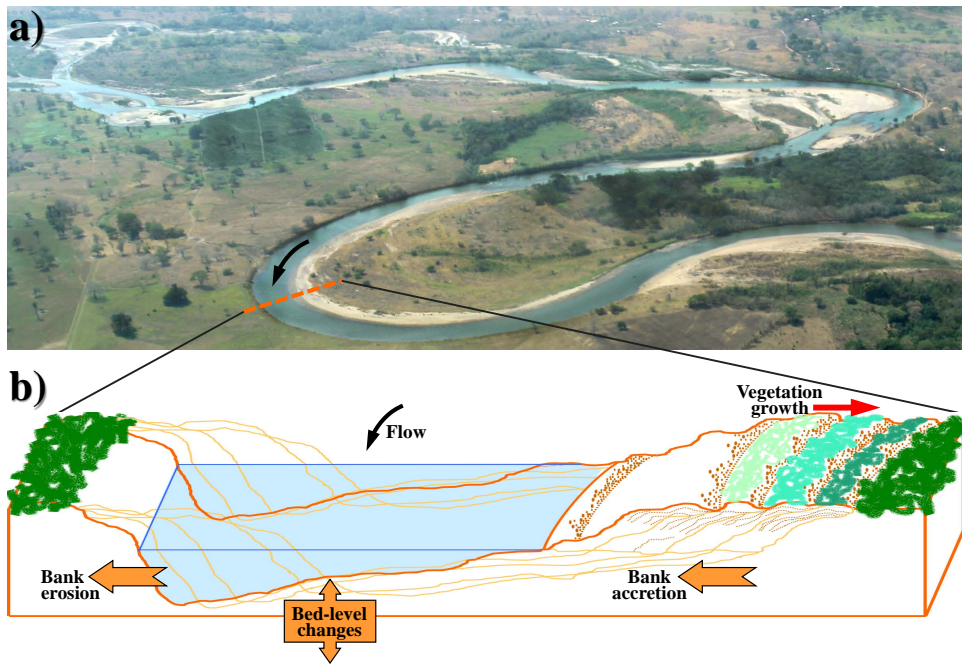


Figure 1.2: (a) Aerial view of the Yopal river, Colombia. Source: Claudia Jara; (b) Schematic representation of the bank erosion and accretion sequences in the bend shown in (a).

River planforms are the result of the interaction among several environmental agents related to hydrology, sediment and vegetation, which are dependent on geology and climate. The interplay between bank dynamics and channel bed dynamics becomes visible

in the varied channel patterns of fluvial systems, see Figure 1.3. In braiding systems the equilibrium width and depth are driven by the dominant influence of bank and bed erosion. Widening and deepening processes stop when erosion stops, see Figure 1.3a. In meandering rivers, instead, the equilibrium channel is the result of the combined influence of erosion and accretion. Erosion occurs near the outer bank of bends generated by near-bank flow entrainment and bank failure, while accretion occurs close to the inner bank due to the low-flow velocities and shallow water depths characterizing this area, see Figure 1.3b. Anabranching rivers (Figure 1.3c) are generally associated with high water discharges and low gradients. Their planform results from the combination of erosion and accretion processes as well, but operating on multiple channels (Latrubesse, 2008; Lewin and Ashworth, 2014).

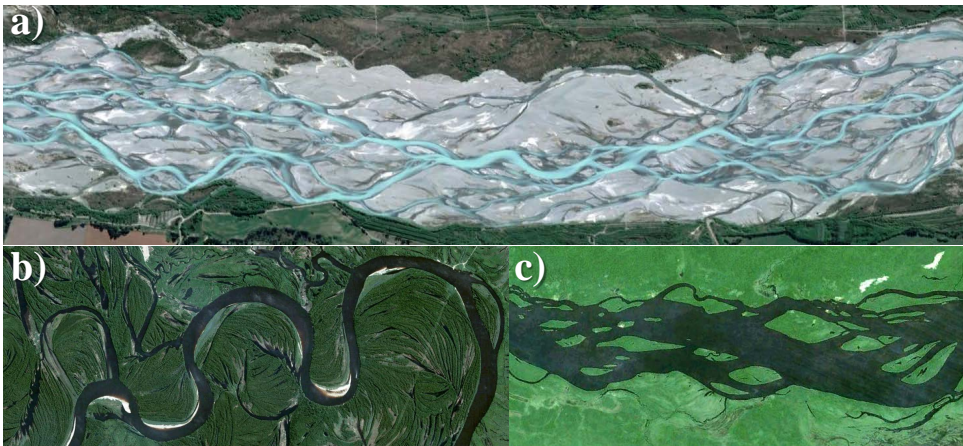


Figure 1.3: Examples of river planform styles: a) Braided system (Waimakariri river, New Zealand); b) Meandering river (Agan river, Russia); and c) Anabranching river (Negro river, Brazil). Source: Google Earth.

Changes of climate, alterations of floodplain vegetation (often related to land use) and human interventions, such as damming, water withdrawal and sediment extraction, result in morphological adaptation of river channels. These alterations can lead to significant morphological changes as the evolution of a braided system into a meandering river and vice-versa. State-of-the-art morphodynamic models are able to simulate meandering and braiding processes, but only few of them are able to simulate the evolution from one planform to another. One-dimensional models have been successful in describing the planimetric changes of meandering rivers assuming equilibrium between the migration rates of opposite banks, relating it to bank erosion, and assuming constant width (e.g. Ikeda et al., 1981; Crosato, 1989; Odgaard, 1989a; Chen and Duan, 2006). Most two-dimensional morphodynamic models including bank erosion can reproduce channel widening until an equilibrium width is achieved (e.g. Spruyt et al., 2011; Canestrelli et al., 2016). Only few 2D morphological models can simulate river-width variations and the evolution of a braided system into a meandering river and vice-versa, because they treat bank erosion and accretion separately, but their representation of river bank accretion is still very simplified (e.g. Asahi et al., 2013; Bertoldi et al., 2014).

A process-based description of river bank accretion includes sediment deposit formation and bar development, as well as bar stabilization by several processes, mainly the establishment of vegetation and soil reinforcement and vertical growth of the deposit. In particular, the physics-based estimation of river bank accretion requires the definition of:

1. The evolution of 2D bed topography (bar and point bar development, scour and deposits forming).
2. The effects of vegetation on water flow and sediment processes.
3. Vegetation processes (colonization, growth, succession, etc.).
4. Soil compaction and reinforcement.
5. Vertical accretion.

For this, the proper identification of the spatiotemporal scales involved in the phenomena is a key aspect. Previous studies showed that riparian vegetation and soil compaction depend on discharge variability and climate (e.g. [Nanson, 1980](#); [Provansal et al., 2010](#); [Hooke, 2006](#)). In particular, vegetation colonization and soil dewatering occur during low-flow stages, whereas bar formation, plant eradication and bed erosion occur during high-flow stages. Seasonal variations of temperature, water discharge and vegetation characteristics interact with the sub-surface flow resulting in bank erosion or accretion. To address these points, more research is needed on the spatiotemporal upscaling of the processes observed in small-scales to the real river scale including seasonal, inter-annual and long-term variations of the flow regime, soil structure and vegetation properties.

This research studies the role of vegetation on the river morphology with particular attention to bank accretion, focusing on lowland streams in temperate climates. The results of this study are relevant for river restoration projects to design successful strategies and interventions and for the prediction of the effects of their implementation. An accurate prediction of the morphological processes in restoration projects is crucial to improve the traditional landscape-oriented design strategies. Restoration projects based on this approach have caused in the USA, for instance, undesired morphological changes (e.g. [Kondolf et al., 2001](#); [Simon et al., 2007](#); [Kondolf, 2011](#)).

1.2. RESEARCH AIMS

THE main objective of this research is to establish the role of vegetation on the river morphology focusing on bank accretion in lowland streams in temperate climates. The research questions are:

What is the role of vegetation in river bank accretion?

The dynamics of opposite banks is a key aspect in establishing the formation of channel-width and planform style of a river. However, physics-based descriptions of the bank accretion processes are still at their infancy. Establishing the role of vegetation on bank accretion is important for the understanding of the river adaptation to changes in climate. Improvements in the prediction of the morphological changes of rivers are also necessary to predict the response of these systems to river training and other human altering flow field, sediment transport and riparian vegetation.

Which method should be used to estimate the effects of vegetation on river morphology?

Physical and numerical models need representing vegetation in a schematic easily-quantifiable way, despite the variety of sizes, shapes and flexibility of real plants. Common approaches represent plants as rigid cylinders, however, comparative studies and validation of these methods on extensive data sets are lacking. Moreover, the ability of this rigid-cylinder schematization to reproduce the effects of vegetation on morphodynamic processes has never been analysed and compared systematically. The rigid-cylinder schematization of plants is practical and promising for applications in numerical models. Nevertheless, it is not clear how to characterize different types of vegetation in terms of arrays of cylinders, considering plant flexibility, foliage, vertical variations and the large ranges of plant density present in nature, covering from high density grass to isolated stems (trees).

What effects does vegetation growth have on the morphological evolution of lowland streams?

Understanding the effects of vegetation on the morphological evolution of lowland rivers in which vegetation on banks and floodplain plays a major role is key to the restoring and maintaining of these ecosystems. Field observations provide valuable information of both morphological evolution and vegetation development. However, following up studies are scarce and therefore evaluating the effects of plants is not always possible. Complementary information about these processes is obtained by performing experiments and conducting numerical exercises. Laboratory experiments provide a considerable amount of data under controlled conditions, whereas numerical models are useful tools for scenario analysis and upscaling processes. It is rather important to combine different types of information, scales and analytical tools to reveal the effects of vegetation growth on the streams morphology.

What is the role of seasonal variations of vegetation and can they be included in modelling bank accretion?

Common practices in morphodynamic modelling accounting for the effects of vegetation only consider plants in a simplified way, maintaining their characteristics invariant in time. This simplification overlooks the effects of the seasonal variations of vegetation that are relevant especially in temperate climates. Establishing the relevance of including the seasonal variability of vegetation characteristics is therefore relevant for modelling purposes and in general for the prediction of the morphological adaptation of river channels after interventions affecting riparian vegetation.

1.3. GENERAL APPROACH

THE work is carried out by combining field observations, extensive laboratory experiments, and numerical simulations, starting from a thorough literature review. This allows establishing the state of the art, selecting the most promising tools and the acquisition of a broader view by observing the processes in varied set-ups and at different spatiotemporal scales and resolutions.

The work starts with an extensive study of state-of-the-art methods and the assessment of their performance on experimental data. This part of the work allows for: identifying the dominant processes responsible for river bank accretion; establishing the most promising method for representing the effects of vegetation on the river morphology; defining the applicability ranges of the selected method; and determining the consequences of using simplified methods to represent vegetation in models.

Field observations provide information about the processes at the real river scale, identifying particularities and complexities of the bank accretion process. This part of the work is important to keep a strong link with reality and to observe the result of the multiple factors existent in lowland streams acting simultaneously.

Experiments in the laboratory are relevant because they are carried out under controlled conditions allowing for the measurement of a considerable amount of data. This is important to analyse in detail specific aspects of the processes of interest for this research. For this work, laboratory experiments are necessary for establishing the applicability of the rigid-cylinder schematization of plants and for understanding the role of vegetation on bank accretion. The following facilities are available at the Environmental Fluid Mechanics Laboratory of Delft University of Technology (see Figure 1.4):

- Two tilting flumes of $L=14.0\text{ m} \times W=0.4\text{ m}$ (Figure 1.4a).
- Two small-scale mobile-bed flumes of $L=2.5\text{ m} \times W=1.2\text{ m}$ (Figure 1.4b), and $L=5.0\text{ m} \times W=1.2\text{ m}$ (Figure 1.4c).
- One large-scale mobile-bed flume of $L=45.0\text{ m} \times W=5.0\text{ m}$ (Figure 1.4d).

The last one (Figure 1.4d) is large enough to perform flow velocity measurements and to reduce the scaling issues that are common for small flume experiments.

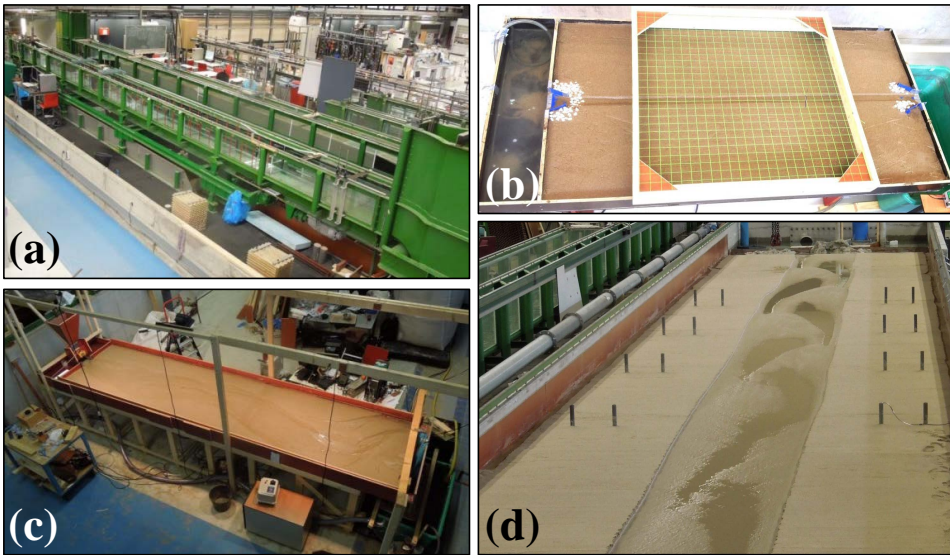


Figure 1.4: Facilities at the Environmental Fluid Mechanics Laboratory of Delft University of Technology.

The effects of vegetation on the river morphodynamics include the influence of plants on global flow resistance, sediment transport and soil erodibility. This influence is studied by analysing and comparing channel bed topographies, vertical velocity profiles, vertical mixing, water levels, bed-shear stresses and soil strength with and without plants.

Numerical simulations enable freedom to study scenarios that are impossible to find in the field and difficult to obtain in the laboratory. For instance, numerical simulations can provide important information on the relevance of seasonal variations of vegetation for the river morphology, which can be obtained by studying and comparing different scenarios of vegetation dynamics. The Delft3D code appears to be the most suitable one for this type of studies (<http://oss.deltares.nl/web/delft3d/source-code>) because the model includes the effects of vegetation and estimates bank erosion, although in a simplified way.

The combination of literature review, field work, laboratory experiments and model runs is the only way to overcome the shortcomings of the single approaches, covering a wide range of scales that are useful for varied purposes in the fields of ecohydraulics, morphodynamics and biogeomorphology.

1.4. STRUCTURE OF THE THESIS

CHAPTER 2 presents a literature review about river bank accretion as well as the state of the art of its modelling. Chapter 3 presents a description of the interaction between vegetation and river dynamics, whereas Chapter 4 includes a description of riparian vegetation dynamics and the inclusion of these processes in morphodynamic

models. The selection of the best method to represent the effects of vegetation available for morphological modelling purposes is presented in Chapter 5. Chapter 6 discusses the implications of representing plants as rigid cylinders in laboratory experiments and numerical modelling, including the results of new experimental tests on the applicability of the rigid-cylinder schematization. The field observations performed to study the morphological effects of vegetation growth are presented and analysed in Chapter 7. Chapter 7 also includes the simulations executed with a numerical model constructed with the Delft3D code analysing the applicability of this numerical tool on predicting the morphodynamic evolution observed in the Lunterse beek and assessing the relevance of considering the seasonal variations of vegetation to study this type of streams. Chapter 8 comprises the description of the laboratory experiments carried out to study the effects of plant establishment on new sediment deposits on the river morphology. Lastly, the main findings and relevant recommendations of the study are given in Chapter 9.

2

RIVER BANK ACCRETION

“Men argue; nature acts.”

Voltaire

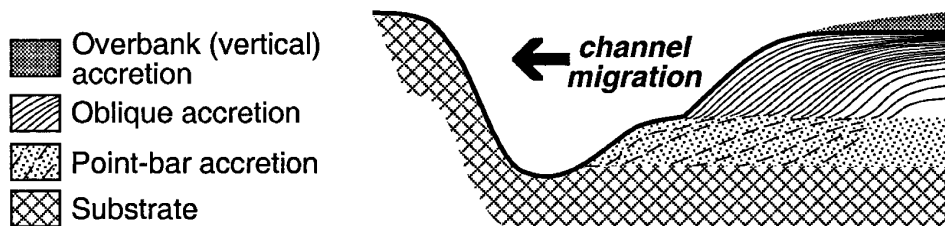


Figure 2.1: Schematic distribution of accretionary deposits on meandering floodplain formation (source: [Page et al., 2003](#)).

In this chapter the key aspects of river bank accretion are presented as well as the state of the art of its modelling.

Parts of this chapter have been published by the author in *River Research and Applications* **32**(2): 164-178, doi:10.1002/rra.2910 ([Solarì et al., 2015](#)) and in the *REFORM project* ([Gurnell et al., 2014](#)), Influence of natural hydromorphological dynamics on biota and ecosystem function. Deliverable 2.2, Part 1 (<http://www.reformrivers.eu/results/deliverables>).

2.1. GENERAL DESCRIPTION

THE morphological response of rivers results from a combination of changes of bed material, bed level variations, as well as erosion and accretion of river banks. River migration and planform configurations are established by the combined action of sequences of bank erosion and accretion, processes that actively interact establishing the channel-width. Accretion processes regard to the formation of new landforms at riverbanks, a fundamental process for the river width adjustment. However, research conducted so far has paid little attention to this process (Solari et al., 2015). These accretional processes result from the interaction of several factors, such as near-bank flow regime, sediment transport and morphological changes, riparian vegetation dynamics and compaction of near-bank deposits.

The interaction between hydrodynamics and the different fractions of the transported sediment defines several types of accretionary deposits, which might result in stratifications, as in the cross-section shown in Figure 2.1. The distribution and relative contribution of different accretionary deposits have been widely discussed in the geomorphological literature (Nanson, 1980; Díaz-Molina, 2009; Page et al., 2003, among others). On the basis of field data Wolman and Leopold (1957) showed the dominance of point bar formation (lateral accretion) with respect to sediment deposition due to over-bank flows (vertical accretion) for the bank accretion processes observed in rivers. The oblique accretion described by Page et al. (2003) for Australian rivers, shows the influence of the bed-load grain size distribution and the relevance of scroll bar formation in this kind of deposits. By combining ground-penetrating radar and core samples Bridge et al. (1995) showed how accretion of sediment together with bar growth processes lead to floodplain construction.

However, these preliminary descriptions do not consider the influence of riparian vegetation and fine sediment processes, which play a key role in the formation and stabilization of new landforms (e.g. Brierley and Hickin, 1992; Hupp and Osterkamp, 1996). Starting with the formation of sediment deposits, such as bars, subsequent vegetation growth and soil compaction cause soil stabilization, which is a prerequisite for the river bank accretion (Wintenberger et al., 2015). These processes are governed by the alternation of low and high flows, through hydrologic regime and climate. Figure 2.2 provides an example of vegetation growth on a point bar leading to the bank accretion in a river bend.

Predicting bar and point bar formation is, therefore, central to studies dealing with the river-width adjustment and river-planform changes (Crosato, 2008). The hydrological regime variability, in terms of magnitude, frequency, and duration of water flows influences soil compaction and vegetation development (Poff et al., 1997). The stability and permanence of the deposited sediment is also influenced by the presence of cohesive material, because consolidation increases the soil resistance to erosive processes.

A common approach in meander migration modelling and river engineering applications is to impose a constant channel width, which is typical of meandering rivers considering equal the long-term rates of bank advance and bank retreat focusing on bank

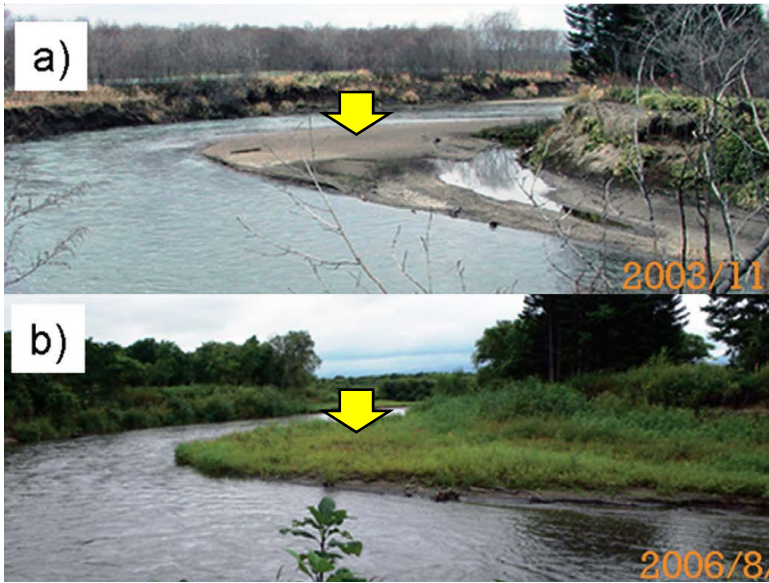


Figure 2.2: Point bar stabilized in the Nakashibetsu River, Hokkaido (Japan) by vegetation growth and fine sediment capture, a) November 2003, b) August 2006 (adapted from: [Parker et al., 2011](#)).

erosion ([Ikeda et al., 1981](#); [Crosato, 1989](#); [Odgaard, 1989b,a](#); [Parker and Johanneson, 1989](#)). Nevertheless, this assumption wrongly implies that both processes are governed by the same factors. Contrastingly, field observations have shown that erosion and accretion processes in rivers vary from reach to reach, operating at different rates and that important temporal lags exist between them which indicates that different factors govern the two processes (e.g. [Li et al., 2007](#); [Kummu et al., 2008](#); [Hobo et al., 2010](#); [Yao et al., 2011](#); [Hossain et al., 2013](#)). These differences can be seen, for instance, in [Figure 2.3](#) showing planimetric and width changes attributable to the bank erosion and accretion of the Ningxia–Inner Mongolia reach of China’s Yellow River over a 50-year period.

The combination of bank erosion and accretion, leads to both width changes and planform style evolution. Bank processes also promote and maintain river ecosystems. River bank accretion form new sites for vegetation colonization and further succession ([Kalliola et al., 1991](#); [Alexander and Marriott, 1999](#)) facilitating, at the same time, habitat development for other species.

2.2. ROLE OF DISCHARGE REGIME

ALLUVIAL rivers are characterized by wide ranges of discharges that are able to erode bed and banks, affecting the fluvial morphology in different ways ([Lane et al., 1996](#)). Thus, in morphodynamic studies, it might be unrealistic to assume that a single value of the discharge can reproduce the effects of the full river flow regime. However, a constant discharge is often used to represent the variable river flow. In the majority of meander

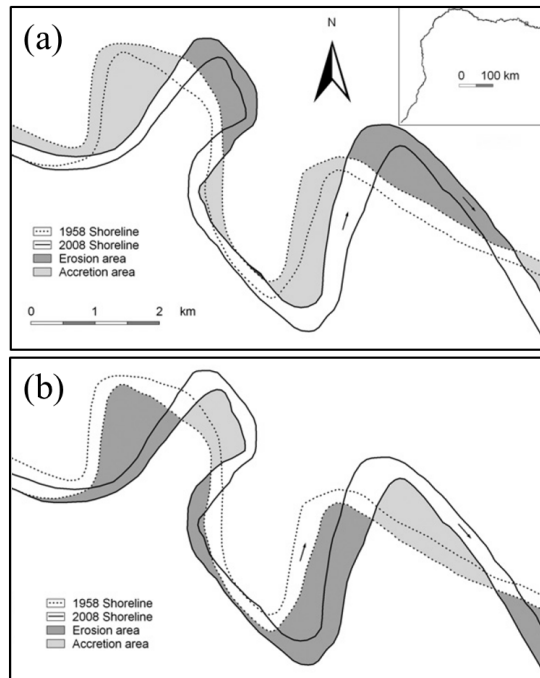


Figure 2.3: Bank erosion and accretion in the Ningxia-Inner Mongolia reach. Flow is from left to right. Displacements observed in a) Left bank, and b) Right bank (source: Yao et al., 2011).

migration models, for instance, it is commonly accepted that a constant discharge (usually taken as the bank-full discharge) is sufficient to describe the effects of the hydrological variability on the river planimetric changes. However, the influence of variable discharge on channel-width adjustments and on changes in erosion and accretion rates in meandering rivers has been identified from field data (e.g. Nanson, 1980; Provansal et al., 2010; Hooke, 2006) and numerical modelling (e.g. Asahi et al., 2013).

The hydrological regime governs the discharge characteristics, such as magnitude, frequency and duration. At the same time, the water flow, together with sediment processes, drives the morphological changes and the ecological development of river channels. The flow strength defines the sediment transport rates and the processes of sediment entrainment and deposition, which shape the bed topography, including the formation of bars and point bars. Vegetation development and survival together with soil consolidation through compaction and de-watering (Section 2.7) are governed by the alternation of high and low flows. Vegetation, in turn, modifies the flow patterns and further stabilizes sediment deposits. Moreover, the spatial distribution and variety of vegetation species on floodplains, in the form of shrubs and trees, is strongly controlled by flood duration and intensity, as well as the sequences of inundations and droughts (Johnson, 2000). The hydrological regime also influences riverbank stability, because the flow variation governs the process of wetting and drying of banks, affecting their

geotechnical response (Thorne, 1982). Thus, water level variability associated with the hydrological regime is strongly related to the river bank accretion processes and the morphodynamic evolution of rivers.

2.3. ROLE OF SEDIMENT TRANSPORT

As river bank accretion starts as a depositional phenomenon, sufficient sediment supply is a prerequisite. In accordance to its origin, the sediment that is transported by rivers can be assigned to two sources: “bed material load” and “wash load”. The bed material load is the coarse component and its transport rate is defined by the flow strength, which means that it is (flow) capacity-limited. Wash load is the fine fraction that is originated through erosive processes at the basin scale. Its rate of transport does not have a relevant dependency on flow strength, but rather on supply, so wash load is supply-limited. Cohesive sediments transported as wash load are important for the creation of accretional structures due to the nutrients they carry (enhancing vegetation growth) and their role in consolidation processes, which will be discussed in Section 2.7.

2.4. ROLE OF RIPARIAN VEGETATION

VEGETATION facilitates the development of new floodplain modifying the morphological environment in a way that favours the establishment of new vegetation, which in turn acts as an ecosystem engineer (Jones et al., 1994; van de Koppel et al., 2001; Gurnell, 2014). By producing hydrodynamic drag vegetation alters the flow pattern and increases the flow resistance, thereby reducing the local flow velocity and the local bed-shear stress and favouring the trapping and deposition of sediment within the plants (Zong and Nepf, 2011). Field experiences (Sand-Jensen and Mebus, 1996; van de Koppel et al., 2005; Cotton et al., 2006; Meier et al., 2013) and laboratory experiments (Zong and Nepf, 2011, 2012) show that vegetation is also effective in trapping and retaining fine sediment. Fine sediments promote vegetation growth due to the presence of nutrients (McBride and Strahan, 1984; Schulz et al., 2003; Meier et al., 2013) and facilitate the development of other species by creating new habitats (Gurnell et al., 2012).

The presence of vegetation favours the stability of recently formed deposits by increasing soil strength due to the mechanical reinforcement derived from root networks including binding, adding of tensile strength, and redistributing stresses (Ott, 2000; Pollen-Bankhead and Simon, 2010). Vegetation furthermore decreases erosion by covering and therefore protecting the bare soil and reduces the pore-water pressure by decreasing the soil moisture content via interception and evapotranspiration (Terwilliger, 1990). However, the hydrological effects of vegetation may also decrease bank stability, because of the increased infiltration rates during rainfall events (Collison and Anderson, 1996; Simon and Collison, 2002) and the additional weight on banks (Abernethy and Rutherford, 2000), for instance derived from trees. Numerical exercises have shown that vegetation growth strongly affects morphodynamic processes and that model responses are highly sensitive to the temporal scales of vegetation development (Murray and Paola, 1994, 1997; Perucca et al., 2007; Crosato and Samir Saleh, 2011).

2.5. ROLE OF OPPOSITE BANK DYNAMICS

RESEARCH conducted in meandering rivers has also shown that bank erosion processes play an important role in river bank accretion, and eventually the advance of river banks (Crosato, 2008). Moreover, it has also been shown that the accretional deposits deflect the main flow towards the opposite bank promoting erosion (Dietrich and Smith, 1983). It is actually the direct communication and permanent feedback between erosional and depositional processes at opposite banks that determine the river-width dynamics in these systems. However, it is still unclear if the equilibrium river-width found in meandering rivers is governed by the newly formed banks (bar push) or the eroding banks (bank pull) (van de Lageweg et al., 2014; Eke et al., 2014a).

2.6. ROLE OF CLIMATE

CLIMATE affects the hydrologic cycle, altering also the stability and composition of soils, and vegetation processes. Therefore, climate modifies the morphodynamic response of river systems. Changes in temperature and precipitation regimes might therefore lead to substantial variations in the water balance of catchments (Parmet et al., 1995). These variations may then induce changes in land use, altering soil organic carbon content as well as evapotranspiration rates and runoff processes. These modifications affect also flow discharges, which in turn cause an immediate alteration of sediment transport rates (Asselman, 1995).

Changes of local climate may directly (by changes in temperature) or indirectly (by land use changes) affect also soil properties by modifying the organic matter status. Considering that soil particles and aggregates are adhered by binding forces that are controlled by organic matter, changes in climate can therefore alter the soil structure stability and degradation (van der Drift, 1995) and therefore the sediment supply to the river. Furthermore, climate change can affect the availability of loose material at the catchment scale, altering fine sediment supply as wash load. On the basis of field data, significant impacts of climate change on soil erosion, transport and deposition have been reported at the catchment scale (e.g. Asselman et al., 2003).

Climate alterations involving the intensity and frequency of events (drought or flood episodes) can cause also enormous impacts on vegetation processes, diversity, and spatial distribution. In forest ecosystems, for instance, climate-related vegetation mortality events have been observed with increasing frequency during the last decades (Allen et al., 2010). These events are commonly associated with droughts and have been observed in temperate systems (e.g. van Mantgem et al., 2009; Carnicer et al., 2011), and in tropical rainforests (Phillips et al., 2009). Summarising, climate affects the discharge and sediment regimes as well as riparian vegetation and soil compaction processes, which in turn can substantially affect the morphological evolution of river systems. As a result, bed-level changes and bank erosion and accretion along river systems may be altered by climate changes.

2.7. ROLE OF SOIL CONSOLIDATION

CONSOLIDATION processes increase the soil resistance to fluvial disturbances and hence facilitates the creation of new landforms. Soil consolidation occurs during low flows due to the presence of cohesive material trapped in vegetation patches. This process starts with the loss of water from the pores which is not replaced by water or air, and is reinforced by the presence of plants because they reduce the water content (Allmendinger et al., 2005). The resistance to erosion of the newly formed deposits due to soil consolidation gives the possibility to resist against subsequent floods, creating new structures in alluvial rivers. Harvey and Watson (1986), for instance, found evidences of bank advance enhancement in incised rivers in Mississippi related to the deposition of wash-load with clay content in recently-established shrubs. Moreover, the presence of fine sediment favours the growth of plants, which increases local sediment deposition (van de Koppel et al., 2001; Meier et al., 2013) and stability.

2.8. SPATIOTEMPORAL SCALES

THE morphodynamic response of river systems is characterized by different length and time scales (Church, 2007). For modelling purposes it is therefore important to identify the dominant processes acting at the different spatial and temporal scales (Wright and Crosato, 2011). Special considerations should also be taken into account to provide the linkage between temporal and spatial scales when including vegetation processes (Phillips, 1995). River bank accretion operates at a wide range of spatiotemporal scales which are discussed below and summarized in Table 2.1.

The smallest spatial scale at which the accretional structures can be distinguished is the scale of the water depth, for which sediment deposits formation and vegetation processes can be established with variations on the vertical. Flow and sediment transport interact locally with the vegetation elements. At this spatial scale, a single flood event has a correspondent temporal scale of hours to days and weeks (according to the size of the drainage area). At the cross-sectional scale and larger spatial scales, the accretion and erosion rates are defined by the horizontal cross-stream shift of the river margins, displacements named as bank advance and retreat, respectively. The combined effect of the bank retreat and opposite bank advance defines the channel width at each location of the river. The sediment deposits and vegetation patches distribution can be spatially identified at this spatial scale and flow-sediment-vegetation interactions set flow patterns, bar formation and vegetation survival. The related temporal scale is that of months to years, including a series of flood events. Considering a river reach, changes in geomorphological forms and the vegetation distribution establish the river planform style which can be additionally described by channel sinuosity, braiding index and the longitudinal slope. Reach-averaged properties of channel and floodplains control vegetation development, see Table 2.1. At the reach scale, the typical temporal scale is that of years to tens of years.

Table 2.1: Spatiotemporal scales of the river bank accretion and related processes.

Spatial scale	Temporal scale	Typical length	Morphodynamic processes	Riparian vegetation dynamics	Vegetation influence on flow	Flow influence on vegetation
Water depth	Up to weeks	Water depth (h)	Bank failure; entrainment of bank material by water flow; near-bank deposition/erosion of bed sediment; soil de-watering	Colonization of vegetation on banks; plants and root system growth	Flow velocity and sediment transport reduction; sediment and organic material accumulation; increased soil resistance by root systems	Soil moisture setting; local stability and permanence: burial and uprooting of plants
Cross-section	Months to years	Channel width (B)	Bank retreat; bank advance; local width adjustment; bar development; sediment deposition forming new levees (levee formation)	Riparian vegetation distribution	Deflection of water flow; protection against erosion of vegetated areas; increase of flow resistance; increase of water levels	Inundated areas: decreasing productivity or increasing mortality; vegetation patches spatial distribution
Reach	Years to tens of years	Water depth to energy slope ratio (h/t_i)	Reach-averaged floodplain rise and width adjustment; planform changes; longitudinal slope adaptation; change in reference bed level and water depth	Vegetation succession; self-thinning	Alteration of water levels and planform styles affecting global conveyance	Seed dispersal; transport of nutrients and organic matter; groundwater levels

2.9. MODELLING ATTEMPTS

SCIENTIFIC contribution to river bank accretion within the field of river morphodynamics mainly deals with observations and strongly simplified numerical modelling, but research describing its evolution in a physics-based, quantitative way is still lacking (Crosato, 2008). The aim of this section is to describe the present state of the art and the knowledge gaps that still impede a physics-based description of river bank accretion. One of the first contributions to river bank accretion modelling was provided by Parker (1978a,b). He assumed that there was a transverse sediment balance between accretion and erosion, including an accretion submodel caused by near-bank settling of fine sediments. With the help of a depth-averaged numerical model, Tsujimoto (1999) studied the effects of vegetation invasion on a river bank at the cross-sectional scale. Tsujimoto's model combined variable discharge and the colonization of vegetation. Bed level degradation occurs above a certain critical velocity, and then degraded areas are colonized by plants during low flows (see Figure 2.4). Nevertheless, this model does not include bank erosion which would take place in most real cases at the opposite side and it is presumed that plant properties are static in time, thus resulting in an incising river.

Only a few models consider the migration of a river as a coupled action of the eroding and depositing processes occurring on opposite banks. The first of them, proposed by Mosselman et al. (2000), was formulated to analyse the effects of bank stabilization on anabranches of a braided river. The authors described channel migration as a combination of retreat and advance along the Brahmaputra-Jamuna River in Bangladesh. A submodel based on the bed shear-stress excess of an analogous shape of the equation proposed by Osman and Thorne (1988), as shown in Figure 2.5, was used to simulate bank erosion and accretion. For the purposes of the case study, they obtained good qualitative results showing the importance of treating the erosion and accretion processes independently, however quantitative estimations deviated from the observations.

Most meander migration models assume that the rate of bank advance is equal to the rate of bank retreat at the opposite side of the channel (Ikeda et al., 1981; Crosato, 1989; Odgaard, 1989b,a; Chen and Duan, 2006). This assumption is a basic long-term characteristic of meandering rivers, but it wrongly implies that both processes of erosion and accretion depend on the same factors (Crosato, 2008). In the case of meandering rivers, some of the most recent approaches have attempted to overcome the limitations of Ikeda et al.'s (1981) model, such as the simplified relationship that allows interaction between eroding and depositing banks defining both migration and evolution of the channel width, proposed by (Parker et al., 2011). The latter model also includes the effects of slump blocks on bank protection against erosion and sediment trapping by vegetation on vertical bank accretion.

On the basis of Parker et al.'s (2011) model, two approaches have been developed. In the first attempt, Asahi et al. (2013) included the combined effects of vegetation colonization, recruitment and establishment in a land accretion module, see Figure 2.6. New land forms when cells remain dry for a period longer than a certain user-defined time, which means that all the vegetation processes are encapsulated in a time-dependent

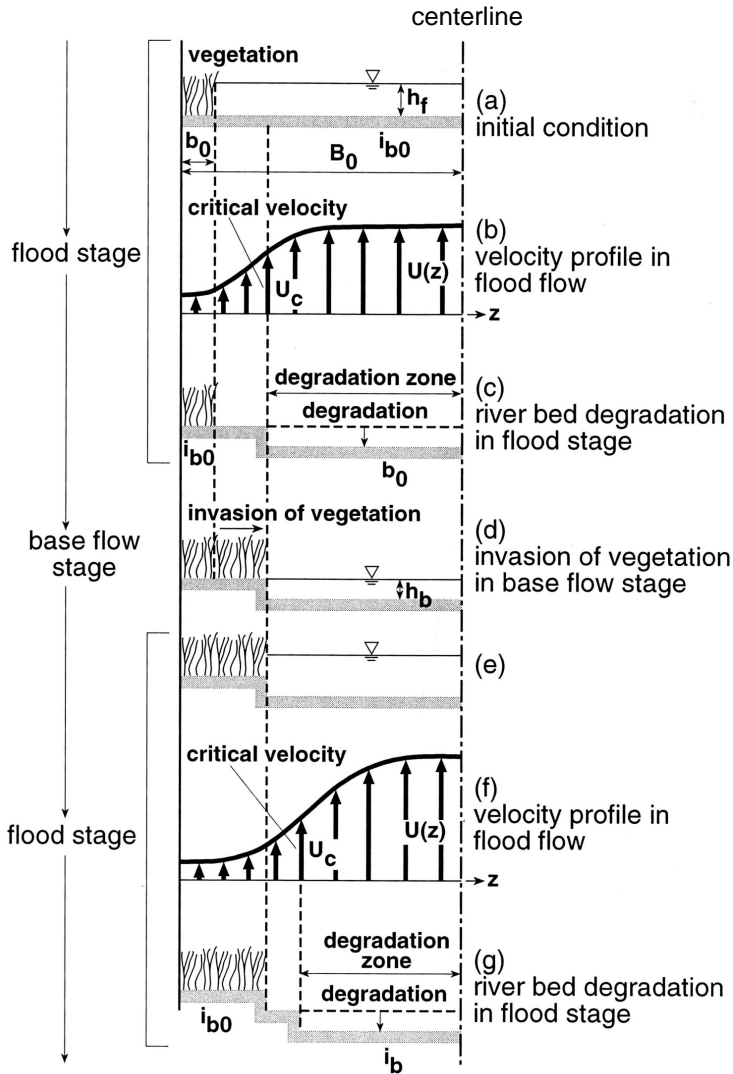


Figure 2.4: Schematic representation of Tsujimoto's model (source: [Tsujimoto, 1999](#)).

parameter. Channel cut-offs and other morphological phenomena are also included in this approach, forming the model Nays2D (see [Asahi et al., 2013](#); [Schuurman et al., 2016](#)). However, the influence and development stages of vegetation and soil consolidation processes among other relevant factors governing the river bank accretion processes are neglected. Additionally, comparisons between estimations and experimental or field data are lacking. For the second approach, based on bed-shear stress forcing and including the effects of vegetation in a simplified way, [Eke et al. \(2014a,b\)](#) proposed a bank deposition model, allowing for the river channel-width evolution (See [Figure 2.7](#)).

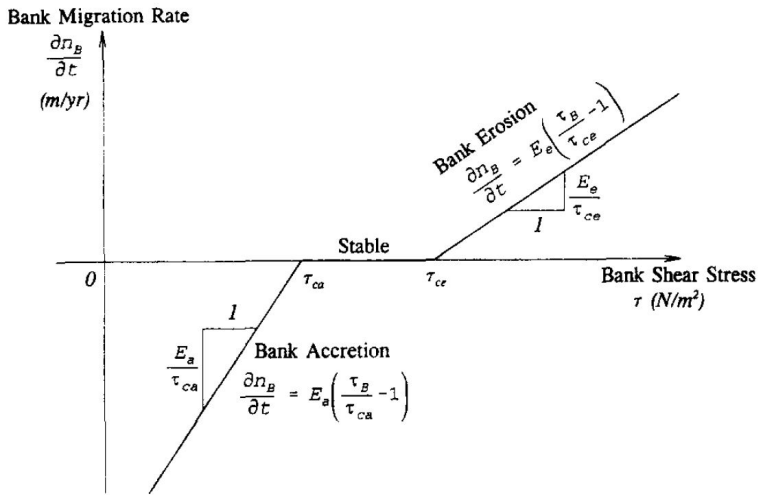


Figure 2.5: Schematization for bank erosion and accretion processes (source: Mosselman et al., 2000).

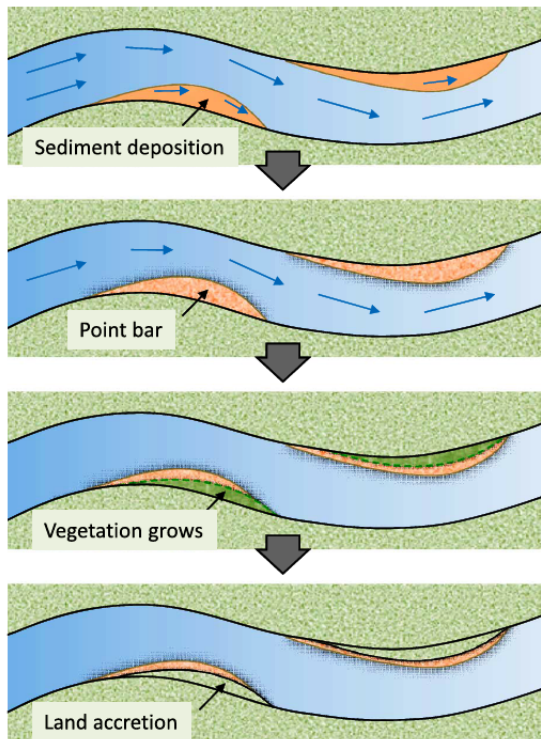


Figure 2.6: Land accreting process in Asahi et al. (2013)'s model (source: Asahi et al., 2013).

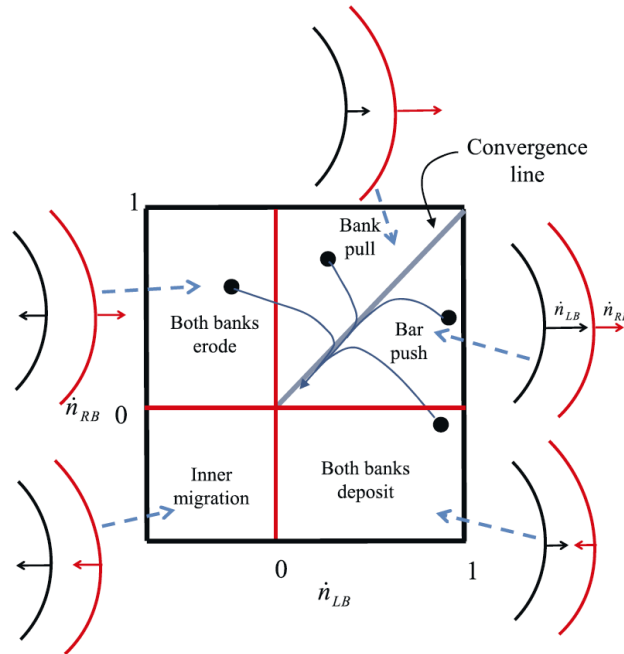


Figure 2.7: Bank migration phases proposed in Eke et al. (2014)'s model (source: Eke et al., 2014a).

The first attempt to include vegetation dynamics on bars in a morphodynamic model is recently presented by Bertoldi et al. (2014). In the two-dimensional morphodynamic model BASEMENT (www.basement.ethz.ch), the authors include the possibility of vegetation development on sediment deposits. Vegetation properties and dynamics are described in terms of the dimensionless biomass density, which distribution is described as a function of elevation. Simple rules considering vegetation growth and plant removal are also included. The scenarios presented by Bertoldi et al. show the potential of including vegetation dynamics for river management and restoration. In Figure 2.8 an application of this model to a case with similar characteristics to those of the Magra river in Italy is shown. After four flooding events the biomass distribution is shown in Figure 2.8(e). A similar numerical exercise was used by Zen et al. (2016) by using a quasi 1D model to study the bank advance of migrating meander bends.

2.10. DISCUSSION

SOME of the processes influencing river bank accretion have been already included in morphological models. However, bank accretion cannot be fully modelled yet, because the models should include the effects of the presence of plants, incorporating their dynamics (colonization, survival, growth, succession, etc.) which are influenced by flow-plant interactions and changes over time. Including these aspects implies incorporating seasonal variations and geographical considerations, such as climate and

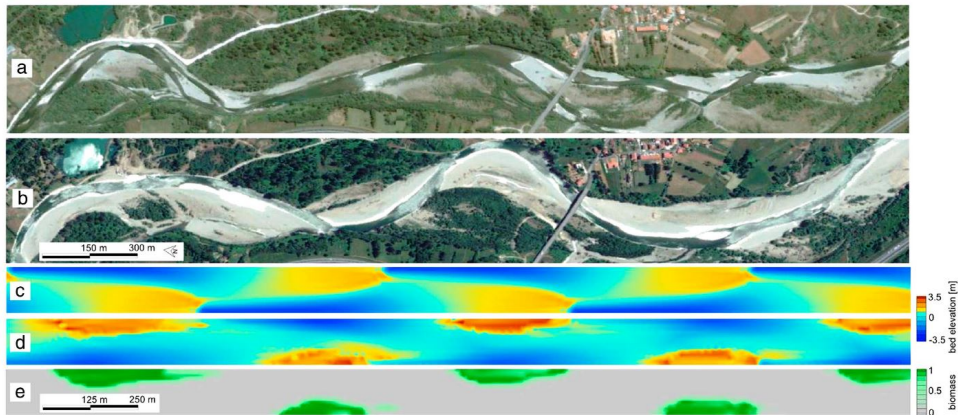


Figure 2.8: Results obtained with Bertoldi et al.'s (2014) model for the case of the Magra river (Italy) (source: Bertoldi et al., 2014).

geology. Moreover, the effects of these processes on groundwater distribution and on the soil properties (composition, consolidation and resistance) should be taken into account as well. Finally, river bank accretion should be described at different scales, starting from the sediment deposition that generate vertical variations on a cross section (at the depth scale) to the bank advance observed in shifting bank lines that eventually leads to channel migration (at the river width scale). This should be addressed by up-scaling processes from the short to the long term in order to reach a temporal scale covering several years or decades. Timescales in river bank accretion are highly relevant, in view of their implications for vegetation development as well as for the physical and mechanical transformations of soils due to the effects of roots and consolidation processes.

3

INTERACTION BETWEEN VEGETATION AND RIVER DYNAMICS

“Water is the driving force of all nature.”

Leonardo da Vinci

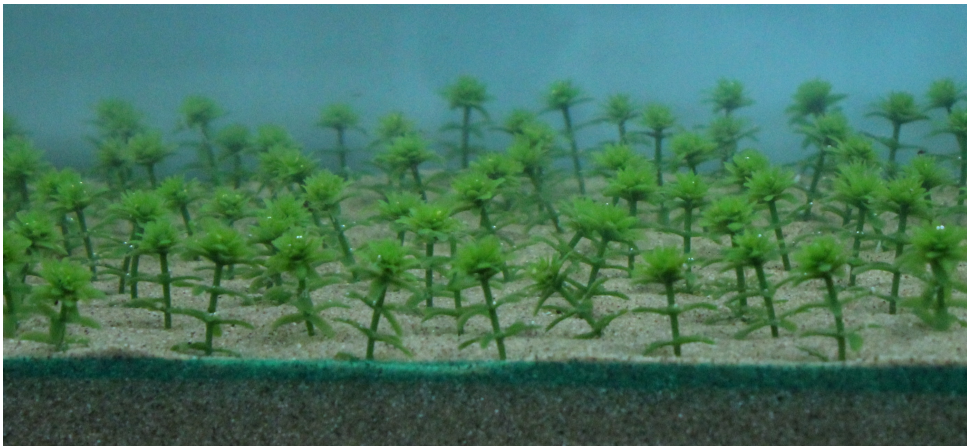


Figure 3.1: Artificial plants used in flume experiments to test the effects of different types of vegetation on flow resistance.

In this chapter the feedback between hydro-morphodynamics and vegetation in riparian areas is addressed.

3.1. THE NEED FOR A BIO-GEOMORPHOLOGICAL APPROACH TO DESCRIBE RIVER DYNAMICS

VEGETATION increases the hydrodynamic resistance (see Figure 3.1), decreasing flow velocities and sediment transport and increasing water depths, at the same time strengthening the soil through its root system. As a result, vegetation can influence the river-width adjustment (Charlton et al., 1978; Andrews, 1984; Allmendinger et al., 2005; Gleason, 2015) and the river-planform changes (Millar, 2000; Murray and Paola, 2003; Tal and Paola, 2010; Crosato and Samir Saleh, 2011). Therefore, it is important to include the effects of vegetation in river studies (Curran and Hession, 2013).

Considering that the highly-active interactions between the river and its floodplains observed in the headwaters decrease as valleys widen more downstream (Brierley and Fryirs, 2013), several floodplain classifications have been proposed on the basis of energy level of the river flow and availability of sediment, among other factors. Nanson and Croke (1992), for instance, based their classification on the specific stream power on which they identify the river processes involved in floodplain genesis, not explicitly considering the role of riparian vegetation. However, riparian vegetation is a strong control for fluvial geomorphology through several types of interactions which determine morphodynamic evolution and landforms (Simon et al., 2004; Corenblit et al., 2007, 2009; Gurnell et al., 2012). Riparian vegetation varies along rivers and its development is vigorously controlled by the hydrological and geomorphologic settings. At the same time, vegetation modifies flow patterns and acts as an ecosystem engineer, controlling sediment and organic matter dynamics, creating the conditions that favour the survival and establishment of new plants and the succession of pioneer plants (Bertoldi et al., 2011; Gurnell, 2014). Once established, vegetation facilitates the reinforcement and development of new landforms modifying the morphological environment. Nevertheless, the influence of vegetation is commonly ignored, or treated merely descriptively, in studies regarding floodplain processes (Hickin, 1984; Osterkamp and Hupp, 2010), with only a few exceptions (e.g. Jeffries et al., 2003; Geerling et al., 2008).

Floodplain vegetation is also key to the river ecosystem considering that biodiversity increases productivity (van Ruijven and Berendse, 2005), stabilizes biomass at the community level (Gross et al., 2014) and reduces plant invasion (van Ruijven et al., 2003). Species richness also influences bank stability (Berendse et al., 2015), sediment trapping and deposition (Owens et al., 2005) and flood control (Mooney et al., 2009; Bullock et al., 2011). Considering these arguments, river management should consider multi-targeted interventions by including the river floodplains with more diverse ecosystems that are also able to cope with floods in the long term. New trends in hydraulic engineering are now considering the paradigm shift from building *in* nature to building *with* nature, which has been applied in the Netherlands through several projects such as the Room for the River project (Rijke et al., 2012; Zevenbergen et al., 2013, 2015).

According to Nanson and Croke (1992), new floodplains in lowland rivers are mainly formed by a combination of lateral (Figure 3.2a) and vertical (Figure 3.2b and 3.2c) accretion mechanisms that are governed by vegetation and fine sediment processes, which in

turn depend on the season (in temperate systems). These factors have been thoroughly discussed in Chapter 2.

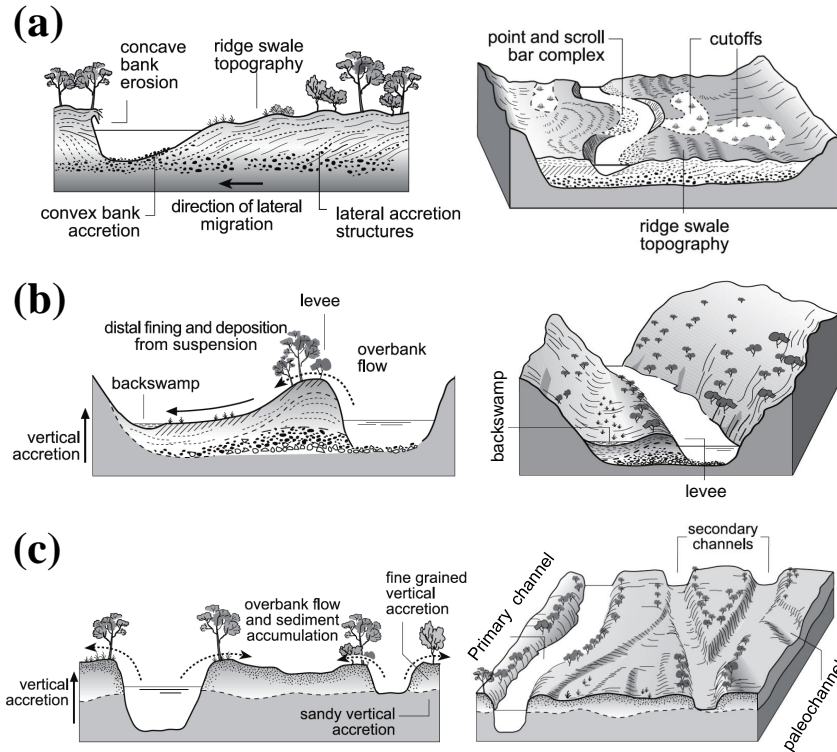


Figure 3.2: Floodplain forming processes according to [Nanson and Croke \(1992\)](#): (a) lateral accretion, (b) vertical accretion in a partly confined valley, and (c) vertical accretion across a wide plain. Adapted from [Brierley and Fryirs \(2013\)](#).

In this chapter, the feedback between hydro-morphodynamics and riparian vegetation is presented, addressing also the state of the art on modelling the effects of vegetation on river flow and morphological changes. The description of these processes pave the way to describe vegetation dynamics and its inclusion in morphodynamic models in Chapter 4.

3.2. EFFECTS OF VEGETATION ON RIVER DYNAMICS

THE main effects of vegetation on river dynamics can be listed as follows:

1. The increase of effective (local) hydraulic roughness ([Cowan, 1956](#)), altering flow patterns and increasing the local flow resistance ([Bakry et al., 1992](#); [Tsujimoto, 1999](#)). This reduces velocities and bed shear stresses, as well as sediment transport in vegetated areas ([Prosser et al., 1995](#); [Ishikawa et al., 2003](#)), promoting sediment

retention between plants (Sand-Jensen and Mebus, 1996; Cotton et al., 2006; Meier et al., 2013).

2. The protection of local soil from erosion directly by covering and indirectly by the reduction of flow velocities (e.g. Gurnell, 2014).
3. The increase of soil strength by roots through binding, addition of tensile strength, and stresses redistribution (Waldron and Dakessian, 1981; Gyssels et al., 2005; Pollen-Bankhead and Simon, 2010; Li and Li, 2011).
4. The drainage of river banks, reducing the effects of waterlogging processes (e.g. Terwilliger, 1990).
5. The damping of turbulence, reducing sediment and plant detachment and entrainment (e.g. Yager and Schmeeckle, 2013).
6. The damping of waves (e.g. Ma et al., 2013; Hu et al., 2014).

The intensity of these effects is highly context-dependent, since several factors play a role, such as the spatial and temporal scales of vegetation development (e.g. Perucca et al., 2007), the type of plants and their seasonality and growth rates (Nadler and Schumm, 1981; Johnson, 1994; Geerling et al., 2008), the riverbank materials (e.g. Labbe et al., 2011), the relative size of vegetation compared with channel size (e.g. Zimmerman et al., 1967; Allmendinger et al., 2005) and climate (e.g. Sandercock et al., 2007), among others.

3.2.1. EFFECTS ON FLOW RESISTANCE

THE hydrodynamic resistance in open-channel flow results in friction at the boundaries due to the characteristics of the channel. For un-vegetated channels, the flow resistance is normally expressed as a combination of factors, such as the hydraulic regime (usually expressed in terms of the Reynolds number and/or Froude number), the relative roughness of the bottom (k_s/R_h , where k_s is the bed surface roughness and R_h is the hydraulic radius), the geometrical shape, and the degree of flow unsteadiness (Rouse, 1965). Since the work of Saint-Venant in the 19th century, it has long been suspected that the hydrodynamic resistance has been related to fluid properties and velocity gradients. Consequently, any alteration of the flow field will have effects on flow resistance. The presence of vegetation on the river bed, banks and floodplains alters the local flow field and therefore the flow resistance and sediment transport of the river at the different flow stages.

After the work of Prandtl, who introduced the mixing-length concept, it is regularly accepted that the vertical distribution of flow velocity in a channel can be divided in two layers: the viscous sublayer and the turbulent layer, see Figure 3.3. The viscous sublayer, δ , is a thin layer above the bottom in which the viscous shear stress, τ_v , is dominant (hence the flow is laminar) and the flow velocity has a linear distribution. The turbulent layer lies above the viscous sublayer and covers the major part of the flow depth, where the turbulent shear stress dominates and the flow velocity exhibits a “logarithmic” profile. Near the bed, the logarithmic velocity profile in this layer is obtained based on the

Prandtl mixing-length theory and on the assumption of a constant total shear stress. Further away from the wall in the outer layer, the total shear stress, τ_t , increases linearly with depth, still supporting a logarithmic profile with a wake correction, see Figure 3.3.

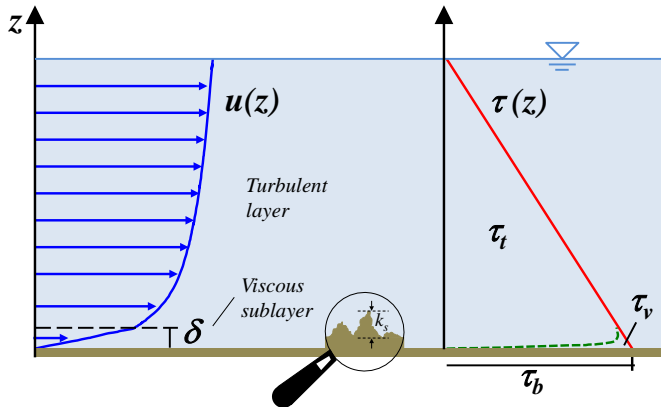


Figure 3.3: Schematic vertical profiles of flow velocity (left) and shear stress (right) for the flow in un-vegetated channels.

These layers and the vertical flow velocity distribution are affected by the bed roughness, an aspect that was first studied in pipe flows (Nikuradse, 1933). If the bed roughness height is much smaller than the viscous sublayer thickness, the bed roughness does not affect the velocity distribution and the flow is considered hydraulically smooth. The flow is considered hydraulically rough when the bed roughness is so large that it produces turbulence close to the bottom. In this case, the flow velocity is independent of viscosity and the viscous sublayer does not exist. A hydraulically transitional flow is then considered when the velocity distribution is affected by both bed roughness and viscosity.

The geometry of plants influences the turbulence characteristics and affects considerably the flow resistance of vegetated beds. Significant research has been performed mainly at the laboratory scale during the last decades providing some understanding on the interaction between flow dynamics and plants (see Green, 2005; Folkard, 2011; Nepf, 2012a; Marjoribanks et al., 2014, for a review), and on the implications for morphodynamic systems (Tal and Paola, 2010). However, the applicability of the obtained results is limited to a few plant species (or plant surrogates in most cases) under controlled flow conditions, which might be far from real conditions (Vargas-Luna et al., 2016b). One of the key problems that limits the understanding of the hydrodynamics of vegetated channels lies in the complexity and variety that riparian vegetation exhibits along river corridors. This diversity combines species, densities and developmental stages in almost each fluvial reach, which are controlled by the hydrologic regime and climate of the area. As the flow field changes considerably when the flow depth exceeds the vegetation height, the study of flow conditions on vegetated beds is here separated in the two

cases of emergent and submerged vegetation. Moreover, for sake of simplicity, vegetation is treated as either rigid or flexible uniform elements.

EMERGENT VEGETATION

FIGURE 3.4 shows the schematized vertical profiles of flow velocity and Reynolds shear stresses for the flow through rigid and flexible emergent plants. The largest vertical variation is attained close to the bottom of the channel, whereas low variation is observed above this level (e.g. Choi and Kang, 2004; Kubrak et al., 2008; Stoesser et al., 2010). This results in low variability of the Reynolds shear stress. On the basis of this behaviour, the flow velocity is commonly assumed to be uniform and the vertical momentum exchange negligible if the vegetation has high density, see Figure 3.4. For sparse vegetation, the vertical velocity profile show less deviation and can be compared to the un-vegetated case (Nepf, 2012a).

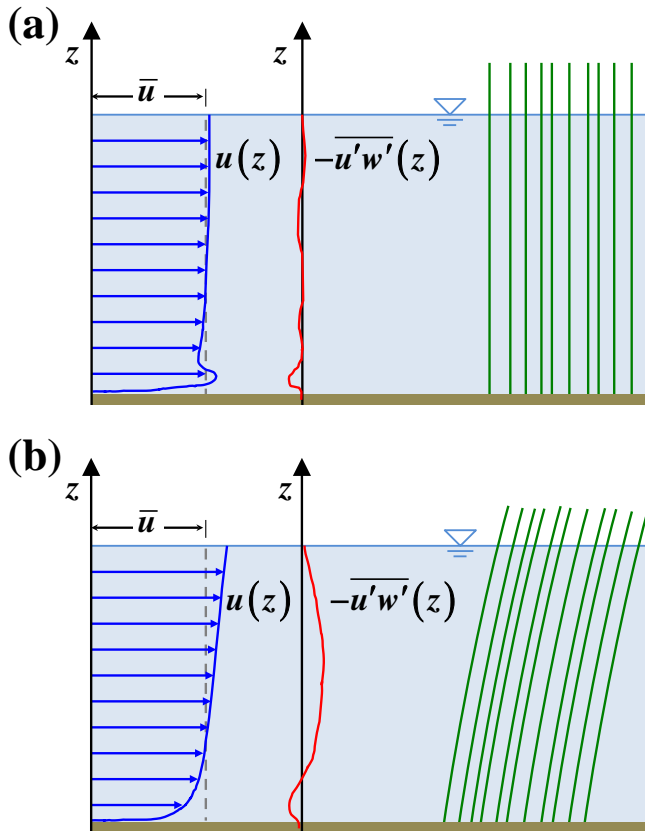


Figure 3.4: Schematic vertical profiles of flow velocity and Reynolds shear stress for channels with emergent: (a) Rigid plants, and (b) Flexible plants.

SUBMERGED VEGETATION

THE schematic vertical profiles of flow velocity and Reynolds shear stresses for the flow on vegetated channels with rigid and flexible submerged plants are shown in Figures 3.5a and 3.5b, respectively. In this case, the flow field is rather complex and the interface between the vegetation layer and the surface layer strongly alters the flow velocity and Reynolds shear stress profiles, creating a strong shear layer, which dominates the transport of mass and momentum between these two layers. Therefore, the main processes are commonly studied by dividing the water depth in three different areas: the lower vegetation zone, the upper vegetation zone, and the non-vegetated zone (surface layer). In the lower vegetation zone, the main forces acting on the water body are gravity and vegetation drag. Since the turbulent shear is relatively small, Reynolds shear stresses are usually ignored (Hu et al., 2013). This area, with negligible shear and more limited water renewal, is named after Ghisalberti and Nepf (2006) as the wake zone. For highly-dense configurations the vegetation drag force generates a shear layer across the vegetation–water interface, along with vortex structures (red cyclic arrows in Figure 3.5), called the upper vegetation zone (or exchange zone according to Ghisalberti and Nepf, 2006). For sparse vegetation the drag force is small compared with bed roughness, thus there is no upper vegetation zone and the flow velocity follows a turbulent boundary-layer profile that is only slightly disturbed (Nepf, 2012a). Based on laboratory investigations several researchers have proposed thresholds to define the transition between sparse to dense configurations (e.g. Belcher et al., 2003; Coceal and Belcher, 2004) and the magnitude of the vortex penetration, δ_e , (Nepf, 2012a). In the surface layer (the non-vegetated zone) there is no vegetation drag force, compared with the upper vegetation zone, and a turbulent boundary-layer profile is normally assumed.

The behaviour of submerged plants can also be divided in different regimes on the basis of the feedback between the hydrodynamic action of the flow and the plant flexibility (Okamoto and Nezu, 2010b). If the plants are not deflected (so their effective height is h_v , see Figure 3.5a) and behave like “rigid elements”, the vortices formed at the shear layer are large, but their penetration (δ_e in Figure 3.5) into the vegetation layer is relatively small. If stems deflect (so their effective height is h_{vd} , see Figure 3.5b) and vibrate exhibiting independent waving, the vortices formed at the shear layer are smaller than in the case of rigid elements, but penetrate more in the vegetation layer. For this case, the Reynolds shear stress distribution has a sharp peak near the vegetation edge (Okamoto and Nezu, 2010b). At higher flow rates, the stems are deflected more significantly and the waving motion becomes coherent (see the left panel of Figure 3.5c) and the Reynolds shear stress distribution has a milder peak structure (Ghisalberti and Nepf, 2006; Okamoto and Nezu, 2010b). When the flow is even stronger or the plants are highly flexible (or both), the stems become bent smoothing the bed surface (right panel of Figure 3.5c). The strong shear layer formed near the vegetation edge of stiffer vegetation generates large-scale coherent structures enhancing momentum transport towards the vegetation layer (Nezu and Sanjou, 2008). Whereas, the reconfiguration exhibited by flexible vegetation increase the momentum absorption near the vegetation canopy decreasing drag (Luhar and Nepf, 2011; de Langre et al., 2012) and creating weaker and smaller vortices (Okamoto and Nezu, 2010b).

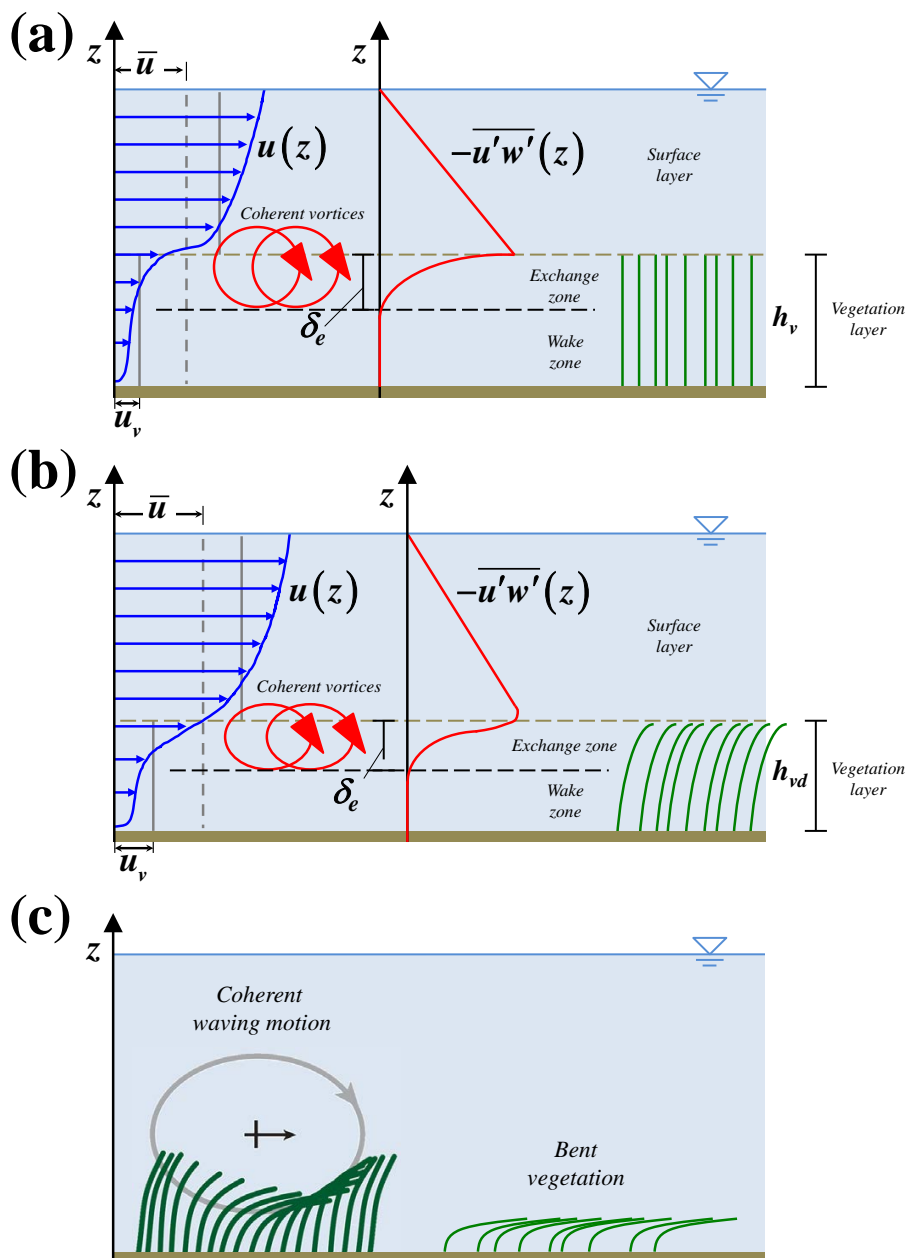


Figure 3.5: Schematic vertical profiles of flow velocity and Reynolds shear stress for channels with submerged: (a) Rigid plants, and (b) Flexible plants. (c) Special behaviour of submerged plants: vegetation with coherent waving motion and prone vegetation.

INFLUENCE OF FOLIAGE

THE quantification of the contribution of the foliage to the flow resistance is a complex issue that remains unsolved mainly due to the high spatial variability of the vegetation geometrical characteristics. Plants with foliage exhibit higher drag than leafless specimens (Järvelä, 2002; Armanini et al., 2005; James et al., 2008; Wilson et al., 2008). The foliage surface area significantly increases the momentum absorbed by the plants, resulting in a decreased mean flow velocity within the vegetation layer (Västilä et al., 2013). However, when plant submergence increases in foliated plants the turbulence magnitude within the vegetation layer remains almost unaltered in comparison to the high variations observed in non-foliated plants. Thus, while the foliage induces larger drag forces, the shear-generated turbulence is reduced due to the inhibition of momentum exchange (Wilson et al., 2003). Additionally, plant foliage shifts the Reynolds shear stress peak to a level above the canopy. It has been found that, at smaller scales, the leaf shape is the most important factor determining hydrodynamic interactions, whereas the flexibility of leaves is the most influential parameter for vegetation reconfiguration (Albayrak et al., 2012).

3.2.2. EFFECTS ON SEDIMENT TRANSPORT

THE presence of vegetation decreases the local sediment transport rates substantially (Prosser et al., 1995; Ishikawa et al., 2003). This reduction is associated with: the decrease of flow velocity and shear stress near the bed (see Figures 3.4 and 3.5) due to the local increase of the hydraulic resistance (Bennett et al., 2008) and the momentum absorbed by vegetation. This results also in decreased turbulence and sediment entrainment (López and García, 1998; Nezu and Sanjou, 2008; Liu et al., 2008). Instead, sediment resuspension occurs within sparse vegetation (Yager and Schmeeckle, 2013). Studies dealing with both bed-shear stress and vegetation drag are scarce and only a few global flow resistance predictors estimate the bed-shear stress for both emergent and submerged vegetation (Vargas-Luna et al., 2015b).

Only a few experimental studies carried out direct sediment transport measurements in vegetated channels and field data are scarce (with a few exceptions: e.g. Temmerman et al., 2003; Lightbody and Nepf, 2006). Li and Shen (1973) described the effects of the spatial distribution of emergent vegetation on flow velocity and sediment transport. Other studies linked bed-material load measurements to numerical modelling (e.g. Okabe et al., 1997; Watanabe et al., 2002) and to estimations by sediment transport capacity formulae (Jordanova and James, 2003; Wu and He, 2009; Kothyari et al., 2009a). For submerged vegetation, López and García (1998) included measurements and modelling of suspended sediment transport.

Many formulae have been designed for the assessment of the sediment transport capacity in non-vegetated streams (e.g. Meyer-Peter and Müller, 1948; Engelund and Hansen, 1967; van Rijn, 1984b; Huang, 2010), but only a few formulae were derived for vegetated channels and most of them are only applicable within a certain flow regime, degree of submergence and canopy properties (Ashida and Michiue, 1972; Li and Shen,

1973; Ishikawa et al., 2003; Jordanova and James, 2003; Kothyari et al., 2009a; Armanini and Cavedon). Direct measurements from a laboratory study with emergent plants have shown that the bed load transport is affected not only by vegetation characteristics, but also by the way that its presence alters the flow conditions (Yager and Schmeckle, 2013). Consequently, including the effects of vegetation on the sediment transport process might be essential to simulate the morphological changes of alluvial rivers.

3

3.2.3. EFFECTS ON BANK DYNAMICS

THE river width depends on the joint action between erosion and accretion processes occurring at the opposite river banks resulting in bank retreat and bank advance, respectively (ASCE Task Committee on Hydraulics, Bank Mechanics, and Modelling of River Width Adjustment, 1998). Vegetation plays a key role in bank dynamics, affecting both processes of bank erosion and bank accretion by modifying the local near-bank fluvial processes and affecting the configuration of banks in various ways (Hickin, 1984; Thorne, 1990). However, it has been shown that these effects are highly scale-dependent (Anderson et al., 2004). Vegetation also affects other processes that are relevant for the bank dynamics such as overbank deposition and levee formation (Nanson and Croke, 1992). These effects have been studied by using laboratory experiments (e.g. Pasche and Rouvé, 1985) and field data in temperate rivers (e.g. Pizzuto, 1987; Lecce, 1997; Walling and He, 1997; Owens et al., 1999; Klasz et al., 2014).

Changes in bank stability due to vegetation are mainly related to mechanical and hydrological effects (Rinaldi and Darby, 2007). The most important mechanical effect of vegetation for bank stability is on the soil strength induced by the root system (Pollen-Bankhead and Simon, 2010). Nevertheless, the net effect of the additional weight of vegetation on the bank surface on bank stability can be either beneficial or detrimental, depending on site-specific factors such as the position of the vegetation on the bank, the slope of the shear surface and the friction angle of the soil (Greenway, 1987; Thorne, 1990; Simon and Collison, 2002). In terms of the influence of riparian vegetation on local scale river bank hydrology, three main effects can be distinguished: vegetation water interception, evapotranspiration and infiltration induced by root pathways. Although these effects are well understood at a conceptual level (Greenway, 1987; Thorne, 1990), they are in practice extremely difficult to quantify. Vegetated banks also decrease the near-bank flow field, altering shear stress distributions and sediment transport processes in these areas and, therefore, reducing bank erosion processes (e.g. McBride et al., 2007). Vegetation is also a key factor on river-bank accretion processes, effects that have been thoroughly discussed in Chapter 2.

3.2.4. EFFECTS ON RIVER BED DYNAMICS

THE river-bed dynamics has an important effect on the morphological evolution of river systems. This important geometrical boundary of the river channel provides the major contribution of flow resistance (Yen, 2002), directly affecting the conveyance of water and sediment fluxes. Therefore, the presence of vegetation on the river-bed may

alter the flow and sediment transport of the system, leading to morphological changes and conveyance losses (Wu and He, 2009).

The river-bed also plays a relevant role on temporary storing of fine sediments (e.g. Collins et al., 2005; Collins and Walling, 2007), which can be remobilized during high flows to be deposited more downstream on river banks and/or floodplains. Additionally, macrophytes have been found fundamental in affecting the nutrient cycles in river systems (e.g. Clarke, 2002).

Bed-level fluctuations contribute in the river-width adjustment as well. In the Plum Creek, Colorado (USA), for instance, the damping of bed-level fluctuations due to vegetation establishment on sediment deposits was found of high importance on the channel narrowing processes observed after high floods (Friedman et al., 1996b,a).

3.3. EFFECTS OF RIVER AND SEDIMENT FLUXES ON VEGETATION

THE major effects of river flow and sediment dynamics on riparian vegetation are:

1. Flow-governed restrictions on the spatial distribution of plants (e.g. Biggs, 1996; Large and Prach, 1999).
2. Plant burial (e.g. Johnson, 2000; Shaw et al., 2013) or uprooting (e.g. Edmaier et al., 2011, 2015) caused by local sedimentation or erosion during high flows.
3. The death or damage of plants during submerged periods (e.g. Blom and Voesenek, 1996; Banach et al., 2009).
4. Groundwater-governed restrictions on plant growth rates and spatial distribution (e.g. Butcher, 1933; Large and Prach, 1999).
5. Vegetation mortality caused by desiccation and nutrients scarcity due to extended droughts (e.g. McDowell et al., 2008).
6. Deposition of fine material fertilizing the soil (e.g. Schulz et al., 2003).

Riparian vegetation mortality is mainly controlled by the environmental setting and climate constrains in temperate river systems, aspects that define the presence of vegetation during the occurrence of hydrodynamic events (e.g. Large and Prach, 1999; Champion and Tanner, 2000). At the reach scale, this process is therefore governed by the flow regime (Gurnell, 2014), which establishes the periods of floods and droughts, both affecting the survival of plants. In fact, it is possible to observe different mortality processes in the same river system according to the season as reported by Johnson (2000) for the Platte River, USA.

3.3.1. EFFECTS OF WATER FLOW

WATER flow can affect vegetation both directly, due to mechanical effects such as excavation, uprooting or burial; and indirectly, due to changes in the transported sediment characteristics (Madsen et al., 2001). The interaction between plants and flow and sediment fluxes can cause their burial (Johnson, 2000) or uprooting (Tanaka and Yagisawa, 2009; Edmaier et al., 2011, 2015). Burial of vegetation leads to death by asphyxia, whereas uprooting causes the direct loss of single elements or complete vegetation specimens (Madsen et al., 2001; Edmaier et al., 2011). Bed erosion and sedimentation can also affect the presence of vegetation, especially related to near-bank stability processes (Simon et al., 2000).

3.3.2. EFFECTS OF FLOODS

EXTENDED inundation periods alter plants development possibly leading to serious physiological damage, affecting larger areas. When riparian vegetation is partially submerged, inundated conditions suppress shoot and root growth, delay leaf formation and accelerate senescence; whereas complete submergence also inhibits photosynthesis and hinders internal oxygen transport (Blom and Voesenek, 1996; Kozłowski, 2002). The severity of the physiological effects depends on the inundation depth and duration, the developmental age of the plant and water temperature (Auchincloss et al., 2012). Additional physiological effects can occur to riparian plants during the post-inundation period due to the re-exposure to light that may cause foliage damage by oxidation (Parolin, 2009). Although research on flood-related tolerance and mortality have been carried out in riparian forests (e.g. Friedman and Auble, 1999; Kozłowski, 2002; Auchincloss et al., 2012), woodlands (e.g. Amlin and Rood, 2001) and other riparian ecosystems (e.g. Blom et al., 1990; Blom and Voesenek, 1996; Banach et al., 2009), quantitative estimations are scarce. The results reported by Auchincloss et al. (2012) show that, for instance, the mortality percentage by drowning of *Freemont cottonwood* varies linearly with the inundation duration.

3.3.3. EFFECTS OF RIVER BED DYNAMICS

THE river-bed is continuously being adapted to the excesses of sediment coming from upstream, supplied mainly during high-flow stages. By creating new sediment deposits, these bed-level fluctuations define the areas that during low flows will be colonized and stabilized by plants (Friedman et al., 1996b,a).

3.4. MODELLING THE EFFECTS OF VEGETATION ON RIVER DYNAMICS

THE main effect of plants on reducing the bed and near-bank shear stresses in river channels and floodplains is usually modelled in terms of increased flow resistance (Vargas-Luna et al., 2015b), whereas other specific effects such as localized erosion or deposition are more difficult to account for (Solari et al., 2015). By using laboratory and

field data, a review on the methods to estimate the global flow resistance due to the presence of vegetation is presented in Chapter 5. The consequences of representing plants as rigid elements in experiments and models is further analysed and described in Chapter 6.

Regarding the soil reinforcement by the root system, recent research (Pollen and Simon, 2005; Pollen-Bankhead and Simon, 2010) has shown that the previously developed model of Wu et al. (1979) tends to overestimate the additional shear strength of the roots because of the assumption that the full tensile strength of each root is mobilized during soil shearing, and that all the roots break simultaneously. Therefore, a new root reinforcement model (RipRoot) was developed based on fibre bundle theory to account for progressive root breaking during shearing (Pollen and Simon, 2005; Pollen-Bankhead and Simon, 2010).

The mechanical effects of vegetation on bank stability are included in mass failure models for banks composed by non-cohesive (Millar and Quick, 1993), cohesive (Millar and Quick, 1998), and composite materials (Eaton, 2006). Some successful attempts to combine these mass failure models with regime theory models have been made to analyse changes in channel patterns (Millar, 2000) and river restoration (Millar and Eaton, 2013). Other efforts on demonstrating the effects of vegetation in reducing bank instability have been made by using cellular automata models (e.g. Murray and Paola, 2003). Nevertheless, the effects of vegetation on riverbank failure are still not incorporated in morphodynamic models.

In contrast to the advances in modelling the effects of vegetation on bank erosion, bank accretion modelling is still in its infancy. Some of the processes influencing the bank accretion have been included in models, but there is no general physics-based model that describes this phenomenon. Most recent morphological models that include vegetation on bank accretion consider their properties invariant in time (Nicholas, 2013; Asahi et al., 2013; Eke et al., 2014a,b) or by assuming vegetation dynamics in very simplified way (Bertoldi et al., 2014; Zen et al., 2016). In fact, it is this simplified description of the vegetation dynamics and interactions that limits the upscaling process from numerical modelling exercises to real-river applications.

3.5. DISCUSSION

VEGETATION alters flow velocity fields, affecting bed-shear stresses and turbulent structures, driving the modification of sediment transport processes and therefore leading ultimately to morphological changes. Understanding these effects is a key step in revealing the interaction between plants and river systems. However, more research is still needed to link the laboratory-based findings observed at the process scale to the effects observed at the cross-sectional and reach scale of real rivers. To improve model estimations it is also important to couple the hydro-morphodynamic forcing to the vegetation dynamics in order to complete the description of the feedbacks present in bio-morphodynamic systems.

4

RIPARIAN VEGETATION DYNAMICS AND ITS MODELLING

“Vegetation is the basic instrument the creator uses to set all of nature in motion.”

Antoine Lavoisier

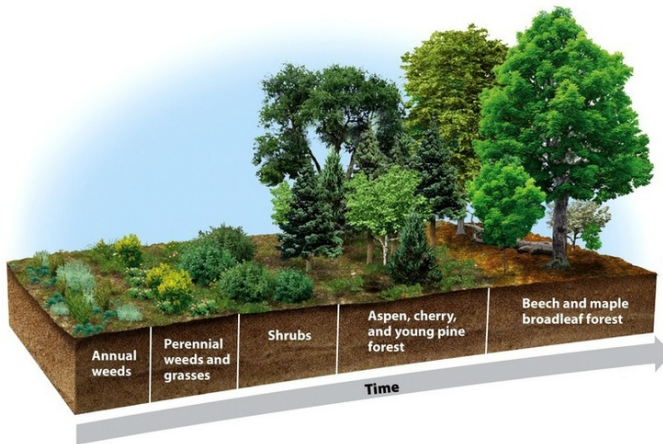


Figure 4.1: Schematic representation of different stages of vegetation development (Source: www.pinterest.com).

This chapter describes the dynamics of floodplain vegetation and the state of the art of its modelling.

Parts of this chapter have been published by the author in the *REFORM project* (Gurnell et al., 2014), Influence of natural hydromorphological dynamics on biota and ecosystem function. Deliverable 2.2, Part 1 (<http://www.reformrivers.eu/results/deliverables>).

4.1. VEGETATION DYNAMICS

RIPARIAN vegetation dynamics refers to the processes that are commonly defined as the adaptive strategies (i.e. dispersal, colonization, recruitment, growth, succession and death) exhibited by plants on river banks and floodplains (e.g. juvenile or mature), see Figure 4.1. These processes are influenced by soil moisture, light, wind, biotic factors (e.g. competition and facilitation), as well as by hydro-morphodynamic forcing (Gurnell et al., 2014). In riverine systems, vegetation appears to be dominated by floods (Bornette et al., 2008) and, therefore, riparian plants have high dispersal rates and are commonly adapted to resist flow (Camporeale et al., 2013). Disturbances caused by floods decline from the main channel towards the floodplains, where competition with other species prevails (Corenblit et al., 2007; Gurnell, 2014). Vegetation is commonly considered in ecological studies in terms of populations. Its dynamics consists in how species change in time in terms of number of individuals or kilograms of biomass of individuals (Volterra, 1926; Lotka, 1956). Jørgensen and Fath (2011) define a population, P_i , as a “collective group of organisms of the same species” that has several characteristic properties, such as density, natality and mortality rates, growth forms and so forth. It is therefore important to study how populations change in time, analysing their rate of change per unit time, dP_i/dt , or the rate of change per unit time per individual, $dP_i/(P_i dt)$, at a particular instant.

4.1.1. SEED DISPERSAL

PLANTS are adapted to have their seeds dispersed by means of animals, wind (anemochory) and water flow (hydrochory); the last adaptation being the most important one in riparian areas (Schneider and Sharitz, 1988; Gurnell, 2014). Hydrochory depends on the synchronization of hydrological regimes with reproduction (Hupp, 1992), increasing its intensity as flood frequency increases (Bornette et al., 2008) and during overbank flows (Nilsson and Svedmark, 2002; Boedeltje et al., 2004). Therefore, along stream channels, the hydrodynamic processes are highly effective as seed dispersal drivers in both longitudinal and lateral directions (Johansson et al., 1996; Merritt and Wohl, 2002).

Several attempts to describe the spatial patterns of seed dispersal and deposition have been made for temperate river systems by using field data (e.g. Gurnell et al., 2008), empirical (e.g. Campbell et al., 2002; Levine, 2003; Steiger et al., 2005), semi-empirical (e.g. Groves et al., 2009), experimental (e.g. Merritt and Wohl, 2002) and physics-based (e.g. Tealdi et al., 2010) approaches. However, there are still many questions that remain unsolved about this process due to its complexity. Moreover, methods to quantify seed dispersal processes in morphological models are still not available.

4.1.2. COLONIZATION

THE colonization process refers to the propensity displayed by vegetation to expand within their ecological range (Grime, 2006). Pioneer plants conquer new areas on alluvial surfaces resulting from sedimentation processes that become exposed during low flows. In temperate regions, the survival of pioneer plants is mainly affected by seasonal

variations of water levels, water-table depths and moisture controlling water availability during establishment stages (Bendix and Stella, 2013). Thus, the plant colonization observed at a specific location is highly dependent on the flow regime and seasonality of the stream (Large and Prach, 1999), inter-annual variations of the amount of vegetation biomass (Dawson et al., 1979; Sand-Jensen et al., 1989, 1999). Water availability has shown to limit population dynamics in snowmelt-dominated rivers (e.g. Lytle and Merritt, 2004) and to be critical in arid and semi-arid regions (e.g. Horton and Clark, 2001; Rood et al., 2003).

The existence of thresholds in plant growth, identifying relevant bio-geomorphological feedbacks between flow and vegetation dynamics, were highlighted in the recent experimental work of (Wang et al., 2016), who studied the vegetation establishment of alfalfa sprouts on bare substrates under different flow regimes. On real rivers, Bradley and Smith (1986) found that, along the Milk River in Canada, pioneer plants develop preferably in horizontal bands that are related with the optimum elevation for seed germination, see Figure 4.2. Relations between water level variability, i.e. flooding, and colonization by plants were observed in pioneer tree communities in USA along the upper Missouri River Auble and Scott (1998), see Figure 4.3, and along the middle Zambezi (Khan et al., 2014).

Colonization of river banks and channels by plants depends on water level variability (Figure 4.3a). Channel narrowing at low-flow periods can lead to the recruitment of plants on the former channel bed (Figure 4.3b). (Auble and Scott, 1998) observed that due to overbank flows, high areas are colonized by pioneer trees on deposit surfaces, see Figure 4.3d. On meandering rivers, vegetation recruitment on point bars promotes bank accretion (Figure 4.3c), which is also described by Mahoney and Rood (1998), see Figure 4.4.

4.1.3. PLANT GROWTH AND VEGETATION SUCCESSION

THE expansion of leaf and root volumes of plants depend on soil moisture, light, and temperature conditions that vary annually and inter-annually (Grime, 2006). The timing, duration and rate of rise and fall of floods affect vegetation growth (Ward, 1989; FISRWG, 1998; Large and Prach, 1999) as well as other vegetation processes (e.g. Puckridge et al., 1998; Boedeltje et al., 2004). Plant growth therefore depends on the flow regime variability through the effects of plant recruitment and survival (Hicks et al., 2007). The temporal scales of plant growth and decay have shown to play a key role on the morphological evolution of rivers (Perucca et al., 2007). This has been addressed, for instance, by relating riparian vegetation development to flood pulses (Junk et al., 1989). Schematic representations of sequences of floods and vegetation growth are shown in Figures 4.5 and 4.6.

Through time and the variability of the hydrological regime, most types of plant populations are exposed to progressive alterations in structure and composition, changes known as succession (Grime, 2006). Ecological succession encompasses structural changes

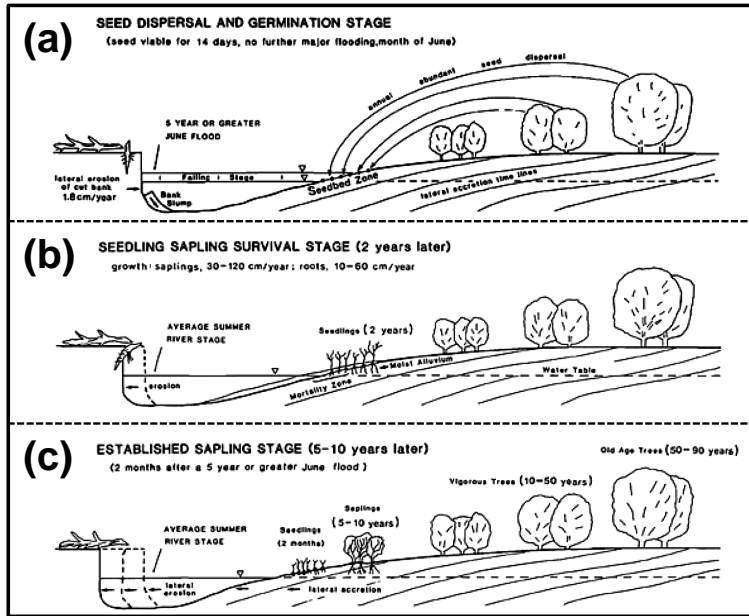


Figure 4.2: Scheme for seeds: (a) dispersal, (b) germination and growth, and (c) establishment, proposed by Bradley and Smith (1986). Adapted from Camporeale et al. (2013).

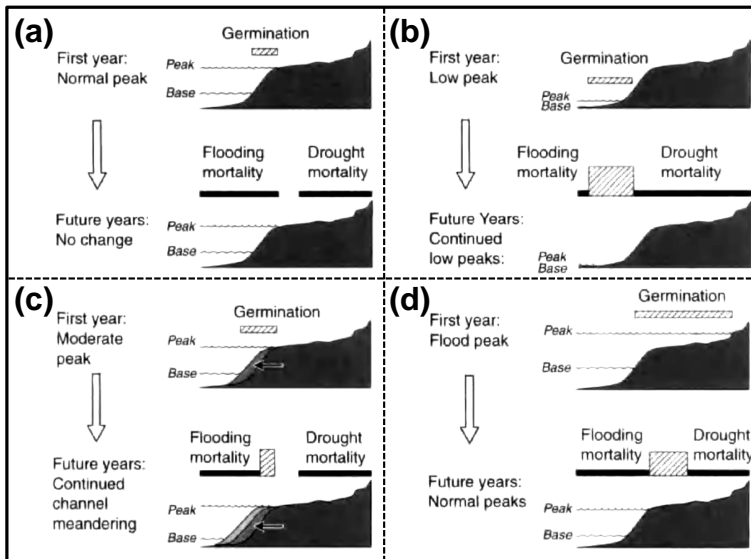


Figure 4.3: Flow variability and its relationship with pioneer trees recruitment: (a) absent, (b) on the former channel, (c) on point bars, and (d) at high elevations. Adapted from Friedman and Auble (2000).

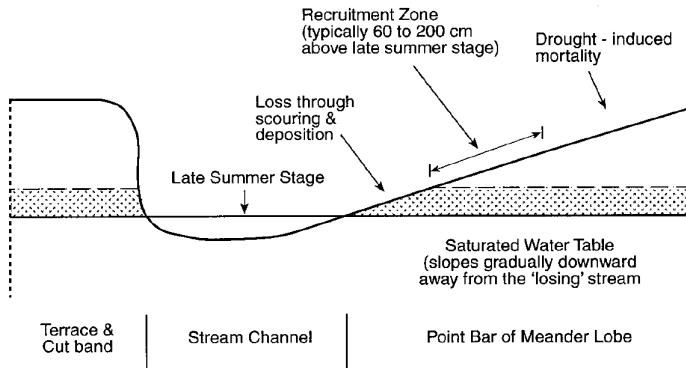


Figure 4.4: Schematic cross-section showing ideal location for germination and survival of cottonwood seedlings (after Mahoney and Rood, 1998).

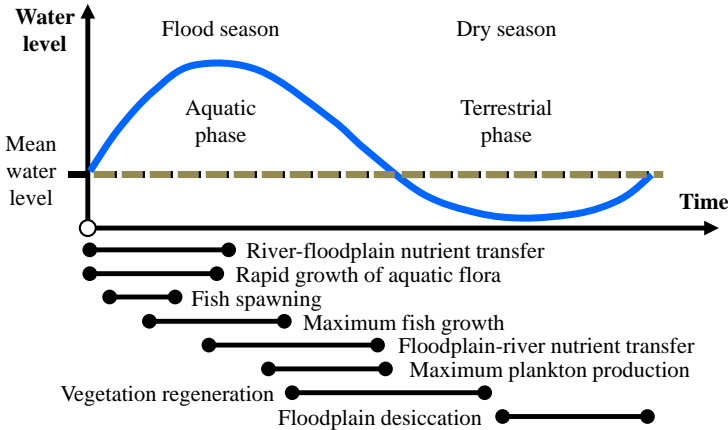


Figure 4.5: The influence of the flood pulse within the river-floodplain complex for yearly fluctuations. (Source: Large and Prach, 1999)

ranging from the establishment of pioneer species to the alteration of shrub communities into woody species that in time will develop in new forest areas. As plants grow, the competition for resources such as light, water, and nutrients increases. When this competence intensifies, some plants die, which results in reduced plant density; and can be seen in the long term as a succession mechanism. In temperate floodplain environments, the plant population is spatially distributed as a mosaic of riparian vegetation patches encompassing a wide range of developmental stages (Ward et al., 2002) due to the interruption of ecological succession by flow disturbances (Large and Prach, 1999; Madsen et al., 2001). Considering this difficulty in achieving a stable equilibrium state, new approaches have migrated from the concept of “climax” communities to the

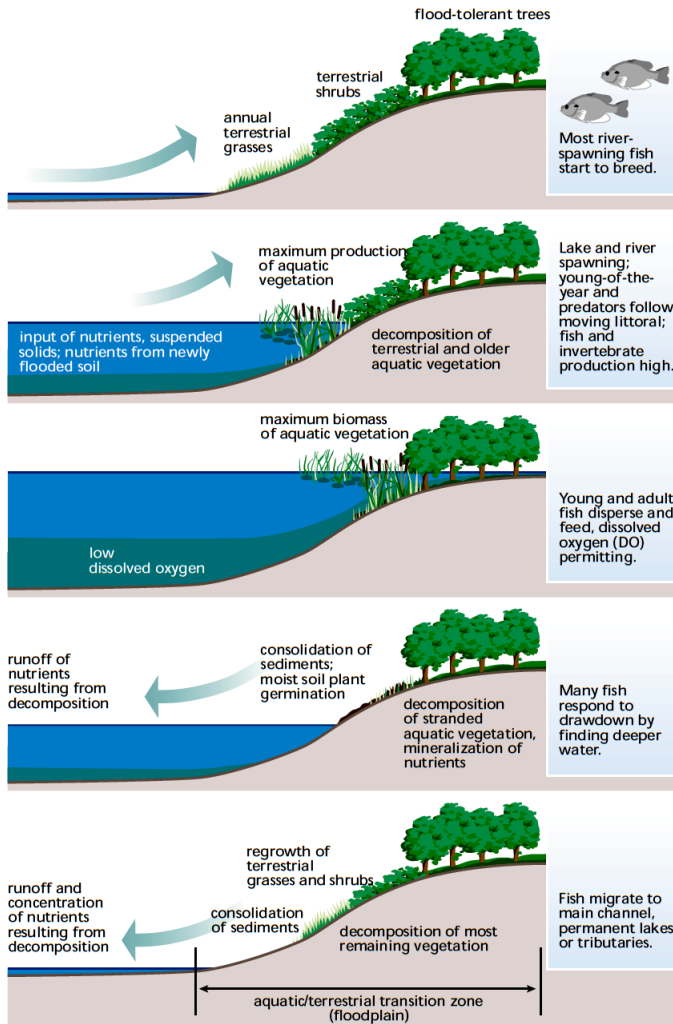


Figure 4.6: Schematic representation of vegetation development by using the flood-pulse concept (After Bayley (1995); Source: FISRWG (1998)).

analysis of riparian vegetation as a collection of numerous patches with varied geometrical characteristics and at different stages of successional development. These complex structures of the riparian vegetation mosaics complicate the distinction between vegetation growth and succession for modelling purposes, especially when the succession of vegetation has been found to be highly sensitive to human interventions (e.g. Egger et al., 2015) and hydrological disturbances (Cline and McAllister, 2012). Bendix and Hupp (2000), for instance, showed how the spatial distribution of vegetation species in temperate floodplains of southern California (USA) is associated with their tolerance to resist different soil moisture, inundation, and shear stress conditions, see Figure 4.7.

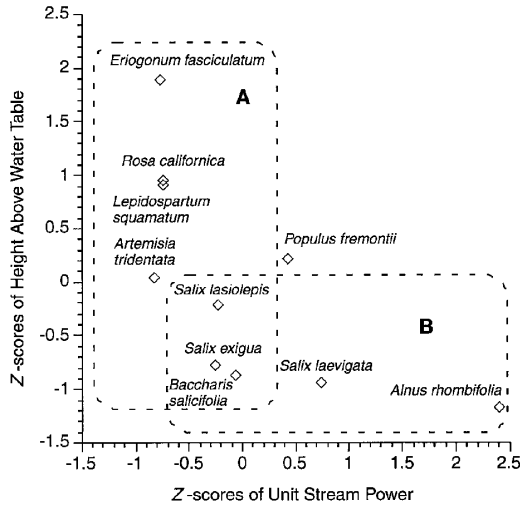


Figure 4.7: Plant species distribution in Southern California as a function of unit stream power and height above the water table (After Bendix and Hupp (2000))

4.2. VEGETATION DYNAMICS MODELLING

CONSIDERING the interaction between riparian vegetation and river morphodynamics, as described in Chapter 3, plants are often included in river morphodynamic models. A common approach to account for vegetation in morphodynamic models is based on a rigid-cylinder representation (Vargas-Luna et al., 2015b, reported in Chapter 5). Although this approach is useful for practical purposes, it was found to be realistic only for restricted flow regimes, whereas at the same time it is difficult to define the real plants that the cylinders represent (Vargas-Luna et al., 2016b, reported in Chapter 6). If plants are described as rigid cylinders in arrays, the dynamics of their population is described in terms of temporal changes of number of cylinders per unit area, their diameter and height..

4.2.1. COLONIZATION MODELLING

THE quantitative estimation of colonization rates and patterns in models is usually based on conceptual models as, for instance, the “recruitment box model” proposed by Mahoney and Rood (1998). Built upon the key role of soil moisture in the colonization process, this model links the seasonal decline of water levels to the release of seeds. Figure 4.8 shows that the seedling success is directly related to the rate of water table decline in this model. A germination module was recently included by (Ye et al., 2013) in a cellular automata model.

Currently, only a few morphodynamic models include colonization processes, and in a simplified way. Phillips (1995) related vegetation development to flooding recurrence intervals, assuming similarity in temporal scales. After channel bed degradation,

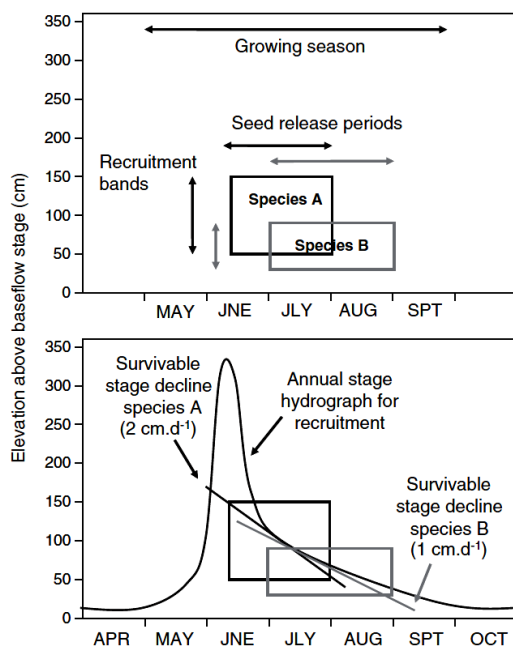


Figure 4.8: Application of the recruitment box model of Mahoney and Rood (1998) adapted by Camporeale et al. (2013).

Tsujimoto (1999) assumed the immediate vegetation colonization of the bank areas that become exposed. With the aim of testing the effects of vegetation on river planforms, Crosato and Samir Saleh (2011) used a physics-based numerical model, based on the Delft3D code, and, assuming that vegetation colonizes every year the areas that become exposed during the low-flow period, showed the relevance of vegetation in obtaining single-thread channels. van Oorschot et al. (2016) proposed an off-line tree colonization module on the basis of mechanisms described by (Corenblit et al., 2009; Gurnell, 2014) and linked it to a morphodynamic model based on the Delft3D code, see section 4.2.2. Different planforms were also obtained with the HSTAR model (Hydrodynamics and Sediment Transport in Alluvial Rivers) by Nicholas (2013), in which channel cells are transformed into vegetated (floodplain) cells by pioneer plant colonization as a function of inundation depth and duration. On the basis of the numerical framework developed by Parker et al. (2011), Asahi et al. (2013) included the combined effects of vegetation colonization, recruitment and establishment in a land accretion module. Based on the dimensionless biomass density of vegetation, varying as a function of elevation, Bertoldi et al. (2014) included the possibility of vegetation colonization and development on sediment deposits in the two-dimensional morphodynamic model BASEMENT. Kim et al. (2014) defined the biomass of pioneer vegetation, M_i , within an invasion area as the differences in ordinary and averaged water levels of the seed dispersal season, see Figure 4.9 and Equation 4.1.

$$M_i = \left(1 - \frac{z}{z_0}\right) M_{i0} + M_{i0\min} \quad (4.1)$$

in which z is the relative height from the ordinary water stage, z_0 is the relative height of the water level of the seed dispersal season from the ordinary water stage, M_{i0} is the initial biomass at the water edge of the ordinary water stage and $M_{i0\min}$ is the initial biomass at $z=z_0$, respectively.

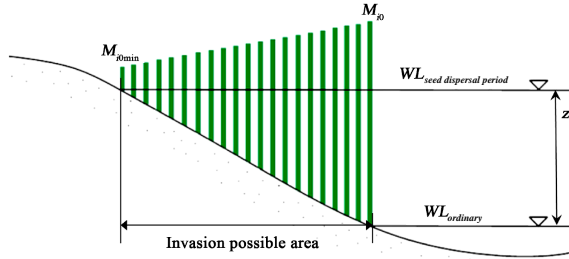


Figure 4.9: Vegetation colonization in Kim et al.(2014)'s model (source: [Kim et al., 2014](#)).

With the exception of few recent modelling exercises ([Bertoldi et al. \(2014\)](#) and [van Oorschot et al. \(2016\)](#)), the approaches that have been included vegetation colonization in morphological models have the limitation of assuming that the properties of the pioneer plants remain constant with time.

4.2.2. PLANT GROWTH MODELLING

TEMPERATURE-DEPENDENT vegetation growth rates have been obtained from the development of certain crops and their relative changes during farming periods, leaving these estimations only applicable to specific crops and seasons ([Omanga et al., 1995, 1996](#); [Craufurd et al., 1998](#); [Yan et al., 1996](#); [Yan and Wallace, 1998](#); [Yin et al., 1995, 1996](#); [Yin and Kropff, 1996](#); [Yan and Hunt, 1999](#); [van der Heide et al., 2006](#)), leaving these estimations only applicable to specific crops and seasons. Without considering hydrological fluxes, some models have been proposed to analyse the growth of trees in forests. One of the first works related to tree growth is the model by [Botkin et al. \(1972\)](#), proposing species-specific formulas for recruitment, growth, and mortality. The long-term growth of even-aged forests has been modelled by considering self-thinning rules, normally used to model vegetation succession (e.g. [Smith and Hann, 1986](#); [Tang et al., 1994](#); [Meng et al., 1997](#); [Vanclay, 2009](#); [Li et al., 2011](#)), see section 4.2.3. Mangrove forests growth and development have been related to ecological variables as salinity ([Chen and Twilley, 1998](#)) or light availability ([Berger and Hildenbrandt, 2000](#)).

Among the few models that include river disturbances on vegetation growth models, [Pearlstone et al. \(1985\)](#) combined flood duration and water level estimations from

stage-discharge relationships with the ecological model FORFLO (Forest Floodplain Succession Model) [Odum \(1983\)](#) into a mathematical model estimating the change in trees diameter as

$$\frac{dD}{dt} = \frac{1 - DH/D_{\max} H_{\max}}{274 + 3b_2D - 4b_3D^2} \cdot p \quad (4.2)$$

where D is the tree diameter at breast, H is the tree height, D_{\max} and H_{\max} are the maximum diameter and height (in cm), t is time (years), p is a site coefficient (that depends on stand density, temperature, shading tolerance and the water table position), and G , b_2 , and b_3 are species-specific growth rate parameters.

Attempting to account for the stochastic nature of plant growth, [Lytle and Merritt \(2004\)](#) described cottonwood development considering drought and flooding seasons. [Perucca et al. \(2006, 2007\)](#) modelled spatially-variable vegetation properties in terms of biomass density by combining meander dynamics (using the shallow water equations and erosion-deposition processes) with the stochastic model of local riparian vegetation developed by [Camporeale and Ridolfi \(2006a\)](#). This is based on vegetation cover variability in cross-sectional direction, assuming that vegetation properties remain constant with time (see [Figure 4.10](#)). By means of a logistic law, the cellular-automata model by [Ye et al. \(2013\)](#) considered vegetation growth and the response of growth rates to floods and droughts. However, this model does not consider morphological evolution.

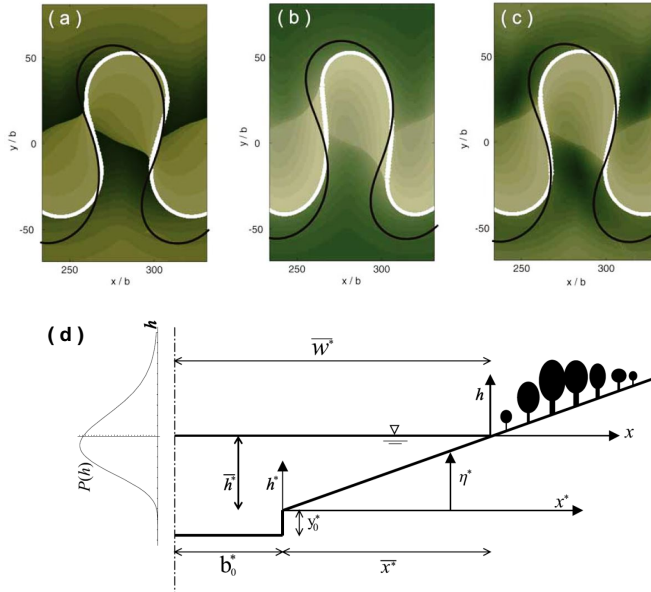


Figure 4.10: River planforms and corresponding vegetation patterns for three (a to c) biomass transversal distributions ([Perucca et al., 2007](#)) considering the Camporeale and Ridolfi's (2006) model shown schematically in (d).

Only a few attempts to include vegetation growth in morphodynamic models are available. [Takebayashi et al. \(2006\)](#) inserted a density-based plant growth rate (see Figure 4.11) in a morphodynamic model for a braided channel in order to analyse the effects of unsteady flow conditions and the presence of vegetation on channel morphology. According to them, the vegetation density, λ_v , is given by

$$\lambda_v = \lambda_{v \max} \left(\frac{t_d}{T_f} \right) \quad (4.3)$$

where $\lambda_{v \max}$ is the maximum vegetation density, t_d is the accumulated time that the bed is dry and T_f is the time wherein the relevant region is filled with vegetation.

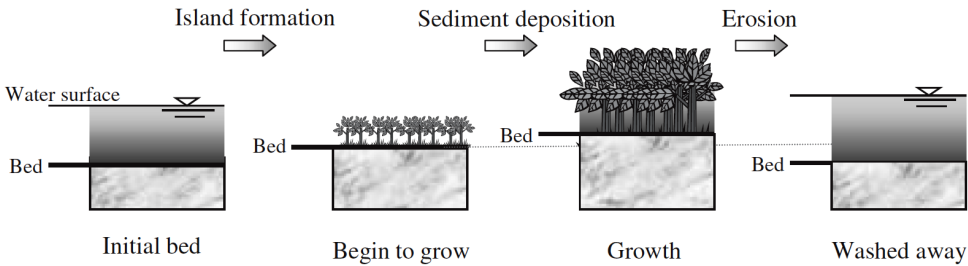


Figure 4.11: Vegetation model considering linear vegetation growth by [Takebayashi et al. \(2006\)](#)'s model (source: [Takebayashi et al., 2006](#)).

[Ye \(2012\)](#) included a diffusive logistic growth (DLG) model in the Delft3D code, which is a two dimensional extension of Fisher's equation ([Fisher, 1937](#); [Holmes et al., 1994](#)). The DLG model has two components: logistic population growth and Brownian random dispersal. The partial differential equation that describes the vegetation dynamics and spatial spread is given by

$$\frac{dP_i}{dt} = r_i P_i \left(1 - \frac{P_i}{K_i} \right) + D_{veg,i} \left(\frac{\partial^2 P_i}{\partial x^2} + \frac{\partial^2 P_i}{\partial y^2} \right) \quad (4.4)$$

where t is the time; r_i the growth/mortality rate, K_i the carrying capacity and D_{veg} the diffusion coefficient of the population, P_i , i ; and x and y represent the spatial coordinates. The properties obtained by the DLG model are linked in [Ye's \(2012\)](#) approach to a physics-based flow resistance estimator that calculates flow resistance and bed-shear stresses for vegetated beds represented as rigid cylinders by [Baptist \(2005\)](#). This method has shown good agreement with laboratory data for both emergent and submerged plants ([Vargas-Luna et al., 2015b](#), reported in Chapter 5). The results of reproducing the spatial patterns of vegetation in a semi-closed artificial inland lake, Lake Veluwe in the northeast side of Amsterdam, obtained with this model are presented in Figure 4.12. [van Oorschot et al. \(2016\)](#) compared the differences between using static vegetation properties and logarithmic growth functions to reproduce riparian tree development. They highlighted the relevance of vegetation dynamics in reproducing the vegetation patterns observed in the field, see Figure 4.13.

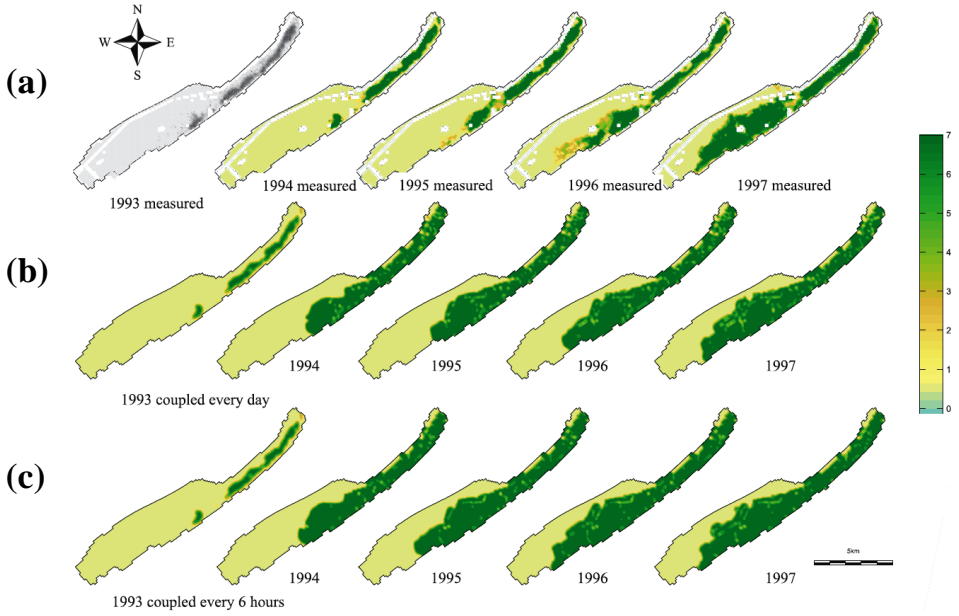


Figure 4.12: *Chara aspera* population densities from 1993 to 1997: (a) measured, (b) simulated with a daily coupling, and (c) simulated with a coupling of 6 hours. Population density is classified from low to high into Class 0 to Class 7. Adapted from Ye (2012).

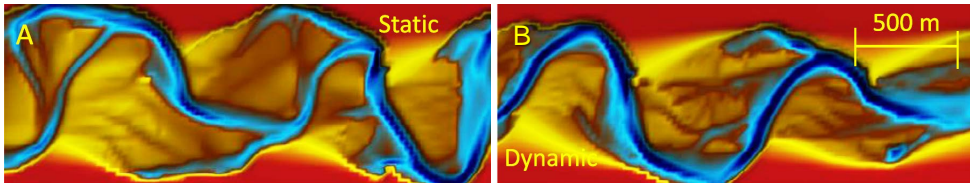


Figure 4.13: Differences in river planform obtained by using vegetation with (a) static characteristics, and (b) dynamic characteristics. Adapted from: van Oorschot et al. (2016).

Kim et al. (2014) adopted an approach similar to Ye's (2012) to analyse the effects of a low-head dam removal on the downstream river vegetation and morphology. By combining the balance between primary production and respiration with a diffusion model they simulated the growth and expansion of riparian vegetation by:

$$\frac{\partial M_i}{\partial t} = Pr_i - R_i + \frac{\partial}{\partial x} \left(k_{xi} \frac{\partial M_i}{\partial x} \right) + \frac{\partial}{\partial y} \left(k_{yi} \frac{\partial M_i}{\partial y} \right) \quad (4.5)$$

where M is the biomass per unit area, Pr is the primary production, R is the respiration of the vegetation type i (grass or trees), and k_{xi} and k_{yi} are the diffusion coefficients for horizontal vegetation expansion in x and y directions, respectively. In Figure 4.14, the results obtained by Kim et al. for the Gongreung river are shown.

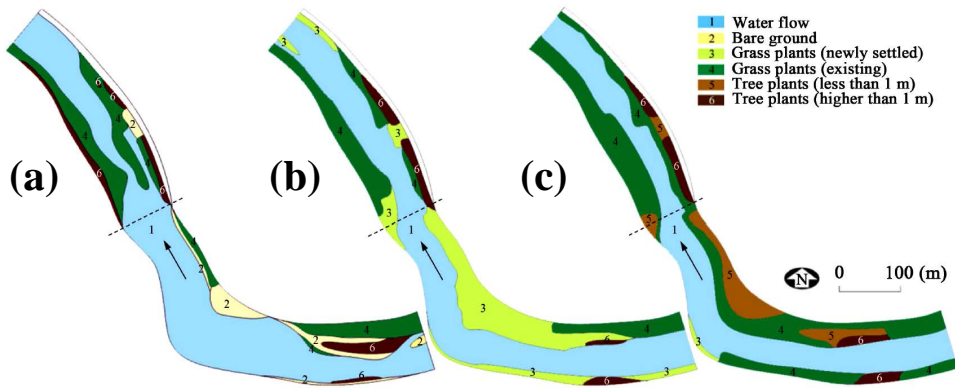


Figure 4.14: Vegetation spatial distribution modelled for the Gongreung river: (a) Initial condition, (b) 1 year after dam removal, and (c) 5 years after dam removal. Adapted from Kim et al. (2014).

Recently, (Bertoldi et al., 2014) coupled the two-dimensional morphodynamic model BASEMENT (www.basement.ethz.ch) with vegetation growth, which they described by equations based on logistic approaches. Similar attempts have been carried out in order to study spatially narrowing rivers (Perona et al., 2014) and the bank advance of meandering rivers (e.g. Zen et al., 2016). However, the effects of vegetation such as increased flow resistance and decreased bed-shear stresses were included only by considering trivial relationships or by assigning fixed values according to user-defined thresholds.

4.2.3. VEGETATION SUCCESSION MODELLING

OPERATING at a the hydrological scale and neglecting the hydrodynamic forcing, vegetation succession processes have been described by using the landscape modelling approach, which are similar to cellular-automata models, since the work of (Baker, 1989). LANDIS, a stochastic individual species model (Mladenoff, 2004) and the transition-matrix probability approach by Perry and Enright (2007), for instance, are based upon probability theory. Whereas, among the rule-based models one can mention, for instance, the Across Trophic Level System Simulation model (ATLSS) by Duke-Sylvester (2006) and the Everglades Landscape Vegetation Succession model (ELVeS) by Pearlstine et al. (2011). As the succession process in temperate floodplains widely varies according to vegetation species and is strongly influenced by the environmental setting, only observations-based descriptions (e.g. Dykaar and Wigington Jr., 2000; Cooper et al., 2003) and conceptual models for specific river systems (e.g. Richter and Richter, 2000; Corenblit et al., 2010; Cline and McAllister, 2012; Egger et al., 2015) are currently available. Thus, models that combine vegetation succession and river morphodynamics are still at their infancy.

As new plant species grow, the competition for resources such as light, water, and nutrients increases, leading to reductions in plant density. Based on a rigid-cylinder

representation of vegetation, which is described by plant diameter and density, the simultaneous increase of diameter and the associated reduction in density due to competition have been addressed by studying “self-thinning” rules. The first description of the self-thinning relationship was proposed by Reineke (1933), defining the tree density in terms of average stand diameter as:

$$m_t = a_1 D_t^{b_1} \quad (4.6)$$

where m_t is the number of trees per unit area, D_t is the average diameter of the trees, and a_1 and b_1 are constants. Reineke found that parameter a_1 is related to the tree species and that the self-thinning rate, b_1 , is equal to -1.605 for the surveyed forests. Based on the relationship between average total plant biomass / volume and number of trees per unit area, Yoda et al. (1963) proposed another model to describe the self-thinning trend:

$$V = a_2 m_t^{b_2} \quad (4.7)$$

where V is the total plant volume per unit area, and a_2 and b_2 are constants. Numerous studies have demonstrated that the exponent, b_2 , can be assumed equal to -1.5 for many plants, whereas the parameter a_2 is species-dependent. Consequently, this relation has been called, among other names, the “-3/2 power law”. However, as some contributions have shown (Enquist et al., 1998; Niklas et al., 2003), this exponent may be slightly different and, therefore, dynamic thinning trajectories (Ogawa, 2005) and species-specific thinning formulations (e.g. Mohler et al., 1978; White, 1981; Weller, 1987a,b; Newton and Smith, 1990; Ogawa, 2009) have been proposed to correct it. Figure 4.15 shows the mean plant volume and the average tree diameter as a function of tree density constructed by using Equations 4.6 and 4.7. Newton (1997) presents a review about obtaining and using these diagrams for management purposes, and Reynolds and Ford (2005) discuss about the fragility of the self-thinning generalizations.

On the basis of the self-thinning rules calibrated empirically, time varying expressions have been obtained to estimate the long-term growth of even-aged forests (e.g. Smith and Hann, 1986; Tang et al., 1994; Meng et al., 1997; Vanclay, 2009; Li et al., 2011).

4.3. INTERACTION BETWEEN PLANT POPULATIONS

DIFFERENT species of plants, cohabiting in the same area, present active interactions competing for the same resources (e.g. nutrients, space, light, etc.) and supporting one another, i.e. facilitation. Facilitation can be either beneficial for both parties (mutualism) or one species creates favourable conditions for another species indirectly (Gurnell et al., 2014). Competition and facilitation are, therefore the main processes driving vegetation succession (Tabacchi et al., 1998; Brooker et al., 2008). So, realistic vegetation dynamics models should contain the interacting plant species as state variables. However, a constant influence between plants is implicitly assumed when the parameters of population growth models are held invariant in time.

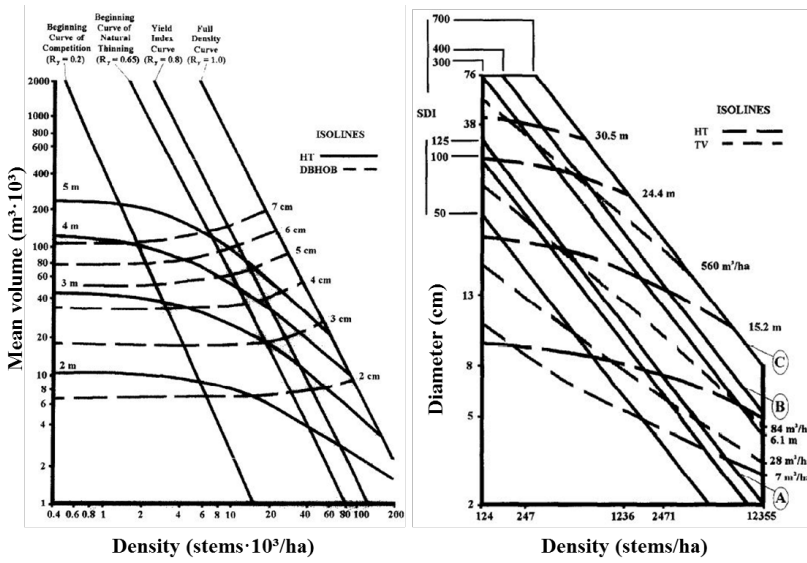


Figure 4.15: Stand-density management diagrams for pines based on Reineke's relation (Left) and on the $-3/2$ power law (Right) (Modified from [Newton, 1997](#))

Only a few models including competition and facilitation are applied in riparian zones. The stochastic hydrodynamic model with long-term vegetation dynamics proposed by [Tealdi et al. \(2013\)](#), for instance, compared two vegetation species with different growth rates, showing the relevance of the facilitation process on plants biomass spatial distribution. At a larger scale, a cellular automate containing ten different herbaceous species competing for the available resources was applied by [Ye et al. \(2013\)](#) along the Lijiang river in China. Their results show how competition can reduce vegetation growth.

The only attempt to include vegetation competition in a morphodynamic model was carried out by [Ye \(2012\)](#), assuming the interaction between two populations (i and j) to be represented by

$$\frac{dP_i}{dt} = p_{c(i-j)} [(P_i - K_i) + (P_j - K_j)] \tag{4.8}$$

where P_i and P_j are the populations density, and K_i and K_j the carrying capacities for both species i and j ; and $p_{c(i-j)}$ is a probabilistic coefficient that needs calibration.

4.4. SPATIOTEMPORAL SCALES

TEMPORAL and spatial aspects of vegetation dynamics are complex settings that play an important role in the biogeomorphological evolution of river systems. However, the unclear relation between time and space in vegetation development, the difficulty in

generalizing the observed processes, and the subjectivity in defining the units of measuring complicates a general consensus. In relation to the temporal aspects, ecological studies dealing with vegetation dynamics have commonly adopted, although arbitrarily, time scales looking at vegetation changes in the: 1) short, 2) intermediate and 3) long term (Glenn-Lewin and van der Maarel, 1992). In the short-term time-scale, vegetation processes, such as colonization and plant growth, affect the relative abundance of vegetation (quantitative change). These ‘fluctuations’ take place at the single plant level over very short time periods, causing a sensitive response to seasonal changes and climatic fluctuation (e.g. van der Maarel, 1981). Conversely, the long-term time-scales cover the domain of vegetation history, reaching periods of the order of centuries.

4

Vegetation succession is related to changes in species composition (qualitative change), operating at an intermediate time-scale, which becomes evident over decades to a century (Pidwirny, 2006). Although the segments of this global time-scale are clear, due to the arbitrary criteria considered in their definition it is difficult to distinguish the boundaries between vegetation processes, such as plant growth and succession, and their associated spatial-scales (Miles, 1979; Austin, 1981; van der Maarel et al., 1985). This can be observed for instance in the need to couple self-thinning rules with plant growth models (see section 4.2.2). Arbitrary distinctions can lead to different conclusions considering that an episode catalogued as vegetation succession for some researchers can be seen as a strong fluctuation that occurred during certain duration. The same difficulty can be found when defining the thresholds between vegetation succession and long-term changes. These limitations on defining time scales impose high uncertainties on important aspects of vegetation dynamics as, for example, calculating rates of change.

It is common to find estimations of time scales for the sequences of succession of different vegetation species in the literature. The values reported in these studies differ widely between each other, not only for the aspects mentioned here, but also because the succession process is highly-dependent on climate (Puhakka et al., 1992). An example gathered from literature is shown in Figure 4.16, providing only qualitative indications because it has been proven that the use of chronological analyses (replacing space for time) in order to study the sequences of succession can be inadequate, as is well documented by Johnson and Miyanishi (2008) and Walker et al. (2010) for instance.

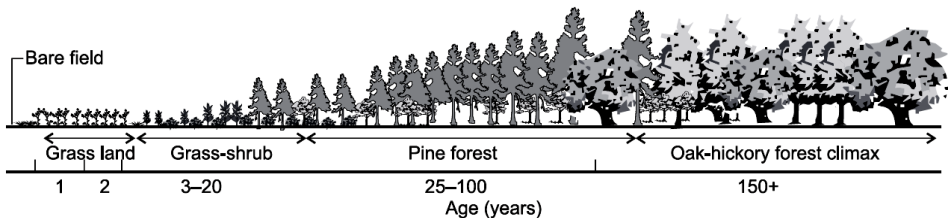


Figure 4.16: Example of the use of chronosequences for establishing succession time scales on North Carolina Piedmont, after: Goudie (1989) (modified from Johnson and Miyanishi, 2008)

Regarding the spatial aspects of vegetation dynamics, the range of scales is also wide and varied. This is especially important as currently vegetation communities are considered as a changing mosaic composed by patches of different characteristics in terms of size, age, structure, and composition, among others (Austin, 1981; Ward et al., 2002). Therefore, vegetation can be analysed at the single plant or at the community level. Moreover, vegetation dynamics can be also conceived as a regional process in which only the global landscape changes are studied. The size of the vegetation unit to consider depends on the degree of isolation of that unit towards its environment and on the level-of-integration required for the specific study (van der Maarel, 1988). Following the approach of van der Maarel (1988), spatial and temporal scales of vegetation dynamics can be integrated in the two-dimensional scheme presented in Figure 4.17.

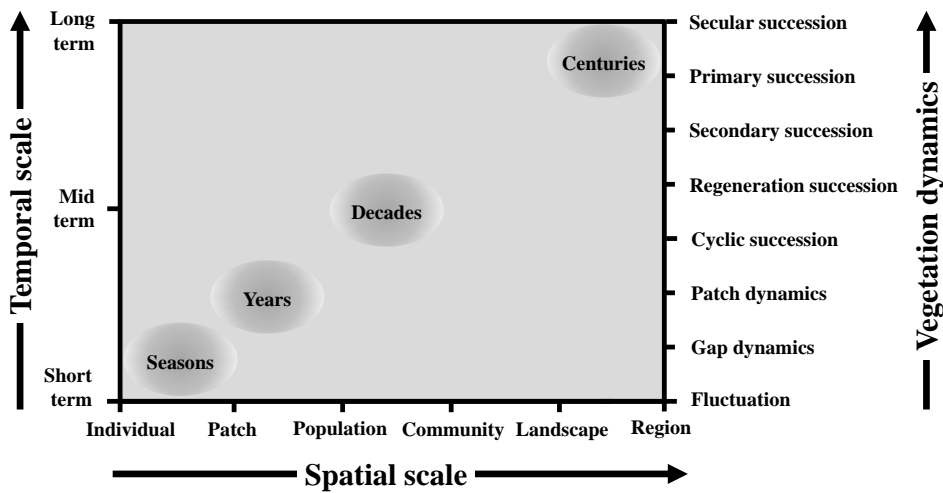


Figure 4.17: Two-dimensional scheme of spatiotemporal scales of vegetation dynamics

Due to the overlaps between plant growth and the succession processes, which increases the complexity of distinguishing their spatiotemporal scales, boundaries and thresholds, it is difficult to include vegetation dynamics in morphodynamic models. Therefore, it is important to understand and describe the mechanisms behind these interactions and their feedbacks to start filling the current knowledge gaps in this matter.

4.5. DISCUSSION

ALTHOUGH there is an increasing recognition of the multiple interactions between vegetation dynamics and river processes, much research is still needed in this topic. The linkages are well recognized, but, as presented in this chapter, the quantification of the feedbacks between flow and sediment fluxes and vegetation dynamics is still poorly understood. In addition to this, the effects of the interaction between the different spatiotemporal time scales of the biotic and abiotic processes are still unclear. Therefore,

multidisciplinary approaches are necessary to reveal the functioning of the complex processes occurring at fluvial systems, and to build up models encapsulating the main effects at the appropriate spatial and temporal scales.

Improvements in predicting the morphological evolution of river systems require including in morphodynamic models process-based descriptions of vegetation dynamics, such as dispersal, adaptation, establishment, growth and succession, among others. Understanding the effect of species interactions and their functional traits for prediction of invasion are important processes that also require the attention of researchers in biogeomorphological approaches.

It is also of high importance to understand better the influence of seasonal variations and the possible response to changes in climate, reducing the uncertainties and associated risks to people and the existent infrastructure.

5

MODELS PREDICTING THE EFFECTS OF VEGETATION ON FLOW AND SEDIMENT FLUXES

*“In nature, nothing is perfect and everything is perfect.
Trees can be contorted, bent in weird ways, and they’re still beautiful.”*

Alice Walker

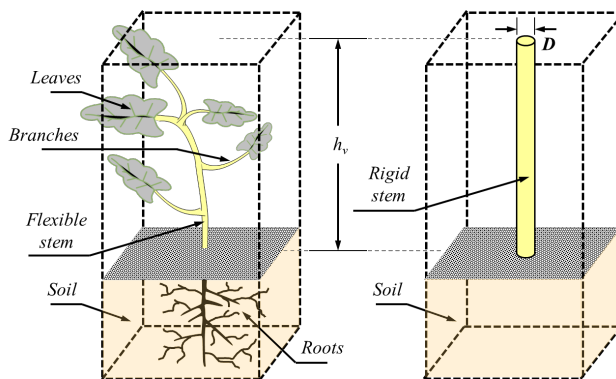


Figure 5.1: Scheme of the geometric properties for real vegetation (left) rigid-cylinder analogy (right).

The performance of a large number of models on flow resistance, vegetation drag, vertical velocity profiles and bed-shear stresses in vegetated channels is analysed.

This chapter has been published by the author in *Earth Surf. Proc. Land.* **40**(2): 157-176, doi:10.1002/esp.3633 (Vargas-Luna et al., 2015b). Only minor changes have been performed for formatting purposes.

5.1. INTRODUCTION

5.1.1. OUTLINE

COLONISATION and growth of vegetation on river banks and floodplains is controlled by the ecological, hydrological and geomorphological settings of these areas. Once established, by increasing the local hydraulic roughness, vegetation reduces the flow velocity and the bed-shear stress (e.g. Tsujimoto, 1999; Bennett et al., 2008), promoting local sedimentation (Wu and He, 2009; Nepf, 2012b,a). Moreover, vegetation cover protects the soil and roots increase the soil strength against erosion. As a result, plants act as ecosystem engineers, since they create the conditions that favour the survival and establishment of new vegetation (Bertoldi et al., 2011; Gurnell et al., 2006; Gurnell, 2012); this makes vegetation processes an important component of the dynamics of river channels. For instance, vegetation growth on bars is the key factor for the creation of new floodplain (Parker et al., 2011; Asahi et al., 2013). This process, known as "bank accretion", is of basic importance for the morphological changes of river channels, in particular for the tendency of rivers towards braiding or meandering. The role of vegetation in reducing the braiding degree of rivers has been observed in laboratory experiments (e.g. Gran and Paola, 2001; Braudrick et al., 2009; Tal and Paola, 2007, 2010), numerical modelling (Murray and Paola, 2003; Camporeale and Ridolfi, 2006b; Perucca et al., 2007; Perona et al., 2009; Crosato and Samir Saleh, 2011) and real rivers (e.g. Ward et al., 2000; Beschta and Ripple, 2006; Hooke, 2007). It is therefore important to consider the effects of vegetation in numerical models simulating the morphological changes of alluvial rivers. In particular, including the effects of vegetation might be essential to simulate the river planimetric changes (e.g. Villada Arroyave and Crosato, 2010; Camporeale et al., 2013) and to fully understand past river conditions (e.g. Montes Arboleda et al., 2010).

This paper provides an overview of the state of the art in modelling the effects of vegetation on water flow and bed material load (capacity-limited sediment transport) and identifies the most important knowledge gaps in this field. The work focuses on the assessment of performance and applicability ranges of several existing models. This procedure is done by comparing their predictions with a vast dataset. The data, gathered from the literature, comprise 743 laboratory tests for artificial vegetation and 279 (including field investigations) for real vegetation. The sources are listed in Table 5.1 (artificial plants) and Table 5.2 (real plants).

A number of previous studies already compared formulae describing the flow in vegetated channels using data from the literature (e.g. Huthoff and Augustijn, 2006; Augustijn et al., 2008, 2011; Galema, 2009; Poggi et al., 2009; Cheng, 2011). However, these compilations combined artificial and real plants, considered only submerged vegetation and did not include sediment transport. Instead, we distinguish artificial from real vegetation and consider both submerged and emergent conditions. For artificial vegetation, we also distinguish flexible from rigid plants. We classify real plants according to type and foliage: aquatic plants, grass and shrubs. Aquatic plants correspond to species permanently under water that are found in river channels. Grass and shrubs are found on river banks and floodplains and are not always submerged. Grass commonly exhibits high densities and is generally composed by single leafless, rigid and flexible, stems.

Shrubs comprise bushy species with many stems and leaves and are distinguished based on their foliage density (see Table 5.2).

Table 5.1: Summary of experiments and their vegetation configuration considering artificial vegetation gathered for the present study.

Authors ^a	Number of tests	T ^b	C ^c	P ^d	a^e (m^{-1})	D^f (mm)	h_v^g (mm)	Stems shape ^h
Kouwen et al. (1969)	27	F	S	S	25.0	5.0	100-2460	FS
Murota et al. (1984) ¹	8	F	S	L	0.96	0.24	47.5-60	C
Shimizu et al. (1991) ³	28	R	S	L	3.75; 10.0	1.0; 1.5	41; 46	C
Tsujimoto et al. (1991) ^{2*}	8	F	S	L	3.75	1.5	23.8-41.9	C
Tsujimoto et al. (1993) ¹	12	F	S	L	6.20	0.62	61-65	C
Dunn et al. (1996)	6	F	S	S	0.27-2.46	6.35	120	C
	12	R	S	S	0.27-2.46	6.35	70-170	C
Ikeda and Kanazawa (1996)	7	F	S	L	4.8	0.24	40-45	C
Meijer (1998a) ¹	7	F	S	L	1.45	5.7	1550-1650	C
Meijer (1998b) ¹	48	R	S	L	0.51; 2.05	8.0	450-1500	C
Stone and Shen (2002) ^{3*}	128	R	S	S	1.10-8.84	3.18-12.7	124	C
Ishikawa et al. (2003)	31	R	E	S	1.00-6.41	4.0; 6.4	200	C
Jordanova and James (2003)	9	R	E	S	6.24	5.0	21-111	C
Thompson et al. (2004)	16	R	E	S	0.10-1.58	9.5-36.1	22-58	C; R; T
Sharpe and James (2007)	17	R	E	S	1.04-3.12	10	62-234	C
Murphy et al. (2007) [*]	28	R	S	R	2.50-8.0	6.4	70-139	C
Kubrak et al. (2008) [*]	25	F	S	L	2.06-8.25	0.825	131-164	C
Velasco et al. (2008)	4	F	S	L	0.51	2.5	102-112	FS
Liu et al. (2008)	9	R	S	L; S	0.62-3.15	6.35	76	C
	9	R	E	L; S	0.62-3.15	6.35	55-74	C
Nezu and Sanjou (2008)	9	R	S	L	7.6-29.4	8.0	50	FS
Yan (2008) ³	12	R	S	L	3.0-12.0	6.0	60	C
Yang (2008) ³	2	R	S	S	2.8	2.0	35	C
	5	F	S	S	2.8	2.0	23-34	FS
Kothyari et al. (2009a)	55	R	E	S	1.08-3.06	2.0-5.0	28-61	C
Okamoto and Nezu (2010a)	28	F	S	L	7.61	8.0	30-96	FS
Cheng (2011)	23	R	S	S	1.78-18.43	3.2-8.3	100	C
Cheng and Nguyen (2011)	142	R	E	S	1.71-18.24	3.2-8.3	20-100	C
King et al. (2012)	2	R	E	R	4.0	3.1; 25.3	194	C
	26	R	S	R	1.0-4.0	3.1-25.3	194	C

^a Datasets indicated with a number, were taken from a secondary reference: ¹: from Baptist (2005); ²: from Galema (2009); and ³: from Cheng (2011). Datasets indicated with * were used to compare the mean flow velocity in the vegetation layer.

^b Vegetation Type= F: Flexible; R: Rigid.

^c Condition= E: Emergent; S: Submerged.

^d Pattern= L: Linear; R: Random; S: Staggered.

^e Plant area per unit of volume.

^f For rectangular, trapezoidal and flat strips, D is taken as stem width.

^g For flexible vegetation h_v is taken as deflected height.

^h C: Cylindrical; FS: Flat strip; R: Rectangular; T: Trapezoidal.

The work considers the effects of vegetation on flow resistance, flow velocity and bed-shear stress. It also includes the analysis of model performance in describing the vertical velocity profile with vegetated beds and comprises a trend analysis of the (apparent) drag coefficient under different hydraulic conditions and for several types of vegetation. The work ends with the assessment of the performance of the sediment transport capacity formulae by Engelund and Hansen (1967) and van Rijn (1984b) in view of extending their application to vegetated beds.

The results of this work can also be applied to tidal environments, where salt marshes and sea-grass beds significantly contribute in shaping estuarine channels and intertidal

flats (e.g. Temmerman et al., 2005, 2007; Van der Wal et al., 2008). Particularly relevant for tidal areas are the parts dealing with flow resistance, flow velocity and bed-shear stress, as well as the estimates of apparent drag coefficient, since the performed analyses deal with the effects of both emergent and submerged vegetation on water flows. In tidal systems, however, vegetated beds may be composed by fine, cohesive material and sediment is mainly transported in suspension (Temmerman et al., 2003; Lightbody and Nepf, 2006). Focusing on capacity-limited sediment transport, the results of the other part of the work are therefore applicable only to the sandy areas of these systems. Moreover, mangrove swamps (e.g. Bird, 1986; Furukawa et al., 1997; Wu et al., 2001; Anthony, 2004) and waves are not considered (e.g. Massel et al., 1999). These might become relevant for the morphodynamic behaviour of tropical and wide estuaries, respectively.

Table 5.2: Summary of measurements using real vegetation gathered for the present study.

Authors ^a	Number of tests	Type of vegetation	Foliage ^b	Location ^c	Condition ^d
Ree and Crow (1977) ¹	24	Grass, Shrubs	NL; LL	F	E
	31				S
Turner and Chanmeesri (1984)	17	Wheat	NL	L	E
Hall and Freeman (1994)	12	Bulrush	NL	L	E
Meijer and van Velzen (1999)	2	Reeds	NL	L	E
Freeman et al. (2000)	37	Shrubs	NL; HL	L	E
	50				S
Wilson and Horritt (2002) [*]	20	Grass	NL	L	S
Järvelä (2003)	12	Wheat and Sedges	NL	L	S
James et al. (2004)	8	Reeds	NL	L	E
Armanini et al. (2005) [*]	4	Willows	NL	L	E
	16		LL	L	E; S
Velasco et al. (2008)	9	Barley	NL	L	S
Nikora et al. (2008)	1	Aquatic	-	F	E
	24				S
Righetti (2008)	2	Willows	LL	L	E
	4				S
King et al. (2012)	2	Aquatic	-	L	E
	4				S

^a ¹: Only the experiments that include a clear definition of vegetation density from this study are considered (series J, K and L); Datasets indicated with ^{*} were used only for the drag coefficient analysis.

^b NL: No leaves; LL: Low concentration of leaves, and HL: High concentration of leaves.

^c F: Field; L: Laboratory.

^d E: Emergent; S: Submerged.

5.1.2. THEORETICAL BACKGROUND

PLANTS have different size and shape according to species, growth stage and environmental conditions. Moreover, each plant has an almost unique combination of height, stem diameter and stiffness, foliage and other properties. Nevertheless, it is commonly accepted to represent vegetation as a collection of uniformly distributed identical stems, assumed as cylindrical (Figure 5.1).

Plants are generally described by a characteristic diameter, D , and height, h_v , with an average distance between elements, s (Figure 5.2). The surface density of stems, m , is defined as the number of stems, N , per unit bed surface area. The surface density of vegetation is often represented by the following parameter:

$$\lambda = \frac{m\pi D^2}{4} \quad (5.1)$$

as well as by the projected plant area per volume (Nepf, 2012b,a):

$$a = mD \quad (5.2)$$

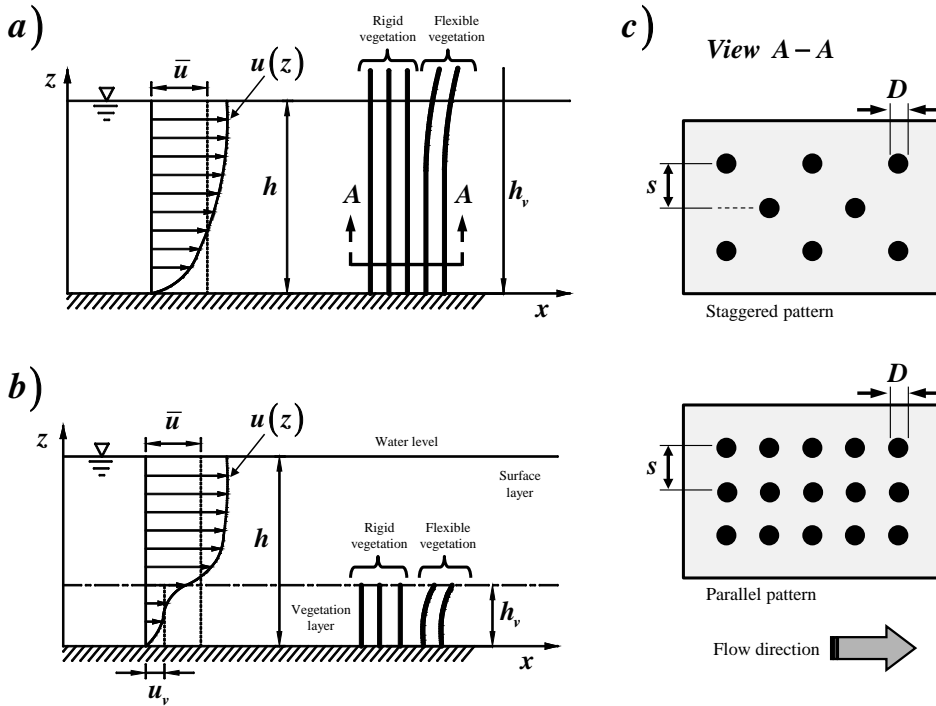


Figure 5.2: Main characteristics of rigid and flexible vegetation in open channels. Left: side view of emergent vegetation (above) and submerged vegetation (below) [Adapted from: Wu and He (2009)]. Right: plan view of staggered and parallel patterns.

The hydraulic resistance of vegetated beds is described by empirical equations or by either (semi-)empirical or physics-based models (Galema, 2009). The physical background of these models is based on specific conditions for vegetation that range from rigid to flexible stems, and from submerged to emergent (see Figures 5.2a and 5.2b). The parameters used have been mostly obtained from laboratory experiments for specific hydrodynamic conditions and types of vegetation (from artificial to real), leaving questions on their applicability ranges. For instance, in the laboratory, artificial and real canopies are often spatially distributed with parallel (called linear by some authors) or staggered patterns (Figure 5.2c), which are not easily found in nature.

Most existing models are based on the rigid-cylinder analogy, whereas only a few address flexible plants (e.g. Dijkstra and Uittenbogaard, 2010). The models predicting the

flow resistance (resistance predictors) based on the rigid-cylinder analogy consider either submerged or emergent vegetation or both. Petryk and Bosmajian (1975), Ishikawa et al. (2003), James et al. (2004) and Hoffmann (2004) consider only emergent vegetation. Klopstra et al. (1997), Van Velzen et al. (2003), Huthoff (2007) and Yang and Choi (2010), among others, consider only submerged vegetation. Stone and Shen (2002), Baptist (2005) and Cheng (2011) consider both emergent and submerged vegetation (models described in Appendix A).

In-stream vegetation, composed mainly by macrophytes, is submerged most of the time, whereas emergent vegetation is the most common in floodplain areas. Instead, vegetation on tidal marshes and recently-formed sediment deposits, such as river bars, frequently change from emergent to submerged. In such cases, the model used to estimate the flow resistance should consider both conditions. This situation means that only a limited number of models are available for the description of the bank accretion process and estuarine morphodynamics. After the pioneer work performed by Schlichting (1936), a common way to analyse the flow resistance in vegetated channels splits the total shear stress into bed-shear stress, τ_{bv} , and shear stress due to vegetation (or vegetation drag), τ_v , by assuming a linear superposition:

$$\tau = \rho g R_h i_b = \tau_{bv} + \tau_v \quad (5.3)$$

where ρ is the fluid density, g is the acceleration due to gravity, R_h is the hydraulic radius, and i_b is the channel slope.

Raupach (1992) proposed an analytical approach to assess the ratio between the bed-shear stress and the total shear stress, τ_{bv}/τ . Originally designed for aeolian processes, the method has been applied to vegetated channels by, for example, Thompson et al. (2004) and Baptist (2005).

For the assessment of the bed-shear stress, τ_{bv} , the methods by Barfield et al. (1979), Stone and Shen (2002) and Baptist (2005) consider both emergent and submerged vegetation. Other methods are only applicable to emergent plants (e.g. Ishikawa et al., 2003; Kothyari et al., 2009a).

For the assessment of the vegetation drag, τ_v , Järvelä (2004) expresses the drag exerted by emergent plants as a friction factor using the leaf area index (LAI), defined as the ratio of the one-sided leaf area to the ground area. Applications showed that this formulation provides good estimates (Jalonen et al., 2013; Västilä et al., 2013), but more efforts in parametrizing the species-dependent coefficients of this methodology are needed.

The drag exerted by vegetation has been commonly included in flow resistance predictors by means of the drag force approach, in which the drag force per unit bed area due to vegetation is expressed as:

$$\tau_v = \frac{1}{2} \rho C_D a h_v u_v^2 \quad (5.4)$$

where C_D is the apparent drag coefficient and u_v the mean flow velocity in the vegetation layer. Note that for emergent vegetation $u_v = \bar{u}$, see Figure 5.2a. C_D is here defined as "apparent drag coefficient" because it is derived for a set of hydraulic parameters which may not represent the physics of the flow around plant stems (Hygelund and Manga, 2003).

The flexibility of real plants and the presence of foliage considerably affect the apparent drag coefficient and hence the assessment of the flow resistance (Freeman et al., 2000; Järvelä, 2004; Jordanova et al., 2006; Folkard, 2011; Wunder et al., 2011; Aberle and Järvelä, 2013; Västilä et al., 2013). Selecting the value of the apparent drag coefficient from the literature is complicated even further by a number of factors (Cheng and Nguyen, 2011). The most important one is that the measured values are not comparable; this is due to the different experimental set-ups, techniques and equipment used. Additionally, only a few studies considered real plants, so the application of the results to real cases is difficult. Finally, there is no agreement in the way the results are presented. For instance Wu et al. (1999), Armanini et al. (2005) and Wilson (2007), among others, provide the parameter aC_D instead of C_D . Sand-Jensen (2003), O'Hare et al. (2007) and Wunder et al. (2011) present the apparent drag coefficient as a function of flow velocity, others as a function of the Reynolds number. But, more importantly, the definition of the Reynolds number is not unique. For instance, some authors compute it using the inundated depth of vegetation and the mean flow velocity (e.g. Wu et al., 1999; Wilson, 2007), whereas others consider other vegetation-related length scales, such as stem thickness or diameter, together with the mean velocity through vegetation (e.g. Tanino and Nepf, 2008; Kothyari et al., 2009b; Cheng and Nguyen, 2011) or the mean flow velocity (e.g. Wilson and Horritt, 2002; Armanini et al., 2005). Although previous studies have shown that the apparent drag coefficient is a function of the Reynolds number, in practical applications this coefficient is normally assumed as constant. Considering the importance of an overview, we have put together the measured values of vegetation drag coefficients reported in the literature, showing its trends according to the type of vegetation.

The vertical velocity profile is significantly affected by the presence of vegetation. A precise description is necessary for the understanding of the flow-sediment interaction (Hu et al., 2013). For emergent vegetation, the shape of the vertical velocity profile is related to the density and the vertical distribution of foliage (Aberle and Järvelä, 2013). For submerged vegetation, the vertical velocity profile mainly depends on the density and flexibility of the plants and on their degree of submergence, represented by the relation between water depth and vegetation height, h/h_v (Nepf, 2012b,a). According to vegetation and flow properties, the vertical velocity profile presents several vertical zones that for convenience are usually treated separately. However, most of them require a layer-thickness pre-definition or a calibration of length-scale related parameters (e.g. Huai et al., 2009; Hu et al., 2013).

The presence of vegetation decreases the local sediment transport rates substantially (Prosser et al., 1995; Ishikawa et al., 2003). This reduction is associated with: the decrease of flow velocity and shear stress at the bed due to the local increase of the hydraulic resistance (Bennett et al., 2008) and the momentum absorbed by dense vegetation, resulting

in decreased turbulence and sediment entrainment (López and García, 1998; Liu et al., 2008; Nezu and Sanjou, 2008; Neary et al., 2012). Instead, resuspension occurs within sparse vegetation (Yager and Schmeeckle, 2013). Only a few experimental studies carried out direct sediment transport measurements in vegetated channels and field data are scarce (with a few exceptions: e.g. Temmerman et al., 2003; Lightbody and Nepf, 2006). Li and Shen (1973) described the effects of the spatial distribution of emergent vegetation on flow velocity and sediment transport. Other studies linked bed-material load measurements to numerical modelling (e.g. Okabe et al., 1997; Watanabe et al., 2002) and to estimations by sediment transport capacity formulae (Jordanova and James, 2003; Wu and He, 2009; Kothyari et al., 2009a). For submerged vegetation, López and García (1998) included measurements and modelling of suspended sediment transport. However, due to scarcity of data on the effects of vegetation on suspended sediment transport, this work examines only bed-material load.

Many formulae have been designed for the assessment of the sediment transport capacity in non-vegetated streams (e.g. Meyer-Peter and Müller, 1948; Engelund and Hansen, 1967; van Rijn, 1984a; Huang, 2010), but only a few formulae were derived for vegetated channels and most of them are only applicable within a certain flow regime, degree of submergence and canopy properties (Ashida and Michiue, 1972; Li and Shen, 1973; Ishikawa et al., 2003; Jordanova and James, 2003; Kothyari et al., 2009a). Direct measurements from a laboratory study with emergent plants have shown that the bed load transport is affected not only by the vegetation density and properties, but also by the way that its presence alters the flow conditions (Yager and Schmeeckle, 2013).

Using a general sediment transport capacity formula in vegetated beds would allow estimating the morphological changes of natural rivers, including the combined effect of sediment movement on bare soil and through vegetation. With this aspect in mind, we have assessed the performance of two well-known sediment transport capacity formulae, Engelund and Hansen (1967) and van Rijn (1984b) derived for alluvial channels without vegetation, on vegetated channels.

5.2. MATERIALS AND METHODS

5.2.1. ACCURACY

To estimate and quantitatively compare the accuracy of the analysed models, we used the Root Mean Square Error (*RMSE*), and the coefficient of determination (R^2) given by Eqs. 5.5 and 5.6, respectively.

$$RMSE = \sqrt{\frac{1}{n} \sum_{i=1}^n (x_{o_i} - x_{e_i})^2} \quad (5.5)$$

$$R^2 = \frac{\left[\sum_{i=1}^n (x_{o_i} - \bar{x}_o) \cdot (x_{e_i} - \bar{x}_e) \right]^2}{\sum_{i=1}^n (x_{o_i} - \bar{x}_o)^2 \cdot \sum_{i=1}^n (x_{e_i} - \bar{x}_e)^2} \quad (5.6)$$

where x_{o_i} and x_{e_i} represent the observed and estimated values, respectively; \bar{x}_o and \bar{x}_e are their corresponding averages and n is the sample size.

5.2.2. GLOBAL FLOW RESISTANCE

WE assessed the performance of the models calculating the global flow resistance (resistance predictors) of vegetated channels by comparing their assessments with the measured data. This analysis was performed considering the Chézy equation for uniform flow:

$$\bar{u} = C_r \sqrt{hi_b} \quad (5.7)$$

where, h is the water depth and C_r is the global flow resistance coefficient for the vegetated channel, expressed as a Chézy coefficient. The global resistance predictors are listed in Table 5.3, and their mathematical description is given in the Appendix A. The models were selected based on the availability of data fulfilling the conditions for which they were designed.

Table 5.3: Summary of methods considered in the analysis carried out.

Model	Global flow resistance	Number of layers	Profile equation	Bed-shear stress
<i>Emergent vegetation</i>				
Petryk and Bosmajian (1975)	Yes	One	No	No
Raupach (1992)	No	-	-	Yes
Ishikawa et al. (2003)	Yes	One	No	Yes
James et al. (2004)	Yes	One	No	No
Hoffmann (2004)	Yes	One	No	No
Kothyari et al. (2009a)	No	-	-	Yes
<i>Submerged vegetation</i>				
Klopstra et al. (1997)	Yes	Two	Yes	No
Van Velzen et al. (2003)	Yes	Two	No	No
Huthoff (2007)	Yes	Two	No	No
Yang and Choi (2010)	Yes	Two	Yes	No
<i>Emergent and Submerged vegetation</i>				
Barfield et al. (1979)	No	-	-	Yes
Stone and Shen (2002)	Yes	Two	No	Yes
Baptist (2005)	Yes	One	No	Yes
Cheng (2011)	Yes	Two	No	No

5.2.3. VERTICAL VELOCITY PROFILES

THE vertical velocity profile and the mean velocity in the vegetated layer were analysed for the case of submerged vegetation. The assessment of model performance was carried out for the formulations which do not need any calibration of length-scale parameters: Klopstra et al. (1997) and Yang and Choi (2010), see Table 5.3. The mathematical description of these models is given in the Appendix A. Six datasets of point velocity measurements, of which characteristics are shown in Table 5.4, were used for the analysis. The models of Petryk and Bosmajian (1975), Stone and Shen (2002), Van Velzen

et al. (2003), James et al. (2004), Hoffmann (2004), Baptist (2005), Yang and Choi (2010) and Cheng (2011) allow computing the mean velocity in the vegetation layer. The accuracy of their results is compared using the statistical methods described in section 5.2.1.

Table 5.4: Experiments used for the analysis of vertical velocity profiles.

Authors	Test	Type ^a	D (m)	m (m ²)	h_v (m)	h/h_v	C_D	i_b (m/m)
Velasco et al. (2008)	T3-3	F	0.0025	205	0.110	1.87	1.20	4.00 E-04
Shimizu et al. (1991)	A31	R	0.0015	2500	0.046	2.03	1.00	3.00 E-03
Ghisalberti and Nepf (2004)	H	R	0.0064	1250	0.138	3.38	0.61	1.00 E-04
Nezu and Sanjou (2008)	A-10	R	0.0080	3676	0.050	3.00	2.25	7.77 E-04
Carollo et al. (2002)	1	Re	0.0440	31000	0.048	2.48	1.00	1.00 E-02
Tinoco Lopez (2011)	M4	Re	0.0043	500	0.250	1.48	5.88	2.00 E-05

5.2.4. BED-SHEAR STRESS

ONLY the methods by Stone and Shen (2002) and Baptist (2005) allow estimating the global flow resistance and the bed-shear stress of a vegetated channel for both emergent and submerged plants. Barfield et al. (1979) and Raupach (1992) models estimate the bed-shear stress without calculating the global flow resistance. Ishikawa et al. (2003) and Kothyari et al. (2009a) models are only applicable to emergent plants. The mathematical description of these models is given in the Appendix A. To compare the performance of all these models, the analysis considered only the data relative to artificial emergent vegetation. These are provided by four independent studies counting 111 configurations, see Table 5.5.

Table 5.5: Summary of bed-shear stress and sediment transport measurements gathered for the present study.

Authors	No. of tests	Vegetation		Flow		Sediment	
		D (mm)	a (m ⁻¹)	u (m/s)	h (mm)	D_{50} (mm)	q_t (m ² /s)
Ishikawa et al. (2003)	31	4.0; 6.4	1.00-6.41	0.23-1.14	25-114	1.8	-
Jordanova and James (2003)	9	5.0	6.24	0.15-0.18	21-111	0.45	1.89E-06-6.94E-06
Thompson et al. (2004)	16	9.5-36.1	0.10-1.58	0.39-0.78	22-58	-	-
Kothyari et al. (2009a)	55	2; 4; 5	1.08-3.06	0.34-0.94	28-61	0.60-5.90	5.00E-07-3.97E-03

5.2.5. APPARENT DRAG COEFFICIENT

FROM the gathered dataset (Tables 5.1 and 5.2), it is possible to observe that some studies included the measurement of the drag force for the assessment of the drag coefficient, C_D . These experimentally-derived values were analysed to assess the relation between (apparent) drag coefficient and type of vegetation and the variation of drag coefficient as a function of the element Reynolds number, Re_D :

$$Re_D = \frac{\bar{u}D}{\nu} \quad (5.8)$$

where \bar{u} is the mean flow velocity, ν is the kinematic viscosity, and D the characteristic plant diameter. As reported in the literature, C_D decreases as Re_D increases (e.g. Tanino and Nepf, 2008; Kothyari et al., 2009b).

5.2.6. SEDIMENT TRANSPORT

SEDIMENT transport was measured in the framework of two studies using emergent metal rods as artificial vegetation (64 tests), see Table 5.5. For this reason, it was analysed only for the emergent condition. For the prediction of sediment transport with vegetated beds, we compared the performance of the models by Barfield et al. (1979), Stone and Shen (2002) and Baptist (2005), which apply also to the case of submerged vegetation, coupled to the sediment transport capacity formulae by Engelund and Hansen (1967) and van Rijn (1984b). We estimated the global flow resistance coefficient, the mean flow velocity, and the bed-shear stress with either the models of Barfield et al., Stone and Shen or Baptist and then computed the sediment transport rate using the formulae of Engelund and Hansen and van Rijn. Finally, these estimations were compared with the measured values.

5.3. RESULTS

5.3.1. GLOBAL FLOW RESISTANCE

ARTIFICIAL VEGETATION

FOR artificial submerged vegetation, the computed values of global flow resistance, in terms of Chézy coefficient, are plotted against the measured ones in Figures 5.3a-5.3g. Table 6 lists the values of ($RMSE$) and (R^2) relative to the considered models, showing the degree of accuracy of the results. The model of Stone and Shen exhibits the lowest performance. The model by Huthoff has a low performance too, and in addition it is highly dependent on the degree of submergence, see Appendix A. The models of Klopstra et al. (1997), Van Velzen et al. (2003) and Baptist (2005) present a similar behaviour for rigid and flexible vegetation, whereas the methods proposed by Yang and Choi (2010) and Cheng (2011) have higher performance for the type of vegetation on which they based the derivation of their formulation. Thus, the method by Yang and Choi fits better the measurements relative to flexible vegetation, whereas the method of Cheng exhibits the best results for the rigid case. Despite the fact that most of considered models are based on the rigid-cylinder analogy, they work reasonably well for flexible vegetation as well, as long as the vegetation height used in the equations corresponds to its deflected height. This conclusion is in accordance to observations previously made by Baptist (2005), and Galema (2009), among others.

For artificial emergent vegetation, the computed and the measured values of global flow resistance are plotted together in Figures 5.4a-5.4g. Table 5.7 lists the values of ($RMSE$) and (R^2) relative to the considered models, showing the degree of accuracy of the results. The results show that there is no noticeable difference between the estimations made by using the models of Stone and Shen (2002), James et al. (2004), Cheng (2011)

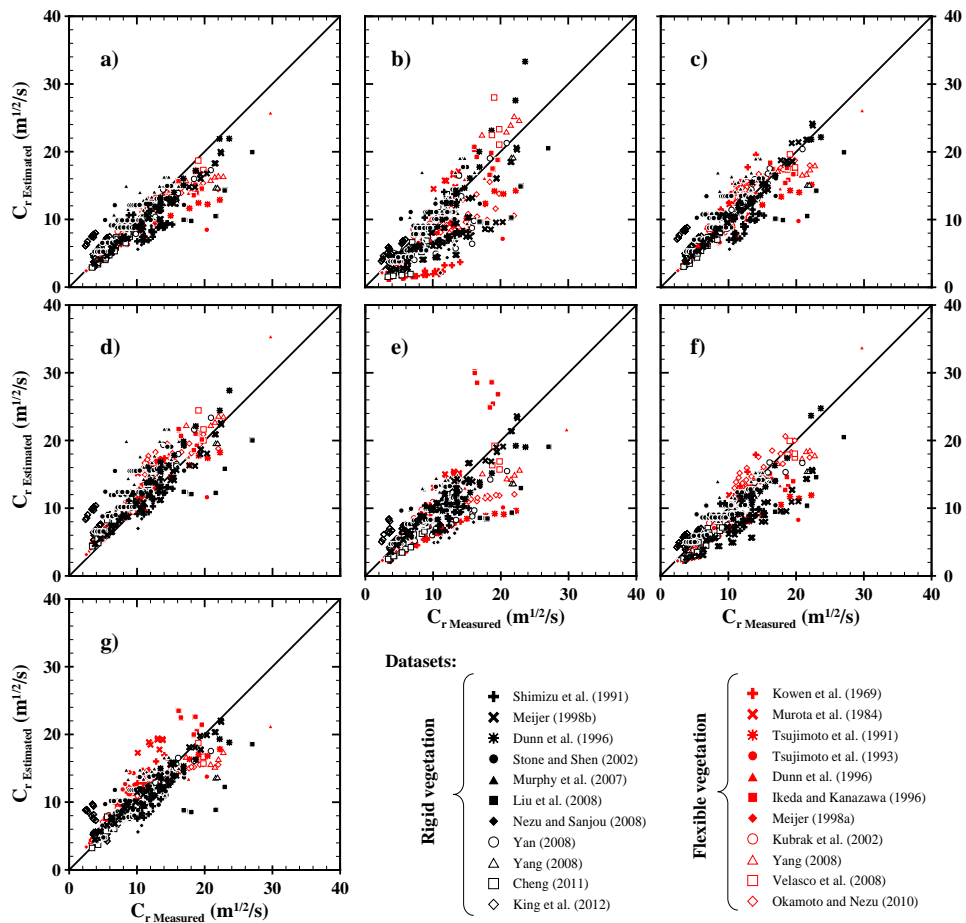


Figure 5.3: Submerged artificial vegetation: measured against estimated global flow resistance for: (a) Klopstra et al. (1997), (b) Stone and Shen (2002), (c) Van Velzen et al. (2003), (d) Baptist (2005), (e) Huthoff (2007), (f) Yang and Choi (2010), and (g) Cheng (2011)

and Petryk and Bosmajian (1975), whereas the models of Ishikawa et al. (2003) and Baptist (2005) provide a substantial improvement (Figure 5.4). This aspect is especially true for the data measured by Ishikawa et al. (2003), Thompson et al. (2004) and Cheng and Nguyen (2011). The summary presented in Table 5.7 shows that the best fit is accomplished by the model by Baptist (2005), whereas the model by Hoffmann (2004) has the lowest performance. According to the results presented in Figures 5.3 and 5.4, the methods of Klopstra et al. (1997), Van Velzen et al. (2003) and Baptist (2005) are the best-fitting formulations for submerged vegetation, whereas the models of Ishikawa et al. (2003) and Baptist (2005) present the best fit for the emergent case.

Table 5.6: Submerged artificial vegetation: statistical estimators obtained by comparing measurements with estimations.

Models	RMSE ($m^{1/2}/s$)		R^2	
	Rigid	Flexible	Rigid	Flexible
Klopstra et al. (1997)	6.49	6.93	0.71	0.85
Stone and Shen (2002)	12.21	23.89	0.59	0.66
Van Velzen et al. (2003)	6.38	5.56	0.69	0.80
Baptist (2005)	9.73	7.09	0.68	0.88
Huthoff (2007)	8.15	20.08	0.66	0.52
Yang and Choi (2010)	9.47	7.80	0.65	0.79
Cheng (2011)	6.39	9.17	0.69	0.70

Table 5.7: Emergent artificial vegetation: statistical estimators obtained by comparing measurements with estimations.

Models	RMSE ($m^{1/2}/s$)	R^2
Petryk and Bosmajian (1975)	33.92	0.82
Stone and Shen (2002)	25.75	0.81
Ishikawa et al. (2003)	13.55	0.79
James et al. (2004)	33.59	0.82
Hoffmann (2004)	92.76	0.81
Baptist (2005)	9.17	0.85
Cheng (2011)	52.79	0.80

REAL VEGETATION

FOR real vegetation, we analysed the performance of the models by Stone and Shen (2002) and Baptist (2005) for both submerged and emergent conditions, considering that these methods also allow bed-shear stress estimations. Measured and estimated values are shown in Figure 5.5. The results show that Baptist model reproduces reasonably well the global flow resistance and performs similarly for submerged and emergent conditions (Figure 5.5a), whereas the Stone and Shen method tends to overestimate the global flow resistance. In Figure 5.5, ellipses encircle some specific groups of data. Group A encloses data from experimental set-ups for which the global flow resistance is underestimated by Baptist (2005). This group mainly consists of submerged shrubs with high density of leaves (values of parameter a between 1.45 and 3.25 m^{-1}). It also includes one case corresponding to low density of leaves and relatively high degree of submergence ($a=0.04 m^{-1}, h/h_v=2.1$). Group B includes data obtained from a set of experiments (Series J – Grass type) performed by Freeman et al. (2000), for which the Baptist model overestimates the global flow resistance. Group C encloses two experimental set-ups for which the Stone and Shen model underestimates the global flow resistance (higher estimated Chézy coefficients), both with high degrees of submergence, one with low and one with high density of leaves ($a=1.20 m^{-1}, h/h_v=7.9$). Group D encloses data from experimental set-ups characterized by high values of aD , to which the Stone and Shen model is extremely sensitive. Based on these observations, it is clear that vegetation density and degree of submergence play a key role for the ranges of applicability of the selected flow resistance models. An analysis that includes these parameters is performed in the next subsection.

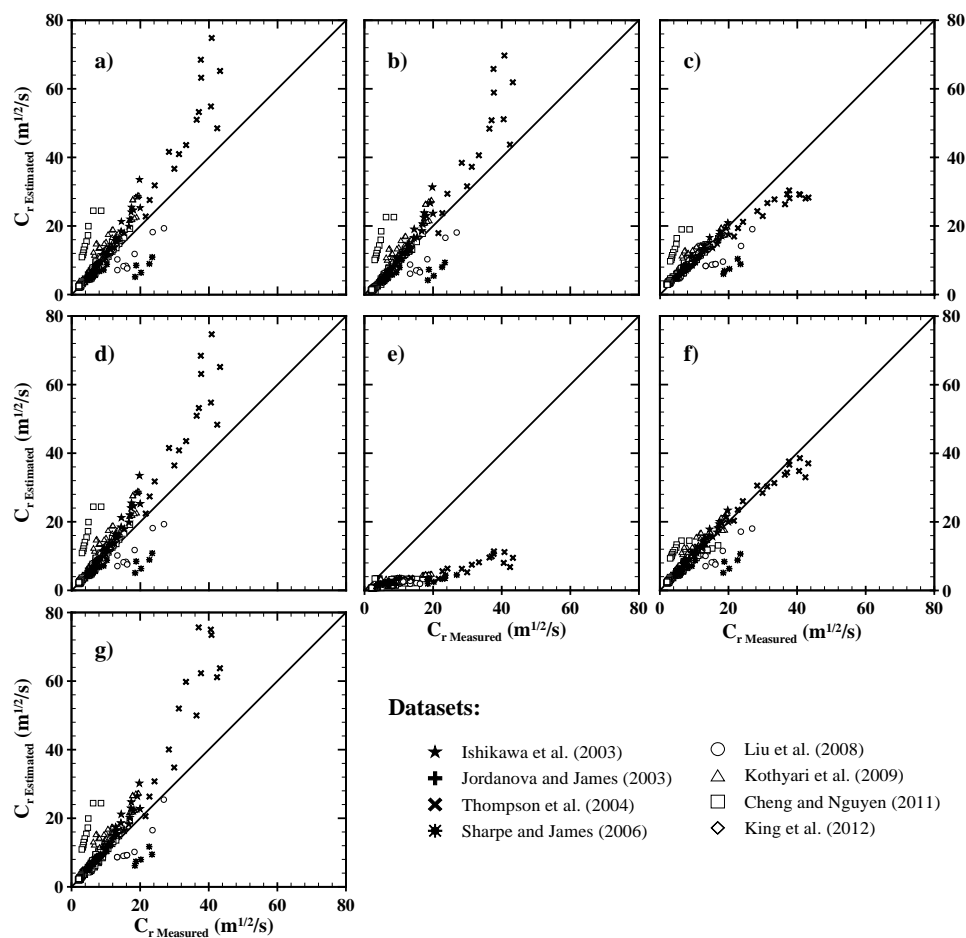


Figure 5.4: Emergent artificial vegetation: measured against estimated global flow resistance for: (a) Petryk and Bosmajian (1975), (b) Stone and Shen (2002), (c) Ishikawa et al. (2003), (d) James et al. (2004), (e) Hoffmann (2004), (f) Baptist (2005), and (g) Cheng (2011).

ROLE OF THE DEGREE OF SUBMERGENCE ON GLOBAL FLOW RESISTANCE ESTIMATIONS

THE response of the methodologies of Stone and Shen (2002) and Baptist (2005) was analysed as a function of submergence degree. For this analysis, we considered a vegetated channel with bed roughness, C_b , equal to $50 \text{ m}^{1/2}/\text{s}$, vegetation patch with drag coefficient, C_D , equal to 1.0, and characteristic diameter, D , equal to 0.004 m . Assuming two different vegetation densities (250 and 750 m^{-2} , which correspond to a plant area per unit of volume, a , of 1.0 and 3.0 m^{-1}) and two vegetation heights (0.05 and 0.25 m), we varied the water levels obtaining degrees of submergence fluctuating between 0.04 and 17.0 . The results of this analysis are shown in Figure 5.6. In this figure, it is possible to observe the influence of the canopy density and the vegetation height on the obtained global flow resistance values. For the less dense canopy (Figure 5.6a), there are no large

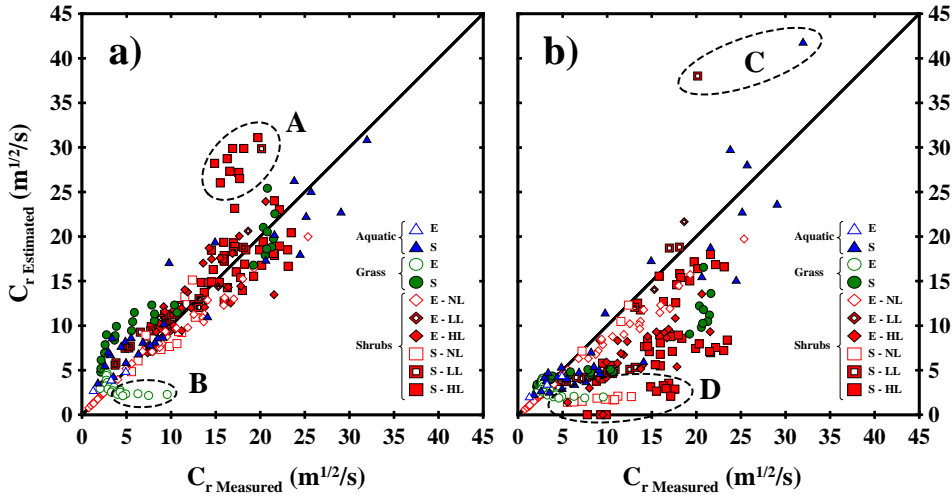


Figure 5.5: Real vegetation: measured against estimated global flow resistance for: (a) Baptist (2005), and (b) Stone and Shen (2002). The conditions considered were: *E*= Emergent; *S*= Submerged; *NL*= No leaves; *LL*= Low concentration of leaves; and *HL*= High concentration of leaves. The ellipses define groups with different characteristics with respect to vegetation properties, see the text.

differences between the estimations of the two models for tall vegetation, whereas substantial deviations are observed for the shorter plants. These deviations lead to unrealistic estimations of the global flow resistance coefficient with the Stone and Shen method (i.e. Chézy coefficient higher than the one representing the bed roughness). For denser canopies, lower deviations between the two methods are observed in case of emergent plants. The method by Stone and Shen shows high sensitivity to water level variations in case of submerged plants (see Figure 5.6b). In general, it is more sensitive to water depth variations than the Baptist method, which leads to some discrepancies in the estimations.

5.3.2. VERTICAL FLOW VELOCITY PROFILE WITH SUBMERGED VEGETATION

THE vertical velocity profiles estimated with the selected formulations and the point velocity measurements are plotted together in Figure 5.7. This figure shows that predicted velocity profiles have a good agreement with measurements only for certain combinations of vegetation properties and flow conditions. The Yang and Choi model predicts the velocity in the vegetation layer reasonable well, but not the velocity in the upper layer. This formulation performs best for the dataset of Velasco et al. (2008) (see Figure 5.7a). For the other datasets (Figures 5.7e and 5.7f), the model by Yang and Choi overestimates the flow velocity in the upper layer for dense canopies and underestimates it for the sparse ones. The higher the values of the projected plant area per volume; the higher are the deviations from the measured values (see Table 5.5 and Figure 5.7. This tendency is attributed to the parameter C_{u} , defined by Yang and Choi (see Appendix).

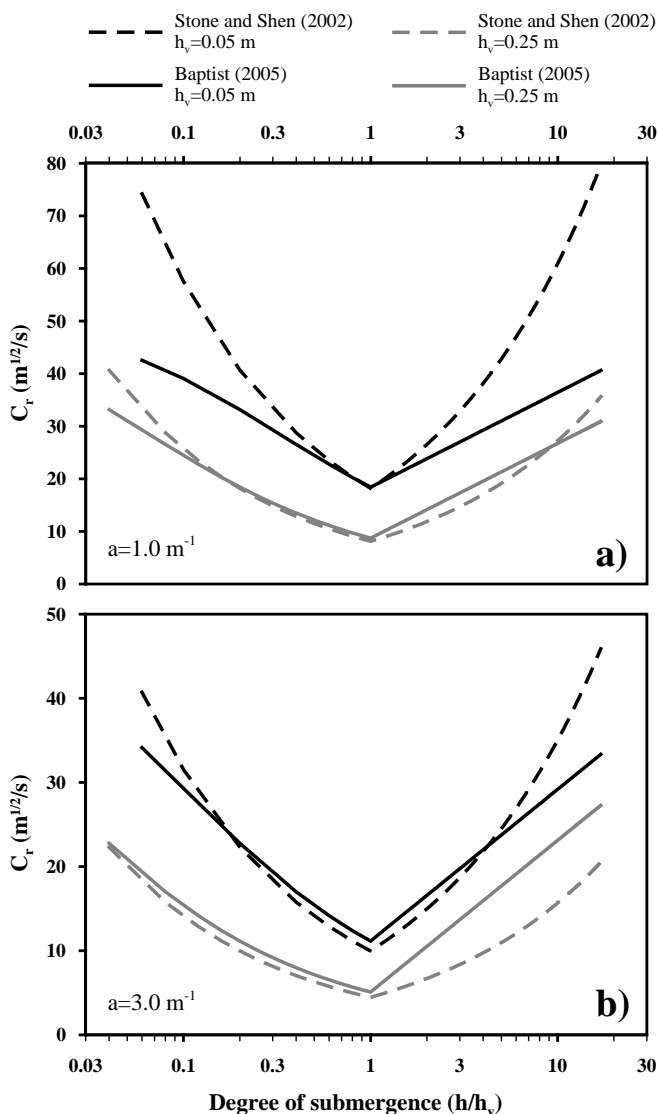


Figure 5.6: Global flow resistance coefficient as a function of the degree of submergence according to [Stone and Shen \(2002\)](#) and [Baptist \(2005\)](#) for a plant area per unit of volume, a , of (a) 1.0 m^{-1} and (b) 3.0 m^{-1} . Two heights of the vegetated layer were considered: 0.05 m and 0.25 m .

The model developed by [Klopstra et al. \(1997\)](#) provides good assessments for some combinations of flow and vegetation properties (see Figs. 5.7c and 5.7d), whereas in other cases the predicted upper-layer velocity is lower than the vegetation-layer velocity (see Figs. 5.7a, 5.7b and 5.7f). This result disagrees with both theory and laboratory observations (e.g. [Dunn et al., 1996](#); [Murphy et al., 2007](#); [Velasco et al., 2008](#)). Klopstra

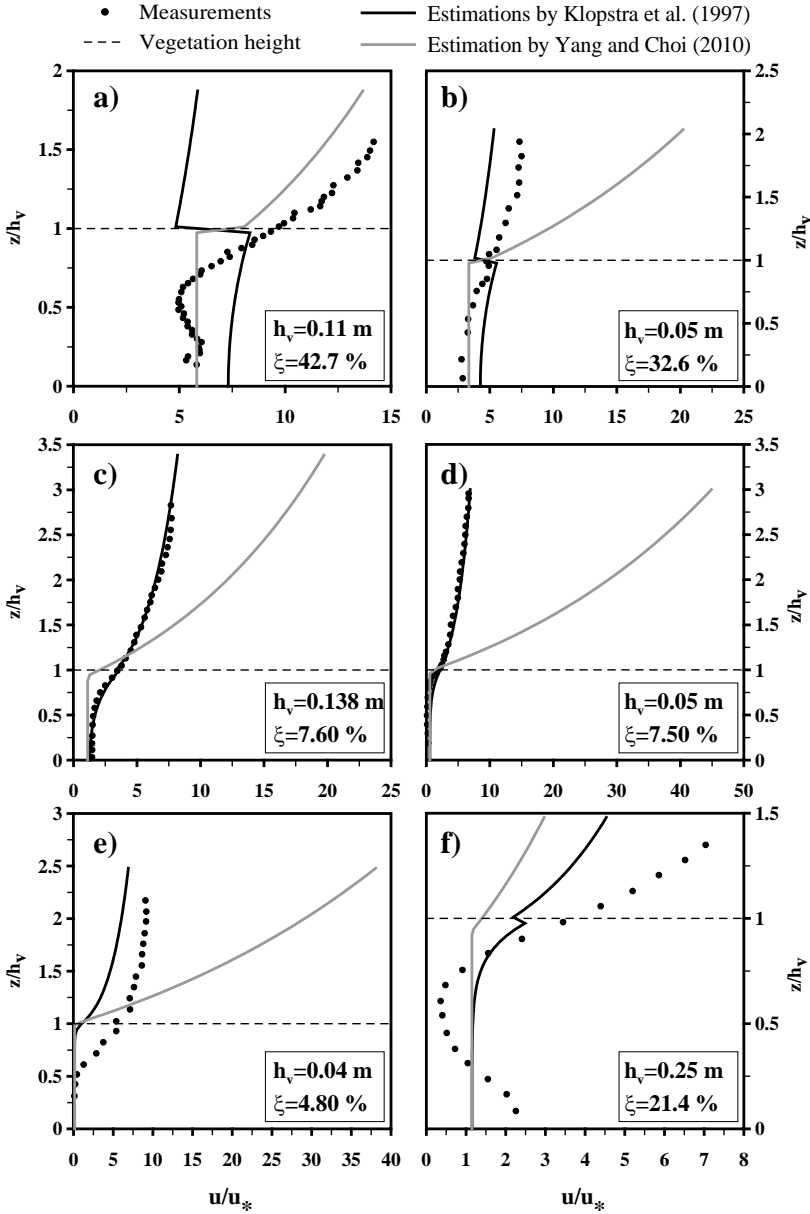


Figure 5.7: Submerged vegetation: measured against estimated vertical velocity profiles according to Klopstra et al. (1997) and Yang and Choi (2010). Datasets: (a) Velasco et al. (2008) (Test T3-3), (b) Shimizu et al. (1991) (Test A31), (c) Ghisalberti and Nepf (2004) (Test H), (d) Nezu and Sanjou (2008) (Test A-10), (e) Carollo et al. (2002) (Test 1), and (f) Tinoco Lopez (2011) (Test M4). Degree of discontinuity, ξ , defined in Eqs. 5.9, 5.10 and the Appendix A

et al. used two different equations, one for the vegetation layer and one for the upper layer, meeting at the vegetation top. However, the procedure does not guarantee that the velocity estimated at this point is the same for both equations and in fact it is possible to obtain two different values. When the difference between the two velocities is small, the velocity profile does not present irregularities, but when this difference increases the irregularities are noticeable. Based on the equations proposed by Klopstra et al. (1997), given in the appendix, is possible to formulate an equation for this degree of discontinuity, ξ , expressed as

$$\xi (\%) = \left(1 - \frac{u(h_v)_{K[Equation(A13)]}}{u(h_v)_{K[Equation(A18)]}} \right) \cdot 100 \quad (5.9)$$

where the relation between the velocities is represented by

$$\frac{u(h_v)_{K[Equation(A13)]}}{u(h_v)_{K[Equation(A18)]}} = \frac{\kappa \sqrt{\bar{u}_{P \& B}^2 + 2C_2 \text{Sinh}(Ah_v)}}{u_{*K} \ln\left(\frac{h_s}{k_p}\right)} \quad (5.10)$$

The degree of discontinuity, ξ (%), represents the deviation between the velocity estimated at the top of the vegetation layer from the velocity estimated at the same position for the upper layer. Mathematical definition of each term in Equation 5.10 is given in the Appendix. Calculated values of the discontinuity degree ξ (%) are indicated in Figure 5.7.

Based on the results, the model by Klopstra et al. performs well for values of degree of discontinuity, ξ , lower than 10% for sparse canopies, and lower than 15% for dense canopies (Figure 5.7). The degree of discontinuity proposed here and the values obtained for sparse and dense canopies could be used as a criterion of the applicability of this method. Considering that the method proposed by Van Velzen et al. (2003) for the global flow resistance derives from the velocity profile by Klopstra et al. (1997), the same considerations could be applied to the van Velzen et al. method.

Regarding the mean flow velocity in the vegetation layer, Table 5.8 lists the values of *RMSE* and R^2 describing the level of agreement between measured and values estimated by several models. It is possible to observe that the mean flow velocity prediction in this layer can be obtained equally well with formulations that assumed emergent conditions (except from the model by Hoffmann) as with the model by Cheng for the submerged case.

5.3.3. BED-SHEAR STRESS

IN Figure 5.8 computed values of the bed-shear stresses are plotted against the corresponding measured values. The model by Raupach exhibits the lowest performance (see Figure 5.8b), whereas the models of Stone and Shen (2002) and Baptist (2005) provide slightly better estimations, however, these models have the tendency to underestimate the bed-shear stress, see Figures 5.8c and 5.8e. The models by Ishikawa et al. (2003) and Kothyari et al. (2009a), applicable only to emergent vegetation, predict the measured

values quite well. The simple analogy proposed by Barfield et al. (1979) presents a good agreement with the measurements, see Figure 5.8a. All models present higher dispersion for the lowest values of the bed-shear stress; this could be related to variations in the mobility thresholds for vegetated beds (Larsen et al., 2009).

Table 5.8: Velocity in the vegetation layer: statistical estimators obtained by comparing measurements with estimations.

Model	RMSE x 10 ⁻⁴ (m/s)	R ²
<i>Submerged conditions</i>		
Stone and Shen (2002)	11.93	0.91
Van Velzen et al. (2003)	22.83	0.94
Baptist (2005)	24.18	0.94
Yang and Choi (2010)	25.93	0.94
Cheng (2011)	7.49	0.94
<i>Emergent conditions</i>		
Petryk and Bosmajian (1975)	8.67	0.92
Stone and Shen (2002)	6.32	0.91
James et al. (2004)	8.18	0.92
Hoffmann (2004)	55.68	0.89
Baptist (2005)	8.07	0.92
Cheng (2011)	10.04	0.94

Ishikawa et al. (2003) and Baptist (2005) allow computing also the ratio between bed-shear stress and total shear stress, f , which is shown as a function of the non-dimensional product, ah_v , in Figure 5.9. These two models provide similar results and responds better to high values of ah_v (dense canopies). They should be used for ah_v higher than 0.01.

The dependency of the considered methodologies on length scales (water depth or vegetation height) was analysed in Figure 5.10. In this figure, the behaviour of the ratio between the bed-shear stress and the total shear stress, is shown as a function of the degree of submergence for the values of the vegetation canopies considered in Figure 5.5. The models by Barfield et al. (1979) and Baptist (2005) have similar trends for both submerged and emergent conditions, whereas the Stone and Shen model exhibits an opposite behaviour for the submerged case. The method by Baptist shows low values of f for denser canopies and higher vegetation heights, and has a wider range of variation compared with the model of Barfield et al. (1979) for the submerged condition.

5.3.4. APPARENT DRAG COEFFICIENT

FIGURE 5.11 shows the values of the apparent drag coefficient obtained for different types of artificial and real vegetation as a function of the element Reynolds number. This figure confirms the results of previous studies. It reveals also the difficulty in obtaining general formulations describing the trends of this coefficient, which is due to the substantial difference among the different types of vegetation under similar flow conditions. As a starting point, we would like to draw the reader's attention to the values close to unity obtained with rigid artificial vegetation for both submerged Murphy et al. (2007) and emergent conditions Kothyari et al. (2009b). About the results obtained

by [Wilson and Horritt \(2002\)](#) for real grass, we can observe how the apparent drag coefficient rapidly decreases (from a value close to 1 to almost 0.05) for relatively small variations of element Reynolds number. Higher values of the apparent drag coefficient are observed for reeds and bulrushes under emergent conditions derived from the data of [Jordanova et al. \(2006\)](#), which is in agreement with other studies. For instance, [Hall and Freeman \(1994\)](#) observed values of the apparent drag coefficient up to 15 (see [James et al., 2004](#)).

Datasets:

⊕ Ishikawa et al. (2003) ● Thompson et al. (2004) ▲ Jordanova and James (2003) □ Kothiyari et al. (2009)

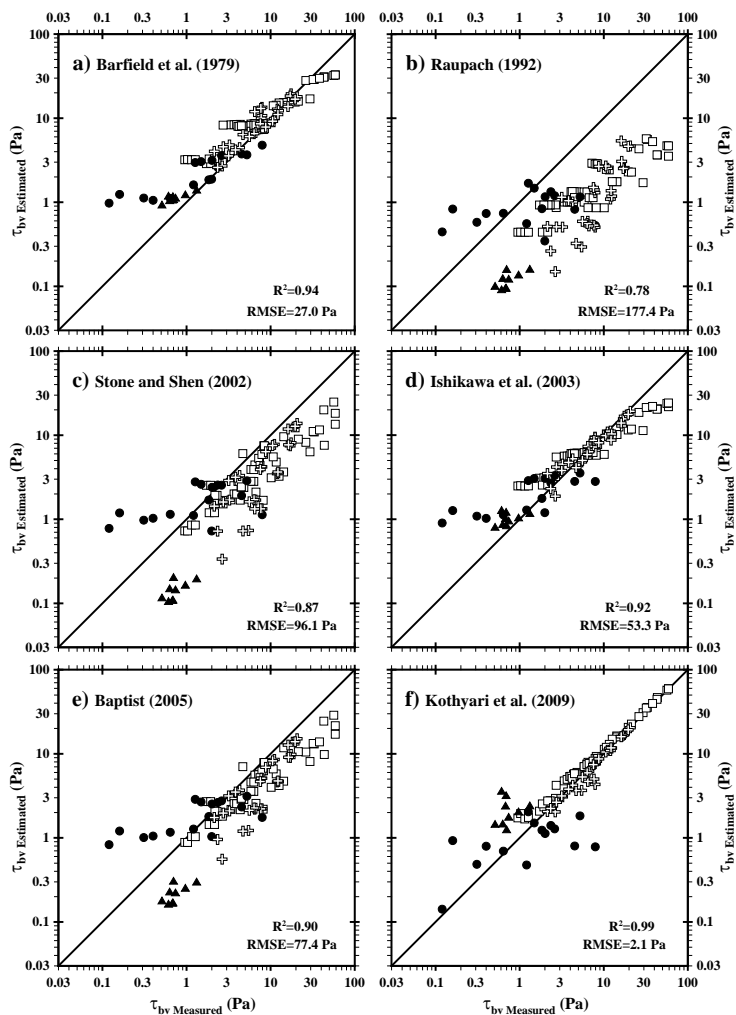


Figure 5.8: Emergent artificial vegetation: Comparison between the bed-shear stresses measured in vegetated flumes and the estimated values by (a) [Barfield et al. \(1979\)](#), (b) [Raupach \(1992\)](#), (c) [Stone and Shen \(2002\)](#), (d) [Ishikawa et al. \(2003\)](#), (e) [Baptist \(2005\)](#), and (f) [Kothiyari et al. \(2009a\)](#).

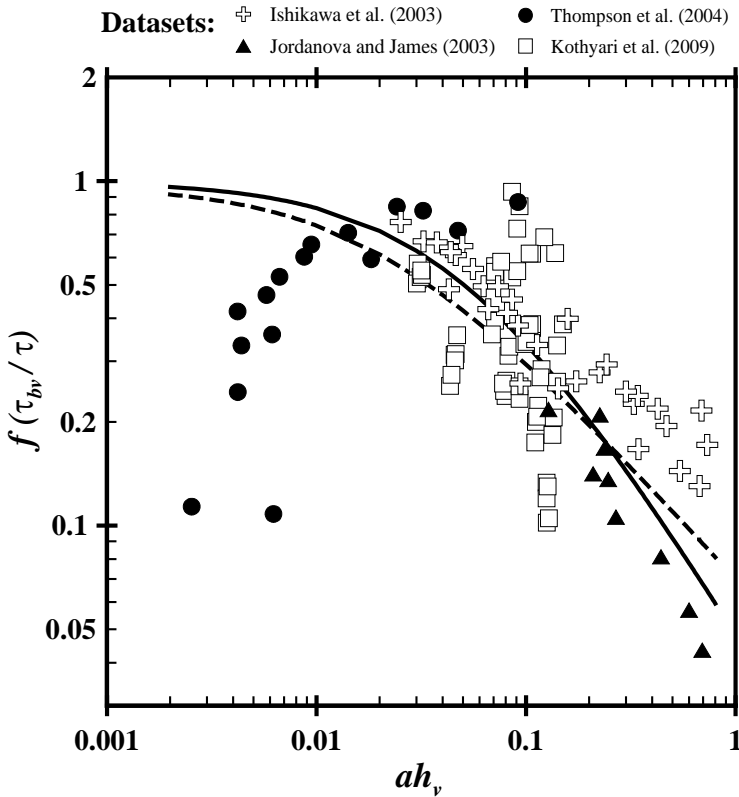


Figure 5.9: Emergent artificial vegetation: ratio between bed-shear stress and total shear stress for vegetated beds as a function of ah_v . Measured values against estimated by [Baptista \(2005\)](#) (Continuous line), and [Ishikawa et al. \(2003\)](#) (Dashed line).

From the dataset of [Armanini et al. \(2005\)](#), it is possible to see how foliage affects the drag coefficient (emergent vegetation). Armanini et al. show that if plants are defoliated the drag coefficient decreases and becomes similar to the drag coefficient of artificial vegetation. This behaviour was also observed by [James et al. \(2004\)](#) and [Jordanova et al. \(2006\)](#).

Regarding submerged bulrushes, two behaviours are observed: for low values of the element Reynolds number (lower than 10 000) the apparent drag coefficient varies between 1 and 3 (data from [Armanini et al., 2005](#)), whilst for larger element Reynolds numbers its values are found smaller than 0.30 (data from [Freeman et al., 2000](#)). Similar values were also reported by [Sand-Jensen \(2003\)](#); this shows the high reduction in the drag exerted by foliage due to reconfiguration effects for the case of real vegetation ([Statzner et al., 2006](#); [Aberle and Järvelä, 2013](#)). This reconfiguration is related to streamlining and bending exerted by real plants under flow action which decreases the projected area and drag forces ([Gosselin et al., 2010](#); [de Lange et al., 2012](#); [Dittrich et al., 2012](#); [Siniscalchi and Nikora, 2013](#); [Albayrak et al., 2014](#)).

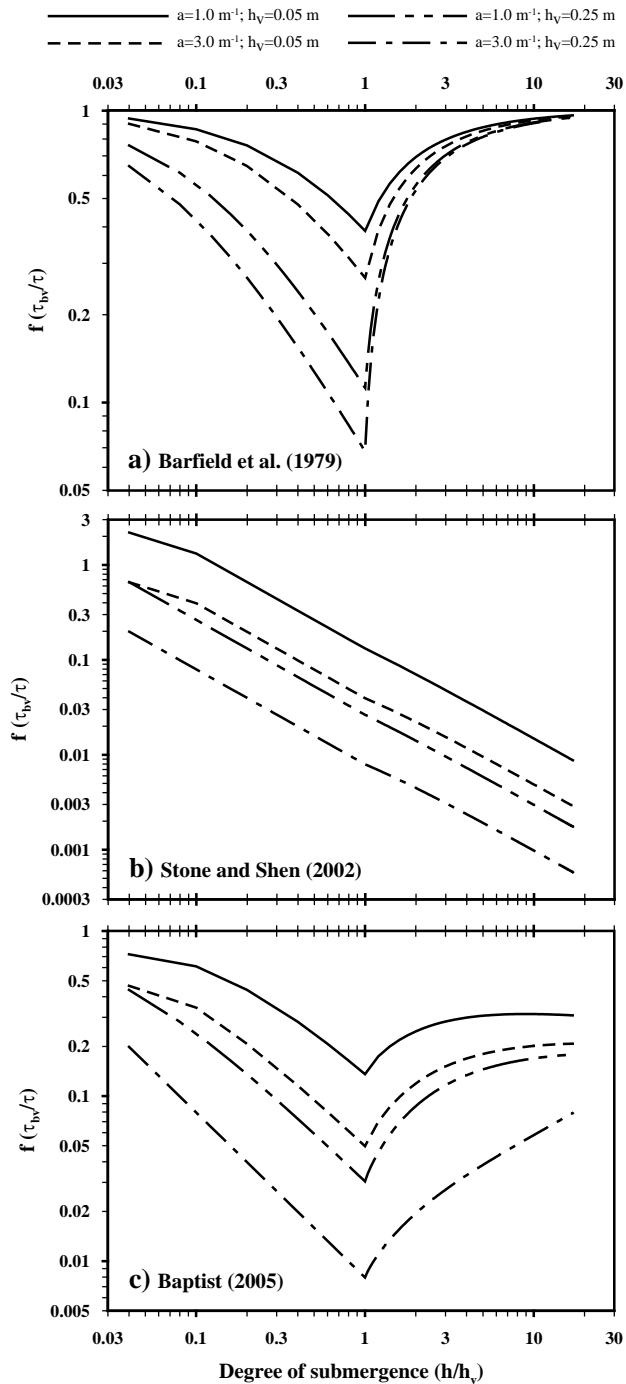


Figure 5.10: Ratio between bed-shear stress and total shear stress for vegetated beds as a function of the degree of submergence for: (a) Barfield et al. (1979), (b) Stone and Shen (2002), and (c) Baptist (2005).

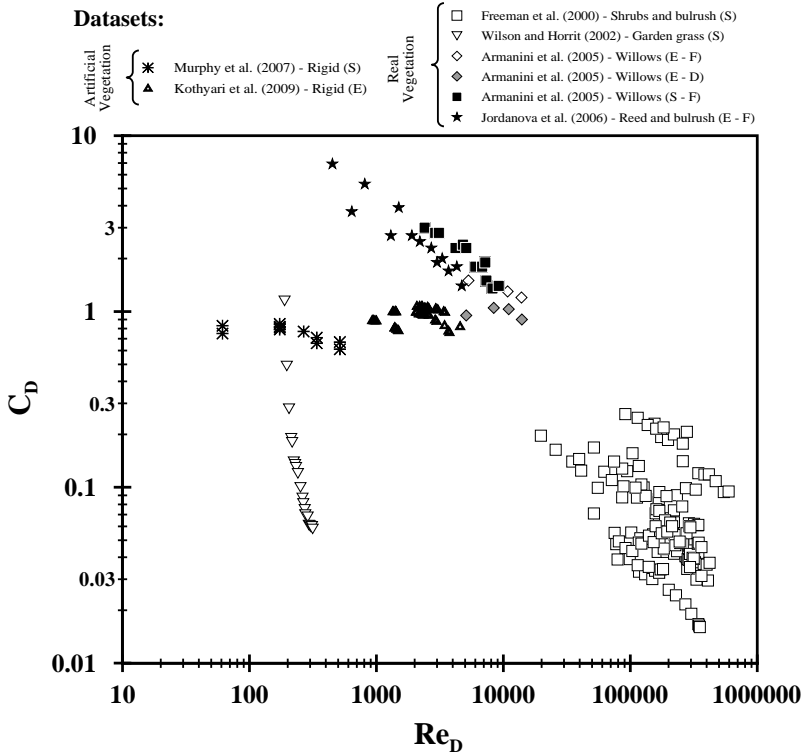


Figure 5.11: Apparent drag coefficient as a function of the element Reynolds number reported in previous studies. Vegetation condition: S= Submerged, E= Emergent, F= Foliated, and D= Defoliated.

5.3.5. SEDIMENT TRANSPORT

FIGURE 5.12 allows comparison of the measured sediment transport rates with the predicted ones. The model proposed by Barfield could be coupled to van Rijn (1984a) sediment transport formula only, because the Barfield method does not allow estimating the global flow resistance coefficient. In some cases, the models by Stone and Shen, and Baptist estimated bed-shear stresses that were lower than the critical shear stress in van Rijn (1984a) formula. In these cases, the sediment transport formula of van Rijn predicts zero sediment transport.

The results show that the two sediment transport capacity formulae provide similar results for high sediment transport rates (above $4 \times 10^{-5} \text{ m}^2/\text{s}$). For low sediment transport rates, the Engelund and Hansen (1967) formula provides better results; this outcome might be due to the different applicability ranges of the two formulae. The high dispersion in the lower sediment transport rates could be related to modifications in the bed-shear stress thresholds for vegetated beds or to the possibility that the sediment and flow characteristics did not fall within the applicability ranges of the two formulae anymore. Additionally, Figure 5.12 shows also that both flow resistance predictors (Stone and Shen and Baptist) can be used with the same accuracy, at least for emergent conditions.

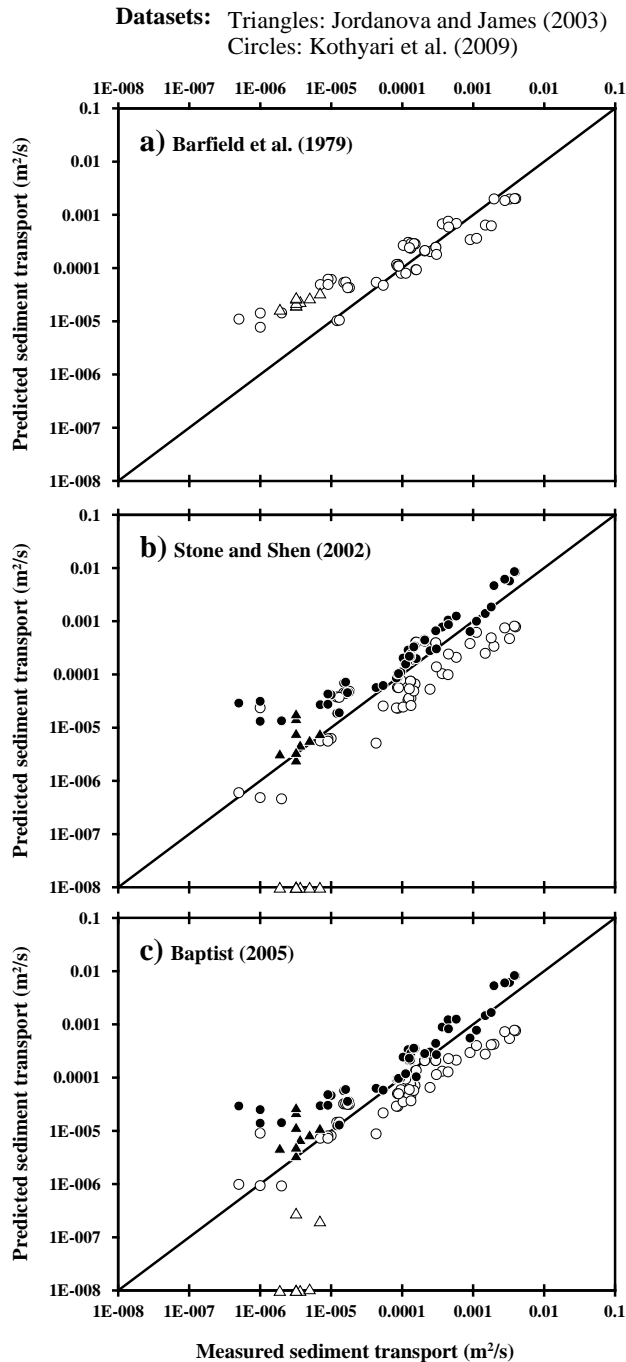


Figure 5.12: Comparison between measured and predicted sediment transport rates per unit width using the estimations of (a) Barfield et al. (1979), (b) Stone and Shen (2002), and (c) Baptist (2005). Markers in black: computed by applying Engelund and Hansen (1967). Markers in white: computed by applying van Rijn (1984a).

5.4. DISCUSSION AND CONCLUSIONS

5.4.1. MODEL EVALUATION

THE extensive dataset gathered from the literature allowed analysing the performance of existing models for the assessment of the global flow resistance for different vegetation types and under several degrees of submergence. We distinguished artificial vegetation with rigid or flexible stems, under emergent or submerged conditions, from real vegetation. The results show that for submerged vegetation the degree of submergence is a key parameter for the global flow resistance. The discrepancies between model results and measurements may reflect not only the variety of vegetation types and laboratory techniques used in each experiment, but also the differing data formats. Although no model can represent equally well both emergent and submerged conditions, the [Baptist \(2005\)](#) model provided the best fitting with the measurements, for both artificial and real vegetation. To apply this model to flexible plants, it is recommended to use the deflected vegetation height with a parameter ah_v larger than 0.01.

Formulations that allow estimating the vertical velocity profiles based on the properties of the vegetation canopy perform well only for certain cases. The major discrepancies are observed for the case of real vegetation, since the influence of foliage and plant flexibility is usually not included in the estimators. The model by [Klopstra et al. \(1997\)](#) showed the best performance, but its application should fulfil the criterion of low degree of discontinuity (Equations 5.9, 5.10 and Appendix). Mean flow velocity prediction in the vegetation layer could be performed equally well using the other formulations that apply to emergent conditions (except from the model by Hoffmann) and the model by Cheng for the submerged case.

The additional drag exerted by vegetation diminishes the flow velocity in the vegetation layer leading to a reduction of the bed-shear stress. Since this variable directly influences sediment entrainment from the bed, its accurate estimation is of high relevance for the assessment of sediment transport rates and bed level changes. However, studies dealing with both bed-shear stress and vegetation drag are scarce. From the analysed global flow resistance predictors only the [Stone and Shen \(2002\)](#) and [Baptist \(2005\)](#) methods estimate the bed-shear stress for both emergent and submerged conditions. Nevertheless, for submerged vegetation, the Stone and Shen model results in a decrease of the ratio between bed-shear stress and total shear stress if the submergence degree increases, which is against expectations. The model proposed by [Barfield et al. \(1979\)](#) and the models by [Ishikawa et al. \(2003\)](#) and [Kothyari et al. \(2009a\)](#), which are only applicable to emergent conditions, performed also well.

Even though the data used in this analysis refer to emergent vegetation and bed material load, the results show that the sediment transport capacity formulae of [van Rijn \(1984a\)](#) and [Engelund and Hansen \(1967\)](#) derived for non-vegetated channels can be applied to vegetated channels. However, the performance of these formulae was not satisfactory for low sediment transport rates, which is here attributed to possible variations in the mobility thresholds for vegetated beds or to the possibility that the sediment and flow characteristics did not fall within the applicability ranges of these formulations. The possibility of using general sediment transport capacity formulas on vegetated channels

allows estimating the morphological changes in rivers including the combined effect of the sediment moving on bare soil and through plants.

5.4.2. RESEARCH NEEDS

ADDITIONAL research is needed to accurately reproduce the effects of natural vegetation on water flow and sediment transport, notwithstanding the great progress made in the last decades. The effects of vegetation on both bed-material and suspended loads have received little attention so far. Proper parametrisation of these effects for studies at larger spatial scales will be the following necessary step to reproduce and study the morphodynamic behaviour of rivers and estuaries at different spatial and temporal scales.

The additional drag exerted by vegetation diminishes the flow velocity in the vegetation layer leading to a reduction of the bed-shear stress. Since this variable directly influences sediment entrainment, its accurate estimation is of high relevance for sediment transport calculations. Nonetheless, studies dealing with both bed-shear stress and vegetation drag are scarce, which means that more research in this field is required.

The (apparent) drag coefficient is a key parameter for the assessment of vegetation drag. Research performed during the last decades allowed progress in this field, but the value of this coefficient to be applied for different plant species and wide ranges of the element Reynolds number is still only partly known. Additionally, it is difficult to correlate the results of different studies to assess the apparent drag coefficient for different vegetation types and hydraulic conditions. Although the study of the drag coefficient of vegetation mixtures is relevant when dealing with real plants, this aspect remains almost unexplored.

Flow resistance estimators applicable for both emergent and submerged vegetation and dealing with the complex geometry and flexibility of real plants are still lacking. These estimators are necessary for sediment transport computations, and in particular for applications on tidal areas where the submergence degree of vegetation continuously varies with time.

Regarding the study of the flow field through and above vegetation, it is not yet understood how the turbulent coherent structures identified in hydrodynamic applications with fixed geometries (e.g. [Uijttewaal, 2014](#)) are modified by vegetation and how these structures affect sediment entrainment.

More research on sediment transport through and above vegetated beds is also needed ([Camporeale et al., 2013](#)). The formulation of sediment transport formulae incorporating the properties and effects of vegetation requires further attention. Sediment transport measurements, especially for the submerged conditions, are also a subject for future work. More laboratory set-ups are needed to investigate a wider range of sediment transport rates with varied vegetation and flow characteristics, and to analyse the behaviour of the different methodologies in estimating the sediment transport rates under submerged conditions. Field measurements are not available, thus, intensive field campaigns including different climatic conditions, vegetation species, flow regimes, hydraulic conditions and environmental set-ups (riverine and tidal) are also recommended.

Finally, assessing the long-term effects of vegetation on the river morphology requires new approaches incorporating the seasonal variations of vegetation characteristics (on yearly basis) and vegetation dynamics (colonization, survival, growth, succession, etc.) on new deposits and floodplains operating at a larger time scale (decades).

6

REPRESENTING PLANTS AS RIGID CYLINDERS IN EXPERIMENTS AND MODELS

“Uniformity is not nature’s way; diversity is nature’s way.”

Vandana Shiva

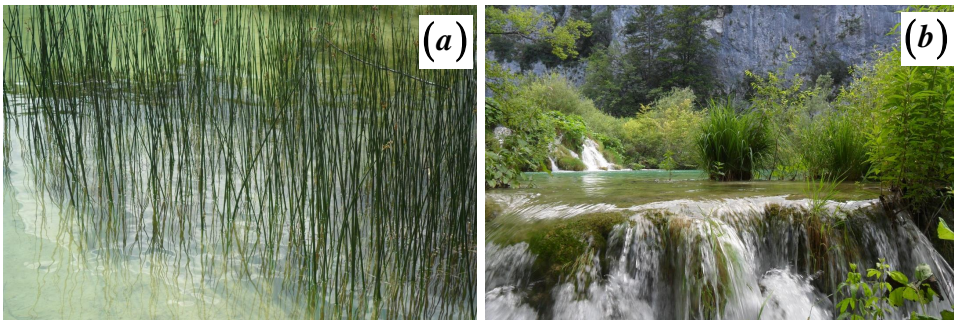


Figure 6.1: Comparison of geometric characteristics of plants: (a) Uniform, cylindrical and leafless; and (b) Irregular, with high variability in density and foliage. Photo taken at Plitvice, Croatia.

The consequences of representing plants as rigid cylinders by comparing the effects of real plants to those of rigid cylinders in a large number of laboratory tests and numerical simulations are analysed, focusing on different morphodynamic processes.

This chapter has been published by the author in *Advances in Water Resources* **93**, Part B: 205-222, doi:10.1016/j.advwatres.2015.10.004 (Vargas-Luna et al., 2016b). Only minor changes have been performed for formatting purposes.

6.1. INTRODUCTION

THERE is increasing awareness of the need to include the effects of vegetation in studies dealing with the morphological response of rivers and estuaries (e.g. [Hickin, 1984](#); [Nepf, 2012a](#)). Numerical models and laboratory experiments (e.g. [Tal and Paola, 2007](#)) have recently shown that riparian vegetation can reduce river braiding and vegetation growth on point bars has been recognized as one of the major factors governing river meandering (e.g. [Parker et al., 2011](#); [Asahi et al., 2013](#); [Eke et al., 2014a](#); [Bertoldi et al., 2014](#)).

Plants increase the local hydraulic roughness, reducing flow velocity and bed-shear stress (e.g. [Tsujiimoto, 1999](#); [Bennett et al., 2002](#)) and promoting sedimentation ([Wu and He, 2009](#); [Zong and Nepf, 2011](#)). Vegetation cover protects the soil, and root systems increase the soil strength against erosion. In the end, plants act as ecosystem engineers since they create the conditions that favour the survival and establishment of new vegetation ([Bertoldi et al., 2011](#); [Gurnell, 2014](#); [Gurnell et al., 2006](#); [Gurnell, 2012](#)). The relevance of vegetation processes for the morphological response of rivers and estuaries has resulted in an increased amount of research from several disciplines based on field investigations, laboratory experiments, and numerical models (e.g. [Murray and Paola, 2003](#); [Camporeale and Ridolfi, 2006a](#); [Perucca et al., 2007](#); [Perona et al., 2009](#); [Crosato and Samir Saleh, 2011](#); [Villada Arroyave and Crosato, 2010](#); [Camporeale et al., 2013](#); [Solari et al., 2015](#)).

Considering the relevance of vegetation for flow resistance, much research focused on calculating the hydraulic roughness of vegetated beds (e.g. [Stone and Shen, 2002](#); [Baptist, 2005](#); [Baptist et al., 2007](#)), and on the drag imposed by arrays of cylinders under submerged ([Nepf, 1999](#); [Tang et al., 2014](#)) and emergent conditions ([Tanino and Nepf, 2008](#); [Kothyari et al., 2009b](#); [Cheng, 2011](#)).

A number of mobile-bed laboratory experiments used alfalfa sprouts to analyse the morphological changes caused by the presence of vegetation ([Tal and Paola, 2007](#); [Gran and Paola, 2001](#); [Braudrick et al., 2009](#); [Tal and Paola, 2010](#)), the influence of riparian vegetation on bank erosion ([Jang and Shimizu, 2007](#)), and the morphological effects of its spatial distribution ([van Dijk et al., 2013](#)), among other aspects (e.g. [Paola et al., 2009](#); [Kleinhans et al., 2014](#)). More recently, the use of alfalfa sprouts has been combined with the supply of wooden dowels in order to reproduce the combined effects of living vegetation and floating logs ([Bertoldi et al., 2015](#)). These works showed important aspects of the effects of vegetation on the morphology of river systems, but provided mere qualitative results due to the difficulty of translating the laboratory results to the real river scale (upscaling).

The study of the flow around isolated cylindrical elements started in the early 1950's (e.g. [Finn, 1953](#); [Tritton, 1959](#)), but it was only twenty years later that arrays of cylinders were considered in laboratory experiments to simulate vegetation (e.g. [Li and Shen, 1973](#); [Petryk and Bosmajian, 1975](#); [Tollner et al., 1977](#)). These studies helped identifying the relevance of the stems density and spatial distribution on flow resistance, flow

field and sediment processes. Other studies showed that the representation of plants as rigid cylinders neglects the reconfiguration of plant foliage under flowing water (Statzner et al., 2006; Aberle and Järvelä, 2013) which decreases the projected area and drag forces (Gosselin et al., 2010; de Langre et al., 2012; Dittrich et al., 2012; Siniscalchi and Nikora, 2013; Albayrak et al., 2014). Several research contributions have advanced our understanding of how an array of cylinders modifies vertical velocity profiles (Kubrak et al., 2008; Huai et al., 2009; Liu et al., 2008) and turbulent structures (Nepf, 1999; Ghisalberti and Nepf, 2006; Stoesser et al., 2009), affecting bed load (Jordanova and James, 2003; Kothyari et al., 2009a) and suspended load (López and García, 1998; Sharpe and James, 2007), as well as depositional processes (Zong and Nepf, 2011; Yager and Schmeeckle, 2013).

Rigid cylinders have been used in laboratory experiments also to analyse the flow-vegetation interaction in vegetated patches and on floodplains. Regarding vegetated floodplains, a considerable amount of experimental work has been carried out to study the effects of vegetation on overbank flow (Pasche and Rouvé, 1985), shear-stresses at cross-sectional interfaces (Thornton et al., 2000), hydraulic conveyance (Oldham and Sturman, 2001), stream-bank erosion (Wynn and Mostaghimi, 2006), near-bank turbulence (McBride et al., 2007), turbulent coherent structures (White and Nepf, 2008; Sanjou et al., 2010), and flow field alterations (Jahra et al., 2011). A few studies have considered wake structures and flow field alterations on finite vegetation patches in channels with fixed beds (Takemura and Tanaka, 2007; Nicolle and Eames, 2011; Zong and Nepf, 2012) and even fewer studies have considered bed level changes around vegetation patches (Kim et al., 2015).

From the available modelling approaches that have been proposed to describe plants in a schematic easily-quantifiable way, the most common one represents vegetation as a set of rigid cylinders with given height, diameter, stem distribution and density (a review can be found in Vargas-Luna et al., 2015b). However, linking the settings of rigid cylinders to real vegetation is an important unsolved issue. In nature it is possible to find plants that can be well represented by cylindrical rigid stems (Figure 6.1a), but in most cases it is simply impossible to represent the variability of their geometrical and physical characteristics by this basic approach (Figure 6.1b). Plant flexibility is considered only by a few models (e.g. Dijkstra and Uittenbogaard, 2010), but these models are not suitable for practical applications, which reinforces the common practice of using simpler approaches.

Experiments with rigid cylinders have the advantage of using the approach adopted by a number of numerical models (e.g. Stone and Shen, 2002; Baptist, 2005; Wu et al., 2005; Cheng, 2013). This allows using the numerical models to interpret the laboratory results for real systems, since upscaling is a known problem for all experiments dealing with vegetation and sediment. However, it is still unclear whether numerical models based on the rigid cylinder representation of vegetation provide realistic results at the scale of real rivers and estuaries.

This work explores the implications of representing plants as rigid cylinders by means

of new laboratory experiments and by reviewing the results of published model simulations. The first set of experiments, carried out in a straight flume with glass walls (Flume No. 1), studies the correspondence between the effects of real and artificial vegetation and those of rigid cylinders on water flows. This aspect is addressed by comparing the hydraulic roughness of channel beds covered either with plants or with rigid cylinders under the same flow regimes. The second set of experiments analyses the evolution of a channel with erodible bed and banks (Flume No. 2) to explore the feasibility of using rigid cylinders to simulate the effects of floodplain vegetation on the channel width formation. A third set of experiments, carried out in a similar, but larger, flume (Flume No. 3), explores the feasibility of using rigid cylinders to simulate vegetated bank dynamics.

The work is complemented by a thorough review of the results obtained by two-dimensional (2D) morphodynamic models adopting Baptist's method (Baptist, 2005) to evaluate the consequences of using a rigid-cylinder schematization for the simulation of the morphological developments of real rivers. To substantiate the analysis of model results, the predictive capacity of the method developed by Baptist (2005) in estimating water depth and mean flow velocity is assessed by comparing the results to the data obtained from the first set of experiments.

This paper represents a first step in assessing the effects of representing real vegetation with rigid cylinders in laboratory experiments and numerical models. The results allow identifying the limitations of the approach and provide some preliminary guidelines on its application.

6.2. THEORETICAL BACKGROUND: BAPTIST'S MODEL

THE flow resistance estimator for vegetated beds considered in this study was developed by Baptist in 2005 (Baptist, 2005). It is based on a rigid-cylinder representation of vegetation and can be considered as representative of the models adopting this approach. Baptist's method (Baptist, 2005) predicts the total flow resistance of a river bed covered by vegetation, which forms the base for water depth predictions. Sediment transport and bed level changes predictions, instead, are derived by considering the bed shear stress, which is reduced by the presence of vegetation, resulting in more realistic bed level changes in the vegetated areas (Baptist et al., 2003). The method is implemented in the open-source Delft3D software (www.deltares.nl), computing the morphological changes of rivers, estuaries and coasts in two and three dimensions. Delft3D was used in the simulations reviewed in Section 6.5. Baptist's method (Baptist, 2005) performance was analysed and compared to the performance of a number of other models (Vargas-Luna et al., 2015b), where it proved to be one of the most complete vegetation models, since it is valid for both submerged and emergent plants, and it is the most accurate one with respect to predictions of laboratory data.

Baptist described plants as sets of rigid cylinders with a characteristic diameter, D , height, h_v , and stem surface density, m , defined as the number of stems, N , per bed surface area (Figure 6.2). The basic assumption is that vegetation has high density so

that the vertical velocity profile of the flow within the plants can be assumed uniform and constant in vertical direction. It is important to note that the approach does not allow for combinations of different vegetation types, such as grass and trees, at the same location.

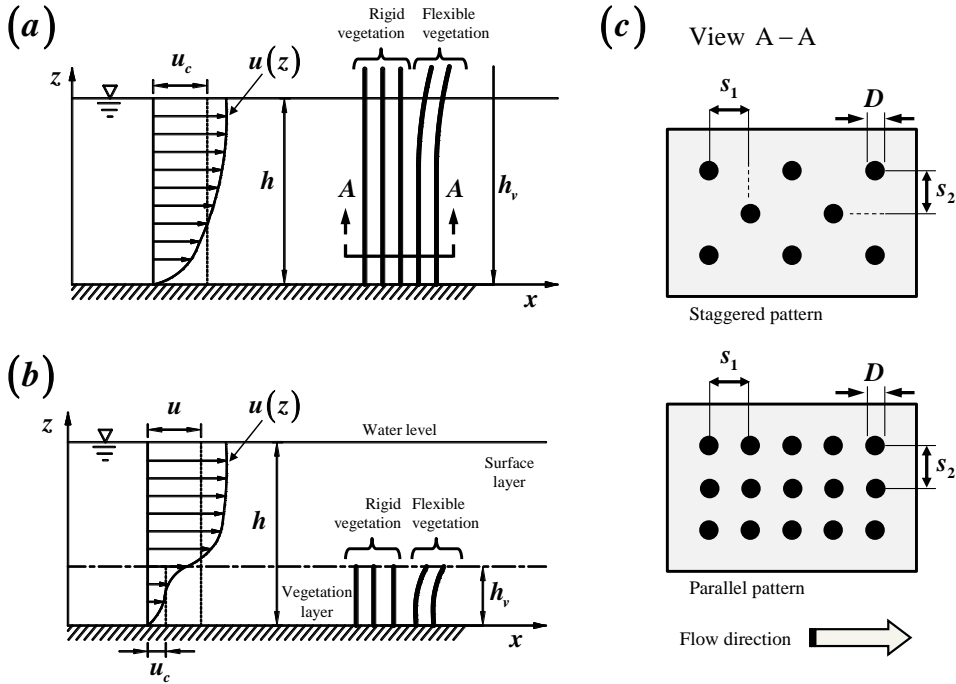


Figure 6.2: Main characteristics of rigid and flexible vegetation in open channels. Left: side view of emergent vegetation (above) and submerged vegetation (below), Adapted from: Wu and He [10]. Right: plan view of staggered and parallel patterns. Variables and units shown in the notation section.

Baptist derived an expression for the hydraulic resistance to a flow over (submerged) and through (emergent) vegetation from the momentum balance, based on the following assumption:

$$\rho g h i_b = \tau_{bv} + \tau_v \tag{6.1}$$

where ρ is the mass density of water (kg/m^3); g is the acceleration due to gravity (m/s^2); h is the water depth (m); i_b is the longitudinal water surface slope (-); τ_{bv} is the bed shear stress (N/m^2) and τ_v is the extra shear stress caused by vegetation (N/m^2).

According to Baptist, the bed shear stress, τ_{bv} , in case of emergent vegetation (wet vegetation height is equal to water depth h), is given by

$$\tau_{bv} = \frac{\rho g}{C_b^2} u_c^2 \tag{6.2}$$

and the extra shear stress exerted by the plants is expressed as

$$\tau_v = \frac{1}{2} \rho C_D a h u_c^2 \quad (6.3)$$

where C_b is the Chézy coefficient of the bare soil ($m^{1/2}/s$); C_D is the drag coefficient of the plants (-) (Baptist suggests using $C_D = 1$); a is the projected cylinders area per unit of volume (m^{-1}) (Nepf, 2012a): (m being the number of stems, N , per bed surface area in m^{-2} and D the reference cylinder diameter in m). Typical ranges for natural vegetation are 0.1 to 1.0 m^{-1} for open herbaceous and marsh types of vegetation (Baptist, 2005), and 10 to 15 m^{-1} for natural grasslands. The depth averaged flow velocity through vegetation, u_c (m/s), is given by:

$$u_c = C_r \sqrt{h i_b} \quad (6.4)$$

where C_r represents the total friction coefficient expressed in terms of Chézy coefficient ($m^{1/2}/s$), given by the expression

$$C_r = \sqrt{\frac{1}{1/C_b^2 + C_D a h / 2g}} \quad (6.5)$$

It is important to note that a larger value of the canopy density leads to a smaller value of C_r corresponding to a larger bed roughness.

For submerged vegetation, it is assumed that the water depth is much larger than the plant height and that the flow velocity is uniform between the plants, but has a logarithmic profile above them, starting from the value u_c , obtained by substituting the water depth h (m) with the plant height h_v (m) in Equation 6.3. The bed shear stress becomes

$$\tau_b = \frac{\rho g}{C_b^2} u^2 \quad (6.6)$$

where C'_b represents the flow resistance of the bed between the plants in case of submerged vegetation, given by the expression

$$C'_b = C_b + \frac{\sqrt{g}}{\kappa} \sqrt{1 + \frac{C_D a h_v C_b^2}{2g} \ln\left(\frac{h}{h_v}\right)} \quad (6.7)$$

in which κ ($=0.41$) is the Von Kármán constant. It is important to note that Equation 6.7 results in a reduction of the bed shear stress with respect to bare soil and emergent vegetation, since C'_b is larger than C_b .

Considering the total water flow, including the flow between and above vegetation, the depth averaged flow velocity results

$$u = C'_r \sqrt{h i_b} \quad (6.8)$$

in which C'_r is the total friction coefficient expressed in terms of the Chézy coefficient ($m^{1/2}/s$), given by:

$$C'_r = \sqrt{\frac{1}{1/C_b^2 + C_D a h_v / 2g}} + \frac{\sqrt{g}}{\kappa} \ln\left(\frac{h}{h_v}\right) \quad (6.9)$$

It is important to observe that higher canopy density a , and plant height h_v , result in a smaller value of C'_r and therefore larger bed roughness. The first term of Equation 6.9 is equivalent to C_r (Equation 6.5) with the water depth substituted by the plant height. The logarithmic term appears only for $h > h_v$ and in such case it increases the value of C'_r , decreasing the average resistance, for larger submergence (water-depth to plant-height) ratios. The submergence ratio (h/h_v) has also shown to be of relevance for the study of turbulent structures (e.g. Nepf and Vivoni, 2000; Neary et al., 2012; Luhar and Nepf, 2013) and longitudinal mixing processes (Murphy et al., 2007; Shucksmith et al., 2011) in vegetated channels.

6.3. MATERIALS AND METHODS: LABORATORY EXPERIMENTS

6.3.1. REPRESENTATION OF VEGETATED FLOWS USING RIGID CYLINDERS

TO assess the capability of representing the effects of real and artificial vegetation by using uniformly distributed arrays of rigid cylinders, we used the tilting glass-walled flume 14 m long and 0.40 m wide available at the Environmental Fluid Mechanics Laboratory of Delft University of Technology (Figure 6.3a). We compared the effects of four types of vegetation on hydraulic resistance considering several densities and plant heights.

To represent plants, we used rigid cylinders (wooden sticks with diameter, D , equal to 2×10^{-3} m and total height, H , equal to 0.20 m, Figure 6.3b), two flexible artificial plants, composed by either plastic grass (Figure 6.3c) or by leafy plastic plants (*Egeria densa*, Figure 6.3d) and real plants belonging to the Piperaceae family (*Peperomia rotundifolia*, Figure 6.3e). The plants were inserted in a 0.15 m layer of sand with median diameter, D_{50} , equal to 5×10^{-4} m and sorting index, $I = 0.5(D_{50}/D_{16} + D_{84}/D_{50})$, equal to 1.23 (Figure 6.4) in staggered patterns (Figure 6.2c). The characteristic diameter for the real and artificial plants was derived by dividing the frontal area of the plant by its height. Vegetation properties are summarized in Table 6.1.

Water and sediment were recirculated. Water level and bed surface profiles were measured with lasers located in a movable carriage above the flume. The mean water depth was calculated as the difference between the water level and bed surface profiles. The discharge was measured in the supply system with an ultrasonic flowmeter. Mean flow velocities were derived by dividing the discharge by the total cross-sectional area.

Bed slopes in the flume were set to 0.002 or 0.004 m/m, but these did not coincide with the slope of the water surface. The flow resistance in terms of the friction coefficient, C_f , of the vegetated bed was obtained by using the one-dimensional steady flow momentum equation per unit width, valid for gradually varying flow:

$$u \frac{du}{dx} + g \frac{dz}{dx} + g \frac{dh}{dx} + \frac{C_f u^2}{R_h} = 0 \quad (6.10)$$

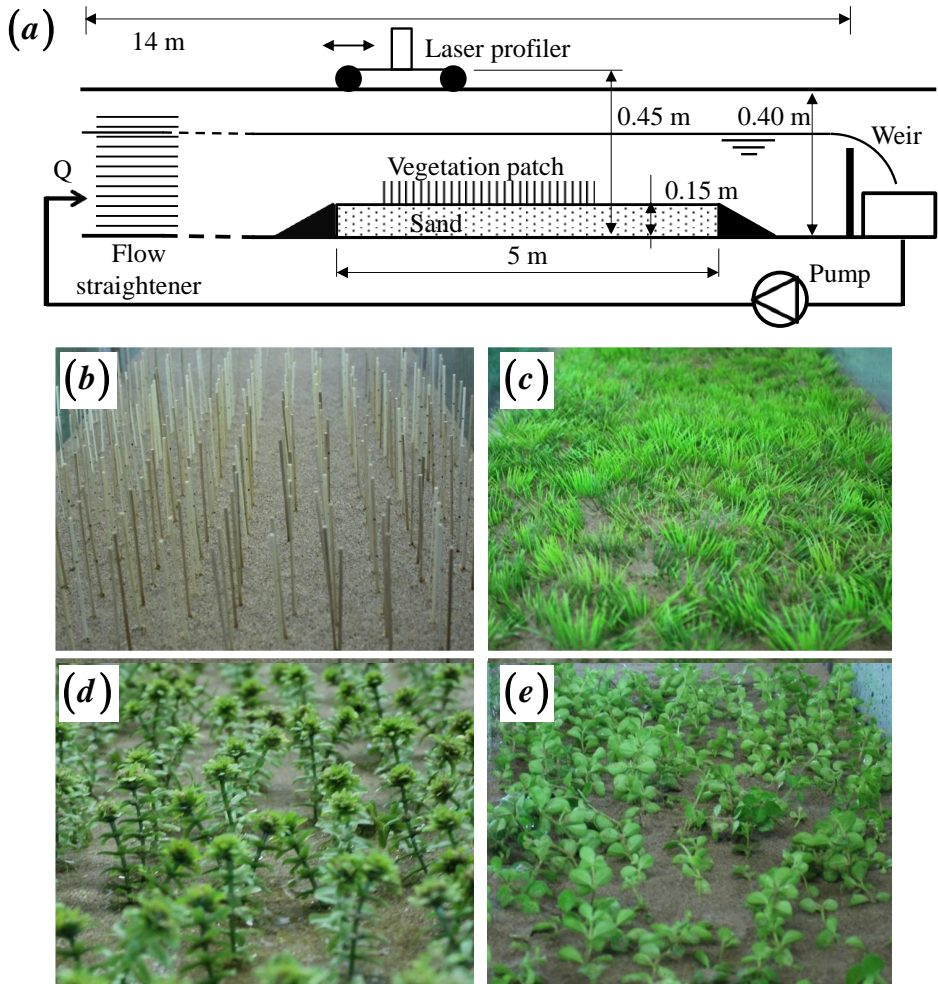


Figure 6.3: Experimental set-up for Flume No. 1. (a) and vegetation arrays used: (b) Rigid (Wooden) sticks [Test W11], (c) Artificial Grass [Test G2], (d) Artificial with Leaves (*Egeria densa*) [Test ED3], (e) Real (*Peperomia rotundifolia*) [Test R2]. Vegetation properties are presented in Table 6.1.

where z is the bed level elevation (m) in the longitudinal direction x (m), C_f is the friction coefficient (-), and R_h is the hydraulic radius (m), expressed as the cross-sectional area over the wetted perimeter. The friction coefficient can straightforwardly be linked to the Chézy coefficient by the expression $C_f = g/C_z^2$. As a glass-sided flume was used, sidewall corrections were applied by using the method proposed by Vanoni and Brooks (1957).

The flow velocity in the experiments was imposed below the condition for sediment motion to avoid important hydrodynamic effects of excessive bed scouring and deposition. However, some additional trials were performed at the end of each test with higher

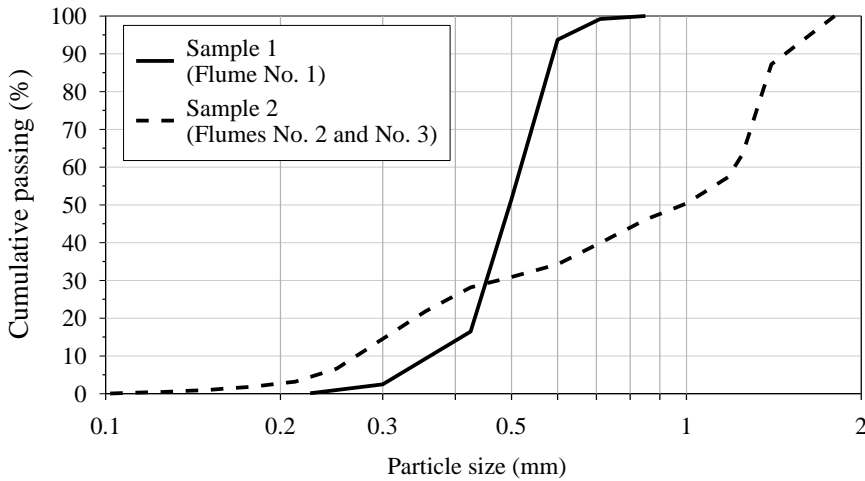


Figure 6.4: Sediments used in the laboratory experiments.

flows to observe the influence of vegetation on sediment transport and bed development. The changes in bed surface were recorded by a video camera from the lateral glass wall at specific locations. The differences between the initial and final bed surface profiles extracted from the measurements were used to roughly analyse the erosion and deposition patterns.

6.3.2. REPRESENTATION OF THE CHANNEL-WIDTH FORMATION USING RIGID CYLINDERS

ANOTHER set of experiments was carried out to qualitatively study the effects of rigid cylinders on floodplains on the main channel-width formation, the major question being whether rigid cylinders (wooden sticks) inserted in the banks of an excavated channel would decrease bank erosion as real vegetation in similar experimental tests (e.g. Tal and Paola, 2010). The tests were carried out in a 2.25 m long, 1.2 m wide and 0.20 m deep mobile-bed flume (Flume No. 2, see Figure 6.5) with fixed inlet and outlet. A pump placed in a tank beneath the flume outlet provided the flow discharge by recirculating the water to a basin located behind the inlet, where waves were dissipated by a set of vanes. The pump was connected to a power-regulated supply system enabling flow discharge variation. The flume was filled with sand having median diameter, D_{50} , equal to 9.5×10^{-4} m and sorting index, I , equal to 2.32 (Figure 4). A straight 0.09 m wide channel was excavated in the centre of the flume with an initial bed slope of 0.01 m/m. Vegetation was represented by arrays of toothpicks with diameter, D , of 2×10^{-3} m and a total height of 0.08 m, considering several combinations of patterns and densities (Figure 6.5b). The toothpicks were inserted in the sand, leaving just 0.02 m above the surface (i.e. $H_1=0.08$, and penetration depth $H_2=0.06$ in Figure 6.5c). The characteristics of the parallel and staggered vegetation arrays are listed in Table 6.2.

Table 6.1: Vegetation arrays considered in the experiments in Flume No. 1.

Test ^a	h_v (m)	m (m^{-2})	D (m)	a (m^{-1})
W1	0.025	761	0.0020	1.5
W2	0.025	1294	0.0020	2.6
W3	0.025	2755	0.0020	5.5
W4	0.025	10280	0.0020	20.6
W5	0.050	761	0.0020	1.5
W6	0.050	1294	0.0020	2.6
W7	0.050	2755	0.0020	5.5
W8	0.050	10280	0.0020	20.6
W9	0.075	761	0.0020	1.5
W10	0.075	1294	0.0020	2.6
W11	0.075	2755	0.0020	5.5
W12	0.075	10280	0.0020	20.6
DG1	0.025	208	0.0100	2.1
DG2	0.025	656	0.0100	6.6
DG3	0.025	1296	0.0100	13.0
ED1	0.025	761	0.0088	6.7
ED2	0.025	2755	0.0088	24.2
ED3	0.050	761	0.0097	7.4
ED4	0.050	2755	0.0097	26.7
R1	0.060	761	0.0150	11.4
R2	0.060	2755	0.0150	41.3

^a W: Rigid (Wooden) sticks; DG: Artificial Grass; ED: Artificial with Leaves (*Egeria densa*); R: Real (*Peperomia rotundifolia*). See Figures 6.2 and 6.3 for graphical description.

Three discharge hydrographs, including constant and variable flows, having the same averaged value, were applied to each of the seven configurations described in Table 6.2. The hydrographs were selected on the basis of the intensive laboratory experiments performed by Byishimo (2014) (Figure 6.5d). The width changes with time were tracked by recording the evolution of the channel with a video camera located at the top of the flume with the help of a squared grid (0.05×0.05 m) placed above the flume. By analysing the central part of the channel at three locations far from the inlet and outlet, the average channel width was measured each 5 minutes from the recorded videos.

Table 6.2: Vegetation arrays considered in the experiments in Flume No. 2 (for the spatial distribution see Figure 6.5).

Test ID	s_1 (m)	s_2 (m)	Vegetation pattern	m (m^{-2})	a (m^{-1})
W-NV	-	-	-	-	-
W-V1	0.02	0.02	Parallel	2500	5
W-V2	0.01	0.02	Staggered	2500	5
W-V3	0.01	0.02	Parallel	5000	10
W-V4	0.02	0.01	Parallel	5000	10
W-V5	0.01	0.01	Staggered	5000	10
W-V6	0.01	0.01	Staggered	10000	20

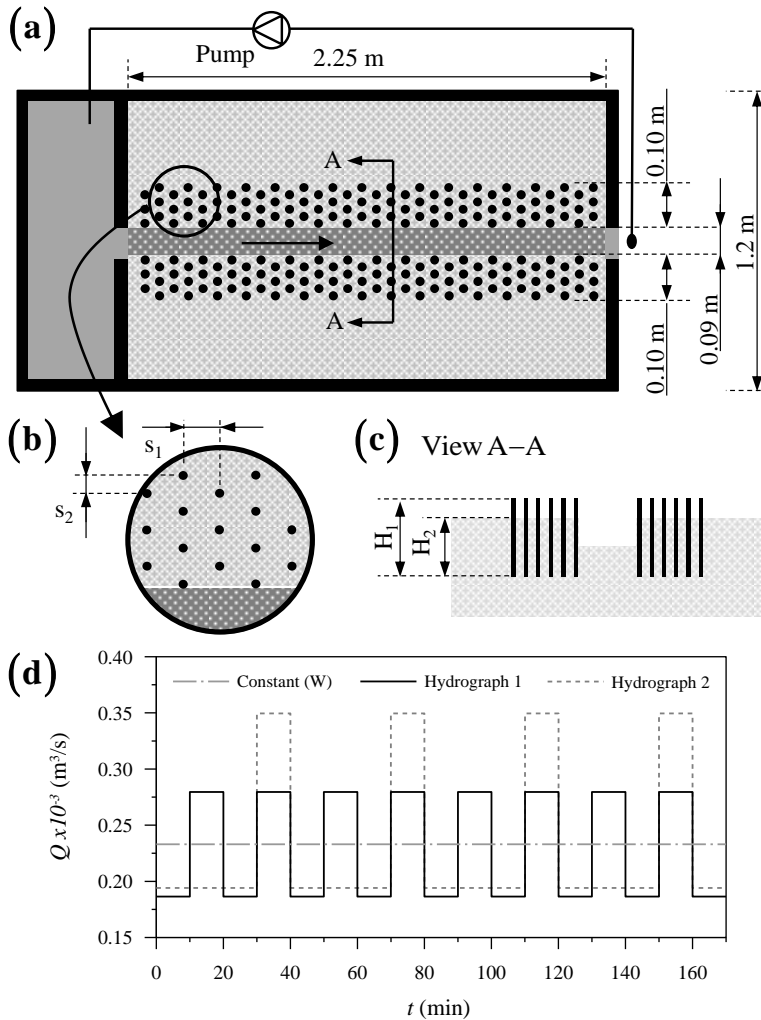


Figure 6.5: Experimental set-up for Flume No. 2. (a) Plan view, (b) Vegetation distribution on the floodplains, (c) Typical cross-section, and (d) Hydrographs used in the experiments. Initial bed slope = 0.01 m/m .

6.3.3. REPRESENTATION OF BANK DYNAMICS USING RIGID CYLINDERS

A third laboratory set-up, Flume No. 3, was used to analyse the effects of vegetation and flow variability on channel planform formation, see Figure 6.6a. The mobile-bed flume was 5.0 m long, 1.2 m wide and 0.25 m deep. An initial 0.08 m wide channel was excavated in the centre of the flume, filled with the same sand used in Flume No 2 (Figure 6.4). The initial bed slope was 0.010 m/m . For this set of experiments a curved bend made from a PVC elbow was used as a geometrical perturbation at the inlet of the flume, see Figure 6.6. This time, only the 0.20 m wide inlet was fixed, whereas the outlet was let free to allow lateral channel migration.

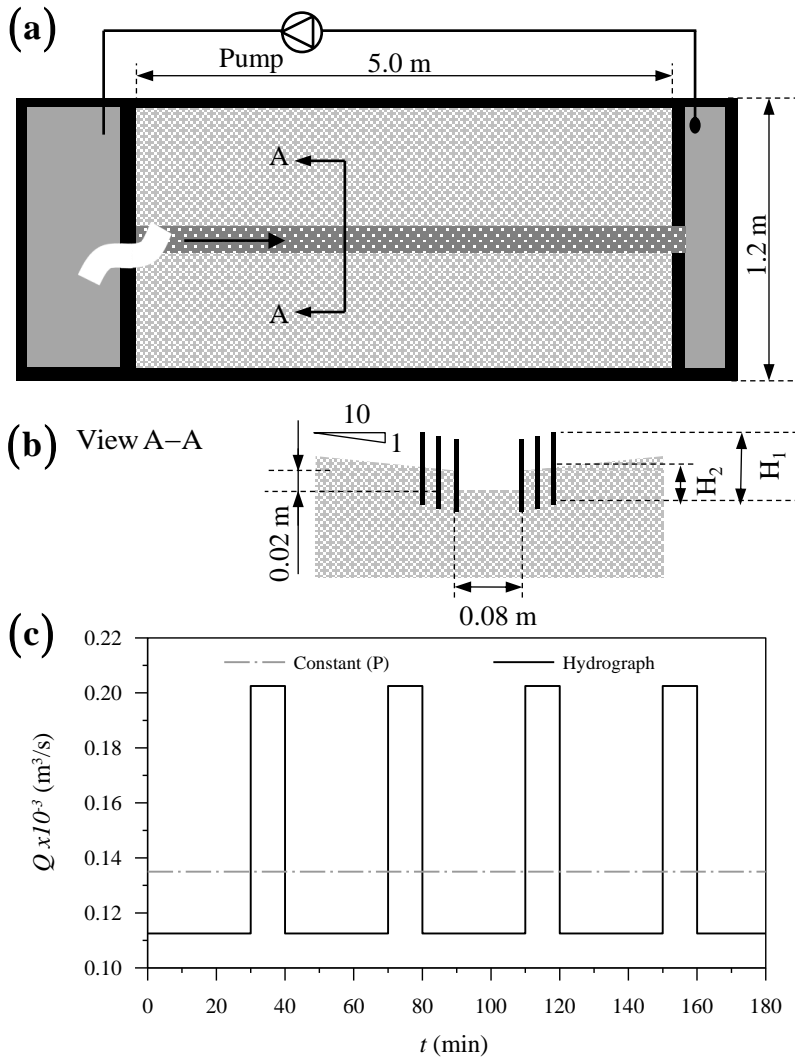


Figure 6.6: Experimental set-up for Flume No. 3. (a) Plan view, (b) Typical cross-section, and (c) Hydrographs used in the experiments. Initial bed slope = 0.01 m/m .

The same type of wooden toothpicks of the previous set-up was used, this time considering only parallel arrays, but including different heights, H_1 , and penetration depths, H_2 (see Table 6.3 and Figure 6.6b). The flow was regulated as in Flume No. 2. The constant and variable discharges, having the same averaged value, are given in Figure 6.6c. The planform changes in time were tracked by recording the evolution of the channel with a video camera.

Table 6.3: Vegetation arrays considered in the experiments in Flume No. 3 (for the spatial distribution see Figures 6.5 and 6.6).

Test ID	s_1 (m)	s_2 (m)	H_1 (m)	H_2 (m)	m (m^{-2})	a (m^{-1})
P-NV	-	-	-	-	-	-
P-V1	0.04	0.02	0.08	0.06	1250	2.5
P-V2	0.04	0.02	0.08	0.01	1250	2.5
P-V3	0.04	0.02	0.04	0.01	1250	2.5
P-V4	0.02	0.02	0.08	0.06	2500	5.0

6.4. RESULTS OF LABORATORY EXPERIMENTS

6.4.1. REPRESENTATION OF VEGETATED FLOWS USING RIGID CYLINDERS

CONSIDERING that the flow resistance of a vegetated bed depends on the combination of flow and vegetation properties, the results are presented as a function of the element Reynolds number, with the uniform diameter of plants as characteristic length, given as

$$Re_D = \frac{uD}{\nu} \quad (6.11)$$

where ν is the cinematic viscosity of the fluid (m^2/s). The results are presented in Figure 6.7. The first observation is that for all vegetation types the flow resistance decreases as the element Reynolds number increases. The trend is more evident for real plants and plastic grass (Figures 6.7a and 6.7b), as well as for low density plastic *Egeria Densa* (Figure 6.7c), for which the points appear clearly aligned on a curve. Only for wooden sticks, the friction coefficient increases as the density increases (Figure 6.7d). Our results show that the friction coefficients obtained with wooden sticks (Figure 6.7d) have the same order of magnitude as the ones obtained with real and plastic plants, with only a few exceptions. The wooden sticks, however, present the smallest element Reynolds numbers, which is due to their small diameter (2 mm). Other experiments found in the literature (Cheng, 2011) show that rigid cylindrical rods with larger diameters have friction coefficients and element Reynolds numbers similar to those observed for real and artificial plants in our experiments, see Figure 6.7d. As they offer more realistic results, it might be better to use rigid stems or wooden sticks with larger diameters (of about 8 mm). Experiments reported in (Cheng, 2011) have comparable flow velocities (0.077 - 0.342 m/s) and submergence ratios (1.3 - 2.0) with the experiments reported here. For *Egeria Densa*, the highest density results in more scattered points (Figure 6.7c), whereas for the other vegetation types low and high densities result in similar friction coefficients (Figures 6.7a and 6.7b).

The possible effects of foliage and flexibility can be analysed by comparing the results provided by the two types of plants with leaves: real vegetation and plastic *Egeria Densa*. Both plant types have similar leaf volumes, but the leaves of the real plants have lower stiffness than the plastic ones, see Figures 6.3d and 6.3e. With 2755 plants/ m^2 (high density), the leaves of the more rigid *Egeria Densa* act as obstacles to the flow and result in higher roughness than the more flexible leaves of real plants (compare Figures 6.7c and 6.7a). This means that for plants with foliage the flow resistance is not only affected by

vegetation density (expressed as number of plants per unit area), but also by foliage and plant flexibility. Therefore, another definition of plant geometry and density should be adopted when describing foliated plants in order to include the effect of these properties on the flow resistance. Contrary to what previously found by other researchers (e.g. [Nepf and Vivoni, 2000](#)), the submergence ratio, h/h_v , does not appear to affect the flow resistance coefficients in our experiments.

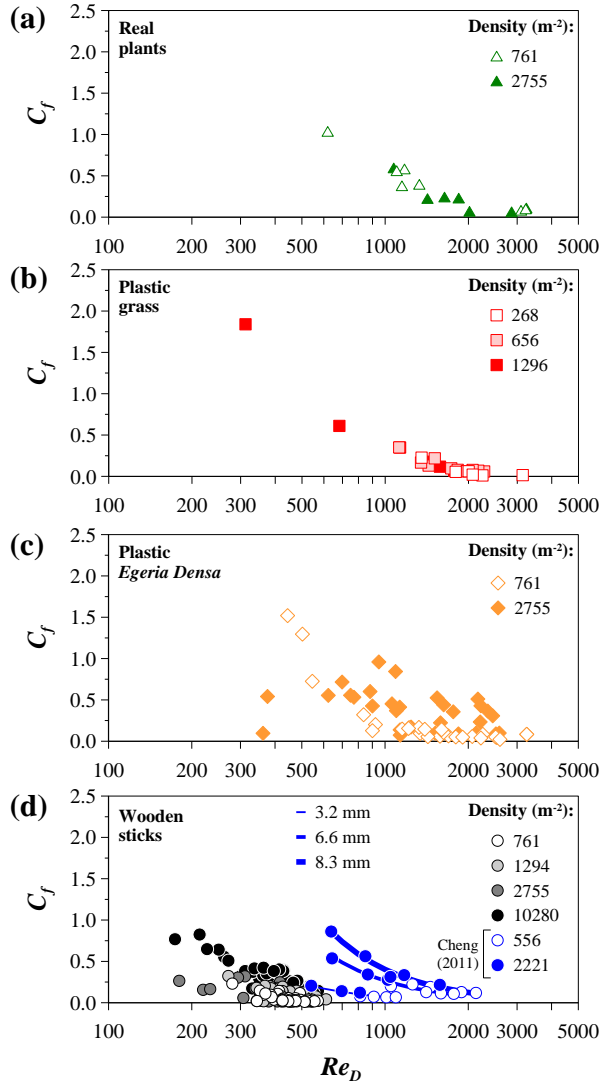


Figure 6.7: Friction coefficient (C_f) as a function of the element Reynolds number (Re_D) for: (a) Real plants [h/h_v : 2.0 - 3.6], (b) Plastic grass [h/h_v : 4.7 - 8.7], (c) Plastic *Egeria Densa* [h/h_v : 1.8 - 8.8], and (d) Wooden sticks [h/h_v : 1.5 - 7.8] and cylindrical rods by [Cheng \(2011\)](#) [h/h_v : 1.3 - 2.0]. Vegetation properties are listed in [Table 6.1](#).

About the additional trials with flow velocities higher than the conditions for sediment motion, bedforms formed downstream and upstream of the vegetation patch for all vegetation types and densities, with different erosional and depositional patterns. With low and medium density artificial grass (DG1 and DG2) local erosion and deposition patterns formed within the vegetation patch. In some cases the plants were completely covered by sediment in certain areas. High density grass (DG3) produced local erosion at the upstream end of the vegetation patch, but in this case much less sediment was deposited more downstream inside the vegetation patch. Erosion occurred at end of the flume. High density vegetation with leafs (real plants and artificial *Egeria Densa*) produced local erosion at the upstream end of the vegetated patch, but the sediment settled just downstream of the patch and not within vegetation. With low density, erosion and deposition patterns resembled those obtained with low density grass. With wooden sticks, much less sediment was trapped within the elements. At the highest flow velocities local scour occurred around each rigid cylinder.

The results show the relevance of vegetation foliage and high density in general in reducing flow velocities within the plants, affecting sediment transport processes as well as erosional and depositional patterns.

6.4.2. REPRESENTATION OF THE CHANNEL-WIDTH FORMATION USING RIGID CYLINDERS

FIGURE 6.8 shows the channel-width evolution as a function of time for the three considered discharge conditions. As expected, most changes occurred in the first 20 minutes of the experiments. The equilibrium width as well as the time required to achieve it decrease as vegetation density increases. This figure also shows that the response in time of the channel-width and the equilibrium width reached at the end of each experiment are substantially different for each discharge regime. This behaviour shows that the frequency and magnitude of high and low flow sequences have a major impact on the channel formation. The response of the channel-width to the bank erosion pulses driven by the peak flows is more noticeable in the variable regime with less frequent but higher flow peaks (Hydrograph 2). In all cases, the bank erosion rates decrease with time until the equilibrium width is reached, which is clearly attributed to the decrease of water depth caused by channel widening.

The values of the equilibrium width of the channels are shown in Figure 6.9. The experiments with vegetated banks lead to smaller widths compared to the cases without vegetation for the same flow conditions. Larger width reductions occurred with dense vegetation. Regarding the influence of the vegetation pattern, both the separation between elements (along the parallel and perpendicular direction of the flow) and the arrangement (staggered or parallel) were found relevant for the final channel width. Experiments with the same density and parallel pattern but different interchanged separation distances S1 and S2 in Figure 6.5b (tests W-V3 and W-V4) showed similar behaviour for the variable discharge tests. However, a shorter interchanged separation of the elements in the perpendicular direction, S2, reduces the initial bank erosion rates and the equi-

librium widths with constant discharge. According to our observations parallel configurations appear to be more effective on reducing bank erosion than the staggered ones, when comparing the equilibrium width obtained in experiments with the same density.

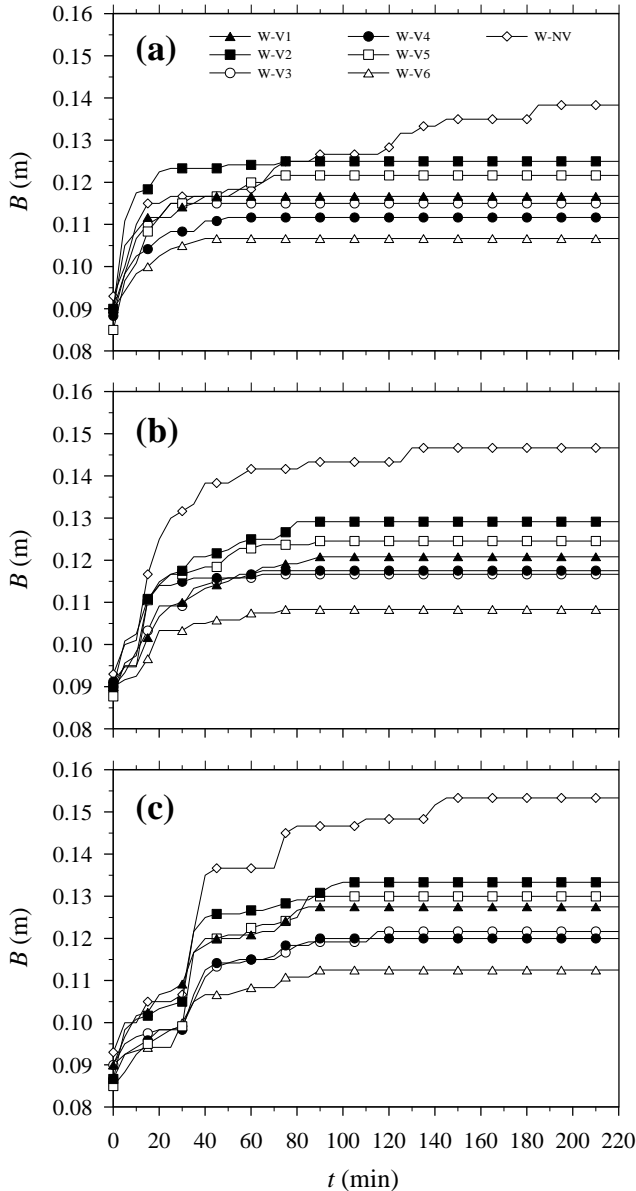


Figure 6.8: Channel-width (B) variation with time in the experiments carried out in Flume No. 2 for: (a) Constant discharge, (b) Hydrograph 1, and (c) Hydrograph 2. The vegetation properties are summarized in Table 6.2 and the hydrographs are shown in Figure 6.5d.

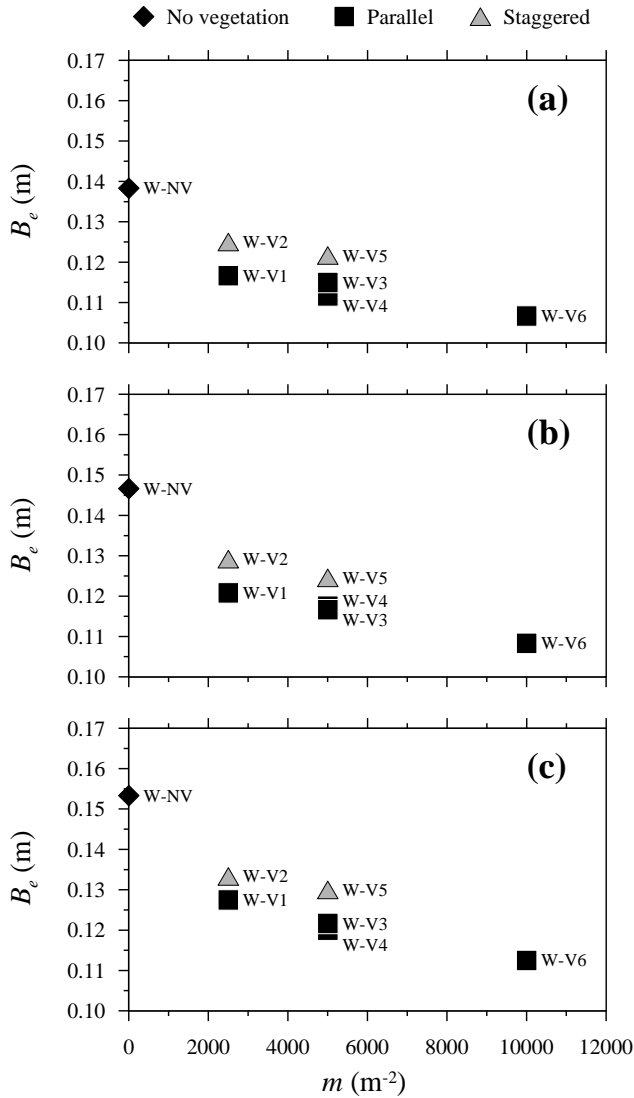


Figure 6.9: Equilibrium channel width (B_e) for the experiments carried out in Flume No. 2 for: (a) Constant discharge, (b) Hydrograph 1, and (c) Hydrograph 2. The vegetation properties used are summarized in Table 6.2 and the hydrographs are shown in Figure 6.5d.

6.4.3. REPRESENTATION OF BANK DYNAMICS USING RIGID CYLINDERS

THE tests allowed observing several typical processes of real rivers with vegetated floodplains: sinuosity formation, braiding index evolution, bank failure, scroll bar formation, and floating vegetation. Since no substantial difference between constant and variable discharge was found for the un-vegetated cases, the tests including vegetation were performed only under variable flow regimes. In general, narrower and more

stable channels were obtained for the experiments with vegetated banks, as in the previous section. The planform evolution for the tests performed in this section is given as supplementary material at: <http://dx.doi.org/10.1016/j.advwtres.2015.10.004>.

CHANNEL SINUOSITY

FIGURE 6.10 shows the evolution of channel sinuosity as a function of time. Variations in sinuosity appear related to discharge variability and vegetation density. In the experiments without vegetation the overall sinuosity of the channel was relatively similar for constant (P-NV(C)) and variable discharges (P-NV), even if the bank erosion pulses driven by the high flows can be easily identified. In general, discharge variability provided a more stable channel. This can be attributed to channel incision during low flows. Comparing the results of tests shown in Figure 6.10, it is possible to observe that the sinuosity is lower with denser vegetation, demonstrating the effectiveness of the rigid cylinders in increasing the bank strength. Figure 6.10 shows also that a smaller penetration depth increases sinuosity significantly (compare P-V1 with P-V2 and P-V3, having the same vegetation density). Nevertheless, in the experiment P-V3 a significant reduction of the channel sinuosity was observed after the peak discharge at 240 minutes. This change in sinuosity occurred because the wooden sticks that were deposited on bars were suddenly transported downstream by the peak flow, reducing bank protection.

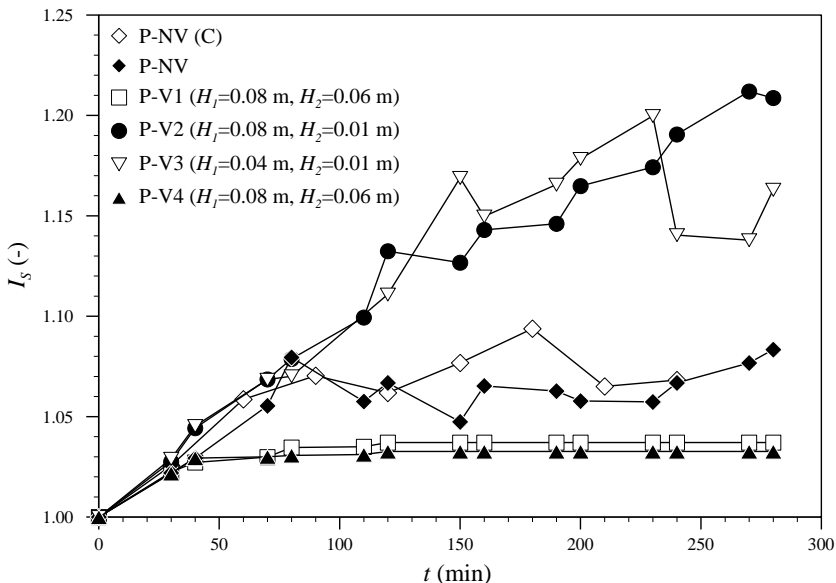


Figure 6.10: Channel sinuosity (I_s) variation with time for the experiments carried out in Flume No. 3. The letter C indicates the experiment that was performed with constant discharge. The vegetation properties used are summarized in Table 6.3 and the hydrographs are shown in Figure 6.6c.

BRAIDING DEGREE

FIGURE 6.11 shows the planform obtained at the end of each experimental test, and emphasizes the difference between the tests without vegetation (P-NV) and the tests with vegetation (P-V1 to P-V4). Un-vegetated channels eventually evolve in wide braided systems (Figures 6.11b and 6.11c). Moreover, it is relevant to highlight the large difference among tests P-V1, P-V2, and P-V3 differing in penetration depth and vegetation length, see Table 6.3 and Figures 6.11d, 6.11e, and 6.11f. A higher penetration depth results in a drastically more stable channel (Figure 6.11d); larger plants with the same penetration depth (PV-2 and PV-3) result in larger eradication rates and a wider channel (compare Figs 6.11e and 6.11f).

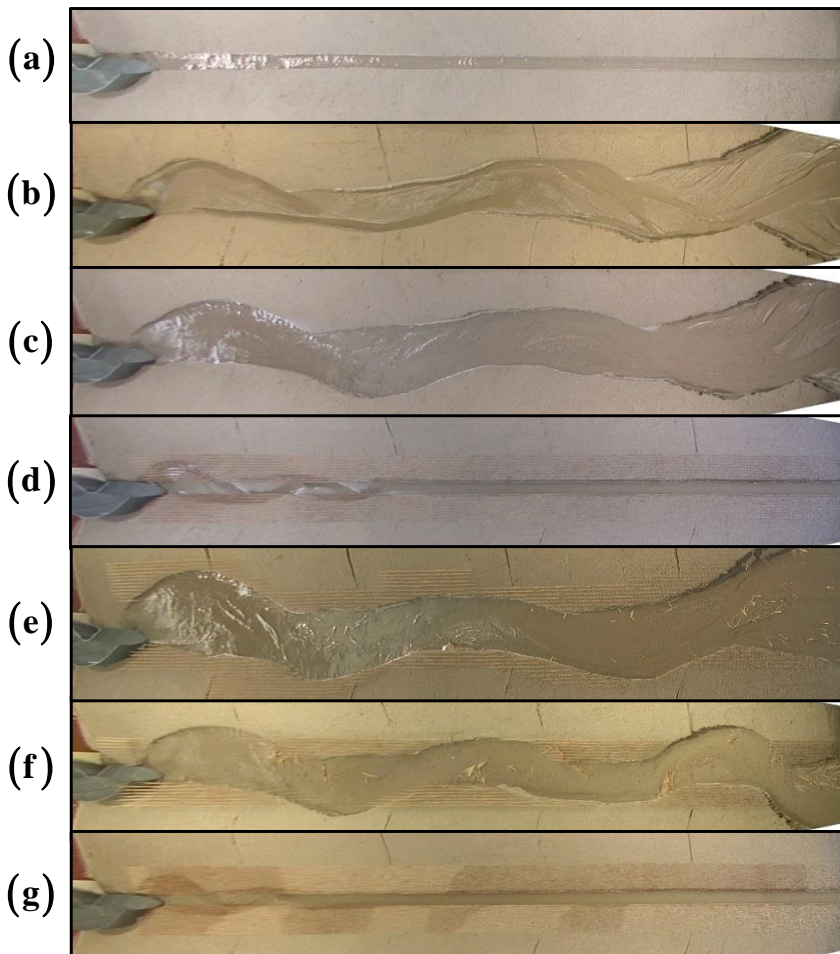


Figure 6.11: Common initial configuration (a) and channel planform after 240 minutes for the experiments in Flume No. 3: (b) Test P-NV (constant discharge); (c) Test P-NV (variable discharge); (d) Test P-V1; (e) Test P-V2; (f) Test P-V3; (g) Test P-V4. Vegetation properties are listed in Table 6.3.

The results show that the reduction of the braiding degree in channels found in former laboratory experiments with the addition of real vegetation, (Tal and Paola, 2007; Gran and Paola, 2001; Braudrick et al., 2009; Tal and Paola, 2010) can be also obtained with rigid sticks.

BANK FAILURE AND LARGE FLOATING DEBRIS

BANK failure occurred due to toe erosion, as shown in Figure 6.12a. Subsequently, the material fallen in the channel acted as bank protection, retarding the next failure episode. This process has been identified also at the outer bends of real meandering rivers (e.g. Dulal et al., 2010). Figure 6.12b shows how the eradicated sticks were later deposited on the bars more downstream, particularly at the bar edge, stabilizing and retaining sediment, deflecting the water flow and promoting erosion near the opposite bank, thus increasing channel sinuosity. Moreover, the sticks on bars increased channel stability in such a way that only one main channel was observed for a longer period, contrary to observations in tests with fixed vegetation or with un-vegetated banks. Assuming that the rigid elements used in these experiments have comparable relative size and properties to woody debris, it is possible to state that the observed processes resemble those occurring in real rivers in U.S.A. (Abbe and Montgomery, 2003; Brummer et al., 2006; Collins et al., 2012) and Europe (e.g. Gurnell et al., 2001; O'Connor et al., 2003; Gurnell et al., 2006; Corenblit et al., 2010). Results shown in Figure 6.12b also agree with the recent findings of the experimental work carried out by Bertoldi et al. (2015).

SCROLL BARS

THE formation of scroll bars along the channel is recognizable due to sediment sorting. Figure 6.12c shows that fine sediment is deposited at the edge of a bar, whereas the coarser fraction settled more downstream as described in most meandering rivers (e.g. Nanson, 1980).

6.5. REPRESENTATION OF RIVERS PROCESSES ADOPTING BAPTIST'S METHOD

THE performance of numerical models adopting Baptist's method (Baptist, 2005) is here assessed based on additional analysis based on our experimental findings and the comparative review of a number of published numerical tests. The numerical simulations were all carried out with similar, and therefore comparable, two-dimensional (2D) models developed from the open-source physics-based morphodynamic software Delft3D solving the Reynolds equations for incompressible fluid and shallow water.

The computations were carried out using a depth-averaged model provided with a parametrization of the 3D effects that become relevant for curved flow (Struiksma et al., 1985) and accounting for the effects of gravity on bed load direction (Bagnold, 1966; Ikeda, 1982). The effects of vegetation on bed roughness and sediment transport were accounted for according to Baptist's method (Baptist, 2005), described in Section 6.2, computing the sediment transport rate as a function of τ_b (Equation 6.2 or 6.6) and the water depth as a function of the total bed shear stress, $\tau_b + \tau_v$ (Equations 6.1 to 6.9). Bed

load was computed using Meyer-Peter and Muller's sediment transport capacity formula (Meyer-Peter and Müller, 1948). Suspended load was computed adopting the method developed by Galappatti and Vreugdenhil (1985).

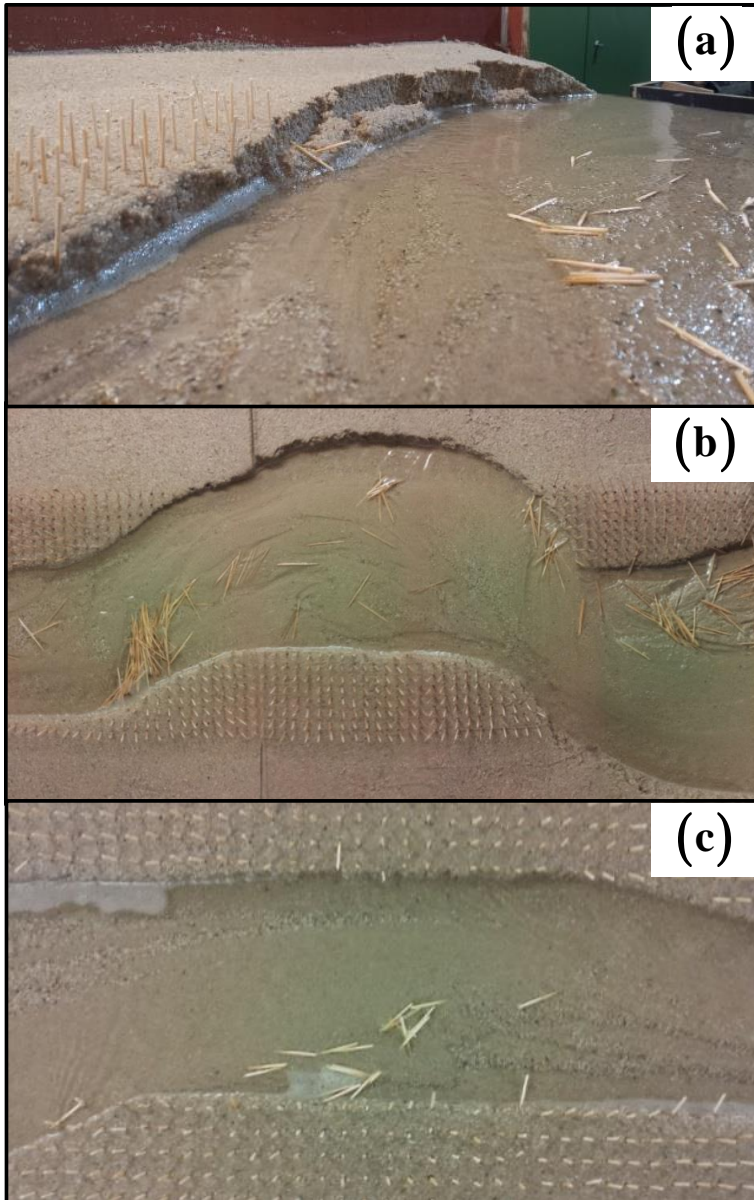


Figure 6.12: Processes observed in the experiments carried out in Flume No. 3: (a) bank failure (view from upstream); (b) large wood deposition (view from above), and (c) Scroll bars formation (view from above).

Delft3D computes the local bed level changes by means of sediment balance equations, resulting in temporal bed level changes in case of spatial imbalance of the sediment transport. Two different approaches are adopted: Exner's approach, valid for immediate adaptation of sediment transport to flow velocity, for bed load; and 2D advection-diffusion equations with sediment entrainment and deposition appearing as forcing terms, for suspended load. Bank erosion is computed relating bank retreat to bed degradation at the toe of the bank (van der Wegen and Roelvink, 2008).

The characteristics of all underlying mathematical equations and their numerical representation are described more in detail in the manuals, which can be downloaded from <http://oss.deltares.nl/web/delft3d/manuals>. The software can be downloaded from <http://oss.deltares.nl/web/delft3d/source-code>.

6.5.1. REPRODUCTION OF THE MORPHOLOGICAL EFFECTS OF VEGETATION OBSERVED IN EXPERIMENTS BY BAPTIST'S METHOD

TO study how well Baptist's method (Baptist, 2005) predicts the global flow resistance and mean flow velocity over vegetated beds we compared the values measured in the experiments carried out in Flume No 1 with model predictions. Measured Chézy coefficients were derived from the friction coefficients, C_f , by using the relation $C_r'_{Measured} = \sqrt{g/C_f}$. Predictions for the wooden sticks were calculated with the properties of each tested array of cylinders. For the case of real and artificial plants, predictions were obtained by representative arrays of rigid cylinders with the vegetation height of each type of plant, but the characteristics of the highest-density wooden-stick configurations (see Section 6.4.1). The drag coefficient, C_D , was here assumed equal to unity and the Chézy coefficient for the bare soil, C_b , was obtained from the results of the experiments for the un-vegetated conditions.

The comparison between measured and estimated Chézy coefficients and mean flow velocities for the real and artificial plants, and rigid cylinders is shown in Figs 6.13 and 6.14, respectively. The most consistent predictions for the wooden sticks are obtained for the highest density configurations, which is in accordance with the assumptions of the method. The results show that Baptist's method (Baptist, 2005) leads to an overestimation of Chézy coefficients and mean flow velocities, for real and artificial plants as well as for rigid cylinders, producing the underestimation of water depths. This is attributed here to: 1) the uncertainty in the value of the Chézy coefficient for the bare soil, which was here assigned on the basis of the un-vegetated cases, and 2) excessive reduction of global flow resistance as a function of the submergence ratio (see Equation 6.9), considering the small values of the Chézy coefficient that were derived for the experiments. A similar function of the submergence ratio appears also in equation 6.7, used for the computation of sediment transport in vegetated areas. Overestimation of the effects of the submergence ratio on the reduction of flow resistance explains both the reduction of morphological changes (Equation 6.9) and the overestimation of mean flow velocity (Equation 6.9). The term including the submergence ratio is related to a logarithmic velocity profile above vegetation, but corrections accounting for turbulence effects are not included. Baptist et al. (2007) identified that the method performs better in cases with high values of the Chézy coefficient, but without providing explanations.

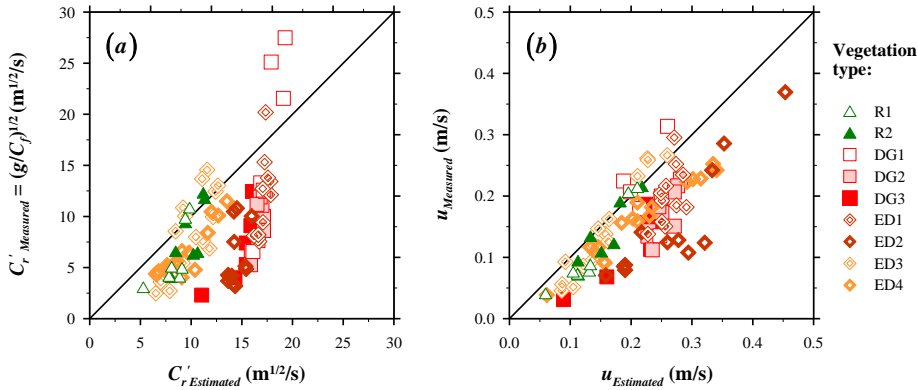


Figure 6.13: Measured and estimated Chézy coefficient and mean flow velocity for real and artificial plants at submerged conditions: (a) Chézy coefficient, and (b) mean flow velocity. Vegetation properties are listed in Table 6.1.

Figure 6.13 also shows that the estimated Chézy coefficients exhibit a noticeable variation only for the highest density configurations of rigid cylinders, whereas very similar values are obtained for each vegetation height in the other configurations. This behaviour results from the increase of the hydraulic roughness due to vegetation in Baptist's method (Baptist, 2005) which also depends on the magnitude of the Chézy coefficient for the bare soil, C_b . This can be seen if C_b is extracted from the squared root of the first term of Equation 6.9, obtaining the expression

$$C'_r = C_b \sqrt{\frac{1}{1 + C_D a h_v C_b^2 / 2g}} + \frac{\sqrt{g}}{\kappa} \ln\left(\frac{h}{h_v}\right) \quad (6.12)$$

The first term of equation 6.12 shows that noticeable reductions of C_b are obtained with high values of $C_D a h_v C_b^2 / 2g$, which are not only reached with high densities, but also with relatively high values of C_b . However, values of C_b over $20 \text{ m}^{1/2}/\text{s}$ lead to similar estimations of this first term for a wide range of densities. This fact is especially important in mobile bed laboratory experiments in which low values of the Chézy coefficient for the bare soil are normally observed, pointing out relevant issues for upscaling processes as well.

6.5.2. REPRODUCTION OF THE EFFECTS OF FLOODPLAIN VEGETATION ON RIVER MORPHOLOGY WITH BAPTIST'S METHOD

THIS part of the study reviews the numerical investigations performed by Baptist and de Jong (2005) and by Crosato and Samir Saleh (2011) on the Allier River upstream of Moulins, France. In the study area, the Allier is a highly-dynamic gravel-bed river at the transition between meandering and braided (e.g. Crosato and Mosselman, 2009), forming large meanders with side channels and central bars. Floodplain vegetation is characterized by pioneer species and grass on the lowest and highest parts of point bars, as well as by softwood forest in the highest and oldest parts of the floodplains.

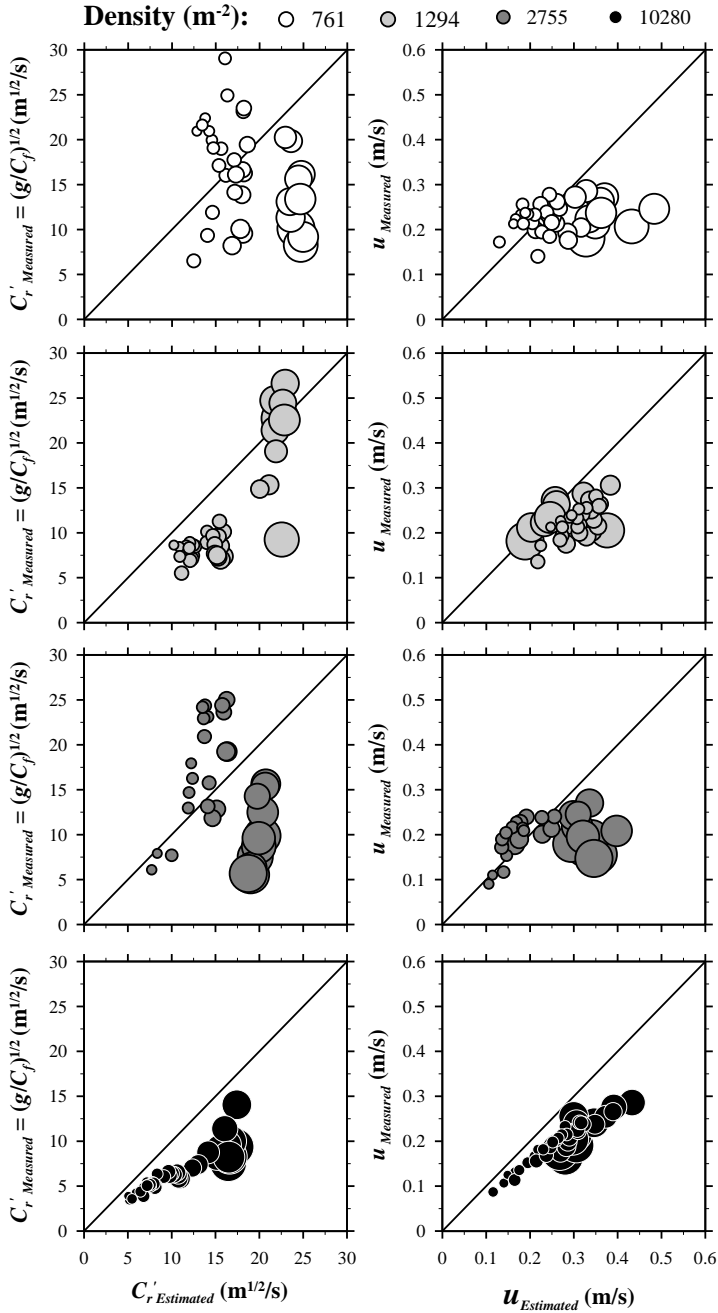


Figure 6.14: Measured and estimated Chézy coefficient and mean flow velocity for submerged rigid cylinders with different densities. Left panels: Chézy coefficient; right panels: mean flow velocity. Larger marker sizes indicate larger submergence ratios.

The simulations of [Baptist and de Jong \(2005\)](#) regarded the prediction of the morphological changes during one year characterized by a major flood event. [Crosato and Samir Saleh \(2011\)](#) simulated the effects of floodplain vegetation on the river planform formation. The model by Crosato and Samir Saleh was set up to represent a river having the characteristics of the Allier near Moulins, starting from a straight channel. Several cases were analysed, including bare floodplains and floodplains uniformly covered by either pioneer vegetation or grass, with constant or variable discharge. For variable discharge and vegetated floodplains, the sediment deposits that became dry during low-flows were colonized by plants having the same characteristics as floodplain vegetation (either pioneer vegetation or grass). The sediment was assumed uniform with particle diameter equal to $5 \times 10^{-3} \text{ m}$ with the same characteristics in the entire model domain, including channel and floodplains.

Both studies adopted a Chézy value of $50 \text{ m}^{1/2}/\text{s}$ to represent bare-bed roughness and considered only bed load transport. Coherently with the rigid-cylinder representation, assuming turbulent flow ([Baptist, 2005](#)), both studies imposed $C_D = 1$ for all vegetation types. The values used for plant height, h_v , stem diameter, D , and density, m , are listed in [Table 6.4](#).

By comparing model results to measurements, [Baptist and de Jong \(2005\)](#) show the importance of including floodplain vegetation to simulate the effects of floods on the Allier River morphology. Their model generally underestimated the morphological changes in both cases, with and without floodplain vegetation. In particular, the model under predicted the erosion rates and did not simulate the observed sedimentation in the higher floodplain parts covered by forest (trees), as well as the filling of the oxbow lake. Without vegetation, the model strongly under predicted bed erosion in the main channel bed, but led to more realistic bed erosion in the floodplain area.

Considering that in the study area sediment varies from sand to coarse gravel, the under prediction of the morphological changes can be partly attributed to not accounting for sediment grading. Finer sediment is more mobile: it is more easily eroded and more easily transported to the upper parts of the floodplains. Accounting for sand could have allowed simulating the filling up of the oxbow lake and the sedimentation in the higher parts of the floodplains. Moreover, the model did not include bank erosion, which was one of the major causes of erosion.

As bed erosion within trees is not reproduced by the model with floodplain vegetation, but is observable in the model without vegetation, we can conclude that the problem is due to the representation of vegetated flows in the model. Moreover, the water flow within trees is not uniform and presents accelerations and decelerations leading to bed erosion and sedimentation, respectively. Assuming uniform flow between the plants is therefore a clear shortcoming of the model in case of sparse vegetation, with the result of neglecting important morphological changes.

Table 6.4: Characteristics of vegetation adopted by: Baptist and de Jong (2005) (1); Facchini et al. (2009) (2); Montes Arboleda et al. (2010) (3).

Vegetation type	Plant height h_v (m)	Stem diameter D (m)	Density m (m^{-2})	Canopy density $a=mD$ (m^{-1})	C_D (-)	Product $a \times C_D$ (m^{-1})
Production forest (1)	10	0.042	2	0.0840	1.0	0.0840
Close floodplain forest (1)	10	0.042	1.2	0.0504	1.0	0.0504
Open floodplain forest (1)	10	0.042	0.4	0.0168	1.0	0.0168
Close shrub (1)	5	0.010	10.2	0.1020	1.0	0.1020
Open shrub (1)	5	0.010	3.4	0.0340	1.0	0.0340
Herbaceous vegetation (1)	0.5	0.005	400	2	1.0	2
Floodplain grassland (1)	0.2	0.003	3000	9	1.0	9
Production grassland (1)	0.1	0.003	4000	12	1.0	12
Pioneer vegetation (1)	0.1	0.003	50	0.1500	1.0	0.1500
Pioneer vegetation (2)	0.15	0.003	50	0.150	1.8	0.270
Production grassland (2)	0.06	0.003	15,000	45	1.8	81
Natural grassland (2)	0.10	0.003	4000	12	1.8	21.6
Herbaceous vegetation (2)	0.20	0.003	5000	15	1.8	27
Dry herbac. vegetation(2)	0.56	0.005	46	0.230	1.8	0.414
Shrubs (2)	6	0.034	3.8	0.130	1.5	0.195
Softwood forest (2)	10	0.140	0.2	0.028	1.5	0.042
Natural grassland (3)	0.1	0.003	4000	12	1.8	21.6
Reed (3)	2.5	0.0046	80	0.368	1.8	0.660
Softwood forest (3)	10	0.14	0.2	0.028	1.5	0.042

Starting from a straight channel having the characteristics of the Allier River, by [Crosato and Samir Saleh \(2011\)](#) obtained a strongly braided channel without floodplain vegetation, a channel with drastically lower braiding intensity with low-density pioneer vegetation, and a channel at incipient meandering conditions with low-density grass on floodplains.

A number of laboratory experiments show similar results (e.g. [Tal and Paola, 2007](#)), whereas similar effects of vegetation are observable also in real rivers (e.g. [Gibling and Davies, 2012](#)). However, it seems not realistic to assume that pioneer vegetation with the very low density of 4.5 elements per square meter has such a strong effect on real rivers. The results therefore indicate that the vegetation model most probably over predicts the stabilizing effects of low-density vegetation, which can be due to overprediction of bed roughness reduction within the plants, as presented in Section 6.5.1.

6.5.3. REPRODUCTION OF SEDIMENTATION RATES ON VEGETATED FLOODPLAINS WITH BAPTIST'S METHOD

THIS part of the study reviews the results of the investigations carried out by [Facchini \(2009\)](#); [Facchini et al. \(2009\)](#); [Montes Arboleda et al. \(2010\)](#) to investigate the capability of the model in representing the effects of floodplain vegetation on local sedimentation rates.

[Facchini \(2009\)](#) and [Facchini et al. \(2009\)](#) simulated the short-term sedimentation rates on the Ewijkse Plaat, a floodplain of the Waal River, near Nijmegen, the Netherlands for the period 1990-1997 for which measured bed topographies, erosion and sedimentation maps and averaged sedimentation rates in the study areas as well as the temporal evolution of vegetation were available ([Bouwman, 1999](#); [Geerling et al., 2008](#)). The model used daily measured discharges and included both bed load and suspended load. Three sediment fractions were considered: coarse sand, medium sand and silt. Sediment inputs were derived by [Asselman \(1997\)](#). Vegetation was represented as in Table 6.4.

[Montes Arboleda et al. \(2010\)](#) simulated the floodplain sedimentation rates along the Waal River on the long term and compared the model results with the average sedimentation rates derived from the analysis of coring data carried out by [Middelkoop \(2002\)](#). The study site is the floodplain of the Waal River between the cities of Nijmegen and Tiel including the Ewijkse Plaat. The major difference between the two studies lies in the time period, since [Montes et al.](#) studied the river in 1800 A.D.

The daily discharges were derived from the water levels measured at Arnhem and the discharges measured at Cologne using the Q-h relationships derived by [van Vuuren \(2005\)](#). [Montes et al.](#) considered two sediment types: sand and silt. Assuming that the incoming sediment concentrations were the same as at present, the same rating curve developed by [Asselman \(1997\)](#) was used as upstream boundary condition. Vegetation data were derived from the ecotope maps reconstructed by [Maas et al. \(1997\)](#), showing that also at that time the dominant floodplain vegetation was herbaceous or grass. Three vegetation types were considered: natural grass, reed and softwood forest (Table 6.4).

The results of [Facchini et al. \(2009\)](#) show that the model reproduces the averaged short-term bed level rises quite well (period 1994-1995: computed 0.081 m, measured 0.080 m; period 1994-1997: computed 0.101 m, measured 0.090 m).

The results of [Montes Arboleda et al. \(2010\)](#) show that the model reproduces well also the long-term floodplain sedimentation rates. The averaged historical sedimentation rates derived from coring of the floodplain soil for the period around 1800 AD ranges between 5 and 16 mm/year, whereas the computed sedimentation rates ranged between 6.3 and 13.5 mm/year. Moreover, the results show that vegetation results in higher sedimentation rates in the areas close to the main river channel and lower sedimentation rates in the farther areas of the floodplain, confirming the observations by [Pizzuto \(1987\)](#). The increased flow resistance exerted by vegetation leads to flow concentration in the main channel and reduces flow velocity, as well as suspended solids concentration over the floodplains, as reported also by [Villada Arroyave and Crosato \(2010\)](#). Even though flow velocity reduction enhances sediment deposition, the reduction of sediment concentration over the floodplain results in lower sedimentation rates, especially in the areas that are far from the channel.

6.6. CONCLUSIONS

IN this chapter we have managed to combine experimental work from three experimental settings, ranging from flow interaction with vegetation to vegetation induced bank migration. The first laboratory set-up shows that the hydraulic roughness of vegetated beds decreases for increasing element Reynolds numbers, which is according to expectations. Rigid cylinders show the same trends and have friction coefficients of the same order of magnitude, but are characterized by element Reynolds numbers which are significantly smaller than the ones of real and plastic plants. Diameters of 8.3 mm used by [Cheng \(2011\)](#) offer the best resemblance with the results of our real and plastic plants. Plant flexibility was detected to be relevant for the flow resistance particularly for plants with foliage. Surprisingly, the submergence ratio (h/h_v) was not found to affect the flow resistance in our laboratory experiments.

Laboratory set-ups two and three allowed establishing the applicability of rigid cylinders to qualitatively represent the morphodynamic processes of channels with vegetated floodplains. Results obtained in Flume No. 2 showed the potential of using rigid cylinders to study the influence of vegetation on the channel-width formation. Parallel configurations of rigid cylinders were found more effective in reducing the channel-width than staggered configurations. The results of the experiments carried out in Flume No. 3 show that it is possible to qualitatively reproduce bank dynamics-related processes and reduce the river braiding degree by placing rigid cylinders on the floodplains. The height of the rigid cylinders above the bed and the penetration depth into the bed were found of relevance for the channel planform formation.

Numerical models adopting Baptist's method ([Baptist, 2005](#)) to reproduce the effects of plants provide satisfactory results for high-density grass and herbaceous vegetation.

Particularly satisfactory are the predictions of sedimentation rates on vegetated floodplains. The method performed well also for the reproduction of the effects of floodplain vegetation on the river planform formation, although the results are only qualitative. However, in general Baptist's method (Baptist, 2005) leads to overestimation of the bed protection effects of low-density vegetation, in particular for trees and pioneer plants. This overestimation is mainly due to the basic assumption that the flow velocity is uniform among the plants, which is not true for low-density vegetation. In some cases, trees are found to enhance rather than prevent bed erosion, since they act as isolated roughness elements (e.g. Coulthard, 2005). Therefore Baptist's method does not appear suitable to reproduce the effects of trees and isolated plants nor of patchy vegetation distributions (e.g. Temmerman et al., 2007).

Representation of the effects of vegetation in the model is based on three parameters: the vegetation density, a , the plant height, h_v , and the drag coefficient, C_D . These parameters are multiplied to each-other to form a bulk parameter weighing the effects of plants on the bed shear stress in Equations 6.5, 6.7 and 6.9. The plant height appears again in the submergence ratio in Equations 6.7 and 6.9, in which higher values of the ratio result in smoother channels beds.

Comparison between data measured in the laboratory and predictions show that Baptist's method (Baptist, 2005) overpredicts mean flow velocities, underpredicting water depths. This can be attributed to an excessive reduction of global flow resistance related to the submergence ratio of vegetation, especially for low Chézy coefficients (rough beds). This leads also to overestimations of the effects of submerged vegetation in reducing local morphological changes (erosion and deposition).

Baptist (2005) assigns a value between 1 and 2 to the drag coefficient, whereas a number of researchers (e.g. Fischer-Antze et al., 2001; Helmiö, 2002; Stoesser et al., 2003) suggest using $C_D = 1$ for multiple cylinders and high Reynolds numbers (turbulent flows). We argue that a coherent representation of plants as rigid cylinders requires adopting always the same value for the drag coefficient, this being the value derived for cylinders. We therefore suggest imposing C_D equal to unity in numerical models. In this case, vegetation is basically distinguished by canopy density, a , and plant height, h_v . This simpler characterization would allow for a clearer interpretation of the morphodynamic effects of different types of vegetation.

7

MORPHOLOGICAL EFFECTS OF RIPARIAN VEGETATION GROWTH AFTER STREAM RESTORATION

“Nature did all things well.”

Michelangelo



Figure 7.1: The Lunterse Beek stream, Renswoude, The Netherlands.

Based on the field campaigns carried out in a lowland restored stream in the Netherlands, the Lunterse Beek, the morphodynamic effects of riparian vegetation growth are presented by combining several information types and sources. A numerical model is used in order to test its capability in predicting the evolution of the field observations and to identify the relevance of including seasonal variations of vegetation.

This chapter has been submitted to *Earth Surface Processes and Landforms* and is currently under peer review.

7.1. INTRODUCTION

A large number of lowland rivers has been severely altered by humans to lower flood levels, reduce natural channel migration, increase land drainage and improve navigation (Brookes, 1988; Gleick, 2003). Channelization is one of the most common interventions, leading to a considerable number of unnatural rivers around the world. Channelized rivers are often also straightened, with long-term consequences that include: increased flood risk downstream, channel incision, decreased communication between main channel and floodplains, lowered groundwater tables and reduction or elimination of bars and point bars. The result is a general loss of morphological complexity, as well as biodiversity and productivity in both main channel and floodplains (Goodwin et al., 1997; van Ruijven and Berendse, 2005; Richardson et al., 2007; Gross et al., 2014).

Considering the importance of preserving riverine ecosystems (Brachet et al., 2015), there has been an increasing awareness of the need to halt degradation and rehabilitate rivers through restoration programs since the early 1980s (e.g. Buijse et al., 2002; Bernhardt and Palmer, 2007). Currently, most river restoration projects are found in U.S.A. and Europe (River Restoration Organization, <http://www.riverrestoration.org/>; European Centre for River Restoration, www.ecrr.org; the River Restoration Centre, <http://www.therrc.co.uk/>), particularly in the most populated areas, characterized by temperate climates. Here, vegetation shows a clear seasonal cycle (Peel et al., 2007) with larger plant coverage in summer and lower in winter and spring when hydrodynamic forcing is at maximum.

River restoration projects can be divided in two categories (Parker, 2004): landscape-design-based and process-based. The first category includes the projects aiming at increasing the aesthetical value of the riverine area, restricting or impeding any morphological adaptation. Projects of this type are often carried out in urban contexts to create recreational areas (PUB, 2014, e.g.). The second category comprehends all projects aiming at restoring a certain degree of natural river dynamics, including some morphodynamic processes (e.g. Beechie et al., 2010). A large part of these projects include channel re-meandering (Kondolf, 2006, e.g.), but in most cases the freedom of the river to migrate laterally remains limited to avoid damages to agricultural land and private property (Piégay et al., 2005, e.g.). This means that some morphological processes, such as bank erosion, bank accretion and channel widening, are often seen as undesirable (e.g. Kondolf et al., 2001). Moreover, in many cases floodplain vegetation is regularly cut to limit flood levels (Nienhuis and Leuven, 2001). In general, the quantification of the effects of restoration projects remains a difficult task for practitioners, scientists and managers (Walker et al., 2007; Schirmer et al., 2014; González et al., 2015) and, despite their increasingly large number, only few projects include post-restoration monitoring activities (Kondolf and Micheli, 1995; Bernhardt et al., 2005, 2007). In addition, there is no consensus on the criteria to be adopted to evaluate the effectiveness of restoration measures (Palmer et al., 2005). The experience gained from the past has always been important for future projects (Kondolf and Micheli, 1995). Learning from others' experience enables professionals in river restoration to set more realistic goals and improve design procedures and standards, as well as reduce maintenance costs (Kondolf and Micheli,

1995; van Breen et al., 2003; Dufour and Piégay, 2009). The proper setting of achievable and measurable goals in stream restoration programs is, therefore, an important activity, which in turn requires a clear understanding of the morphodynamic processes of these systems (Hobbs, 2005; Kondolf, 2011). Such knowledge would allow assessing the geomorphological and ecological conditions that can be obtained after restoration measures, avoiding unwanted morphodynamic responses. However, only few post-restoration studies analysed the river eco-geomorphological response (González et al., 2015) and even less analysed the effects of floodplain vegetation growth and maintenance to establish whether the initial goals have been achieved.

There are two-way interactions between riparian vegetation and fluvial geomorphology. Plants alter water flow, soil resistance and sediment processes, which in turn determine plant settlement, establishment and survival (Simon et al., 2004; Corenblit et al., 2007; Gurnell, 2012). In particular, riparian vegetation decreases soil and bank erosion and increases sediment deposition by locally reducing flow velocity (e.g. Owens et al., 2005; Facchini et al., 2009; Montes Arboleda et al., 2010; Västilä et al., 2016) and through the additional soil-binding action of roots, riparian vegetation also increases bank stability (Hickin, 1984; Thorne, 1990; Gyssels et al., 2005; Berendse et al., 2015; Pollen-Bankhead and Simon, 2010).

Considering the importance of these feedbacks, morphodynamic models including vegetation dynamics are being considered as a valuable tool to predict the evolution of river systems (Solari et al., 2015). However, current state-of-the-art models only consider plants in a strongly simplified way, disregarding seasonal variations (Camporeale et al., 2013; Vargas-Luna et al., 2016b), an aspect of special relevance in temperate climates, not yet quantitatively addressed (e.g. Champion and Tanner, 2000; Cotton et al., 2006; Jankowska et al., 2014).

This study analyses the morphological evolution of a small lowland river located in the Netherlands, the Lunterse Beek (see Figure 7.1). Re-meandered in 2011, this stream is assumed to be a representative of small restored rivers in temperate climates, as many in U.S.A. (e.g. Kondolf et al., 2013, <http://www.riverrestoration.org/>) and Europe (Mohl, 2004; Madsen and Debois, 2006, www.ecrr.org; <http://www.therrc.co.uk/>).

The goal is to obtain data and insight on the morphodynamic effects of riparian vegetation, and in particular its seasonality, on the morphological developments of small water courses. The work is made possible by the availability of detailed data covering the first 5 years of development after restoration, in which the river floodplains evolved from completely bare to richly vegetated.

To study the applicability of state-of-the-art numerical tools for predicting the evolution of restored streams, a 2D morphodynamic model (Delft3D) is setup and applied to reproduce the observed behaviours. The model is also used as a tool to assess the relevance of considering the seasonal variations of vegetation to study the morphological evolution of this type of streams.

7.2. STUDY AREA DESCRIPTION

THE Lunterse Beek is a lowland stream located in the central part of the Netherlands, see Figure 7.2a. The stream has a catchment area of 63.6 km^2 , of which 80 % is used for agriculture, and a mean daily discharge of $0.36 \text{ m}^3/\text{s}$. The relevant catchment characteristics are listed in Table 7.1. In October 2011, a restoration project was conducted on this stream over a reach of 1.6 km , located to the north of Renswoude, a municipality of the province of Utrecht. A bare soil channel (6.5 m wide and 0.4 m deep) with a longitudinal slope of $0.96 \text{ m}/\text{km}$, lowered floodplains and a sinuous planform was excavated to replace the former straightened channel, see Figure 7.2a. The overall restoration goal was meant to improve the ecological conditions of the riverine area while maintaining flood safety and appropriate groundwater levels for agriculture. The study area is a 200 m long reach where detailed field work has been undertaken since restoration. A series of weirs, and a bridge and a gauging station are located upstream and downstream of the study area, respectively, defining well marked boundary conditions (Figure 7.2a). The river bed material is composed by medium to fine sand with median diameter, D_{50} , equal to $258 \mu\text{m}$, with the exception of a 20m -long reach in which the channel bed is excavated in a peat deposit (Figure 7.2b). Previous studies have shown that there are no noticeable temporal variations in the bed material composition (Eekhout et al., 2014; Eekhout and Hoitink, 2015).

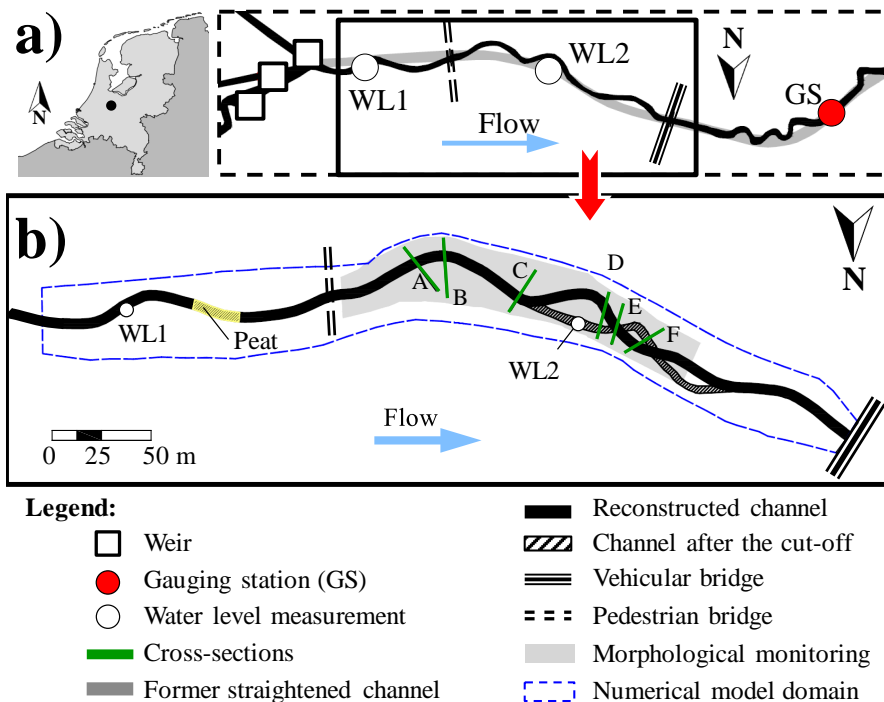


Figure 7.2: Study area. (a) Localization and boundary conditions of the reconstructed channel, and (b) Sketch of the stream employed in this study

Table 7.1: Catchment characteristics in the study area for the Lunterse Beek.

Attribute	Value
Latitude	52° 4' 46" N
Longitude	5° 32' 37" E
Altitude (m.a.s.l)	5.2
Catchment area (km ²)	63.6
Annual average rainfall (mm) ^a	820.4
Annual average temperature (°C) ^a	9.8
Mean daily discharge (m ³ /s) ^b	0.36
Maximum daily discharge (m ³ /s) ^b	4.26
Sediment size (x 10 ⁻⁶ m) ^c	258

^a Calculated from data recorded at Wageningen-Veenkampen in 1971-2015.

^b Calculated from data recorded at Barneveldsestraat between January 2011 and April 2016.

^c As reported by [Eekhout et al. \(2014\)](#).

A cutoff, triggered by the formation of a bar, occurred a very short time after channel re-meandering when vegetation was still absent.

7.3. MATERIALS AND METHODS

THIS study combines the analysis of detailed field observations and 2D morphodynamic modelling, based on the Delft3D code, covering the first 5 years after restoration. Field data include hydrological time-series, high-resolution bathymetric data, photos acquired with an unmanned aerial vehicle and standard aerial photographs. The analysis of field data allows describing the processes that occurred in the study area. The comparison between modelled and observed evolution allows establishing whether a state-of-the-art numerical tool including the effects of vegetation can be used to optimize stream restoration projects by predicting the channel response beforehand. The comparison of different modelled scenarios, in which vegetation properties are either kept constant or changed over time and space according to observations, allows assessing the importance of including seasonality and/or other vegetation dynamics for this type of investigations.

7.3.1. DATA SOURCES, DATA COLLECTION AND PROCESSING

TIME-SERIES of discharges and water levels, measured at Barneveldsestraat, downstream of the study reach (GS in Figure 7.2a), were provided by the Water board (Waterschap Vallei en Veluwe) who provided also water level time series at two other locations along the study reach (WL1 and WL2 in Figure 7.2a). Daily precipitation and mean air temperature time-series were provided by the Royal Netherlands Meteorological Institute (KNMI) ([Klein Tank et al., 2002](#)). The station Wageningen-Veenkampen (ID 8555) is the nearest to the study reach (51° 58' 53" N, 5° 37' 18" E).

The bed topography, including channel and floodplains, was measured in the framework of this study over a length of almost 200 m every two months on average. The information about the surveys is listed in Table 7.2 and the monitored area is indicated in

light grey in Figure 7.2b. Real Time Kinematic (RTK) GPS equipment (Leica 1200+ for surveys 1 to 13 and Leica Viva GS10 for surveys 14 to 26, see Table 7.2) was used to measure channel-bed and floodplain surface elevations with an accuracy of 1-2 *cm*. Longitudinal water surface profiles were measured during the surveys with the RTK-GPS equipment, following the method proposed by Milan et al. (2011).

Table 7.2: Summary of the field campaigns carried out.

No.	Q (m^3/s)	Date (Y-M-D)	Days after restoration	Point density ($points/m^2$)
1	1.19	2011-10-12	0	0.16
2	0.48	2012-01-13	93	0.32
3	0.40	2012-02-22	133	0.27
4	0.16	2012-04-20	191	0.20
5	0.10	2012-05-30	231	0.31
6	0.11	2012-07-26	288	0.35
7	0.03	2012-09-17	341	0.33
8	0.24	2012-10-23	377	0.43
9	0.77	2012-12-11	426	0.39
10	0.46	2013-01-08	454	0.37
11	0.44	2013-02-12	489	0.35
12	0.28	2013-03-20	525	0.38
13	0.11	2013-04-22	558	0.31
14	0.01	2013-06-19	616	0.34
15	0.02	2013-08-14	672	0.45
16	0.05	2013-10-09	728	0.43
17	0.26	2013-11-27	777	0.43
18	0.57	2014-01-29	840	0.28
19	0.16	2014-04-09	910	0.39
20	0.19	2014-07-09	1001	0.32
21	0.17	2014-11-12	1127	0.34
22	0.26	2015-02-12	1219	0.45
23	0.23	2015-04-09	1275	0.49
24	0.02	2015-06-09	1336	0.45
25	0.06	2015-08-12	1400	0.39
26	0.29	2015-10-22	1471	0.45
27	0.28	2015-12-29	1539	0.40
28	0.23	2016-04-05	1637	0.38

Digital Elevation Models (DEMs) were constructed using the data set obtained with the RTK-GPS equipment, as described by Eekhout et al. (2014). The DEMs were then used to study the morphological evolution of the stream. DEMs of difference (DoDs) were produced for the analyses of seasonal changes (see Table 7.3) (Lane et al., 2003).

Vegetation coverage was monitored with several approaches, at different scales and from different information. Dominant vegetation species were identified for the first two years after restoration during two independent field campaigns (September 2012 and July 2013) by Eekhout et al. (2014). In this study, the seasonal changes and colonization processes were tracked with oblique and in-stream terrestrial photographs that were correlated with the riparian vegetation patterns obtained from aerial photographs.

Table 7.3: Summary of the constructed DODs.

Identifier in Figure 7.7	Difference considered between seasons	Selected campaigns ^a
a	Spring 2012 – Winter 2011	4-2
b	Summer 2012 – Spring 2012	6-4
c	Autumn 2012 – Summer 2012	8-6
d	Winter 2012 – Autumn 2012	11-8
e	Spring 2013 – Winter 2012	13-11
f	Summer 2013 – Spring 2013	15-13
g	Autumn 2013 – Summer 2013	16-15
h	Winter 2013 – Autumn 2013	18-16
i	Spring 2014 – Winter 2013	19-18
j	Summer 2014 – Spring 2014	20-19
k	Autumn 2014 – Summer 2014	21-20
l	Winter 2014 – Autumn 2014	22-21
m	Spring 2015 – Winter 2014	23-22
n	Summer 2015 – Spring 2015	25-23
o	Autumn 2015 – Summer 2015	26-25
p	Winter 2015 – Autumn 2015	27-26
q	Spring 2016 – Winter 2015	28-27

^a Detailed information about campaigns is presented in Table 7.2.

Table 7.4 lists the characteristics of the aerial photographs that were used to establish the vegetation development and its spatial distribution over a length of 300 *m*.

Table 7.4: Summary of the aerial photographs used in the study.

No.	Date (Y-M-D)	Days after restoration	Source	Pixel size (cm)	Season
1	2012-01-17	97	Slagboom & Peters	10x10	Winter
2	2012-07-26	288			Summer
3	2013-02-02	479	Cyclomedia	23x23	Winter
4	2013-07-09	636	Slagboom & Peters	10x10	Summer
5	2014-02-25	867	Cyclomedia	23x23	Winter
6	2014-07-04	996	Dutch cadastre office	60x60	Summer
7	2015-05-11	1307	WUR-UARSF ^a	2x2	Spring
8	2015-06-16	1343			Summer
9	2015-09-09	1428			Autumn
10	2016-01-21	1562			Winter

^a The Unmanned Aerial Remote Sensing Facility of the Wageningen University.

In order to record the development of vegetation after restoration, two types of aerial photographs were used: standard (spatial resolution higher than 10 *cm*) and detailed (spatial resolution smaller than 10 *cm*). The standard aerial photographs were collected from different sources, whereas the detailed ones were taken during the execution of this study, see Table 7.4.

Land cover maps were created from the aerial photographs acquired in 2015 (May 11, June 16 and September 9) and in 2016 (January 21) using an unmanned MAVinci fixed-wing aircraft with an on-board Panasonic Lumix GX1 camera. The raw images were pro-

cessed with Structure-from-Motion photogrammetry (Westoby et al., 2012) using Agisoft Photoscan Professional to create Digital Surface Models (DSM) and orthophotos. The DSM and orthophotos were subsequently used as input for a stratified object-based image classification procedure (Anders et al., 2011) in the software eCognition Developer 9. Here, objects were formed on the basis of clustering DSM and orthophoto image pixels using the multi-resolution image segmentation algorithm (MRS, Baatz and Schäpe, 2000) to distinguish 'water', 'trees', 'bare ground', 'low vegetation' and 'high vegetation' (see Table 7.5). Obvious errors of land cover classifications were corrected manually. Lastly, the same vegetation classes were manually identified in the standard aerial photographs (Photos 1 to 6 in Table 7.4) by using a Geographical Information System (GIS).

Table 7.5: Classification rules for the extraction of vegetation classes from the UAV imagery.

Class	Classifier	5/11	6/16	9/9
Trees	Mean DSM	>5.8	>5.8	>5.8
	Mean DSM	<3.8	<4.6	<4.6
	Mean Blue	55-90	85-120	
	Mean Red	60-130	60-140	60-140
	Stdev Red			<10
Bare ground	Mean Blue	>53	>53	>53
	Stdev Red	>8.5	>8.5	>8.5
	OR			
	Mean Blue	>95		
Low vegetation	Mean Blue	>40	>40	45-75
	Mean Green	<120	<120	<120
High vegetation	All remaining unclassified objects			

7.3.2. MORPHODYNAMIC MODELLING

THE objectives of the numerical investigation were to identify the level of performance of a state-of-the-art 2D morphodynamic model in reproducing the morphological evolution of a small restored stream and to assess the importance of including vegetation and its seasonal cycle in this type of studies. To achieve this, a model was constructed and used to simulate the morphological developments of the Lunterse Beek in the 4-year-long period between Campaign 5 and Campaign 28 (Table 7.2). Four different scenarios were considered: 1) complete absence of vegetation; 2) with short grass, uniformly distributed on colonized banks and floodplains; 3) with herbaceous vegetation uniformly distributed; 4) with the observed seasonal variations of vegetation (type, properties and spatial distribution). Two vegetation types were considered: grass and herbaceous. Although some trees were present in the field, these were not included in the model.

The numerical tool used for this investigation was constructed using the open-source Delft3D software package (<http://oss.deltares.nl/web/delft3d/source-code>). The Delft3D code allows simulating flow, sediment transport and bed level changes in vegetated streams with a simplified representation of bank erosion. The hydrodynamic equations are based on the Reynolds equations for incompressible fluid and shallow water (Lesser et al., 2004) with a parametrization of the 3D effects that become relevant for

curved flow (Struiksmma et al., 1985). The effects of transverse flow convection causing a redistribution of the main flow velocity are accounted for by a correction in the bed friction term. The direction of the sediment transport is corrected by a modification in the direction of the bed shear stress. The model includes the effects of gravity on bed load direction (Bagnold, 1966; Ikeda, 1982). The adopted turbulence closure scheme is a κ - ϵ model, in which κ is the turbulent kinetic energy and ϵ is the turbulent dissipation.

The local bed level changes are derived by means of sediment balance equations. Two approaches are adopted: Exner's approach, valid for immediate adaptation of sediment transport to flow velocity (bed-load) and 2D advection-diffusion equations with sediment entrainment and deposition appearing as forcing terms (suspended load). The mathematical equations and their numerical representation are described more in detail in the manuals, which can be downloaded from <http://oss.deltares.nl/web/delft3d/manuals>.

In Delft3D, bank erosion is currently computed in a strongly simplified way relating bank retreat to bed degradation at the toe of the bank. In practice, the shift of the river bank is obtained by assigning a part of the bed erosion occurring inside the wet cells at the margin of the wet area to their adjacent dry cells, which are then converted in wet cells and become a part of the conveying river channel (van der Wegen and Roelvink, 2008). The effects of vegetation on bed roughness and sediment transport are accounted for according to Baptist's method (2005) which is one of the most complete vegetation models (see Vargas-Luna et al., 2015b, 2016b, for an analysis about the applicability of this method).

7.3.3. MODEL SET-UP AND CALIBRATION

A curvilinear grid following the alignment of the main channel was constructed covering an area 430 m long and 45 m wide, see Figure 1b. To minimize the influence of the boundary the model domain covered an area that is larger than the area of interest (Figure 7.2). The mean grid cell size was 1.5 m with an average aspect ratio of 2.7. The initial bed topography was generated from the elevations measured on 22/02/2012 (campaign 2, Table 7.2), just after the initial cut-off. Daily flow discharge and water level series constituted the upstream and downstream boundary conditions, respectively. The sediment was assumed as uniform, with grain size of 258 μm as observed in the field (Eekhout et al., 2014). The area with the peat bed was not distinguished from the rest.

The morphological evolution and the water level series of the period between Campaign 3 and 5 (see Table 7.2), in which vegetation was not present, were used to calibrate the bare bed roughness, to select the sediment transport formula and to optimize the value of the coefficients weighing the effects of transverse slope. The outcomes of this calibration procedure were: a Chézy coefficient, $C = 45 \text{ m}^{1/2}/\text{s}$ for the areas not covered by vegetation; the Engelund and Hansen (1967) sediment transport formula; and the application of the Koch and Flokstra (1980) approach, extended by Talmon et al. (1995), for the adjustment of the bed-load transport direction on sloping beds.

The adopted density and diameter of the cylinder arrays used in the Baptist method to represent vegetation were derived from calibrated values on real river applications from the literature (Van Velzen et al., 2003; de Jong, 2005; Baptist, 2005). The height of the vegetation was assigned according to the conditions observed in the field during the morphological campaigns, imposing a drag coefficient of 1.0, as suggested by Vargas-Luna et al. (2016b).

7.4. RESULTS OF DATA ANALYSIS

7.4.1. SEASONAL VARIATIONS

THE seasonal variations of climate were identified by analysing the annual and intra-annual variability in precipitation, mean air temperature and flow discharge. Seasonal variations of vegetation characteristics were identified by the data collected in the field.

Figure 7.3 shows the box and whisker plots of the hydrological variables recorded at Wageningen-Veenkampen in the period 1971-2015. The mean air temperature clearly exhibits periods of high (June-August), mean (March-May and September-November) and low (December-February) values, with small intra-annual variability (Figure 7.3a). The monthly total precipitation presents little seasonal variation, but with relatively high intra-annual variability (Figure 7.3b). The water supply to the vegetation remains almost constant throughout the year, which means that seasonal changes in vegetation are mainly driven by temperature variation and flow disturbances. Figure 7.3 shows that most of the outliers recorded within the period of analysis occurred between August and December, defining a period in which the climatic conditions are more unstable. As in most temperate streams, the seasonal variation of vegetation observed along the Lunterse Beek comprises increasing vegetation coverage starting in spring and reaching maximum density in late summer, whilst foliage and root biomass reduction is observed from autumn through winter.

Figure 7.4 shows air temperature and discharge time series indicating also the dates when the aerial photographs were taken and the morphological campaigns were carried out. The highest discharges occur in winter, when the air temperature is at its minimum. It is important to mention that the natural variability of discharge and water levels have been drastically reduced in the study area by the weirs located upstream and the downstream gauging station, controlling the flow and therefore affecting some of the vegetation processes, such as colonization and growth.

7.4.2. MORPHOLOGICAL EVOLUTION

THE DEMs are given as supplementary material A. The first high-flow period that occurred immediately after restoration changed substantially the planform of the Lunterse Beek. No other substantial planform changes were observed in the study period. Figure 7.5 shows the changes between January 2012 and September 2015 (three and a half years). Differences in bed level (Figure 7.5c) emphasize the processes of channel

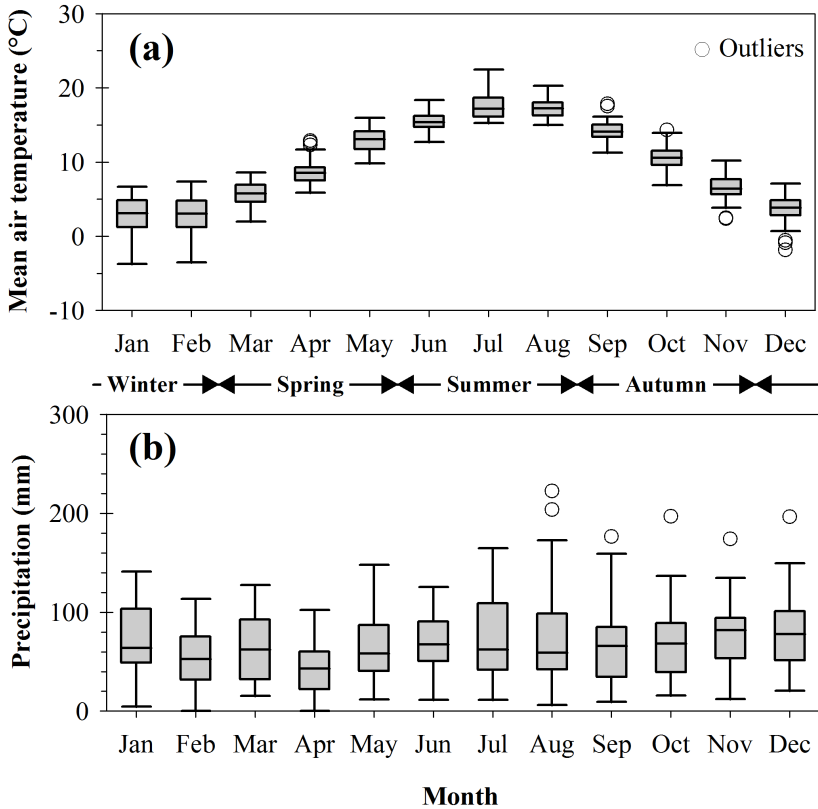


Figure 7.3: Box and whisker plot of the monthly hydrological variables recorded at the Veenkampen station for the period 1971-2015 of: (a) Mean air temperature ($^{\circ}\text{C}$), and (b) Precipitation (mm).

deepening and floodplain rising. Some floodplain soil erosion (lower than 5 cm) occurred far from the channel.

Figure 7.6 shows the temporal evolution of the reach-averaged values of: channel slope, width and bed elevation, floodplain elevation and bankfull water depth, to be compared to the daily discharge time-series. In the study period, the channel slope oscillated between the values of 0.04 and 0.12 (Figure 7.6a) to stabilize around the lowest value. It suddenly decreased in 2011 due to the initial cutoff and later reacted dynamically to deposition and erosion processes as a response to pool migration in the downstream part of the monitored reach. Figure 7.6b shows that the channel-width increased as a retarded response to high flows occurring in autumn and winter, due to bank erosion, and decreased in spring and summer, due to vegetation growth, leading to bank accretion. It is important to note that even though the flow disturbances remained of the same order of magnitude in the study period (Figure 7.6e), the channel-width presented lower variations after the establishment of vegetation, which occurred in the second spring after restoration (2013). The analysis of the channel width evolution indicates

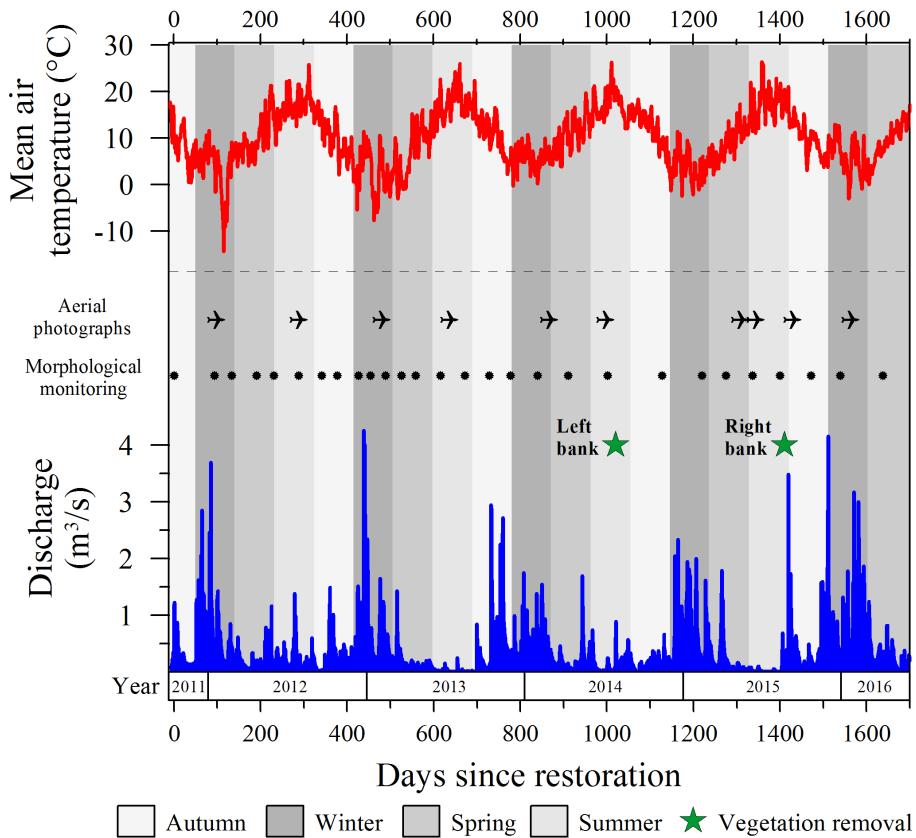


Figure 7.4: Time series of the information available after stream restoration: discharge (m^3/s), mean air temperature ($^{\circ}C$), morphological campaigns and aerial photos. Information about the morphological campaigns and aerial photos can be found in Tables 7.3 and 7.4, respectively.

that the root system plays the major role on bank stabilization. This is deduced from the progressive decrease of channel widening even if high flows systematically occurred in winter when the plant foliage was drastically reduced.

The bankfull water depth, difference between mean floodplain and channel bed elevations (Figure 7.6c), progressively increased as a result of channel incision and sediment deposition on the floodplains. The decrease of reach-averaged floodplain elevation in Summer 2013 is a result of dewatering due to the maintained low flows; its subsequent increase reflects the re-watering and sedimentation processes caused by the high flows that occurred later in autumn, see Figure 7.6e. In Figure 7.6c, C3 and C4 show two episodes of slight decrease of floodplain elevation. These were caused by vegetation cut conducted by the Water Board as a flood-safety measure, see also Figure 7.4.

Erosion and deposition processes can be analysed by using the constructed DEMs of difference (DoD), described in Table 7.4 and shown in Figure 7.7. Bed erosion and verti-

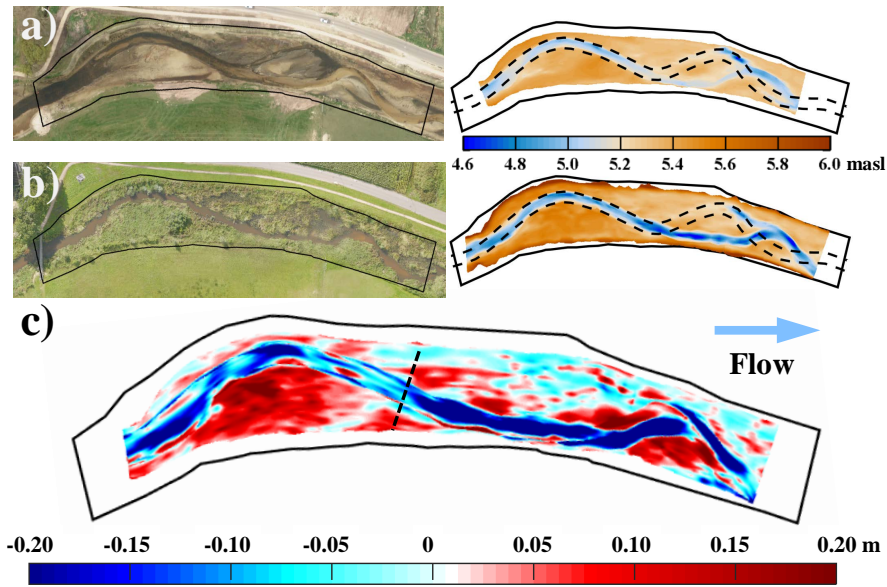


Figure 7.5: Evolution of the Lunterse Beek from (a) January 2012 to (b) September 2015. Left panel: Aerial pictures, Right panel: DEMs with legend indicating the bed level (masl), the initially reconstructed channel is shown in dashed lines. (c) Difference between the two campaigns, erosion is indicated in blue and sedimentation in red. The cross-section is indicated in (c) is used further analyses. Monitoring area enclosed with a black contour.

cal accretion rates are also calculated from three selected cross-sections and presented in Table 7.6. As expected, the relatively high-rate erosion and deposition processes observed in the first three DoDs (Figure 7.7a to 7.7c) are related to the initial cutoff. After this initial channel adaptation, erosion and deposition processes occurred at lower rates, probably associated with vegetation growth and establishment. During the first year (Figure 7.7a to 7.7d), the sediment that settled during the high-flow season on the edges of the banks, forming levees, was washed away during the next winter (Figure 7.7e and 7.7f), because the plants that colonized these areas could not establish. This can also be seen in the negative rates of vertical accretion reported in Table 7.6 for cross-sections A and C during the first year. However, after the high-flow period of the second year, vegetation established on levees (Figure 7.7h), reinforcing them and increasing sediment capture. Consequently, vertical accretion on these areas started to occur after the second year (see Figures 7.7i, 7.7j and Table 7.6).

Levee-formation enhanced channel bed erosion, due to flow concentration (Figures 7.7k and 7.7l). These DoDs and the values reported on Table 7.6 allow identifying that both main channel incision and floodplain rising occurred in the study period. Figures 7.7k and 7.7o show two important episodes of floodplain erosion which were most probably caused by the cutting of vegetation carried out by the Water Board, as a flood-risk reduction measure, in 2014 and 2015. This is also shown by the negative values of vertical accretion reported in Table 7.6 for the last period (Year 4-5).

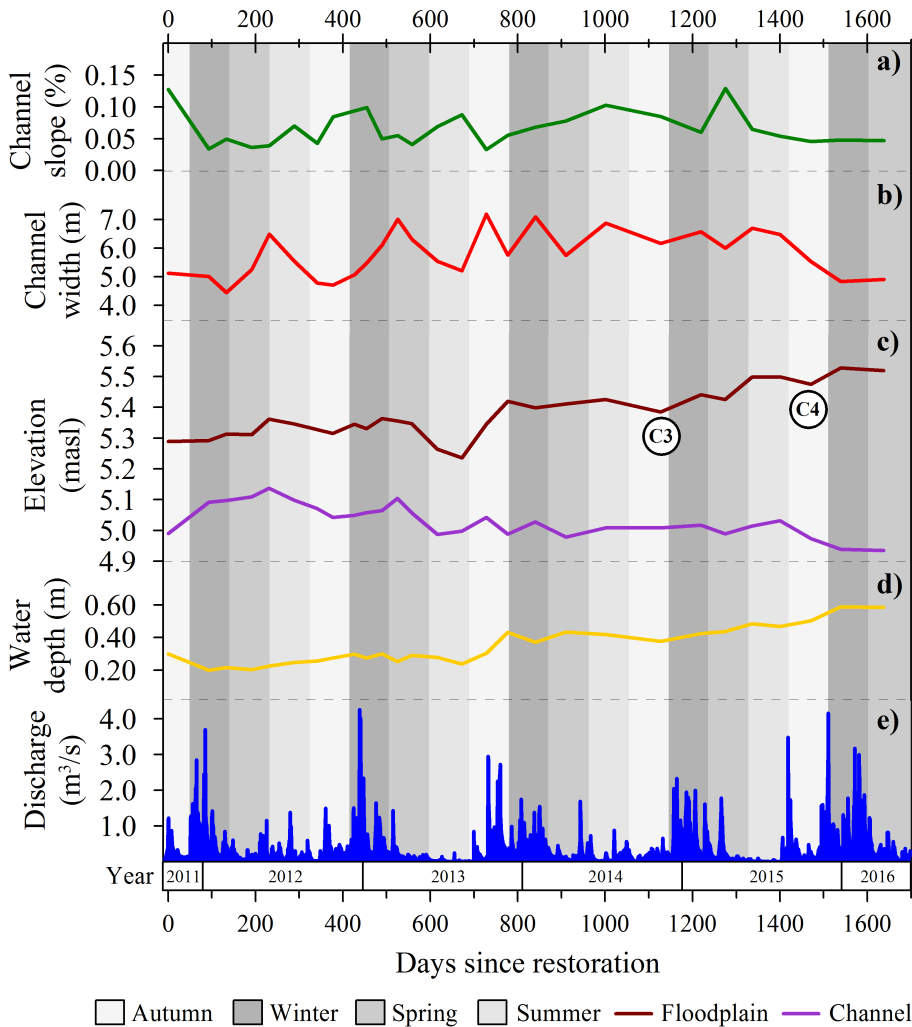


Figure 7.6: Temporal evolution of reach averaged: (a) channel slope (%), (b) channel width (m), (c) elevation of bed channel and floodplains (masl), and (d) bankfull water depth (m), as well as (e) discharge (m^3/s) in the Lunterse Beek after restoration (Day 0).

Table 7.6: Measured erosion and accretion rates between spring seasons. The localization of the selected cross-sections can be seen in Figure 7.2.

Cross Section	Year 1-2			Year 2-3			Year 3-4			Year 4-5		
	BE ^a	VA _{rb} ^b	VA _{lb} ^c	BE ^a	VA _{rb} ^b	VA _{lb} ^c	BE ^a	VA _{rb} ^b	VA _{lb} ^c	BE ^a	VA _{rb} ^b	VA _{lb} ^c
A	5.1	-0.3	-1.5	3.0	2.2	5.6	5.5	-1.3	7.9	4.2	4.1	-4.7
C	13.0	-6.5	-1.3	25.6	2.7	5.5	-8.7	6.6	0.9	0.8	-6.2	7.3
F	25.4	6.2	0.5	14.9	1.2	4.8	9.6	2.1	-2.0	9.4	3.3	8.6

^a BE = Mean bed erosion rate, in centimetres per year.

^b VA_{rb} = Mean vertical accretion rate on the right bank, in centimetres per year.

^c VA_{lb} = Mean vertical accretion rate on the left bank, in centimetres per year.

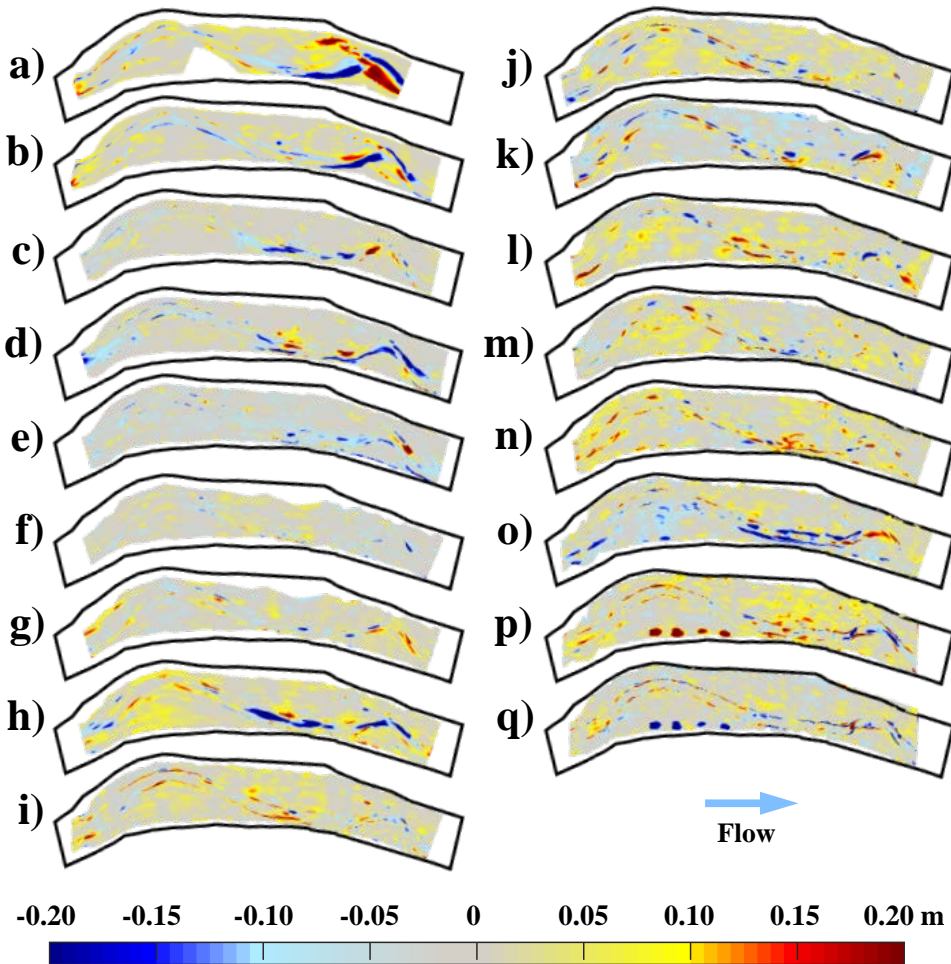


Figure 7.7: DEMs of difference (DoDs) in bed topography occurred in: (a) Spring 2012, (b) Summer 2012, (c) Autumn 2012, (d) Winter 2012, (e) Spring 2013, (f) Summer 2013, (g) Autumn 2013, (h) Winter 2013, (i) Spring 2014, (j) Summer 2014, (k) Autumn 2014 (After vegetation cut on left floodplain), (l) Winter 2014, (m) Spring 2015, (n) Summer 2015, (o) Autumn 2015 (After vegetation cut on right floodplain), (p) Winter 2015, and (q) Spring 2016. The solid black line indicates the monitored area (See Figure 7.2b). Erosion is indicated in blue and deposition in red.

The seasonal variation of the 6 selected cross-sections (see Figure 7.2b) during the study period is given as supplementary material B. The evolution of these cross-sections shows the initial morphological adaptation (cutoff), progressive bed incision, levee formation and the effects of vegetation described in the previous sections (Figures 7.8 and 7.9). Figure 7.9 shows the morphological evolution of cross-section E in the area in which the initial cutoff occurred.

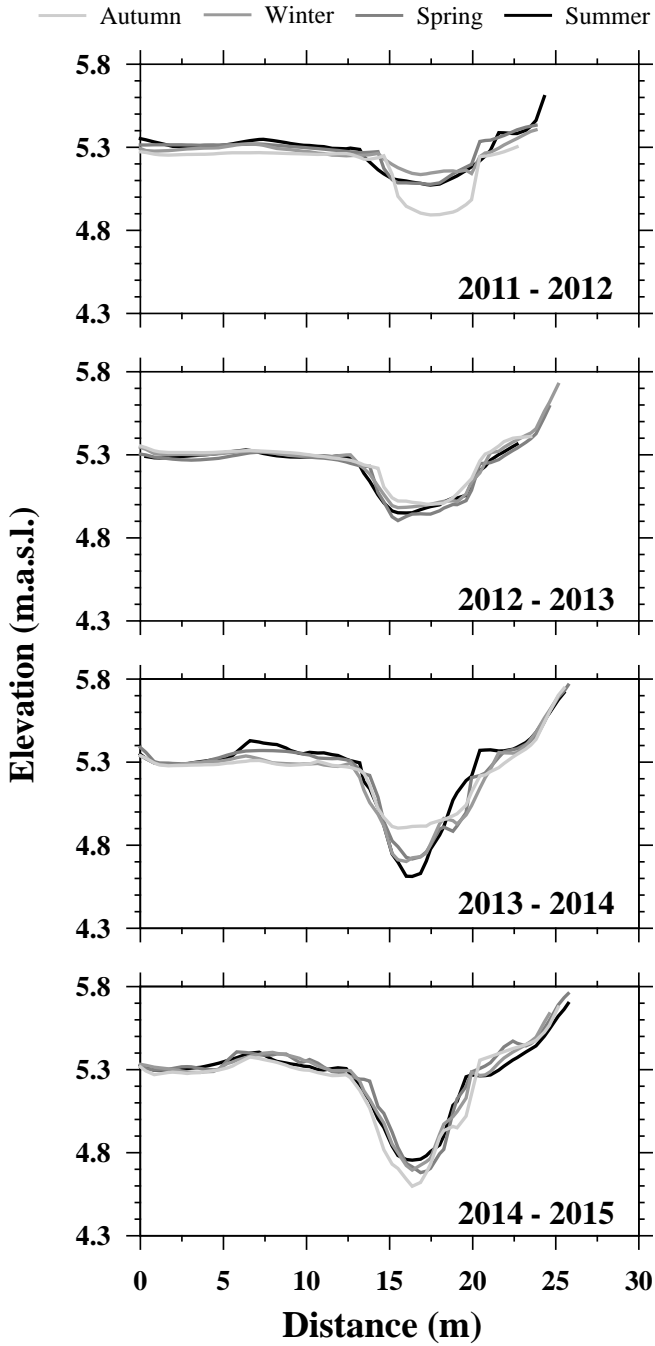


Figure 7.8: Seasonal variation observed on cross-section C, see Figure 7.2.

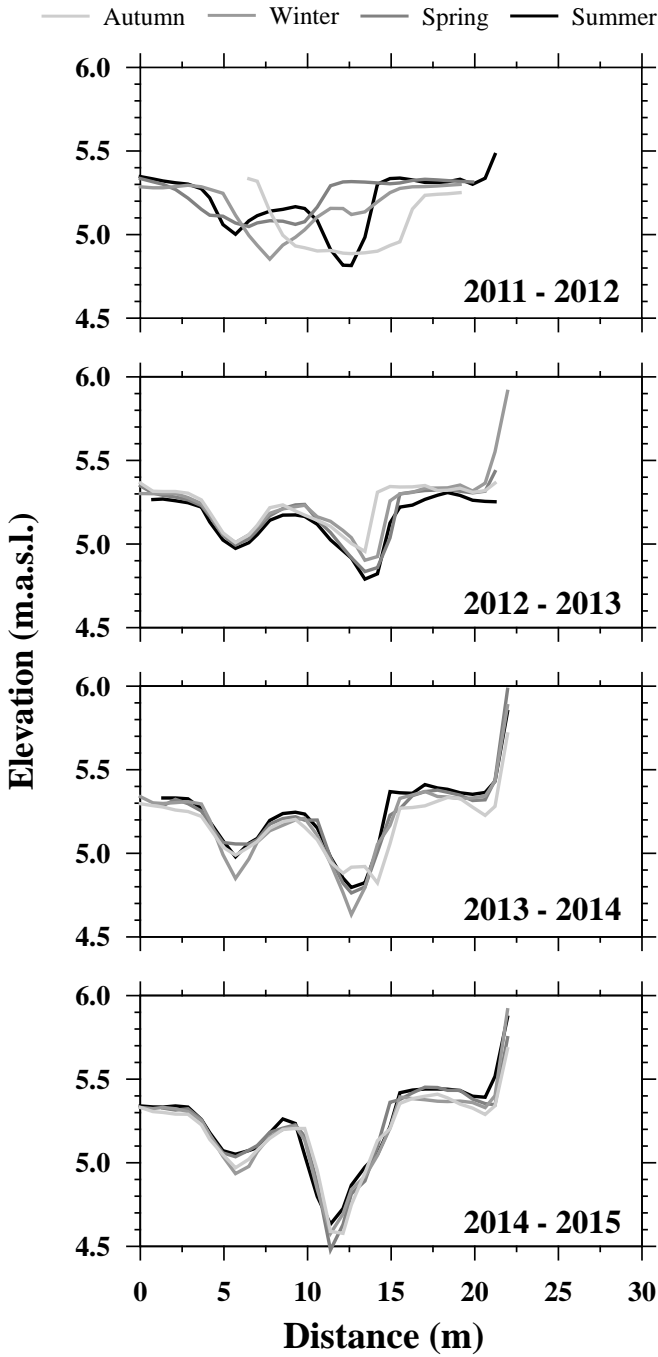


Figure 7.9: Seasonal variation observed on cross-section E, see Figure 7.2.

7.4.3. EVOLUTION OF VEGETATION

THE almost 5-year monitoring activities performed in this study have allowed studying the dynamics and development of vegetation along the Lunterse Beek after re-meandering. The aerial photos and the spatial distribution of vegetation are presented in Figures 7.10 and 7.11 for the summer and winter seasons, respectively. Figure 7.12 shows the evolution of vegetation in the period 2015-2016. Additionally, the seasonal evolution of vegetation has been documented through the photographic annex given as supplementary material C.

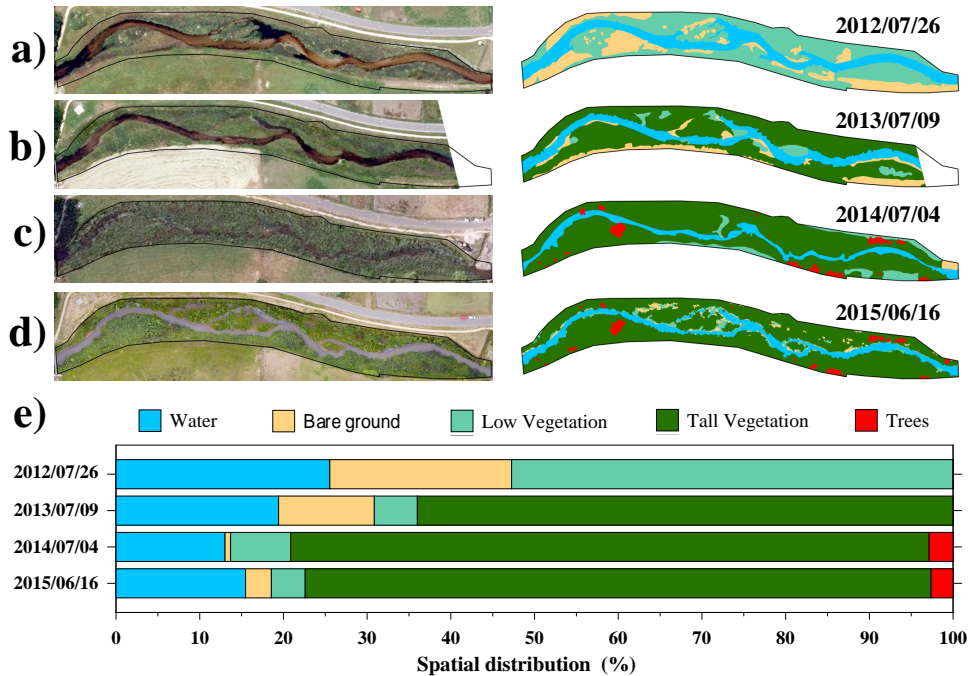


Figure 7.10: (a-d) Aerial photographs and vegetation classification maps of the Lunterse Beek in the summers and (e) spatial distribution in percentage. Information about the aerial photos is presented in Table 7.4.

Riparian vegetation started to appear in this stream during the first spring after restoration. However, the shoots that emerged in the lower areas did not survive the winter due to flow disturbance: the lower areas covered by vegetation in Figure 9a (first summer after restoration) become bare ground in Figure 7.11b (second winter after restoration). A higher coverage was observed in the lower areas of the floodplains in the second annual growth cycle, see Figures 7.10b and 7.11c. By comparing the photos and vegetation classification maps in winter presented in Figure 7.11, it is possible to observe that this time the areas close to the stream are successfully colonized, showing the effectiveness of the re-colonization process and the quick adaptation of pioneer plants. Little organic residuals were observed to remain in these sediment deposits. These are believed to enhance the establishment of new vegetation during the next colonization cycle.

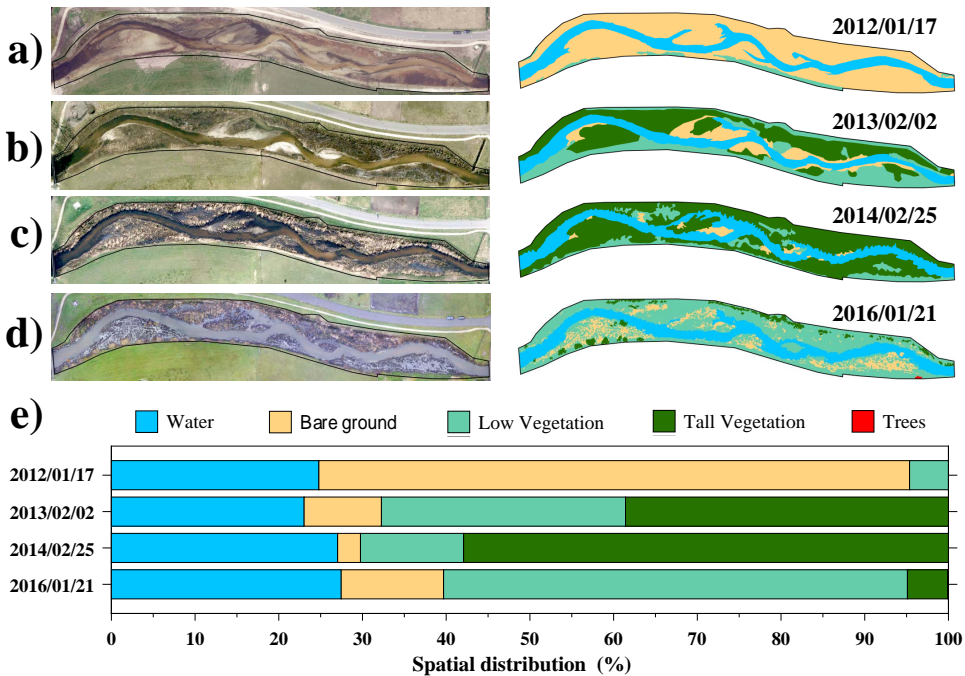


Figure 7.11: (a-d) Aerial photographs and vegetation classification maps of the Lunterse Beek in the winters and (e) spatial distribution in percentage. Information about the aerial photos is presented in Table 7.4.

The amount of grassy and bushy species steadily increased, as did the first phases of softwood trees. Species variety increased every year. Spontaneous regeneration of softwood species in restored streams was found also in previous investigations (e.g. [Friedman et al., 1995](#); [Geerling et al., 2008](#)).

The first stages of ecological succession from grass to shrubs and from grass to woody vegetation (*Salix Alba*) could be observed already in the first 5 years after restoration. In Figure 7.13, two locations (see Figure 7.13a) have been selected to show this process. Figure 7.13b shows the establishment of grassy vegetation on the highest areas, the ones that were first colonized. Figures 7.13c and 7.13d emphasize further developments, i.e.: succession of the first colonized patches and vegetation growth in other areas after only 4 months. Figure 7.13g shows a patch of Willows (*Salix Alba*), which succeeded to the plants that first colonized this area (showed in Figure 7.13f). The first well-developed tree stands with low-dense foliage were observed after 3.5 years, approximately, on the fourth summer after restoration. These young trees started to develop more intensively during the last year, reaching a height of more than 2 m and a mean diameter of the main branch of 2.0 cm. The described areal expansion of these trees and the location of other patches of smaller Willows that were developed during the same period can be identified in Figures 7.12a to 7.12c. Figure 7.12e shows that the area covered by trees increased considerably during a period of four months. The dynamics described in the

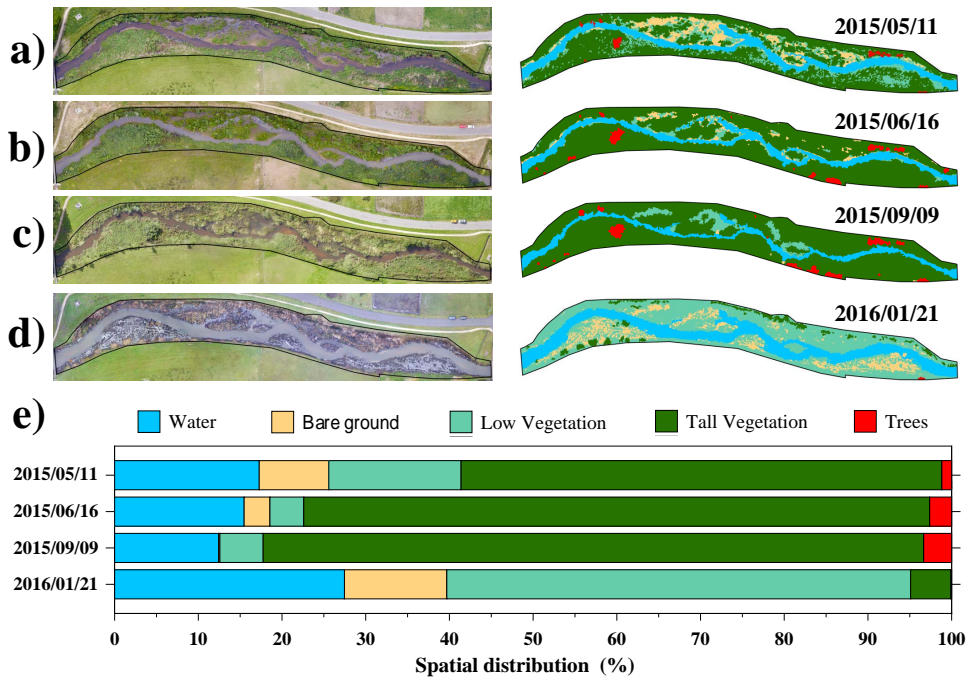


Figure 7.12: (a-d) Aerial photographs and vegetation classification maps of the Lunterse Beek for the vegetation growth and decay observed in 2015 and (e) spatial distribution in percentage. Information about the aerial photos is presented in Table 7.4.

7

examples presented in Figure 7.13 was observed also in other high floodplain areas. The condition of vegetation and trees showed in Figure 7.13 drastically changed at the end of the monitoring campaigns, because of vegetation removal by the Water Board.

7.5. RESULTS OF NUMERICAL MODELLING

THE DEMs of difference obtained between the bed levels calculated with the model and the ones measured during Campaign 28 are presented in Figure 7.14 for the four scenarios. Positive values in red indicate model overestimation whereas negative values in blue indicate model sub-estimation. A cross-section (see Figure 7.5) used to show the cross-sectional developments, is indicated in this figure by a continuous black line. The comparison between the bed levels obtained with the model for the different scenarios and the ones observed in the field at this cross-section are presented in Figure 7.15. This cross-section was chosen because of the high dynamics observed in this bend and the lower accuracy of the model.

From the four simulated scenarios, two different trends can be identified: the first one obtained for the scenarios without plants or low-density vegetation (scenarios 1 and 2, respectively) and the second one obtained for the scenarios including larger plants

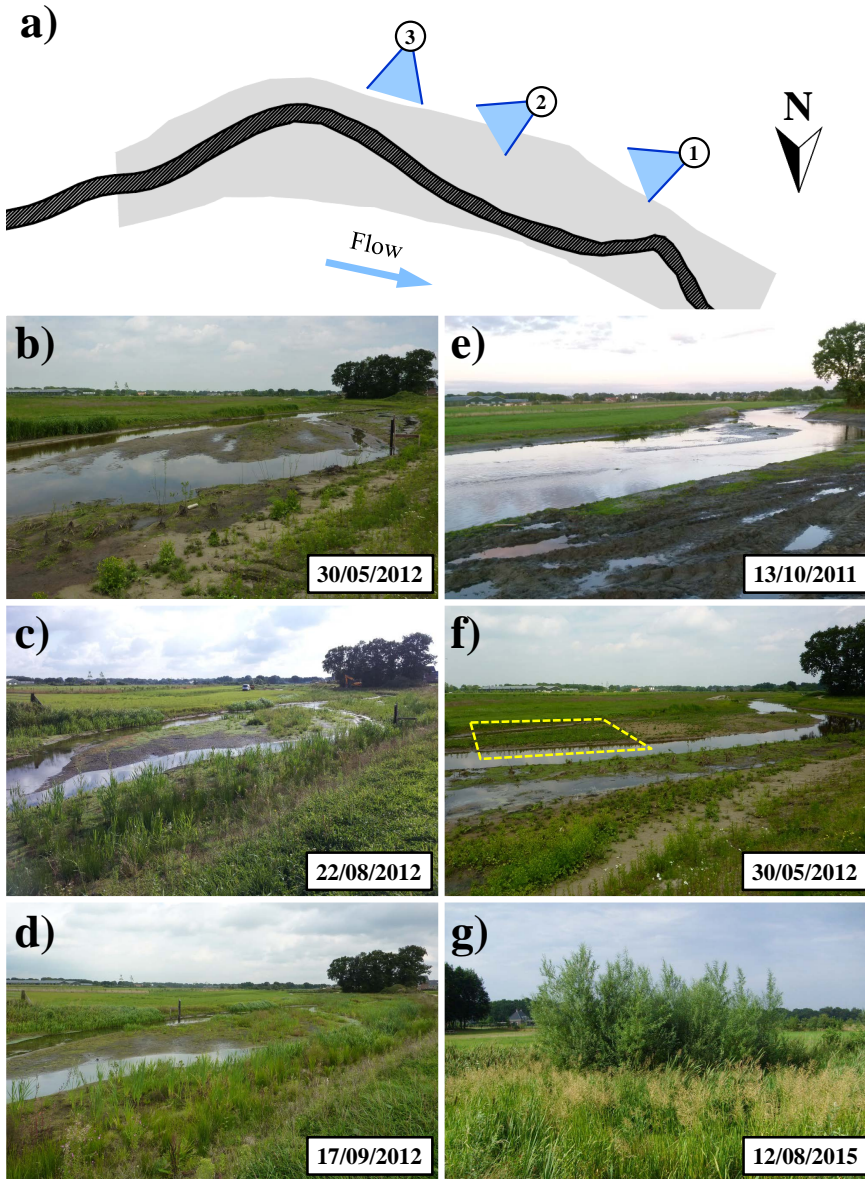


Figure 7.13: Terrestrial photographs highlighting vegetation succession. (a) Scheme indicating the position and direction of the photographs, Vegetation stages from (b) to (g) explained in the text.

(scenarios 3 and 4). When vegetation is not included in the model (scenario 1), a wider and shallower channel than the one observed in the field is obtained. For scenario 2, with uniformly distributed grass, there is little contribution from the increased roughness due to the plants, resulting in a situation similar to the one obtained for scenario 1.

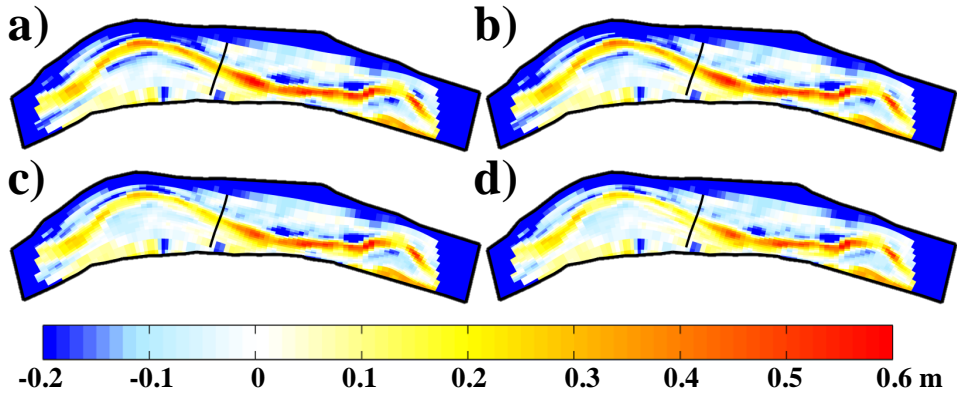


Figure 7.14: DEMs of difference (DoDs) in bed topography at the end of the study between the estimations with the model and the observations for: (a) Scenario 1, (b) Scenario 2, (c) Scenario 3, and (d) Scenario 4.

With herbaceous plants on the floodplains, due to increased flow concentration in the main channel the model better reproduced channel incision. However, the channel-width reproduced by the model is always larger than the one observed in the field and there are some areas in which considerable sedimentation is observed, see Figures 7.14 and 7.15. This is due to not including the effects of the plant roots on the stability of the banks so that the bank accretion process is not well represented and bank erosion is overestimated. Another shortcoming arises from the strongly simplified bank erosion formulation, assigning part of the bed erosion occurring in the wet cells at the channel margin to the adjacent dry cell, in the same way in the entire model domain.

7

The scenario that leads to (slightly) better results is scenario 4, in which the seasonal variations of vegetation are included. In this scenario, the model estimates well the floodplain levels, confirming the ability of Baptist's method of reproducing the effects of vegetation on local sedimentation (e.g. Montes Arboleda et al., 2010). However, the model does not completely capture the flow concentration and the levee formation processes and, therefore, excessive sedimentation is obtained in the main channel.

Regarding the relevance of considering the seasonal variations of vegetation in this type of streams, the results of the model show that the seasonal variations might be important for the evolution of small streams in temperate climates, like the Lunterse Beek. However, maintaining the properties of (an average type) of vegetation constant with time, as done in scenario 3, provides only slightly worse results.

7.6. CONCLUSIONS

THIS investigation is based on the combination of hydrological time series, high resolution bathymetric data, observations of vegetation, aerial photographs and numerical modelling to study the effects of vegetation on a lowland restored temperate-climate stream, the Lunterse Beek. From the morphodynamic changes and the vegetation cover

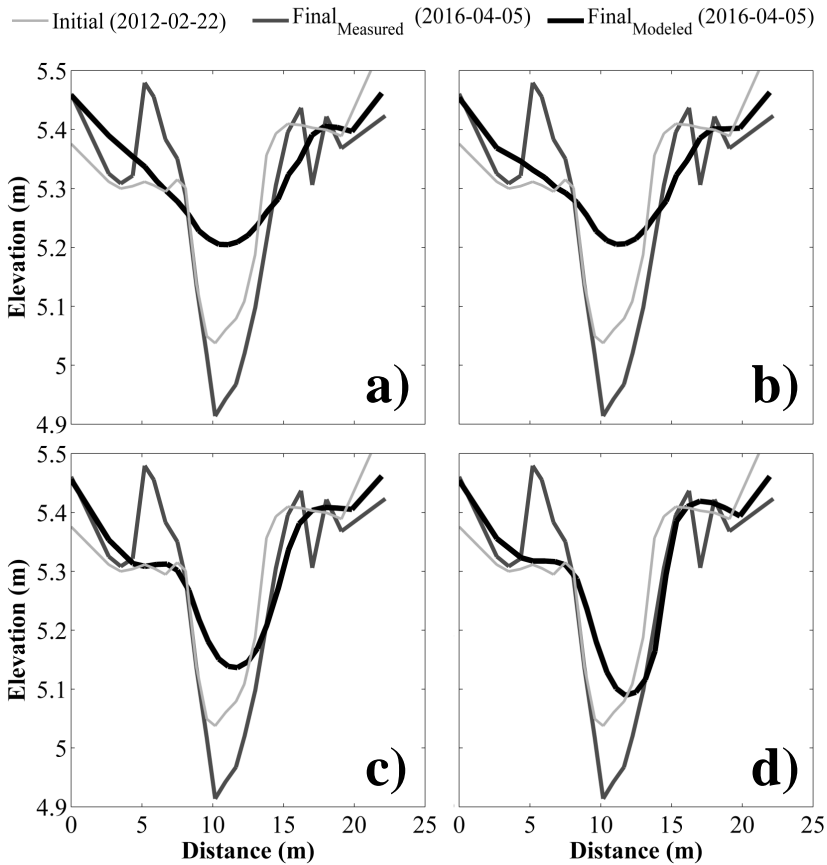


Figure 7.15: Comparison between the initial conditions, and the observed and modelled bed levels at the end of the study for the cross-section indicated in Figure 7.4 for: a) Scenario 1, b) Scenario 2, c) Scenario 3, and d) Scenario 4.

evolution observed in the first five years after channel re-meandering, it was possible to identify the relevance of vegetation establishment on the stabilization of channel width and on the vertical accretion of both levees and floodplains. Without vegetation, the levees that formed during overbank flows were later washed away. After soil stabilization by vegetation, the formed levees remained for later stages inducing channel incision.

The root system of the plants was found to play a key role in counteracting the effects of flow perturbations. Plants were found to protect the bank from erosion even during the winters, when the high flows encounter a substantially reduced vegetation biomass, due to lack of foliage, but an effective root network.

A state-of-the-art 2D morphodynamic model including the effects of vegetation in reproducing the observed morphological floodplain evolution was used to study differ-

ent scenarios, characterized by absence of vegetation, uniform and constant floodplain coverage by grass or herbaceous vegetation, and vegetation following the observed seasonal and inter-annual dynamics. The model reproduced most features observed in the floodplains. However, it could not fully reproduce the bank dynamics because the effects of roots were not included impeding a good representation of bank accretion and because of the strongly simplified bank erosion formulation. The results emphasize the relevance of including vegetation in morphodynamic calculations, demonstrating the relevance of considering the seasonal variability of vegetation, in particular for short-term simulations of small streams in temperate climates.

Quantifying the effects of the plant root system on soil reinforcement and its role on bank accretion is an important issue that should be addressed in future investigations to predict accurately the morphological evolution of river systems. Considering the limitations exhibited by the available estimators on reproducing the effects of isolated vegetation elements, more research is also required on estimating the biomorphological effects of trees on the morphodynamic evolution of lowland streams, taking into account their relative size when compared to the size of these type of rivers.

8

MORPHOLOGICAL EFFECTS OF PLANT COLONIZATION AND BANK ACCRETION

“All life is an experiment. The more experiments you make the better.”

Ralph Waldo Emerson



Figure 8.1: Large-scale laboratory flume for studying bank accretion at Delft University of Technology.

In this chapter the large-scale experimental activities carried out in this research are presented as well as the obtained results.

This chapter is on preparation for future publication in *Journal of Geophysical Research: Biogeosciences*.

8.1. INTRODUCTION

LABORATORY-BASED research is included in this project in order to clarify the mechanisms underlying the effects of vegetation on accretional processes in rivers, see Figure 8.1. The main purpose of these experiments is to quantify the interaction between vegetation and bank dynamics and in particular the role of vegetation colonization of new deposits, at controlled but realistic conditions, minimizing the scale problems observed in previous experiments. The analysis of the results obtained from the laboratory observations performed during this research are presented here.

Considering that the formation and attachment of new sediment deposits to floodplains start with the development of bars, the bar formation process plays a key role in this part of the study. Subsequent colonization by vegetation of emerging areas is what then transforms bars in new islands or floodplain. The experiments are therefore focused on the effects of vegetation colonization in the presence of bars on channel formation. Three typical situations are considered and compared: rivers with un-vegetated banks and floodplains; rivers with vegetation only on the floodplains; and rivers with vegetation on floodplains and on the areas emerging during low flow stages. These three cases can be encountered in nature as a result of interactions between vegetation dynamics and climate. In environments found in arid and cold climates, for instance, colonization by vegetation is slow with respect to the duration of low-flow periods. Whereas in tropical and humid climates the vegetation growth occurs quickly, establishing a fast dynamics.

This chapter includes a short review of the bar formation process as well as previous attempts conducted in the laboratory to reproduce meandering channels and the effects of plants on river planform styles. Single-thread channels with some sinuosity are selected considering that it is in meandering rivers where bank accretion processes can be observed more clearly.

8.2. LITERATURE REVIEW

8.2.1. BAR FORMATION

FOR the sake of clarity, the terminology proposed by Duró et al. (2016) is adopted here. They basically defined three types of bars: free, forced and hybrid. Free bars are formed due to morphodynamic instability. Forced bars are formed locally due to the presence of a geometrical forcing, such as a natural bend or a groyne. Hybrid bars, as free bars, arise from morphodynamic instability, but they are steady and their permanence depends on the existence of forcing.

The major efforts in the research regarding bar formation in river channels focused on the conditions for their formation and on their characteristics, such as length, amplitude, growth rate and migration celerity. Theoretical explanations of bar formation came from the mathematical stability analyses performed on straight channels with non erodible banks by, among others, Hansen (1967), Callander (1969), Engelund (1970), Engelund and Skovgaard (1973), Engelund (1975), Parker (1976) and Fredsøe (1978). These

analyses explained the conditions at which bars (alternate or multiple) form due to inherent instability of the morphodynamic system, named “bar instability” and showed the importance of the channel width-to-depth ratio for bars. Regarding meandering rivers, the first question that intrigued researchers over the years was why a water course tends to become sinuous. Initially, the first way to answer this question was by associating the presence of migrating alternate bars in the river channel with the initiation of meandering. The mathematical stability analysis performed by Ikeda et al. (1981) relating bank retreat to near-bank flow velocity in a mildly-sinuuous channel demonstrated that only bends with a meander wavelength within a certain range tend to grow with time (bend theory). They showed the existence of another kind of instability, called “bend instability”, suggesting that this instability originates river meanders. They also found that the typical wavelengths of free migrating bars are not long enough to fall in the growing range of river bends and for this, migrating bars cannot be the direct cause of meandering. Considering that migrating bars are too fast to lead to localized bank erosion, Olesen (1984) related initiation of meandering to the formation of hybrid bars. This phenomenon was first called “overshooting” (after Struiksmā et al., 1985) or “overdeepening” (after Parker and Johanneson, 1989). In the same period, Blondeaux and Seminara (1985) demonstrated the existence of a resonance phenomenon, which occurs when alternate bars have the same wavelength as growing bends and linked the “bar theory” to the “bend theory”. Free bar formation under resonant conditions occurs at a specific width-to-depth ratio and wavelength. These bars are characterized by celerity equal zero and constant amplitude in longitudinal direction (no growth nor decay). Considering the resonant condition (critical width-to-depth ratio and wavelength) channels with larger width-to-depth ratios are called “super-resonant”, those with smaller width-to-depth ratios “sub-resonant”. Resonance was initially considered the condition for initiation of meandering. Struiksmā and Crosato (1989) showed independently that only steady bars can lead to meandering and found that (non-migrating) hybrid bar formation occurs within a range of width-to-depth ratios and not only at an specific state (resonant condition). One year later, Tubino and Seminara (1990) showed that if a river channel widens the celerity of free migrating bars tends to reduce until becoming zero. This finding led to the idea that only through channel widening free migrating bars could eventually lead to growing bends, so the bar and bend instability theories were connected and the relevance of steady alternate bars in the initiation of meandering was exposed. However, Friedkin (1945) obtained in his experiments initiation of meandering at conditions that were not resonant, showing that resonant conditions cannot be the only cause of meandering (Crosato et al., 2011), which supports the findings by Struiksmā et al. (1985) and Struiksmā and Crosato (1989).

8.2.2. LABORATORY INVESTIGATIONS WITHOUT VEGETATION

OBTAINING a meandering channel in the laboratory has proven to be highly challenging which in many cases reflects the scaling problems and the lack of understanding of the actual causes and processes leading to meandering (Kleinhans, 2010; van Dijk et al., 2012). Considering meandering rivers, after the pioneer work of Friedkin (1945), several laboratory studies in mobile-bed flumes have been performed including some

of the processes present in this type of rivers. Figure 8.2 shows some of the meandering planforms obtained in laboratory experiments without vegetation.

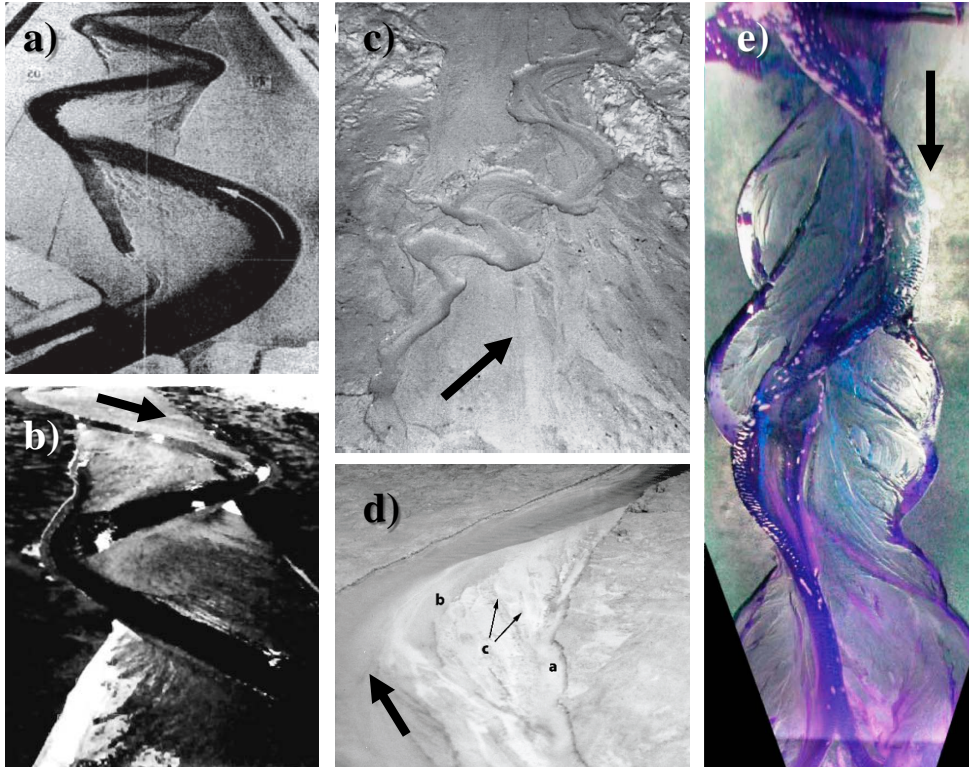


Figure 8.2: Meandering planforms obtained in laboratory experiments without vegetation. Flow direction as indicated. (a) [Friedkin \(1945\)](#), (b) [Schumm and Khan \(1972\)](#), (c) [Smith \(1998\)](#), (d) [Peakall et al. \(2007\)](#), (e) [van Dijk et al. \(2012\)](#).

Although the work by [Friedkin \(1945\)](#) was conducted almost 70 years ago, some of his assumptions are still valid so that his work has been considered as starting point for many laboratory studies. In particular, [Friedkin \(1945\)](#) obtained a meandering system with a mixture of silt and sand (see Figure 8.2a) resulting in some apparent cohesiveness which was enough to obtain vertical eroding banks and large meander amplitudes. There are a few other successful experiences in the production of low-sinuosity channels with some characteristics of meandering using sand as bed material, such as [Schumm and Khan \(1972\)](#), [Jin and Schumm \(1987\)](#), [Peakall et al. \(2007\)](#), and [van Dijk et al. \(2012\)](#), see Figure 8.2. However, after running for a long-enough period the channels widen transforming the meandering river in a braided system. [Smith \(1998\)](#) showed the relevance of cohesive sediment for river meandering in the laboratory and the key role that plays the strength of the river banks, see Figure 8.2c. In the work of [Peakall et al. \(2007\)](#), see Figure 8.2d, the evolution of point bars was studied by analysing their depo-

sitional architecture. These laboratory experiments showed the relevance of bank accretion and the necessity to include a variable discharge in the maintenance of long-term meandering. More recently, [Dulal and Shimizu \(2010\)](#) analysed the influence of layered floodplains in the planform evolution using sediment cohesiveness as a main parameter. [van Dijk et al. \(2012\)](#) produced a meandering bend with scroll and chute bars (see [Figure 8.2e](#)) showing the necessity of a dynamic upstream perturbation for maintaining meandering. Despite all these efforts, not even the laboratory experiments conducted on larger flumes with successful representation of some characteristics of meandering rivers have been able to overcome the difficulties of upscaling the findings in the laboratory to real river cases (e.g. [Fujita and Muramoto, 1982](#)). [Table 8.1](#) summarizes the main characteristics of previous laboratory experiments on meandering planform formation without vegetation.

In one of his multiple configurations with erodible banks, [Friedkin \(1945\)](#) included a test initiating from a sinuous channel pattern and uniform cross-sections. More recently, [Song et al. \(2016\)](#) analysed the planform development of initially constructed sine-generated meandering channels varying the sinuosity, the channel width and the discharge. Although these experiments can be recognized as interesting exercises for analysing the cross-sectional evolution of meandering channels, it is difficult to correlate the imposed channel gradient with the sinuous pattern, in particular considering their short duration.

8.2.3. LABORATORY INVESTIGATIONS WITH VEGETATION

THE influence of vegetation on river patterns has been studied in the laboratory by [Gran and Paola \(2001\)](#), [Braudrick et al. \(2009\)](#), [Tal and Paola \(2007, 2010\)](#), among others. The experiments focused on incrementing the strength of channel banks and on the addition of plants (alfalfa in most cases). Some of the patterns obtained are shown in [Figure 8.3](#). [Gran and Paola \(2001\)](#) and [Tal and Paola \(2007, 2010\)](#) reproduced a single-thread channel trough the seeding of alfalfa sprouts during low flow stages (see [Figures 8.3a](#) and [8.3b](#)) starting from a braided system. [Coulthard \(2005\)](#) showed that vegetation density is a key factor on river planform evolution since a low-density vegetation cover tends to increase the channel braiding index instead of promoting meandering. This fact is also related with the scaling issues regarding the importance of the relative size of the vegetation compared with the size of the river reach (see [Figure 8.3c](#)). [Braudrick et al. \(2009\)](#) obtained some characteristics of meandering starting from a straight channel by seeding alfalfa and blocking small troughs with fine sediment, maintaining a constant discharge (see [Figure 8.3d](#)). More recently, [Bertoldi et al. \(2015\)](#) combined the use of alfalfa sprouts with the supply of wooden dowels in order to reproduce the combined effects of living and death vegetation. All these experiments have shown how vegetation increases the hydraulic resistance of bank and in general the local soil strength, stabilizing the floodplain and deflecting the flow towards the centre of the main river channel. Several aspects influencing the accretional processes observed in rivers have been identified from those experiences, such as: discharge variability, fine sediment deposition and the presence of vegetation. However, it is clear as well that it is not possible yet to scale the observed responses to the real river scale.

Table 8.1: Main characteristics of previous laboratory experiments on river planforms.

Ref ^a	Flume characteristics ^b							Initial channel characteristics ^c				Sediment type ^d	D_{50} (mm) ^e	Q (l/s)	
	W (m)	L (m)	i_b (m/m)	Bend	B (cm)	h (cm)	Shape	B/h	T	h (cm)	Shape				B/h
1	4.0	14.6	0.003 - 0.009	Yes	10-50	1.5-9.0	T	<10					Silt, Sand	0.02 - 1.5	0.28 - 12.2
2	11.6	36.6													
	7.3	30.5	0.0026	Yes	43	4.6	R	9.3					Sand	0.7	4.25
			0.0064		56	4.4		12.7							
			0.0075		61	4.8		12.8							
			0.0085		67	4.9		13.6							
3	7.5	42.8	0.005	No	50	2.3	T	21.7					Sand	0.61	15
4	1.2	3.0	0.015	No	~4	~0.5	R	8.0					DE + CWC	sg=1.35	0.009
			0.020			~0.5		8.0					C + CWC	sg=1.28	0.035
			0.025			~0.7		5.7					RF + K	sg=1.82	0.045
5	3.7	5.5	0.010	Yes	15	2.0	R	7.5					Silica flour	0.21	0.51
					10	2.5	T	6.0							
6	6.0	11.0	0.0055	No	30	1.5	R	20					Sand	0.51	1
7	3.0	12.0	0.005	Yes	10-20	2.4-4.6	R	2.2-7.1					Sand	0.58	0.7-1.4

^a 1) Friedkin (1945), 2) Schumm and Khan (1972), 3) Fujita and Muramoto (1982), 4) Smith (1998), 5) Peakall et al. (2007), 6) van Dijk et al. (2012), 7) Song et al. (2016). From references 2 and 3, only experiments with meandering patterns were included.

^b W = Flume width, L = Length, and i_b = Channel slope.

^c B = Channel width, h = Water depth, Shape: R = Rectangular, T = Trapezoidal.

^d DE = Diatomaceous earth (35 mm); CWC = Calcined White China Clay (4-10 mm); C = Cornstarch (12 mm); RF = Rock flour (4-10 mm); K = Kaolinite (4-10 textitmm).

^e sg = Specific gravity.

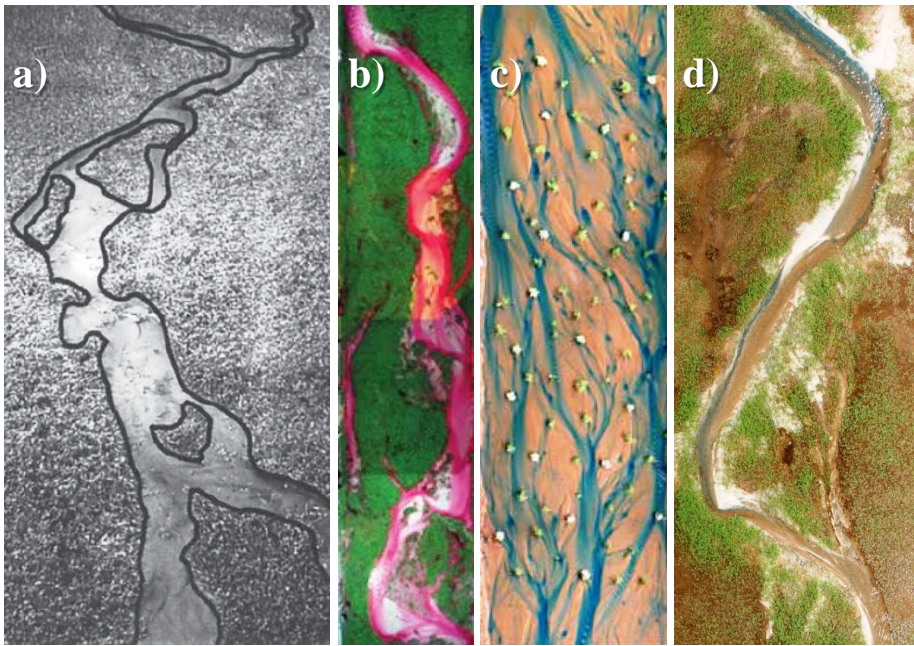


Figure 8.3: Laboratory experiments with vegetation. Flow from top to bottom. (a) [Gran and Paola \(2001\)](#), (b) [Tal and Paola \(2007\)](#), (c) [Coulthard \(2005\)](#), (d) [Braudrick et al. \(2009\)](#).

8.3. EXPERIMENTAL SET-UP

8.3.1. DESIGN

CONSIDERING the importance of the bar formation process on the establishment of channel patterns ([Engelund, 1970](#)), the experimental design of these tests was based on the theory developed by [Struiksmma et al. \(1985\)](#) allowing predicting the expected size (wavelengths) of hybrid bars. These bars were selected because they are steady and tend to form always at the same place if a permanent perturbation exists ([Duró et al., 2016](#)), aspect that ensures obtaining similar configurations for all scenarios even if starting with a flat bed.

8.3.2. FLUME

THE set of experiments was meant to study the effects of vegetation colonization on the channel formation by following the evolution of a zero-slope initially-constructed straight channel with erodible bed and banks. The experimental flume was 5 m wide and 45 m long, but due to the inlet and outlet structures, the effective length became 36 m, see [Figure 8.4a](#). A rectangular channel 80 cm wide and 15 cm deep with floodplains of 1 m at both sides was excavated in the sediment creating as well, see [Figure 8.4b](#). As an example, initial and final planforms of one of the tests is depicted in [Figures 8.4c and 8.4d](#), respectively.

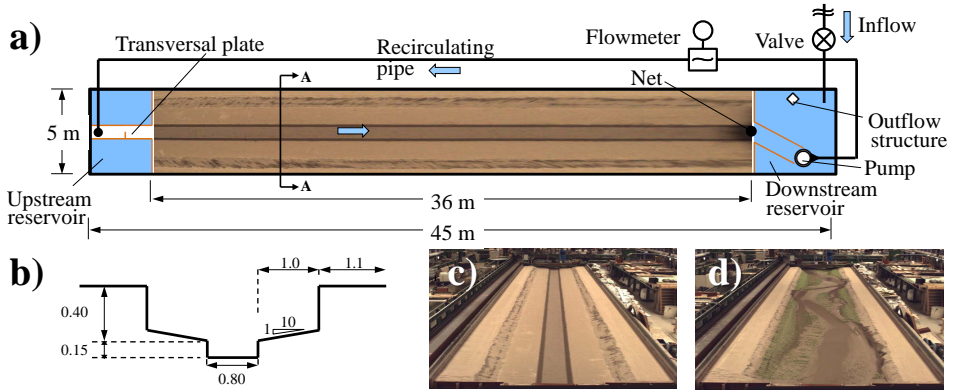


Figure 8.4: Experimental set-up of the mobile-bed flume: (a) Planview, (b) Initial cross-section A-A (Vertically distorted 1V:2H); and Initial (c) and final (d) planforms obtained for Test 3. All dimensions in metres.

The sand used in the experiments had a mean diameter, D_{50} , of 1 mm and was selected after the intense experimental work carried out by [Byishimo \(2014\)](#) and [Byishimo et al. \(2014\)](#). Figure 8.5 shows the grain size distribution of this material.

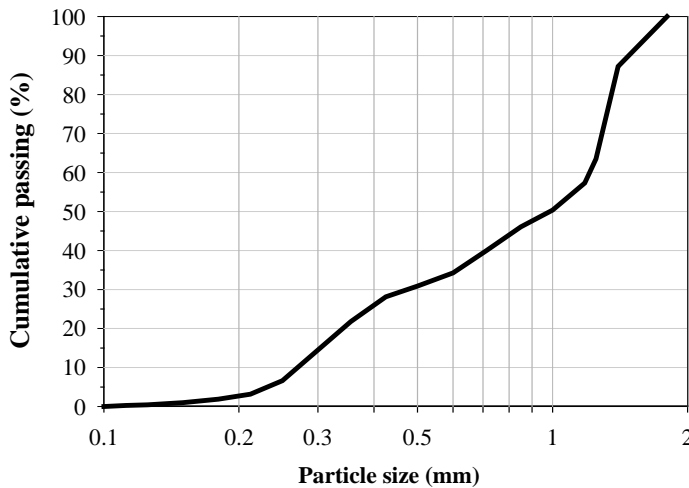


Figure 8.5: Grain size distribution of the sediment used in the laboratory experiments.

An empirical expression for the Chézy coefficient for this sediment, C_b , was proposed conditions by [Vargas-Luna et al. \(2015a\)](#) based on some preliminary tests as:

$$C_b = 1.313Re^{0.2097}i_b^{-0.2243} \quad (8.1)$$

where $Re=uh/\nu$ is the Reynolds number, u is the mean flow velocity (m/s), h is the water depth (m), ν is the kinematic viscosity (m^2/s), and i_b is the energy gradient (m/m).

Equation 8.1 is valid for the considered sediment under Reynolds numbers, Re , between 2.4×10^3 and 2.11×10^5 and energy gradients, i_b , between 0.0005 and 0.002 (m/m), ranges accomplished by our experiments.

The facility was equipped with a reservoir located at the downstream end of the flume in order to control water levels during the tests. From this reservoir water and sediment were recirculated, see Figure 8.4a. A net placed between the mobile bed and the reservoir was used to collect the particles released upstream for flow velocity measurements (see section 8.3.2) and the uprooted pseudo-plants transported by the flow during the experiment. A special sieve was designed and placed in the inlet structure to collect sediment samples and to dissipate the excess of energy of the incoming water. The inlet structure included a 40 *cm* long transversal plate (half of the initial channel width) as a flow perturbation to induce the formation and permanence of the first sediment bar (permanent forcing), see Figure 8.4a.

8.3.3. VEGETATION CHARACTERISTICS

THE same plastic plants of grassy type were used in the experiments to both represent the vegetation on the floodplains and the plants colonizing the emerging deposits. Vegetation selection was performed during some preliminary experimental activities (Vargas-Luna et al., 2015a, 2016b). The medium plant density (112 plants/m^2) was selected among the 3 densities considered in the preliminary tests. Wooden sticks were used as roots considering that they were found to be effective in reinforcing and protecting bare sediment banks and deposits from erosion in a way comparable to real roots (see for instance, Vargas-Luna et al., 2016b). Plants were manually inserted in the sand at the selected density over the area of interest (see Section 8.3.4) following a light pattern projected on the sand surface, as shown in Figure 8.6a. An example of the plant units (root and foliage) used in these experiments is shown in Figure 8.6b, whereas a view of the vegetation pattern seeded on a floodplain can be seen in Figure 8.6c.

8.3.4. TESTS

As the accretional processes of rivers start after the colonization of vegetation on sediment bars, these experiments were carried out including: variable discharge, vegetation and the formation of alternate hybrid bars. The discharge regime included alternating low and high flows. The low flow consisted of 22 *l/s* and was maintained constant during 9 hours, whereas 45 *l/s* during 2 hours were imposed as high discharge condition, see Figure 8.7. Additionally, a difference of 5 *cm* in the water level of the downstream reservoir was defined between high and low flow conditions.

The procedure that is described here was repeated carefully for all the considered scenarios in terms of duration and flow discharges as well as initial and boundary conditions. Considering that measuring the bed topography evolution in mobile-bed laboratory channels with the presence of water is not yet successfully implemented (see Vargas-Luna et al., 2016a), the experiment was stopped at the end of each day and restarted on the next one after scanning the bed surface of the flume.

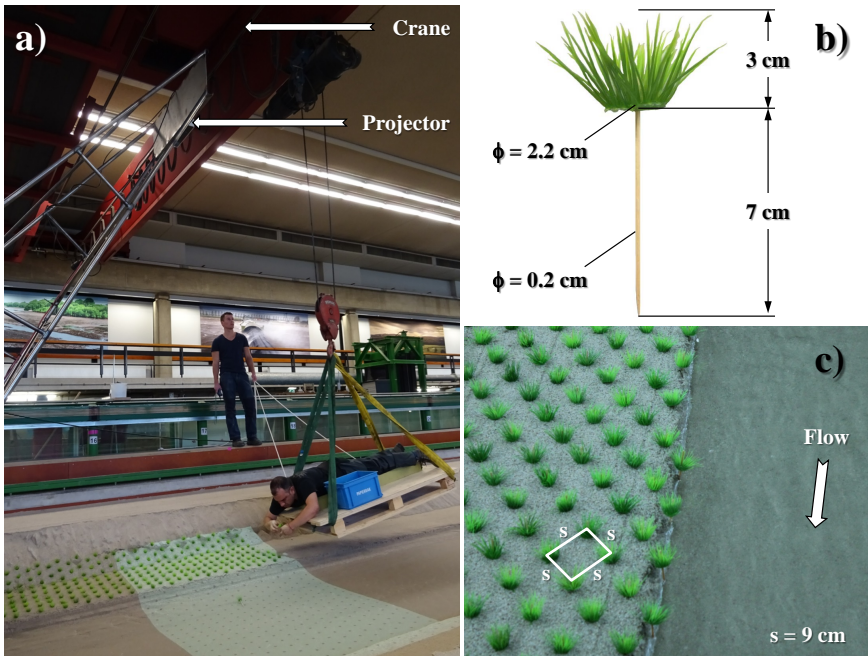


Figure 8.6: Vegetation used in the laboratory experiments: (a) Seeding process, (b) A plant unit, (c) Seeded floodplain.

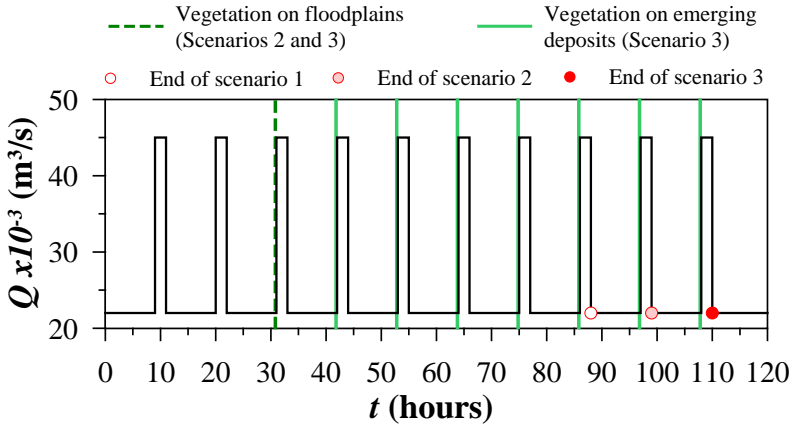


Figure 8.7: Discharge hydrograph indicating the vegetation colonization moments.

The initial conditions of each experiment were obtained as follows. Starting from the straight excavated channel, described in Section 8.3.2, a sequence of low and high discharges as upstream inflow was maintained until bars formed. The first part of the experiment ran during 5 days (31 hours of water flow) until the hybrid bars were fully formed, defining the starting point of all scenarios.

Three tests were carried out. These tests represent three different scenarios, representing: 1) rivers with no vegetation on floodplains and no vegetation colonization of new deposits, 2) rivers vegetated floodplains but no colonization of new deposits; 3) rivers with vegetation on floodplains and colonization of new deposits emerging during low-flow stages.

The first test is here considered as the base case, without vegetation. After the first 31 hours leading to initial bar formation, as described above, the same discharge regime was maintained until the end of the test. This moment was defined when one of the banks reached the end of the floodplain, which occurred after a total duration of 86 hours. In the second test plants were put on the floodplains after the first 31 hours, and then the experiment restarted. The vegetation on the floodplains was put without flow, as shown in Figure 8.6a. The third experiment started as the second one, but after having placed the plants on the floodplains and allowing the bars to adapt to this new condition with an extra cycle of high and low flow, more plants were placed on the areas of the bars emerging during low flow. By repeating this procedure during the subsequent cycles, plant “colonization” was simulated. The “seeding” moments elongated the time of the experiment but this period did not change the bed topography, so this time does not count for for the morphological evolution, see Figure 8.7.

An intense data collection campaign accompanied the execution of these experiments. As explained in Section 8.3.4 the bed surface was scanned daily before re-starting the tests. A FARO Focus 3D laser scanner was used to execute this task. This scanner uses a red laser Class 1, has a range up to 130 *m* and a field of view of 305° vertical and 360° horizontal, shooting up to 976.000 *points/second*, allowing for accurate measurements with a range error of +/- 2 *mm*. More specifications about this equipment can be found at: <http://www.faro.com/>. The obtained point clouds were post-processed by using the Cloud Compare software (<http://www.cloudcompare.org>).

High resolution photos of floating particles were taken hourly from the ceiling of the laboratory in order to obtain the superficial flow velocity field in localized areas of the channel. Flow velocity patterns were later reconstructed by using the time-resolved digital Particle Tracking Velocimetry (PTV) tool for Matlab, developed by Brevis et al. (2011) (see also <http://ptvlab.blogspot.com/>). This technique was selected on the basis of preliminary work on this flume, which demonstrated that for the range of water depths present in these experiments, the immersion of any element in the water to measure vertical flow velocities, as and ADV (Acoustic Doppler Velocimeter) for example, will create considerable local scour altering the channel bed.

Oblique high resolution photos of the entire flume were taken each five minutes in order to record the width adaptation and the planform evolution of the channel. Corrections were applied to this photos to reduce the distortion due to the angle of capture by using the ShiftN software (<http://www.shiftn.de/>). The corrected photos were used to obtain the evolution of the mean channel width and the channel planform during the experiment.

The flow discharge was measured in the recirculation supplying pipe with an acoustic flowmeter, whereas sediment samples were taken hourly by using the special sieve described in Section 8.3.2 at the outlet of this conduit. The collected sediment samples were dried and weighted to estimate the sediment transport rates. Hourly water level profiles were measured with a point gauge installed on the carriage of the flume.

8.4. RESULTS

IN order to prove that the three scenarios started from the same topographic conditions, Figure 8.8 shows the bed-levels after 31 hours of starting the flow when bars formed for the three different tests. Figure 8.9 shows that similar cross sections were obtained. This result confirms previous theoretical and numerical works (Struiksma et al., 1985; Duró et al., 2016) by showing that hybrid bars would always develop at the same location if the flow and sediment conditions as well as forcing are the same.

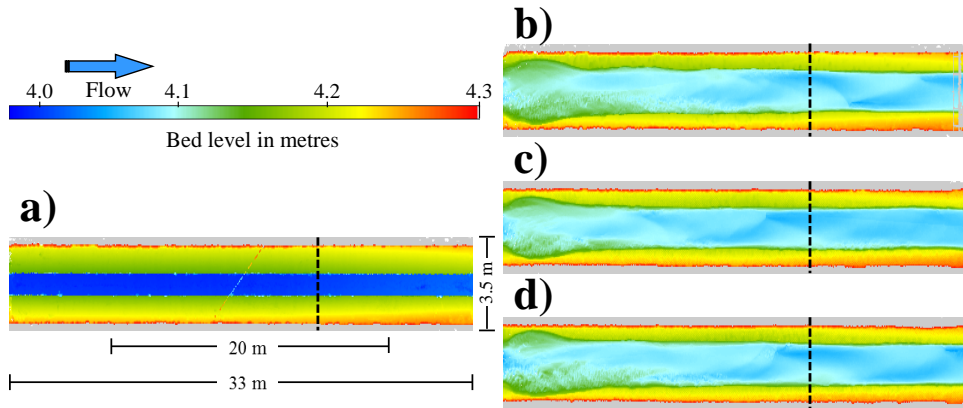


Figure 8.8: Measured bed-levels and planview of the channel for: (a) Initial condition for all the scenarios; and bar pattern after 31 hours for: (b) Scenario 1, (c) Scenario 2, and (d) Scenario 3. Indicated cross-sections are shown in Figure 8.9. Flow from left to right.

8.4.1. EFFECTS OF VEGETATION COLONIZATION ON FLOODPLAINS

POINT clouds highlighting the differences between initial and final bed topographies are shown in Figure 8.10. The wooden sticks used as plants' roots were found highly efficient in increasing the resistance of channel banks, as previously noted in small-scale mobile-bed experiments (e.g. Vargas-Luna et al., 2016b).

Figure 8.11 shows the evolution in time of the wet channel width during the experiments obtained for the three considered scenarios. The values of the wet channel width reported in this figure correspond to the averaged value of the free-surface width calculated by means of imagery analysis for the high-flow conditions in the central 20 m of the flume. The upstream and downstream parts of the flume were excluded from the analysis in order to limit the effects of the boundaries, which were particularly pronounced

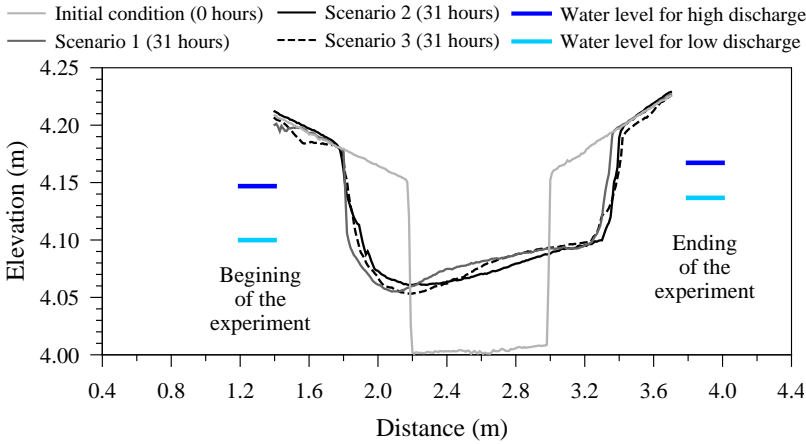


Figure 8.9: Cross-sections comparison between the starting condition and the bar development after 31 hours for the considered scenarios. Localization of the cross-sections shown in Figure 8.8.

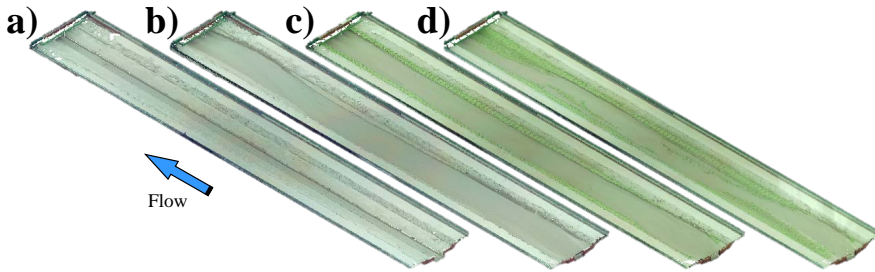


Figure 8.10: Rendered point clouds of the mobile-bed flume. Bed topography of: (a) Initial condition for all the scenarios (0 hours), and after 86 hours for (b) Scenario 1, (c) Scenario 2, (d) Scenario 3.

especially near the upstream end. As expected, the averaged channel width varies as a function of the discharge. Scenario 1 (without plants) shows a similar widening rate during the entire experiment, whereas widening is moderately reduced in scenarios 2 and 3 after the vegetation colonization of floodplains. This can also be noticed from the final planforms shown in Figure 8.12. Figure 8.11 shows also that the final averaged width is reduced in approximately 10 % for the scenarios with vegetation.

Table 8.2 summarizes the characteristics of the main channel (calculated along the thalweg) obtained at the end of each test for the considered scenarios. Narrower channels, as those obtained in scenarios 2 and 3, have shown to have a direct impact on the channel final planform. Vegetation affects also the bar length, as already observed by Jang and Shimizu (2005) using a numerical model. Figure 8.12 shows that the obtained planview exhibits four main bars in scenarios 2 and 3, whereas only three bars were present in scenario 1. This means that the experiments confirm their findings. Crosato (2008) showed that the wavelength of hybrid bars decreases if the width-to-depth ratio decreases.

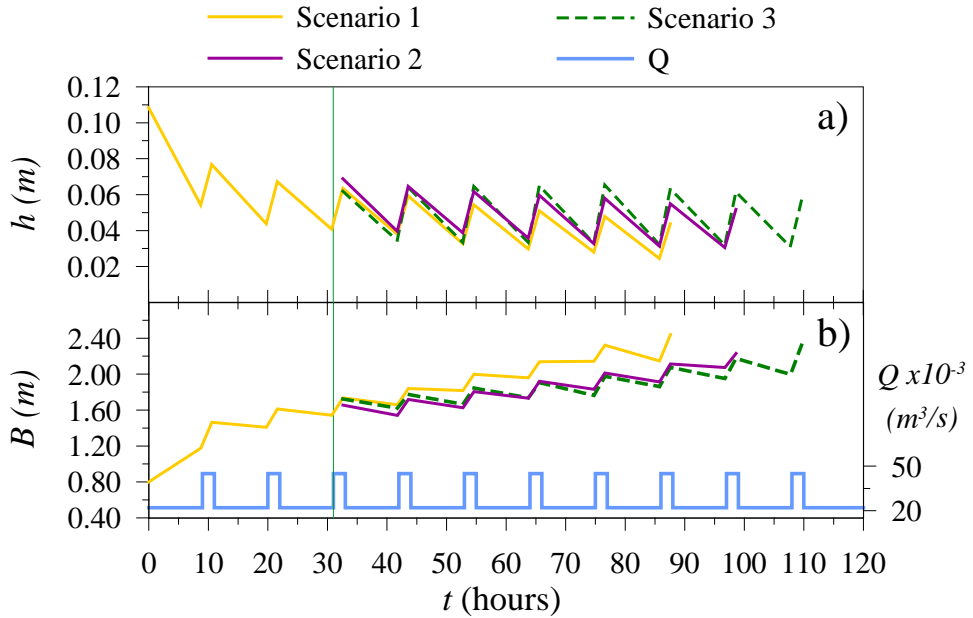


Figure 8.11: Temporal evolution of reach averaged: (a) Water depth, h , and (b) Wet channel width, B , during the experimental tests

Table 8.2: Reach-averaged channel characteristics for the considered scenarios at different times.

Scenario	Wet channel width B (m)	Water depth h (cm)	Slope i_b (m/m)	Sinuosity I_S (-)
1 - After 88 hours	2.44	4.4	0.0020	1.028
2 - After 88 hours	2.11	5.5	0.0015	1.042
3 - After 88 hours	2.08	6.3	0.0021	1.039
2 - After 99 hours	2.23	5.2	0.0016	1.045
3 - After 99 hours	2.18	6.2	0.0023	1.066
3 - After 110 hours	2.32	5.6	0.0024	1.089

8.4.2. EFFECTS OF VEGETATION COLONIZATION ON BARS

FIGURE 8.12 shows the bed level evolution for the considered scenarios. The bed-levels measured at the end of each scenario (Figures 8.12a to 8.12c) show that bank erosion is substantially reduced in scenario 2 due to the vegetated floodplains. This figure also emphasizes the main effects of vegetation colonization on sediment bars. Higher sediment bars and deeper channels are obtained in scenario 3 as well as increased bank erosion due to the sediment trapped by the plants and the flow concentration in the main channel. As a result, the obtained channel sinuosity is much higher than in the other two cases, see Table 8.2. This is here attributed to the flow deflection caused by the vegetation elements and by the sediment trapped by the plants. Figure

8.13 shows typical cross-sections for the considered scenarios taken in regions where bars formed after 86 hours.

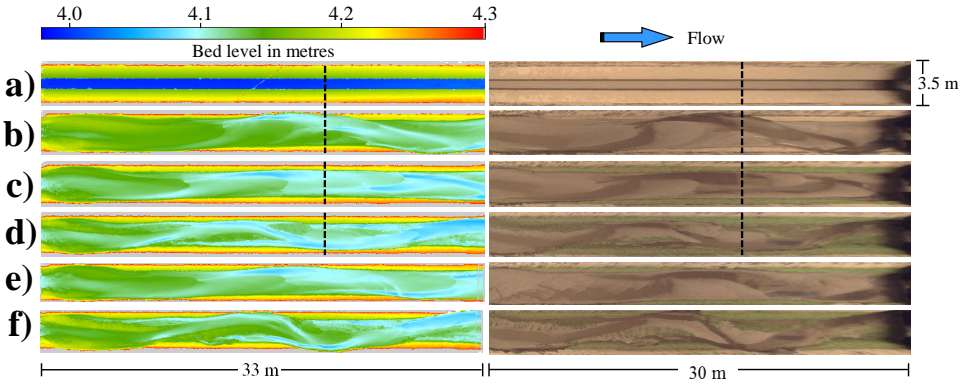


Figure 8.12: Measured bed-levels and planview of the channel for: (a) Initial condition for all the scenarios; after 86 hours for: (b) scenario 1, (c) scenario 2, and (d) scenario 3; after 97 hours for: (e) scenario 2, (f) scenario 3. Indicated cross-sections are shown in Figure 8.13. Flow from left to right.

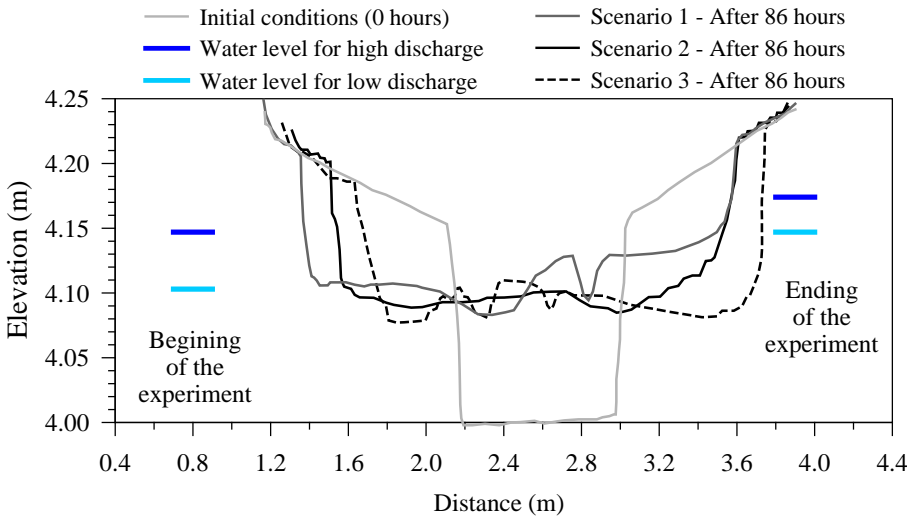


Figure 8.13: Cross-sections comparison between the starting condition and the final configuration of a bar (after 86 hours) for the considered scenarios. Localization of the cross-sections shown in Figure 8.12.

By comparing the results presented in Table 8.2 and Figure 8.12 for scenarios 2 and 3 is evident that these scenarios present similar channel width, sinuosity and longitudinal bed slope. However, in Scenario 3 a deeper channel and higher sediment deposits were obtained in comparison with Scenario 2. This emphasizes the incision by the flow concentration and the sediment deposition induced by the colonizing plants.

The plant units used in our experiments exhibited high resistance to the flow when placed on emerging sediment deposits, avoiding to be uprooted in most cases. So, the collapsed floodplains due to bank erosion (failure) were the primarily source of plants transported downstream by the flow. These highly-resistant new sediment deposits triggered the formation of a side channel and the quick formation of new sediment deposits, see Figure 8.12g. When the main structure of the bars was established, an important fraction of the sediment transported by the flow was captured on bar tops resulting on raise of local bed which often led to the complete submersion of the plants by deposited sediment. In some areas of the flume plants were re-seeded up to 3 layers above the initial one.

8.5. DISCUSSION AND CONCLUSIONS

THE scenarios considered in this experimental work allow observing the effects of vegetation colonization on the strength of the colonized deposits and on the accretional processes in channels. The combined effects of vegetation colonization on the floodplains were found highly affecting the channel width, sinuosity and longitudinal bed slope, leading to noticeable changes in planform configuration.

Although the test with colonization of emerging deposits, scenario 3, exhibits higher bars and lower bed levels, high similarity was found in channel properties with the results obtained for scenario 2, which emphasizes that the main effects of plant colonization are the accretion of sediment deposits (due to sediment trapping and retention) and channel incision (due to the deflection of the flow to the main channel).

Vegetation colonization on bars substantially enhanced opposite bank erosion (bar push effect). However, the resistance of the banks was relatively low considering that non-cohesive material was used in the experiments. It would be important to study the push effect on banks having different resistance against erosion.

The results of these experiments confirm the accretional processes observed in some small streams, such as in the Widden Brook in the Hunter Valley, Australia (see [Erskine et al., 2012](#)) and other large-scale experiments executed in sandy-bed sinuous channels (see [Rominger et al., 2010](#)). The opposite bank erosion observed in the experiments carried out in this work was also observed in the experimental work performed by [Rominger et al. \(2010\)](#) at the Outdoor StreamLab (OSL) of the University of Minnesota's St. Anthony Falls Laboratory. [Rominger et al. \(2010\)](#) also studied the effects of plants colonizing a point bar on altering the secondary circulation observed in river bends.

9

CONCLUSIONS AND RECOMMENDATIONS

“Research is formalized curiosity. It is poking and prying with a purpose.”

Zora Neale Hurston



Figure 9.1: PhD project word cloud (Created with Wordle: <http://www.wordle.net/>)

The main findings and conclusions and recommendations of this PhD project are included in this chapter.

9.1. MAIN CONCLUSIONS

THE results of the study provided the following answers to the research questions:

What is the role of vegetation in river bank accretion?

THIS research addressed this topic by performing an analysis of field observations in a restored lowland stream, the Lunterse Beek (Chapter 7), and by conducting laboratory experiments carried out in a large-scale mobile-bed flume at Delft University of Technology (Chapter 8). The morphological changes and the vegetation cover evolution observed during the five years following the restoration of the lowland stream made it possible to determine how relevant the establishment of vegetation is for the stabilization of the channel width and to see how extensive is the vertical accretion both on levees and floodplains. The levees that formed during overbank flows were only stable if soil was reinforced by vegetation (Section 7.4.2). These findings were confirmed by the experimental tests linked to the evolution of a small straight channel with variable discharge. All tests showed initial channel widening and alternate bar formation which influenced bank erosion and channel evolution. Three scenarios were studied: 1) absence of vegetation, 2) vegetated floodplains and 3) vegetated floodplains and the colonization of deposits emerging during low-flow conditions, namely the bar tops. The scenario that includes the colonization of vegetation, scenario 3, showed a degree of sediment deposition and stabilization (accretion) of colonized deposits as well as general channel incision as observed in the Lunterse Beek after the vegetation had been established (Section 8.4.2).

In the first five years after restoration, the Lunterse Beek presented only limited bank accretion. Apart from an initial cutoff, the channel alignment remained stable. In the laboratory experiments, colonization by plants induced both vertical and lateral accretion, thereby enhancing opposite bank erosion (the bar push effect). Here the different response between field and laboratory observations regarding lateral accretion may be attributed to the relatively high water levels that are artificially maintained during any low-flow stages in the Lunterse Beek, whilst there was no such restriction in the laboratory experiments. High low-flow water levels did not allow top area deposits to emerge, impeding vegetation colonization. This condition shows that low-flow stages are relevant to river bank accretion, since it is during this period that vegetation colonizes emerging new deposits. However, the resistance of the banks in the laboratory experiments was relatively low because banks consisted of sand, in contrast to the conditions present in the Lunterse Beek, where banks tend to be composed of cohesive material. Laboratory studies including variations in the resistance to erosion would therefore be important for studying the push effect in future experimental activities.

The conclusion is that vegetation is an essential component of river bank accretion. Nevertheless, it is important to mention that the results presented in this research exclude incised rivers and rivers formed in clay-dominant environments. Incised rivers

present progressive channel deepening and outer bank erosion, so causing the displacement of the main channel and a corresponding exposure of sediment deposits on the opposite bank which can in fact be seen as bank accretion. Sediment deposits in river systems with banks composed of clay result in lateral bank accretion due to soil stabilization caused by compaction processes which increases the local soil resistance to erosion leading to opposite bank erosion and lateral channel shift.

Which method should be used to estimate the effects of vegetation on river morphology?

THE work carried out to address this issue included two facets: 1) selecting the best methods to estimate the effects of vegetation on flow resistance and sediment transport and the calculation of vertical velocity profiles in vegetated flows, and 2) defining the applicability ranges of the selected methods for the purposes of this research. The work included a literature review, model assessment based on data published in the literature, as well as new experiments carried out in the tilting flumes and in the small-scale mobile-bed facilities at Delft University of Technology that are designed to assess the applicability ranges, and the analysis of the results of 2D numerical simulations presented in previous works. The parts of the study that deal with these aspects are presented in Chapters 5 and 6.

The literature review and the method comparison allowed the main characteristics to be defined that an optimal method describing the effects of vegetation on flow resistance and sediment transport should fulfil if it is to be applied to river morphodynamic modelling. In view of the wide range of water levels to which vegetation in a river system can be exposed, the method should be able to represent the effects of plants under emergent and submerged conditions. In this connection, the results showed that only a few methods are applicable to both situations. For submerged vegetation, the degree of submergence (h/h_v) is a key parameter for estimating the flow resistance exerted by plants (Section 5.3.1). It is also important that the method includes an estimation of the bed-shear stress, since sediment transport depends on this parameter. Although none of the analysed methods can represent both emergent and submerged conditions equally well, the Baptist (2005) method provides the best fitting with respect to the experimental data gathered from the literature, for both artificial and real vegetation (Section 5.3.1). Baptist's method performed well, also regarding the assessment of bed-shear stresses, however, due to limitations in the availability of data for submerged conditions, this aspect was only examined for emergent vegetation and bed-load sediment transport (Section 5.3.3). The bed-shear stress calculation allowed testing the Baptist (2005) method on the assessment of the sediment transport capacity in vegetated channels. This was estimated by combining Baptist's method with the sediment transport capacity formulae of van Rijn (1984a) and Engelund and Hansen (1967) derived for non-vegetated channels. A good correspondence was generally observed. However, poor performance was obtained for low sediment transport rates (conditions close to initiation of motion). This

aspect is attributed to possible variations in the mobility thresholds for vegetated beds or to the possibility that the sediment and flow characteristics did not fall within the applicability ranges of these formulae (Section 5.3.5).

Based on the analysis of the results of numerical simulations obtained from the literature, Baptist's method was found to produce satisfactory estimates of the sedimentation rates on vegetated floodplains. Therefore, the method can be applied to study the effects of floodplain vegetation on river planform development. However, the method overestimates bed protection exerted by low-density vegetation (Sections 6.5.2 and 6.5.3). It is the assumption that there is dense vegetation that lies at the basis of Baptist's method. The tests performed show that applying the method to areas with sparse vegetation results in an underestimation of bed erosion by flowing water. Comparisons between Baptist's method predictions and data obtained from the small-scale experiments performed in this part of the work, proved the method to be suitable for use in this research and was then applied to the numerical simulations performed to analyse the field observations.

After having selected the method proposed by Baptist (2005), the work focused on establishing the applicability ranges. This method schematizes plants as arrays of rigid cylinders with uniform distribution (density), diameter and height. The results obtained (Sections 5.3.3 and 6.5) showed that for numerical modelling purposes the Baptist method:

- Provides better results for high-density grass and herbaceous vegetation.
- Can be used by imposing a drag coefficient, C_D , equal to unity, and establishing the plant characteristics to be described only by two parameters: projected plant area per unit volume including the effects of foliage, a , and plant height, h_v .
- Performs better in vegetation arrays for ah_v larger than 0.01.
- Can be applied to flexible plants and plants with foliage, though it is advisable to use the deflected vegetation height and to calibrate the characteristics of the array of cylinders used to describe the vegetation type considered.
- Is not suitable to reproduce the effects of isolated plants, such as trees.

Regarding the aspect of the work that dealt with velocity profile estimation, it was found that the method proposed by Klopstra et al. (1997) performs best when estimating the vertical velocity profile for the vegetated flows considered. However, as velocity profiles among plants are greatly affected by foliage, the performance of these types of methods is very dependent on the combination of flow characteristics and vegetation properties (Section 5.3.2).

The results obtained from the new small-scale laboratory experiments conducted in the tilting flumes showed that rigid cylinders exhibit the same trends and have friction coefficients of the same order of magnitude as real and plastic plants. However, rigid cylinders have smaller element Reynolds numbers, an aspect that shows the importance

of carefully selecting the diameter of the cylindrical rods (Section 6.4.1). To consider the relevance of the different element Reynolds numbers exhibited by cylinders and plants, one of the tested vegetation types (artificial grass) was selected for the large-scale experiments and the Baptist's method was used for hydrodynamic characterization.

The small-scale laboratory experiments carried out in the mobile-bed flumes also allowed the establishment of the applicability of rigid cylinders to qualitatively represent the morphological processes of channels with vegetated floodplains, such as channel-width development (Section 6.4.2) and bank dynamics (Section 6.4.3) in the laboratory.

What effects does vegetation growth have on the morphological evolution of lowland streams?

THIS part of the study consisted of the combined analysis of the morphological evolution of a lowland stream in the Netherlands, the Lunterse Beek, and the results of a 2D morphological modelling exercise (with Delft3D) using Baptist's method to study different vegetation dynamics scenarios. Experiments done in the large-scale facility at Delft University of Technology that were carried out between December 2015 and March 2016, also contributed to an understanding of the effects of plants on the morphology of small lowland streams.

The results of the field data analysis showed that vegetation processes (colonization, establishment and growth) play a major role in the morphological evolution of lowland streams in temperate climates, such as the Lunterse Beek in the Netherlands. Vegetation contributes to the stabilization of the channel width and enhances the vertical accretion both of levees and floodplains. It is the combination of these processes that leads to channel incision and bed adaptation (Section 7.4.2). The results of field observations showed that the root system of plants plays a key role in reinforcing the soil and counteracting the effects of flow perturbations. This was found to occur even during high-flow periods in winter, when vegetation biomass (foliage) is substantially reduced (Section 7.4.2). It is therefore relevant to include the effects of roots in methods that take into account the morphodynamic effects of vegetation and in models that estimate bank erosion and accretion.

The 2D morphodynamic model reproduced the observed morphological changes rather well. However, the model was not able to completely reproduce the bank dynamics observed in the stream. This limitation was attributed to the simplified description of bank erosion and to the lack of soil reinforcement estimators (Section 7.5).

The results of the experiments showed that there are important differences in bed topography (bar pattern) and final planform between scenarios differing in terms of vegetation cover (Section 8.4). These experiments showed that plant colonization on sediment deposits emerging during low flows induces vertical accretion and channel

incision. These were aspects that were also observed in the Lunterse Beek. Moreover, vegetation colonization increased the amplitude and length of the bars in the main river channel, thus affecting the final river planform. In view of the similarity of scales, the experimental results can be assumed to represent small lowland streams in temperate climates, which clearly demonstrates the major part that vegetation colonization plays on bank resistance and on the accretional processes of these systems.

What is the role of seasonal variations of vegetation and can they be included in modelling bank accretion?

THE role of seasonal variations in vegetation was studied by combining the analysis of field observations with the results of a morphodynamic model (Delft3D) thereby simulating the evolution of the Lunterse Beek in the first five years after restoration for different vegetation scenarios. Seasonal variations included modifications in vegetation characteristics (height, density, etc.) and water flow. Higher discharges characterised the winter seasons, whereas low discharges characterised the summer seasons. Seasonality is typical of temperate climates. The model was found to clearly reproduce the short-term adaptation of the stream morphology to seasonal variations, demonstrating the relevance of seasonal plant variability to short-term predictions. This can, for instance, be relevant to studies dealing with ecological processes. In the long term, however, the establishment of high and dense herbaceous vegetation resulted in negligible effects in terms of seasonal variations. This was attributed to the dominance of the effects of roots, which did not show much seasonal variation, since they remained strong and vital during the winter. Once established, roots had major influence when it came to stabilizing floodplain soil and banks. This explains the minor differences obtained between the results produced by scenarios 3 and 4 (with and without seasonal variation) at the end of the period analysed (Section 7.5).

Quantifying the effects of seasonal variations of plant root systems on soil reinforcement and the role that this has in the stability of soil and banks is an important issue that should be addressed in future investigations in order to more accurately predict the morphological evolution of small river systems.

9.2. GENERAL CONCLUSIONS

THE execution of this research made it possible to identify some general aspects that are relevant to morphodynamic studies.

The first important observation is that the combination of different approaches provides a more complete overview of the problem, which is fundamental to understanding complex physical processes. The importance of analysing observations at different spatial and temporal scales arose during the experimental work. The experiments performed in the small-scale flumes, such as the tilting flume, were relevant to the detailed

study of small-scale processes. This increased the understanding of the fundamental processes to be used later in the designing of large-scale experiments. A large-scale mobile-bed flume is important for creating conditions that are comparable to those observed in real small streams, such as the hydraulic regime (i.e. subcritical) and the presence of sand bars and other bed forms. The size of the large facility available at Delft University of Technology (45 m long x 5 m wide) has allowed for experimental investigations to minimize scale issues. The experiments carried out in small-scale flumes constructed *ad hoc* were determinant in selecting the materials for large-scale experiments, such as the plant density and the sediment type. The versatility of the small-scale facilities was key to time and cost reduction, because not all the combinations of sediment and plants produced the desired conditions. Therefore, the selection of the appropriate materials was found to be an important part of the planning and preparation in these types of experiments.

The conclusion is that the proper design of experiments in a large facility requires the use of quick and numerous tests carried out in small facilities.

9.3. RECOMMENDATIONS

SEVERAL aspects require further investigation. The upscaling of the effects of vegetation on sediment dynamics for applications in large spatial scales requires more attention. The bed-shear stress, decreased by the presence of vegetation, for instance, affects sediment transport between plants. This and its effects on local morphodynamics has been analysed only for specific situations and needs more extensive studies. In particular, only a few efforts have been made to design sediment transport formulae for vegetated beds. New formulae should be valid for different vegetation densities, ranging from bare to vegetated beds. Therefore, more effort needs to be put into incorporating the properties and effects of plants in new sediment transport capacity formulae designed both for vegetated and non-vegetated streams relevant to morphodynamic predictions and simulations. Approaches combining bed-shear stress and vegetation drag are scarce and most assume that there is a linear distribution between these variables. Therefore more research is required to clarify their relative contribution to the total flow resistance of vegetated beds. Sediment transport measurements among and above submerged plants are lacking, so in this regard laboratory experiments are also needed.

During this research, considerable effort was put into the testing of optical techniques (Terrestrial Laser Scanning and Structured Light) to measure the bed-level evolution in mobile-bed flumes through flowing water. Despite the advances made through this activity, low accuracy was obtained in the procedure required to correct the refraction effects of water. Therefore more research also needs to be done in this area.

The inclusion of vegetation dynamics (colonization, survival, growth, succession, etc.) in morphodynamic models was not a part of this research. Efforts to couple these processes with water and sediment flows are highly recommended. This important step

will contribute to the modelling of the long-term effects of vegetation in river morphology.

Field measurements combining vegetation development and morphological evolution are few and far between. Thus, more field campaigns under different climatic conditions and river sizes should be performed. This aspect is especially important for the quantification of the effects of river restoration and training projects and for the validation of new approaches.

APPENDICES

A

LIST OF MODELS PREDICTING THE EFFECTS OF VEGETATION

A.1. MODELS APPLICABLE TO EMERGENT CONDITIONS

A.1.1. PETRYK AND BOSMAJIAN (1975) [P&B]

Based on a force balance, [Petryk and Bosmajian](#) derived the mean flow velocity as

$$\bar{u}_{P\&B} = \sqrt{\frac{2gi_b}{aC_D}} \quad (\text{A.1})$$

which implies that the global flow resistance coefficient is expressed as

$$C_{r\ P\&B} = \sqrt{\frac{2g}{ahC_D}} \quad (\text{A.2})$$

A.1.2. RAUPACH (1992) [R]

The work by [Raupach](#) expressed the bed shear stress as a fraction of the total shear stress as

$$f_R = \frac{1}{1 + ah_v \left(\frac{C_R}{C_P} \right)} \quad (\text{A.3})$$

where C_R is the drag coefficient for a single element, and C_P is the particle drag coefficient without elements. The particle drag coefficient is estimated by applying the equation proposed by [Thompson et al. \(2004\)](#) given as

$$C_P = 0.0016Q^{-0.2266} \quad (\text{A.4})$$

where Q is the discharge in m^3/s .

A.1.3. ISHIKAWA ET AL. (2003) [I]

Based on flume experiments, [Ishikawa et al. \(2003\)](#) provide the following global flow resistance predictor

$$C_{rI} = \sqrt{g} \left(\frac{\bar{u}'}{u'_*} \right) \quad \text{for: } h/h_v \leq 1 \quad (\text{A.5})$$

where

$$\frac{\bar{u}'}{u'_*} = 1.28(ah_v + 0.02)^{-0.534} \quad (\text{A.6})$$

The ratio between the bed-shear stress and total-shear stress is expressed as

$$f_I = 0.0709(ah_v + 0.02)^{-0.67} \quad (\text{A.7})$$

A.1.4. JAMES ET AL. (2004) [J]

James et al. expressed the global flow resistance coefficient as

$$C_{rJ} = \sqrt{1-\lambda} C_{rP\&B} = \sqrt{\frac{2g(1-\lambda)}{ahC_D}} \quad (\text{A.8})$$

A.1.5. HOFFMANN (2004) [HOF]

Based on a space-time porous media averaged model, Hoffmann derived the following global flow resistance coefficient

$$C_{rHof} = \sqrt{h - \frac{\pi D^2}{2S_{Hof}}} C_{rP\&B} = \sqrt{\frac{2g}{ahC_D} \left(h - \frac{\pi D^2}{2S_{Hof}} \right)} \quad (\text{A.9})$$

where the separation between cylinders, S_{Hof} , is given as

$$s_{Hof} = \frac{1}{\sqrt{m}} \quad (\text{A.10})$$

A.1.6. KOTHYARI ET AL. (2009) [KO]

From a momentum balance, Kothyari et al. derived a bed-shear stress given as

$$\tau_{bvKo} = gh \sin \theta - \frac{1}{2} \frac{\rho \bar{u}^2 ahC_D}{1-\lambda} \quad (\text{A.11})$$

where θ is the channel bed angle in radians. The ratio between bed-shear stress and total shear stress is given by

$$f_{Ko} = \frac{2g(1-\lambda) \sin \theta - aC_D \bar{u}^2}{2gi_b(1-\lambda)} \quad (\text{A.12})$$

A.2. MODELS APPLICABLE TO SUBMERGED CONDITIONS**A.2.1. KLOPSTRA ET AL. (1997) [K]**

The Klopstra et al. model subdivide the vertical velocity profile in two layers: vegetation and upper layer. The vertical velocity profile in the vegetation layer is obtained as a solution of the momentum equation

$$u(z)_K = \sqrt{\bar{u}_{P\&B}^2 + C_1 e^{-Az} + C_2 e^{Az}} \quad \text{for: } 0 < z \leq h_v \quad (\text{A.13})$$

A

where $\bar{u}_{P\&B}$ corresponds to the velocity in the vegetation layer proposed by [Petryk and Bosmajian](#) (eqA. A.1); z is the vertical position; C_1 , C_2 , and A are variables, defined as

$$C_1 = \frac{g i_b (h - h_v)}{\ell A (e^{Ah_v} + e^{-Ah_v})} \quad (\text{A.14})$$

$$C_2 = -C_1 \quad (\text{A.15})$$

$$A = \sqrt{\frac{a C_D}{\ell}} \quad (\text{A.16})$$

in which ℓ is the characteristic length scale given by van [Van Velzen et al. \(2003\)](#), tested by [Galema \(2009\)](#):

$$\ell = 0.0227 h_v^{0.7} \quad (\text{A.17})$$

The vertical velocity profile in the upper layer is derived from a modified form of the logarithmic law for turbulent flows. Including the integration constant in the length scale for the bed roughness and assuming a raised zero plane for the logarithmic profile, the velocity profile in this layer becomes

$$u(z)_K = \frac{u_* K}{\kappa} \ln \left(\frac{z - [h_v - h_s]}{k_p} \right) \text{ for } h_v \leq z \leq h \quad (\text{A.18})$$

where $u_* K$ is the shear velocity, κ ($=0.41$) is Von Kármán's constant, k_p is the length scale for bed roughness of the upper layer, and h_s is the distance between the top of the vegetation and the virtual bed of the upper layer defined as follows

$$u_* K = \sqrt{g [h - (h_v - h_s)] i_b} \quad (\text{A.19})$$

$$k_p = h_s e^{-F} \quad (\text{A.20})$$

$$h_s = g \left[\frac{1 + \sqrt{1 + \frac{(2E\kappa)^2 (h - h_v)}{g}}}{2(E\kappa)^2} \right] \quad (\text{A.21})$$

with the help variables

$$E = \frac{C_3 e^{Ah_v}}{2B_1} \quad (\text{A.22})$$

$$C_3 = \frac{C_2}{i_b} \quad (\text{A.23})$$

$$F = \frac{\kappa B_1}{\sqrt{g B_3}} \quad (\text{A.24})$$

$$B_1 = \sqrt{C_3 e^{Ah_v} + u_{v0}^2} \quad (\text{A.25})$$

$$B_2 = \sqrt{C_3 + u_{v0}^2} \quad (\text{A.26})$$

$$B_3 = [h - (h_v - h_s)] \quad (\text{A.27})$$

$$u_{v0} = \frac{\bar{u}_{P \& B}}{\sqrt{i_b}} \quad (\text{A.28})$$

The global flow resistance coefficient is obtained with the integral of the vertical velocity profile defined by eqAs. A.13 and A.18, which can be expressed as

$$C_{rK} = h^{-3/2} \cdot \left\{ \frac{2(B_1 - B_2)}{A} + \frac{u_{v0}}{A} \ln \left[\frac{(B_1 - u_{v0})(B_2 + u_{v0})}{(B_1 + u_{v0})(B_2 - u_{v0})} \right] + \right. \\ \left. \frac{\sqrt{gB_3}}{\kappa} \left[B_3 \ln \left(\frac{B_3}{k_P} \right) - h_s \ln \left(\frac{h_s}{k_P} \right) - (h - h_v) \right] \right\} \quad (\text{A.29})$$

A.2.2. VAN VELZEN ET AL. (2003) [vV]

Based on the Klopstra et al. model, this method estimates the global flow resistance coefficient from the mean flow velocity. This velocity is obtained from the average velocity in the vegetated layer, u_{vvV} , and in the upper layer, u_{svV} , as follows

$$u_{vvV} = \frac{1}{Ah_v} \left\{ 2(B_1 - B_2) + u_{v0} \ln \left[\frac{(B_1 - u_{v0})(B_2 + u_{v0})}{(B_1 + u_{v0})(B_2 - u_{v0})} \right] \right\} \quad (\text{A.30})$$

$$u_{svV} = \frac{u_{*K}}{\kappa(h - h_v)} \left[B_3 \ln \left(\frac{B_3}{k_P} \right) - h_s \ln \left(\frac{h_s}{k_P} \right) - (h - h_v) \right] \quad (\text{A.31})$$

where

$$u_{v0} = \sqrt{\frac{h_v i_b}{\frac{1}{C_b^2} + \frac{ah_v C_D}{2g}}} \quad (\text{A.32})$$

and C_b is the bed roughness, expressed as

$$C_b = 18 \log \left(\frac{12h}{k_s} \right) \quad (\text{A.33})$$

where k_s is the characteristic roughness of the bed, and the variables A , B_1 , B_2 , B_3 , u_{*K} , h_s , and k_P are as defined for the Klopstra et al. model.

The global flow resistance becomes

$$C_{rvV} = \frac{h_v u_{vvV} + (h - h_v) u_{svV}}{h \sqrt{h i_b}} \quad (\text{A.34})$$

A.2.3. HUTHOFF ET AL. (2007) [H]

This model expresses the global flow resistance coefficient as

$$C_{rH} = \sqrt{\frac{2g}{ahC_D}} \left[\sqrt{\frac{h_v}{h}} + \left(1 - \frac{h_v}{h}\right) \left(\frac{h - h_v}{s_H}\right)^{\frac{2}{3}} \left[1 - \left(\frac{h_v}{h}\right)^5\right] \right] \quad (\text{A.35})$$

where s_H is the separation between cylinders given by

$$s_H = \frac{1}{\sqrt{m}} - D \quad (\text{A.36})$$

A.2.4. YANG AND CHOI (2010) [Y&C]

Based on a two-layer schematization and assuming a constant velocity in the vegetation layer, Yang and Choi suggest deriving the flow velocity in the vegetation layer from

$$u_{vY\&C} = \sqrt{\frac{2ghi_b}{C_D ah_v}} \quad \text{for: } 0 < z \leq h_v \quad (\text{A.37})$$

They assume the vertical velocity profile in the upper layer as logarithmic

$$u(z)_{Y\&C} = u_{vY\&C} + C_u \frac{u_{*Y\&C}}{\kappa} \ln\left(\frac{z}{h_v}\right) \quad \text{for: } h_v \leq z \leq h \quad (\text{A.38})$$

with $C_u=1$ for $a \leq 5.0 \text{ m}^{-1}$, $C_u=2$ for $a > 5.0 \text{ m}^{-1}$, $\kappa (=0.41)$ is Von Kármán's constant, and

$$u_{*Y\&C} = \sqrt{g(h - h_v) i_b} \quad (\text{A.39})$$

They obtained the global flow resistance coefficient by integrating the vertical velocity profile defined by eqAs. A.37 and A.39 and is expressed as

$$C_{rY\&C} = \sqrt{\frac{2g}{ah_v C_D}} + \frac{C_u}{\kappa} \sqrt{g \left(1 - \frac{h_v}{h}\right)} \left[\ln\left(\frac{h}{h_v}\right) - \left(1 - \frac{h_v}{h}\right) \right] \quad (\text{A.40})$$

A.3. MODELS APPLICABLE TO BOTH EMERGENT AND SUBMERGED CONDITIONS

A.3.1. BARFIELD ET AL. (1979) [BF]

In this model the general shear stress equation includes a "spacing hydraulic radius", R_{Bf} , defined for the submerged condition as

$$R_{Bf} = h - h_v + \frac{sh_v}{2h_v + s} \quad (\text{A.41})$$

where s is the spacing of the elements in the vegetation canopy. The bed-shear stress is calculated as follows

$$\tau_{bvBf} = \gamma R_{Bf} i_b \quad (\text{A.42})$$

Barfield et al. method expresses the ratio between bed-shear stress and total-shear stress as

$$f_{Bf} = 1 - \frac{2}{2\left(\frac{h}{h_v}\right) + \frac{sh}{h_v^2}} \quad (\text{A.43})$$

For the emergent conditions, $h_v=h$, thus eqAs. A.41 and A.43 are reduced to

$$R_{Bf} = \frac{sh}{2h+s} \quad (\text{A.44})$$

$$f_{Bf} = \frac{s}{2h+s} \quad (\text{A.45})$$

A.3.2. STONE AND SHEN (2002) [S&S]

The Stone and Shen model predicts the flow resistance from the assessment of an apparent velocity derived from the area concentration of the vegetation stems, λ . The global flow resistance coefficient over submerged vegetation is

$$C_{rS\&S} = 1.385 \left(\frac{h}{h_v} - D\sqrt{m} \right) \sqrt{\frac{g}{ah}} \quad \text{for: } h/h_v > 1 \quad (\text{A.46})$$

The bed-shear stress is given as

$$\tau_{bvS\&S} = \frac{\rho g}{C_b^2} u_v^2 (1 - \lambda) \quad (\text{A.47})$$

where the apparent velocity in the vegetation layer, u_v , is estimated from

$$u_v = \bar{u} \sqrt{\frac{h_v}{h}} \quad (\text{A.48})$$

For emergent canopies this method also assumes $h_v=h$, so $u_v=\bar{u}$ from eqA. A.48, and the eqA. A.46 takes the form

$$C_{rS\&S} = 1.385 (1 - D\sqrt{m}) \sqrt{\frac{g}{ah}} \quad \text{for: } h/h_v \leq 1 \quad (\text{A.49})$$

This method expresses the ratio between the bed-shear stress and the total shear stress as

$$f_{S\&S} = \frac{\tau_{bvS\&S}}{\tau} = \left(\frac{C_{rS\&S}}{C_b} \right)^2 \left(\frac{h_v}{h} \right)^2 (1 - \lambda) \quad (\text{A.50})$$

A.3.3. BAPTIST (2005) [B]

From a momentum balance Baptist proposed a resistance coefficient for flow over submerged vegetation defined as

$$C_{rB} = \sqrt{\frac{1}{\frac{1}{C_b^2} + \frac{C_D a h_v}{2g}} + \frac{\sqrt{g}}{\kappa} \ln\left(\frac{h}{h_v}\right)} \quad \text{for: } h/h_v > 1 \quad (\text{A.51})$$

where κ ($=0.41$) is Von Kármán's constant. The bed-shear stress is estimated as follows

$$\tau_{bvB} = \frac{\rho g}{C'_b} \bar{u}^2 \quad (\text{A.52})$$

with

$$C'_b = C_b + \frac{\sqrt{g}}{\kappa} \ln\left(\frac{h}{h_v}\right) \sqrt{1 + \frac{C_D a h_v C_b^2}{2g}} \quad \text{for: } h/h_v > 1 \quad (\text{A.53})$$

Emergent canopies are described by assuming $h_v=h$, so for this condition $C'_b=C_b$ and eqA. A.51 takes the form

$$C_{rB} = \sqrt{\frac{1}{\frac{1}{C_b^2} + \frac{C_D a h}{2g}}} \quad \text{for: } h/h_v \leq 1 \quad (\text{A.54})$$

If the bed roughness is neglected in eqA. A.54, the averaged velocity is reduced to the model proposed by Petryk and Bosmajian for emergent vegetation, eqA. A.1. The ratio between the bed-shear stress and the total-shear stress, is given by

$$f_B = \frac{\tau_{bvB}}{\tau} = \left(\frac{C_{rB}}{C'_b}\right)^2 \quad (\text{A.55})$$

A.3.4. CHENG (2011) [CH]

Based on a two-layer description of the flow, Cheng (2011) derived equations for the calculation of flow velocities in each layer. The mean velocity in the vegetation layer is described with the model proposed by Cheng and Nguyen (2011) as

$$u_{vCh} = \sqrt{\frac{2g r_v i_b}{C_D^*}} \quad (\text{A.56})$$

where

$$C_D^* = \frac{130}{r_{v^*}^{0.85}} + 0.8 \left[1 - \exp\left(-\frac{r_{v^*}}{400}\right) \right] \quad (\text{A.57})$$

with

$$r_{v*} = r_v \left(\frac{g i_b}{v^2} \right)^{1/3} \quad (\text{A.58})$$

$$r_v = \frac{\pi(1-\lambda)D}{4\lambda} \quad (\text{A.59})$$

The mean velocity in the upper layer is given as

$$u_{sCh} = 4.54 \left[\left(\frac{1}{\lambda} - 1 \right) \left(\frac{h-h_v}{D} \right) \right]^{1/16} \sqrt{g(h-h_v) i_b} \quad (\text{A.60})$$

Finally, by calculating the mean flow velocity in the entire section, the global flow resistance coefficient takes the form

$$C_{rCh} = (1-\lambda) \sqrt{\frac{2gr_v}{h_v C_D} \left(\frac{h_v}{h} \right)^{3/2}} + 4.54 \sqrt{g} \left[\left(\frac{1}{\lambda} - 1 \right) \left(\frac{h-h_v}{D} \right) \right]^{1/16} \left(1 - \frac{h_v}{h} \right)^{3/2} \quad (\text{A.61})$$

REFERENCES

- Abbe, T. B. and Montgomery, D. R. (2003). Patterns and processes of wood debris accumulation in the queets river basin, washington. *Geomorphology*, 51(1-3):81–107.
- Aberle, J. and Järvelä, J. (2013). Flow resistance of emergent rigid and flexible floodplain vegetation. *Journal of Hydraulic Research*, 51(1):33–45.
- Abernethy, B. and Rutherford, I. D. (2000). The effect of riparian tree roots on the mass-stability of riverbanks. *Earth Surface Processes and Landforms*, 25(9):921–937.
- Albayrak, I., Nikora, V., Miler, O., and O’Hare, M. (2012). Flow-plant interactions at a leaf scale: effects of leaf shape, serration, roughness and flexural rigidity. *Aquatic Sciences*, 74(2):267–286.
- Albayrak, I., Nikora, V., Miler, O., and O’Hare, M. T. (2014). Flow-plant interactions at leaf, stem and shoot scales: drag, turbulence, and biomechanics. *Aquatic Sciences*, 76(2):269–294.
- Alexander, J. and Marriott, S. B. (1999). *Floodplains: Interdisciplinary Approaches*, chapter Introduction, pages 1–13. Geological Society, London, Special Publications, 163.
- Allen, C. D., Macalady, A. K., Chenchouni, H., Bachelet, D., McDowell, N., Vennetier, M., Kitzberger, T., Rigling, A., Breshears, D. D., Hogg, E. T., Gonzalez, P., Fensham, R., Zhang, Z., Castro, J., Demidova, N., Lim, J.-H., Allard, G., Running, S. W., Semerci, A., and Cobb, N. (2010). A global overview of drought and heat-induced tree mortality reveals emerging climate change risks for forests. *Forest Ecology and Management*, 259(4):660–684.
- Allmendinger, N. E., Pizzuto, J. E., Potter, N., Johnson, T. E., and Hession, W. C. (2005). The influence of riparian vegetation on stream width, Eastern Pennsylvania, USA. *Geological Society of America Bulletin*, 117(1-2):229–243.
- Amlin, N. A. and Rood, S. B. (2001). Inundation tolerances of riparian willows and cottonwoods. *JAWRA Journal of the American Water Resources Association*, 37(6):1709–1720.
- Anders, N. S., Seijmonsbergen, A. C., and Bouten, W. (2011). Segmentation optimization and stratified object-based analysis for semi-automated geomorphological mapping. *Remote Sensing of Environment*, 115(12):2976–2985.
- Anderson, R. J., Bledsoe, B. P., and Hession, W. C. (2004). Width of streams and rivers in response to vegetation, bank material, and other factors. *JAWRA Journal of the American Water Resources Association*, 40(5):1159–1172.

- Andrews, E. D. (1984). Bed-material entrainment and hydraulic geometry of gravel-bed rivers in colorado. *Geological Society of America Bulletin*, 95(3):371–378.
- Anthony, E. J. (2004). Sediment dynamics and morphological stability of estuarine mangrove swamps in sherbro bay, west africa. *Marine Geology*, 208(2-4):207–224.
- Armanini, A. and Cavedon, V. Sediment transport in vegetated streams. *Submitted to Advances in Water Resources*.
- Armanini, A., Righetti, M., and Grisenti, P. (2005). Direct measurement of vegetation resistance in prototype scale. *Journal of Hydraulic Research*, 43(5):481–487.
- Asahi, K., Shimizu, Y., Nelson, J., and Parker, G. (2013). Numerical simulation of river meandering with self-evolving banks. *Journal of Geophysical Research: Earth Surface*, 118:1–22.
- ASCE Task Committee on Hydraulics, Bank Mechanics, and Modelling of River Width Adjustment (1998). River width adjustment. I: Processes and mechanisms. *Journal of Hydraulic Engineering*, 124(9):881–902.
- Ashida, K. and Michiue, M. (1972). Study on hydraulic resistance and bedload transport rate in alluvial streams (in japanese). *Journal of Civil Engineering, Jpn Soc Civil Engineers*, 206:59–69.
- Asselman, N. E. M. (1995). The impact of climate change on suspended sediment transport in the river Rhine. In Zwerver, S., Rompaey, R. S. A. R., van, Kok, M. T. J., and Berk, M. M., editors, *Climate change research: evaluation and policy implications; proceedings of the International Climate Change Research Conference, Maastricht, The Netherlands, 6-9 December 1994. Vol. B*, volume 65 of *Studies in Environmental Science*, pages 937–942. Elsevier.
- Asselman, N. E. M. (1997). *Suspended sediments in the River Rhine*. PhD thesis, University of Utrecht, The Netherlands.
- Asselman, N. E. M., Middelkoop, H., and van Dijk, P. M. (2003). The impact of changes in climate and land use on soil erosion, transport and deposition of suspended sediment in the River Rhine. *Hydrological Processes*, 17(16):3225–3244.
- Auble, G. T. and Scott, M. L. (1998). Fluvial disturbance patches and cottonwood recruitment along the upper Missouri River, Montana. *Wetlands*, 18(4):546–556.
- Auchincloss, L. C., Richards, J. H., Young, C. A., and Tansey, M. K. (2012). Inundation depth, duration, and temperature influence Fremont cottonwood (*Populus fremontii*) seedling growth and survival. *Western North American Naturalist*, 72(3):323–333.
- Augustijn, D., Galema, A., and Huthoff, F. (2011). Evaluation of flow formulas for submerged vegetation. In *EUROMECH Colloquium 523. Ecohydraulics: linkages between hydraulics, morphodynamics and ecological processes in rivers, Clermont-Ferrand, France, 15-17, June 2011*, 147-151.

- Augustijn, D., Huthoff, E., and Velzen van, E. (2008). Comparison of vegetation roughness descriptions. In *4th International Conference on Fluvial Hydraulics, River Flow 2008, September 3-5, 2008, Çeşme, Izmir, Turkey*.
- Austin, M. P. (1981). Role of certain diversity properties in vegetation classification. In Gillison, A. and Anderson, D., editors, *Vegetation classification in Australia: proceedings of a workshop sponsored by CSIRO Division of Land Use Research, Canberra, October 1978*. Canberra, Australia: Commonwealth Scientific and Industrial Research Organization, 1981.
- Baatz, M. and Schäpe, A. (2000). Multiresolution segmentation: an optimization approach for high quality multi-scale image segmentation. *Angewandte Geographische Informationsverarbeitung XII*, pages 12–23.
- Bagnold, R. (1966). An approach to the sediment transport problem from general physics. Technical report, US Geological Survey Professional Paper 422-I, 37 pages.
- Baker, W. L. (1989). Macro- and micro-scale influences on riparian vegetation in Western Colorado. *Annals of the Association of American Geographers*, 79(1):65–78.
- Bakry, M. F., Gates, T. K., and Khattab, A. F. (1992). Field-measured hydraulic resistance characteristics in vegetation-infested canals. *Journal of Irrigation and Drainage Engineering*, 118(2):256–274.
- Banach, K., Banach, A. M., Lamers, L. P. M., De Kroon, H., Bennicelli, R. P., Smits, A. J. M., and Visser, E. J. W. (2009). Differences in flooding tolerance between species from two wetland habitats with contrasting hydrology: implications for vegetation development in future floodwater retention areas. *Annals of Botany*, 103(2):341–351.
- Baptist, M. J. (2005). *Modelling floodplain biogeomorphology*. PhD thesis, Delft University of Technology, ISBN 90-407-2582-9.
- Baptist, M. J., Babovic, V., Rodríguez Uthurburu, J., Keijzer, M., Uittenbogaard, R., Mynett, A., and Verwey, A. (2007). On inducing equations for vegetation resistance. *Journal of Hydraulic Research*, 45(4):435–450.
- Baptist, M. J. and de Jong, J. F. (2005). Modelling the influence of vegetation on the morphology of the Allier, France. In *Final COST 626 Meeting, Silkeborg, Denmark, 19-20 May 2005*, pages 15–22.
- Baptist, M. J., van den Bosch, L. V., Dijkstra, J. T., and Kapinga, S. (2003). Modelling the effects of vegetation on flow and morphology in rivers. *Archiv für Hydrobiologie Supplement 155/1-4, Large Rivers*, 15(1-4):339–357.
- Barfield, B. J., Tollner, E. W., and Hayes, J. C. (1979). Filtration of sediment by simulated vegetation. I steady-state flow with homogenous sediment. *Transactions, American Society of Agricultural Engineers*, 22(3):540–545, 548.

- Bayley, P. B. (1995). Understanding large river-floodplain ecosystems: Significant economic advantages and increased biodiversity and stability would result from restoration of impaired systems. *BioScience*, 45(3):153–158.
- Beechie, T. J., Sear, D. A., Olden, J. D., Pess, G. R., Buffington, J. M., Moir, H., Roni, P., and Pollock, M. M. (2010). Process-based principles for restoring river ecosystems. *BioScience*, 60(3):209–222.
- Belcher, S. E., Jerram, N., and Hunt, J. C. R. (2003). Adjustment of a turbulent boundary layer to a canopy of roughness elements. *Journal of Fluid Mechanics*, 488:369–398.
- Bendix, J. and Hupp, C. R. (2000). Hydrological and geomorphological impacts on riparian plant communities. *Hydrological Processes*, 14(16-17):2977–2990.
- Bendix, J. and Stella, J. C. (2013). Riparian vegetation and the fluvial environment: A biogeographic perspective. In Shroder, J. F., editor, *Treatise on Geomorphology*, volume 12, pages 53–74. San Diego: Academic Press.
- Bennett, S. J., Pirim, T., and Barkdoll, B. D. (2002). Using simulated emergent vegetation to alter stream flow direction within a straight experimental channel. *Geomorphology*, 44(1-2):115–126.
- Bennett, S. J., Wu, W., Alonso, C. V., and Wang, S. S. Y. (2008). Modeling fluvial response to in-stream woody vegetation: implications for stream corridor restoration. *Earth Surface Processes and Landforms*, 33(6):890–909.
- Berendse, E., van Ruijven, J., Jongejans, E., and Keesstra, S. (2015). Loss of plant species diversity reduces soil erosion resistance. *Ecosystems*, 18(5):881–888.
- Berger, U. and Hildenbrandt, H. (2000). A new approach to spatially explicit modelling of forest dynamics: spacing, ageing and neighbourhood competition of mangrove trees. *Ecological Modelling*, 132(3):287–302.
- Bernhardt, E. S. and Palmer, M. A. (2007). Restoring streams in an urbanizing world. *Freshwater Biology*, 52(4):738–751.
- Bernhardt, E. S., Palmer, M. A., Allan, J. D., Alexander, G., Barnas, K., Brooks, S., Carr, J., Clayton, S., Dahm, C., Follstad-Shah, J., Galat, D., Gloss, S., Goodwin, P., Hart, D., Hassett, B., Jenkinson, R., Katz, S., Kondolf, G. M., Lake, P. S., Lave, R., Meyer, J. L., O'Donnell, T. K., Pagano, L., Powell, B., and Sudduth, E. (2005). Synthesizing U.S. river restoration efforts. *Science*, 308(5722):636–637.
- Bernhardt, E. S., Sudduth, E. B., Palmer, M. A., Allan, J. D., Meyer, J. L., Alexander, G., Follstad-Shah, J., Hassett, B., Jenkinson, R., Lave, R., Rumps, J., and Pagano, L. (2007). Restoring rivers one reach at a time: Results from a survey of U.S. river restoration practitioners. *Restoration Ecology*, 15(3):482–493.
- Bertoldi, W., Drake, N. A., and Gurnell, A. M. (2011). Interactions between river flows and colonizing vegetation on a braided river: exploring spatial and temporal dynamics in riparian vegetation cover using satellite data. *Earth Surface Processes and Landforms*, 36(11):1474–1486.

- Bertoldi, W., Siviglia, A., Tettamanti, S., Toffolon, M., Vetsch, D., and Francalanci, S. (2014). Modeling vegetation controls on fluvial morphological trajectories. *Geophysical Research Letters*, 41:7167–7175.
- Bertoldi, W., Welber, M., Gurnell, A. M., Mao, L., Comiti, F., and Tal, M. (2015). Physical modelling of the combined effect of vegetation and wood on river morphology. *Geomorphology*, 246:178–187.
- Beschta, R. L. and Ripple, W. J. (2006). River channel dynamics following extirpation of wolves in northwestern Yellowstone National Park, USA. *Earth Surface Processes and Landforms*, 31(12):1525–1539.
- Biggs, B. J. F. (1996). Hydraulic habitat of plants in streams. *Regulated Rivers: Research & Management*, 12(2-3):131–144.
- Bird, E. (1986). Mangroves and intertidal morphology in Westernport Bay, Victoria, Australia. *Marine Geology*, 69(3-4):251–271.
- Blench, T. (1969). *Mobile-bed fluviology*. University of Alberta Press, Edmonton, Canada.
- Blom, C., Bögemann, G., Laan, P., van der Sman, A., van de Steeg, H., and Voesenek, L. (1990). Adaptations to flooding in plants from river areas. *Aquatic Botany*, 38(1):29–47.
- Blom, C. and Voesenek, L. (1996). Flooding: the survival strategies of plants. *Trends in Ecology & Evolution*, 11(7):290–295.
- Blondeaux, P. and Seminara, G. (1985). A unified bar-bend theory of river meanders. *Journal of Fluid Mechanics*, 157:449–470.
- Boedeltje, G., Bakker, J. P., Ten Brinke, A., Van Groenendael, J. M., and Soesbergen, M. (2004). Dispersal phenology of hydrochorous plants in relation to discharge, seed release time and buoyancy of seeds: the flood pulse concept supported. *Journal of Ecology*, 92(5):786–796.
- Bornette, G., Tabacchi, E., Hupp, C., Puijalón, S., and Rostan, J. C. (2008). A model of plant strategies in fluvial hydrosystems. *Freshwater Biology*, 53(8):1692–1705.
- Botkin, D. B., Janak, J. F., and Wallis, J. R. (1972). Some ecological consequences of a computer model of forest growth. *Journal of Ecology*, 60(3):849–872.
- Bouwman, A. (1999). De netto sedimentatie op de ewijkse plaat berekend met de krigingmethode. Technical report, Technical report 99.118X, Rijksinstituut voor Integral Zoetwaterbeheer en Afvalwaterbehandeling (RIZA) (in Dutch).
- Brachet, C., Magnier, J., Valensuela, D., Petit, K., Fribourg-Blanc, B., Bernex, N., Scoullon, M., and Tarlock, D. (2015). *The handbook for management and restoration of aquatic ecosystems in river and lake basin*. www.inbo.org. ISBN: 978-91-87823-15-2.
- Bradley, C. E. and Smith, D. G. (1986). Plains cottonwood recruitment and survival on a prairie meandering river floodplain, Milk River, southern Alberta and northern Montana. *Canadian Journal of Botany*, 64(7):1433–1442.

- Braudrick, C. A., Dietrich, W. E., Leverich, G. T., and Sklar, L. S. (2009). Experimental evidence for the conditions necessary to sustain meandering in coarse-bedded rivers. *Proceedings of the National Academy of Sciences*, 106(40):16936–16941.
- Brevis, W., Niño, Y., and Jirka, G. H. (2011). Integrating cross-correlation and relaxation algorithms for particle tracking velocimetry. *Experiments in Fluids*, 50(1):135–147.
- Bridge, J. S., Alexander, J., Collier, R. E. L., Gawthorpe, R. L., and Jarvis, J. (1995). Ground-penetrating radar and coring used to study the large-scale structure of point-bar deposits in three dimensions. *Sedimentology*, 42(6):839–852.
- Brierley, G. J. and Fryirs, K. A. (2013). *Geomorphology and river management: applications of the river styles framework*. John Wiley & Sons.
- Brierley, G. J. and Hickin, E. J. (1992). Floodplain development based on selective preservation of sediments, Squamish River, British Columbia. *Geomorphology*, 4(6):381–391.
- Brooker, R. W., Maestre, F. T., Callaway, R. M., Lortie, C. L., Cavieres, L. A., Kunstler, G., Liancourt, P., Tielbörger, K., Travis, J. M. J., Anthelme, F., Armas, C., Coll, L., Corcket, E., Delzon, S., Forey, E., Kikvidze, Z., Olofsson, J., Pugnaire, F., Quiroz, C. L., Saccone, P., Schiffers, K., Seifan, M., Touzard, B., and Michalet, R. (2008). Facilitation in plant communities: the past, the present, and the future. *Journal of Ecology*, 96(1):18–34.
- Brookes, A. (1988). *Channelized rivers: perspectives for environmental management*. Wiley Chichester.
- Brummer, C. J., Abbe, T. B., Sampson, J. R., and Montgomery, D. R. (2006). Influence of vertical channel change associated with wood accumulations on delineating channel migration zones, Washington, USA. *Geomorphology*, 80(3-4):295–309.
- Buijse, A. D., Coops, H., Staras, M., Jans, L. H., Van Geest, G. J., Grift, R. E., Ibelings, B. W., Oosterberg, W., and Roozen, F. C. J. M. (2002). Restoration strategies for river floodplains along large lowland rivers in Europe. *Freshwater Biology*, 47(4):889–907.
- Bullock, J. M., Aronson, J., Newton, A. C., Pywell, R. F., and Rey-Benayas, J. M. (2011). Restoration of ecosystem services and biodiversity: conflicts and opportunities. *Trends in Ecology & Evolution*, 26(10):541–549.
- Butcher, R. W. (1933). Studies on the ecology of rivers: I. On the distribution of macrophytic vegetation in the rivers of Britain. *Journal of Ecology*, 21(1):58–91.
- Byishimo, P. (2014). Effects of variable discharge on width formation and cross-sectional shape of sinuous rivers. Master's thesis, UNESCO-IHE, Institute for Water Education, Delft, The Netherlands.
- Byishimo, P., Vargas-Luna, A., and Crosato, A. (2014). Effects of variable discharge on the river channel width variation. In Augustijn, D. and Warminck, J., editors, *NCR-Days 2014, Book of Abstracts, NCR Publication 38-2014, Nederlands Centrum voor Rivierkunde, 2, 3 October 2014, Enschede, The Netherlands. ISSN: 1568-234X*, pages 31–32.

- Callander, R. A. (1969). Instability and river channels. *Journal of Fluid Mechanics*, 36(3):465–480.
- Campbell, G. S., Blackwell, P. G., and Woodward, F. I. (2002). Can landscape-scale characteristics be used to predict plant invasions along rivers? *Journal of Biogeography*, 29(4):535–543.
- Camporeale, C., Perucca, E., Ridolfi, L., and Gurnell, A. M. (2013). Modeling the interactions between river morphodynamics and riparian vegetation. *Reviews of Geophysics*, 51:379–414.
- Camporeale, C. and Ridolfi, L. (2006a). Convective nature of the planimetric instability in meandering river dynamics. *Physical Review E*, 73(2):026311.
- Camporeale, C. and Ridolfi, L. (2006b). Riparian vegetation distribution induced by river flow variability: A stochastic approach. *Water Resources Research*, 42:W10415.
- Canestrelli, A., Spruyt, A., Jagers, B., Slingerland, R., and Borsboom, M. (2016). A mass-conservative staggered immersed boundary model for solving the shallow water equations on complex geometries. *International Journal for Numerical Methods in Fluids*, 81(3):151–177. FLD-14-0373.R2.
- Carnicer, J., Coll, M., Ninyerola, M., Pons, X., Sánchez, G., and Peñuelas, J. (2011). Widespread crown condition decline, food web disruption, and amplified tree mortality with increased climate change-type drought. *Proceedings of the National Academy of Sciences*, 108(4):1474–1478.
- Carollo, F. G., Ferro, V., and Termini, D. (2002). Flow velocity measurements in vegetated channels. *Journal of Hydraulic Engineering*, 128(7):664–673.
- Champion, P. D. and Tanner, C. C. (2000). Seasonality of macrophytes and interaction with flow in a New Zealand lowland stream. *Hydrobiologia*, 441(1):1–12.
- Charlton, F. G., Brown, P. M., and Benson, R. W. (1978). The hydraulic geometry of some gravel rivers in Britain. Technical report, IT 180, Hydraulics Res. Stn., Wallingford, UK.
- Chen, D. and Duan, J. (2006). Modeling width adjustment in meandering channels. *Journal of Hydrology*, 321(1-4):59–76.
- Chen, R. and Twilley, R. R. (1998). A gap dynamic model of mangrove forest development along gradients of soil salinity and nutrient resources. *Journal of Ecology*, 86(1):37–51.
- Cheng, N. (2013). Calculation of drag coefficient for arrays of emergent circular cylinders with pseudofluid model. *Journal of Hydraulic Engineering*, 139(6):602–611.
- Cheng, N. S. (2011). Representative roughness height of submerged vegetation. *Water Resources Research*, 47(8):W08517.
- Cheng, N. S. and Nguyen, H. T. (2011). Hydraulic radius for evaluating resistance induced by simulated emergent vegetation in open-channel flows. *Journal of Hydraulic Engineering*, 137(9):995–1004.

- Choi, S.-U. and Kang, H. (2004). Reynolds stress modeling of vegetated open-channel flows. *Journal of Hydraulic Research*, 42(1):3–11.
- Church, M. (2007). Multiple scales in rivers. In Habersack, H., Piégay, H., and Rinaldi, M., editors, *Gravel-Bed Rivers VI: From Process Understanding to River Restoration*, volume 11 of *Developments in Earth Surface Processes*, pages 3–28. Elsevier.
- Church, M. and Ferguson, R. I. (2015). Morphodynamics: Rivers beyond steady state. *Water Resources Research*, 51(4):1883–1897.
- Clarke, S. J. (2002). Vegetation growth in rivers: Influences upon sediment and nutrient dynamics. *Progress in Physical Geography*, 26(2):159–172.
- Cline, S. P. and McAllister, L. S. (2012). Plant succession after hydrologic disturbance: inferences from contemporary vegetation on a chronosequence of bars, Willamette River, Oregon, USA. *River Research and Applications*, 28(9):1519–1539.
- Coceal, O. and Belcher, S. E. (2004). A canopy model of mean winds through urban areas. *Quarterly Journal of the Royal Meteorological Society*, 130(599):1349–1372.
- Collins, A. L. and Walling, D. E. (2007). Fine-grained bed sediment storage within the main channel systems of the Frome and Piddle catchments, Dorset, UK. *Hydrological Processes*, 21(11):1448–1459.
- Collins, A. L., Walling, D. E., and Leeks, G. J. L. (2005). Storage of fine-grained sediment and associated contaminants within the channels of lowland permeable catchments in the uk. In Walling, D. E. and Horowitz, A. J., editors, *Sediment budgets 1: proceedings of the International Symposium on Sediment Budgets: held during the Seventh Scientific Assembly of the International Association of Hydrological Sciences (IAHS) at Foz do Iguaço, Brazil, 3-9 April, 2005. International Association of Hydrological Sciences Publication 291. IAHS Press: Wallingford, UK*, volume 1, pages 259–268. IAHS Press.
- Collins, B. D., Montgomery, D. R., Fetherston, K. L., and Abbe, T. B. (2012). The floodplain large-wood cycle hypothesis: A mechanism for the physical and biotic structuring of temperate forested alluvial valleys in the north pacific coastal ecoregion. *Geomorphology*, 139-140:460–470.
- Collison, A. J. C. and Anderson, M. G. (1996). Using a combined slope hydrology/stability model to identify suitable conditions for landslide prevention by vegetation in the humid tropics. *Earth Surface Processes and Landforms*, 21(8):737–747.
- Cooper, D. J., Andersen, D. C., and Chimner, R. A. (2003). Multiple pathways for woody plant establishment on floodplains at local to regional scales. *Journal of Ecology*, 91(2):182–196.
- Corenblit, D., Steiger, J., Gurnell, A. M., and Naiman, R. J. (2009). Plants intertwine fluvial landform dynamics with ecological succession and natural selection: a niche construction perspective for riparian systems. *Global Ecology and Biogeography*, 18(4):507–520.

- Corenblit, D., Steiger, J., and Tabacchi, E. (2010). Biogeomorphologic succession dynamics in a mediterranean river system. *Ecography*, 33(6):1136–1148.
- Corenblit, D., Tabacchi, E., Steiger, J., and Gurnell, A. M. (2007). Reciprocal interactions and adjustments between fluvial landforms and vegetation dynamics in river corridors: A review of complementary approaches. *Earth-Science Reviews*, 84(1-2):56–86.
- Cotton, J. A., Wharton, G., Bass, J. A. B., Heppell, C. M., and Wotton, R. S. (2006). The effects of seasonal changes to in-stream vegetation cover on patterns of flow and accumulation of sediment. *Geomorphology*, 77(3-4):320–334.
- Coulthard, T. J. (2005). Effects of vegetation on braided stream pattern and dynamics. *Water Resources Research*, 41:W04003.
- Cowan, W. (1956). Estimating hydraulic roughness coefficients. *Agricultural Engineering*, 37(7):473–475.
- Craufurd, P. Q., Qi, A., Ellis, R. H., Summerfield, R. J., Roberts, E. H., and Mahalakshmi, V. (1998). Effect of temperature on time to panicle initiation and leaf appearance in Sorghum. *Crop Science*, 38(4):942–947.
- Crosato, A. (1989). Meander migration prediction. *Excerpta, GNI, Publisher Libreria Progetto, Padova, Italy*, 4:169–198.
- Crosato, A. (2008). *Analysis and modelling of river meandering*. PhD thesis, IOS press, Delft University of Technology, The Netherlands.
- Crosato, A. and Mosselman, E. (2009). Simple physics-based predictor for the number of river bars and the transition between meandering and braiding. *Water Resources Research*, 45:W03424.
- Crosato, A., Mosselman, E., Desta, F. B., and Uijttewaal, W. S. J. (2011). Experimental and numerical evidence for intrinsic nonmigrating bars in alluvial channels. *Water Resources Research*, 47:W03511.
- Crosato, A. and Samir Saleh, M. (2011). Numerical study on the effects of floodplain vegetation on river planform style. *Earth Surface Processes and Landforms*, 36(6):711–720.
- Curran, J. C. and Hession, W. C. (2013). Vegetative impacts on hydraulics and sediment processes across the fluvial system. *Journal of Hydrology*, 505:364–376.
- Dawson, F. H., Castellano, E., and Ladle, M. (1979). Concept of species succession in relation to river vegetation and management. *Proceedings-International Association of Theoretical and Applied Limnology*, 20:1439–1444.
- de Jong, J. (2005). Modelling the influence of vegetation on the morphodynamics of the river allier. Master's thesis, Delft University of Technology.
- de Langre, E., Gutierrez, A., and Cossé, J. (2012). On the scaling of drag reduction by reconfiguration in plants. *Comptes Rendus Mécanique*, 340(1-2):35–40.

- Díaz-Molina, M. (2009). *Alluvial Sedimentation*, chapter Geometry and Lateral Accretion Patterns in Meander Loops: Examples from the Upper Oligocene-Lower Miocene, Loranca Basin, Spain, pages 115–131. Blackwell Publishing Ltd.
- Dietrich, W. E. and Smith, J. D. (1983). Influence of the point bar on flow through curved channels. *Water Resources Research*, 19(5):1173–1192.
- Dijkstra, J. T. and Uittenbogaard, R. E. (2010). Modeling the interaction between flow and highly flexible aquatic vegetation. *Water Resources Research*, 46:W12547.
- Dittrich, A., Aberle, J., and Schoneboom, T. (2012). *Environmental Fluid Mechanics: Memorial colloquium on environmental fluid mechanics in honour of Prof. Gerhard H. Jirka*, chapter Drag forces and flow resistance of flexible riparian vegetation, pages 195–215. IAHR Monographs. CRC Press.
- Dufour, S. and Piégay, H. (2009). From the myth of a lost paradise to targeted river restoration: forget natural references and focus on human benefits. *River Research and Applications*, 25(5):568–581.
- Duke-Sylvester, S. M. (2006). *Applying Landscape-scale Modeling to Everglades Restoration*. PhD thesis, University of Tennessee.
- Dulal, K. P., Kobayashi, K., Shimizu, Y., and Parker, G. (2010). Numerical computation of free meandering channels with the application of slump blocks on the outer bends. *Journal of Hydro-environment Research*, 3(4):239–246.
- Dulal, K. P. and Shimizu, Y. (2010). Experimental simulation of meandering in clay mixed sediments. *Journal of Hydro-environment Research*, 4(4):329–343.
- Dunn, C., Lopez, F., and García, M. (1996). Mean flow and turbulence in a laboratory channel with simulated vegetation. Technical report, Hydraulic Engineering Series. 51. University of Illinois at Urbana-Champaign, Urbana, Illinois.
- Duró, G., Crosato, A., and Tassi, P. (2016). Numerical study on river bar response to spatial variations of channel width. *Advances in Water Resources*, 93, Part A:21–38.
- Dykaar, B. B. and Wigington Jr., P. J. (2000). Floodplain formation and cottonwood colonization patterns on the Willamette River, Oregon, USA. *Environmental Management*, 25(1):87–104.
- Eaton, B. C. (2006). Bank stability analysis for regime models of vegetated gravel bed rivers. *Earth Surface Processes and Landforms*, 31(11):1438–1444.
- Edmaier, K., Burlando, P., and Perona, P. (2011). Mechanisms of vegetation uprooting by flow in alluvial non-cohesive sediment. *Hydrology and Earth System Sciences Discussions*, 8(1):1365–1398.
- Edmaier, K., Crouzy, B., and Perona, P. (2015). Experimental characterization of vegetation uprooting by flow. *Journal of Geophysical Research: Biogeosciences*, 120(9):1812–1824.

- Eekhout, J. P. C., Fraaije, R. G. A., and Hoitink, A. J. F. (2014). Morphodynamic regime change in a reconstructed lowland stream. *Earth Surface Dynamics*, 2(1):279–293.
- Eekhout, J. P. C. and Hoitink, A. J. F. (2015). Chute cutoff as a morphological response to stream reconstruction: The possible role of backwater. *Water Resources Research*, 51:3339–3352.
- Egger, G., Politti, E., Lautsch, E., Benjankar, R., Gill, K. M., and Rood, S. B. (2015). Floodplain forest succession reveals fluvial processes: A hydrogeomorphic model for temperate riparian woodlands. *Journal of Environmental Management*, 161:72–82.
- Eke, E., Parker, G., and Shimizu, Y. (2014a). Numerical modeling of erosional and depositional bank processes in migrating river bends with self-formed width: Morphodynamics of bar push and bank pull. *Journal of Geophysical Research: Earth Surface*, 119(7):1455–1483.
- Eke, E. C., Czapiga, M. J., Viparelli, E., Shimizu, Y., Imran, J., Sun, T., and Parker, G. (2014b). Coevolution of width and sinuosity in meandering rivers. *Journal of Fluid Mechanics*, 760:127–174.
- Engelund, F. (1970). Instability of erodible beds. *Journal of Fluid Mechanics*, 42(2):225–244.
- Engelund, F. (1975). Instability of flow in a curved alluvial channel. *Journal of Fluid Mechanics*, 72(1):145–160.
- Engelund, F. and Hansen, E. (1967). A monograph on sediment transport in alluvial streams. Technical report, Copenhagen, Danish Technical Press.
- Engelund, F. and Skovgaard, O. (1973). On the origin of meandering and braiding in alluvial streams. *Journal of Fluid Mechanics*, 57(2):289–302.
- Enquist, B. J., Brown, J. H., and West, G. B. (1998). Allometric scaling of plant energetics and population density. *Nature*, 395:163–165.
- Erskine, W., Keene, A., Bush, R., Cheetham, M., and Chalmers, A. (2012). Influence of riparian vegetation on channel widening and subsequent contraction on a sand-bed stream since european settlement: Widden brook, australia. *Geomorphology*, 147–148:102–114. *Geomorphology of Large Rivers - cases from the 7th {IAG} Conference, Melbourne.*
- Facchini, E. (2009). Morphological aspects of cyclic rejuvenation of the ewijkse plaat, the netherlands. Master's thesis, University of Florence, Faculty of Engineering, Florence, Italy, and UNESCO-IHE, Delft, the Netherlands.
- Facchini, E., Crosato, A., and Kater, E. (2009). La modellazione numerica nei progetti di riqualificazione fluviale: il caso ewijkse plaat, paesi bassi. In *Riqualificazione Fluviale, ECRR-CIRE, No. 2/2009: p. 67-73 (in Italian).*

- Finn, R. K. (1953). Determination of the drag on a cylinder at low Reynolds numbers. *Journal of Applied Physics*, 24(6):771–773.
- Fischer-Antze, T., Stoesser, T., Bates, P., and Olsen, N. (2001). 3D numerical modelling of open-channel flow with submerged vegetation. *Journal of Hydraulic Research*, 39(3):303–310.
- Fisher, R. A. (1937). The wave of advance of advantageous genes. *Annals of Eugenics*, 7(4):355–369.
- FISRWG (1998). Stream corridor restoration: Principles, processes, and practices. Technical report, Federal Interagency Stream Restoration Working Group (FISRWG) (15 Federal agencies of the US gov't). GPO Item No. 0120-A; SuDocs No. A 57.6/2:EN 3/PT.653. ISBN-0-934213-59-3.
- Folkard, A. M. (2011). Vegetated flows in their environmental context: a review. *Proceedings of the Institution of Civil Engineers, Engineering and Computational Mechanics*, 164(1):3–24.
- Fredsøe, J. (1978). Meandering and braiding of rivers. *Journal of Fluid Mechanics*, 84(4):609–624.
- Freeman, G. E., Rahmeyer, W. H., and Copeland, R. R. (2000). Determination of resistance due to shrubs and woody vegetation. Technical report, ERDC/CHL TR-00-25, U.S. Army Engineer Research and Development Center, Vicksburg, MS.
- Friedkin, J. (1945). A laboratory study of the meandering of alluvial rivers. Technical report, Vicksburg, MS: US Army Corps of Engineers, US Waterways Experiment Station.
- Friedman, J. M. and Auble, G. T. (1999). Mortality of riparian box elder from sediment mobilization and extended inundation. *Regulated Rivers: Research & Management*, 15(5):463–476.
- Friedman, J. M. and Auble, G. T. (2000). *Inland Flood Hazards: Human, Riparian, and Aquatic Communities*, chapter Floods, flood control, and bottomland vegetation, pages 219–237. Cambridge University Press, Cambridge, England.
- Friedman, J. M., Osterkamp, W. R., and Lewis, W. M. (1996a). Channel narrowing and vegetation development following a great plains flood. *Ecology*, 77(7):2167–2181.
- Friedman, J. M., Osterkamp, W. R., and Lewis Jr., W. M. (1996b). The role of vegetation and bed-level fluctuations in the process of channel narrowing. *Geomorphology*, 14(4):341–351.
- Friedman, J. M., Scott, M. L., and Lewis, W. M. (1995). Restoration of riparian forest using irrigation, artificial disturbance, and natural seedfall. *Environmental Management*, 19(4):547–557.
- Fujita, Y. and Muramoto, Y. (1982). Experimental study on stream channel processes in alluvial rivers. Technical report, Bull. Disaster Prev. Res. Inst., Kyoto Univ, 32(1), 49–96.

- Furukawa, K., Wolanski, E., and Mueller, H. (1997). Currents and sediment transport in mangrove forests. *Estuarine, Coastal and Shelf Science*, 44(3):301–310.
- Galappatti, G. and Vreugdenhil, C. B. (1985). A depth-integrated model for suspended sediment transport. *Journal of Hydraulic Research*, 23(4):359–377.
- Galema, A. (2009). Vegetation resistance; evaluation of vegetation resistance descriptors for flood management. Master's thesis, University of Twente, Enschede, The Netherlands.
- Geerling, G. W., Kater, E., van den Brink, C., Baptist, M. J., Ragas, A. M. J., and Smits, A. J. M. (2008). Nature rehabilitation by floodplain excavation: The hydraulic effect of 16 years of sedimentation and vegetation succession along the Waal River, NL. *Geomorphology*, 99(1-4):317–328.
- Ghisalberti, M. and Nepf, H. (2006). The structure of the shear layer in flows over rigid and flexible canopies. *Environmental Fluid Mechanics*, 6(3):277–301.
- Ghisalberti, M. and Nepf, H. M. (2004). The limited growth of vegetated shear layers. *Water Resources Research*, 40(7):W07502, doi:10.1029/2003WR002776.
- Gibling, M. R. and Davies, N. S. (2012). Palaeozoic landscapes shaped by plant evolution. *Nature Geoscience*, 5(2):99–105.
- Gleason, C. J. (2015). Hydraulic geometry of natural rivers: A review and future directions. *Progress in Physical Geography*, 39(3):337–360.
- Gleick, P. H. (2003). Global freshwater resources: Soft-path solutions for the 21st century. *Science*, 302(5650):1524–1528.
- Glenn-Lewin, D. C. and van der Maarel, E. (1992). *Plant Succession: Theory and Practice*, chapter Patterns and processes of vegetation dynamics, pages 11–59. Chapman and Hall London, UK.
- González, E., Sher, A. A., Tabacchi, E., Masip, A., and Poulin, M. (2015). Restoration of riparian vegetation: A global review of implementation and evaluation approaches in the international, peer-reviewed literature. *Journal of Environmental Management*, 158:85–94.
- Goodwin, C. N., Hawkins, C. P., and Kershner, J. L. (1997). Riparian restoration in the western united states: Overview and perspective. *Restoration Ecology*, 5(4S):4–14.
- Gosselin, F., de Langre, E., and Machado-Almeida, B. A. (2010). Drag reduction of flexible plates by reconfiguration. *Journal of Fluid Mechanics*, 650:319–341.
- Goudie, A. S. (1989). *The nature of the environment*. Basil Blackwell Ltd., Oxford, UK.
- Gran, K. and Paola, C. (2001). Riparian vegetation controls on braided stream dynamics. *Water Resources Research*, 37(12):3275–3283.

- Green, J. C. (2005). Modelling flow resistance in vegetated streams: review and development of new theory. *Hydrological Processes*, 19(6):1245–1259.
- Greenway, D. R. (1987). *Slope stability: geotechnical engineering and geomorphology*, chapter Vegetation and slope stability, pages 187–230. Wiley and Sons: New York.
- Grime, J. P. (2006). *Plant Strategies, Vegetation Processes, and Ecosystem Properties*. Wiley, Chichester, West Sussex; New York, NY, 2 edition.
- Gross, K., Cardinale, B. J., Fox, J. W., Gonzalez, A., Loreau, M., Polley, H. W., Reich, P. B., and van Ruijven, J. (2014). Species richness and the temporal stability of biomass production: A new analysis of recent biodiversity experiments. *The American Naturalist*, 183(1):1–12.
- Groves, J. H., Williams, D. G., Caley, P., Norris, R. H., and Caitcheon, G. (2009). Modelling of floating seed dispersal in a fluvial environment. *River Research and Applications*, 25(5):582–592.
- Gurnell, A. (2012). Fluvial geomorphology: Wood and river landscapes. *Nature Geoscience*, 5(2):93–94.
- Gurnell, A. (2014). Plants as river system engineers. *Earth Surface Processes and Landforms*, 39(1):4–25.
- Gurnell, A., Thompson, K., Goodson, J., and Moggridge, H. (2008). Propagule deposition along river margins: linking hydrology and ecology. *Journal of Ecology*, 96(3):553–565.
- Gurnell, A. M., Bertoldi, W., and Corenblit, D. (2012). Changing river channels: The roles of hydrological processes, plants and pioneer fluvial landforms in humid temperate, mixed load, gravel bed rivers. *Earth-Science Reviews*, 111(1-2):129–141.
- Gurnell, A. M., Boitsidis, A. J., Thompson, K., and Clifford, N. J. (2006). Seed bank, seed dispersal and vegetation cover: Colonization along a newly-created river channel. *Journal of Vegetation Science*, 17(5):665–674.
- Gurnell, A. M., González Del Tánago, M., O' Hare, M. T., van Oorschot, M., Belleli, B., García De Jalón, D., Grabowski, R., Hendricks, D., Mountford, O., Rinaldi, M., Solari, L., Szewczyk, M., and Vargas-Luna, A. (2014). Influence of natural hydromorphological dynamics on biota and ecosystem function. Technical report, Deliverable 2.2, Part 1, of REFORM (REstoring rivers FOR effective catchment Management), a Collaborative project (large-scale integrating project) funded by the European Commission within the 7th Framework Programme under Grant Agreement 282656.
- Gurnell, A. M., Petts, G. E., Hannah, D. M., Smith, B. P. G., Edwards, P. J., Kollmann, J., Ward, J. V., and Tockner, K. (2001). Riparian vegetation and island formation along the gravel-bed Fiume Tagliamento, Italy. *Earth Surface Processes and Landforms*, 26(1):31–62.
- Gyssels, G., Poesen, J., Bochet, E., and Li, Y. (2005). Impact of plant roots on the resistance of soils to erosion by water: a review. *Progress in Physical Geography*, 29(2):189–217.

- Hall, B. R. and Freeman, G. E. (1994). Study of hydraulic roughness in wetland vegetation takes new look at Manning's n. Technical report, The Wetlands Research Program Bulletin, 4(1): 1-4.
- Hansen, E. (1967). On the formation of meanders as a stability problem. Technical report, Coastal Engineering Laboratory, Techn. Univ. Denmark, Basis Research, Progress Report 13, 9-13, Lyngby.
- Harvey, M. D. and Watson, C. C. (1986). Fluvial processes and morphological thresholds in incised channel restoration. *JAWRA Journal of the American Water Resources Association*, 22(3):359–368.
- Helmiö, T. (2002). Unsteady 1D flow model of compound channel with vegetated floodplains. *Journal of Hydrology*, 269(1-2):89–99.
- Hickin, E. J. (1984). Vegetation and river channel dynamics. *Canadian Geographer / Le Géographe canadien*, 28(2):111–126.
- Hicks, D. M., Duncan, M. J., Lane, S. N., Tal, M., and Westaway, R. (2007). Contemporary morphological change in braided gravel-bed rivers: new developments from field and laboratory studies, with particular reference to the influence of riparian vegetation. In Habersack, H., Piégay, H., and Rinaldi, M., editors, *Gravel-Bed Rivers VI: From Process Understanding to River Restoration*, volume 11 of *Developments in Earth Surface Processes*, chapter 21, pages 557–584. Elsevier.
- Hobbs, R. J. (2005). The future of restoration ecology: Challenges and opportunities. *Restoration Ecology*, 13(2):239–241.
- Hobo, N., Makaske, B., Middelkoop, H., and Wallinga, J. (2010). Reconstruction of floodplain sedimentation rates: a combination of methods to optimize estimates. *Earth Surface Processes and Landforms*, 35(13):1499–1515.
- Hoffmann, M. R. (2004). Application of a simple space-time averaged porous media model to flow in densely vegetated channels. *Journal of Porous Media*, 7(3):183–192.
- Holmes, E. E., Lewis, M. A., Banks, J. E., and Veit, R. R. (1994). Partial differential equations in ecology: Spatial interactions and population dynamics. *Ecology*, 75(1):17–29.
- Hooke, J. M. (2006). *Hydromorphological adjustment in meandering river systems and the role of flood events*, chapter Hydromorphological adjustment in meandering river systems and the role of flood events, pages 127–135. Wallingford, International Association of Hydrological Sciences.
- Hooke, J. M. (2007). Spatial variability, mechanisms and propagation of change in an active meandering river. *Geomorphology*, 84(3-4):277–296.
- Horton, J. L. and Clark, J. L. (2001). Water table decline alters growth and survival of *Salix gooddingii* and *Tamarix chinensis* seedlings. *Forest Ecology and Management*, 140(2-3):239–247.

- Hossain, M. A., Gan, T. Y., and Baki, A. B. M. (2013). Assessing morphological changes of the ganges river using satellite images. *Quaternary International*, 304:142–155.
- Hu, Y., Huai, W., and Han, J. (2013). Analytical solution for vertical profile of stream-wise velocity in open-channel flow with submerged vegetation. *Environmental Fluid Mechanics*, 13(4):389–402.
- Hu, Z., Suzuki, T., Zitman, T., Uittewaal, W., and Stive, M. (2014). Laboratory study on wave dissipation by vegetation in combined current-wave flow. *Coastal Engineering*, 88:131–142.
- Huai, W., Zeng, Y., Xu, Z., and Yang, Z. (2009). Three-layer model for vertical velocity distribution in open channel flow with submerged rigid vegetation. *Advances in Water Resources*, 32(4):487–492.
- Huang, H. Q. (2010). Reformulation of the bed load equation of Meyer-Peter and Müller in light of the linearity theory for alluvial channel flow. *Water Resources Research*, 46(9). W09533.
- Hupp, C. R. (1992). Riparian vegetation recovery patterns following stream channelization: A geomorphic perspective. *Ecology*, 73(4):1209–1226.
- Hupp, C. R. and Osterkamp, W. (1996). Riparian vegetation and fluvial geomorphic processes. *Geomorphology*, 14(4):277–295.
- Huthoff, F. (2007). *Modelling hydraulic resistance of floodplain vegetation*. PhD thesis, Department of Water Engineering, University Twente.
- Huthoff, F. and Augustijn, D. C. M. (2006). Hydraulic resistance of vegetation: predictions of average flow velocities based on a rigid-cylinders analogy. Technical report, Project no. U2/430.9/4268. University of Twente, The Netherlands.
- Hygelund, B. and Manga, M. (2003). Field measurements of drag coefficients for model large woody debris. *Geomorphology*, 51(1-3):175–185.
- Ikeda, S. (1982). Lateral bed slope transport on side slopes. *Journal of the Hydraulics Division ASCE*, 108(11):1369–1373.
- Ikeda, S. and Kanazawa, M. (1996). Three-dimensional organized vortices above flexible water plants. *Journal of Hydraulic Engineering*, 122(11):634–640.
- Ikeda, S., Parker, G., and Sawai, K. (1981). Bend theory of river meanders. part 1. linear development. *Journal of Fluid Mechanics*, 112:363–377.
- Ishikawa, Y., Sakamoto, T., and Mizuhara, K. (2003). Effect of density of riparian vegetation on effective tractive force. *Journal of Forest Research*, 8(4):235–246.
- Jahra, F., Kawahara, Y., Hasegawa, F., and Yamamoto, H. (2011). Flow-vegetation interaction in a compound open channel with emergent vegetation. *International Journal of River Basin Management*, 9(3-4):247–256.

- Jalonen, J., Järvelä, J., and Aberle, J. (2013). Leaf area index as vegetation density measure for hydraulic analyses. *Journal of Hydraulic Engineering*, 139(5):461–469.
- James, C. S., Birkhead, A. L., Jordanova, A. A., and O'Sullivan, J. J. (2004). Flow resistance of emergent vegetation. *Journal of Hydraulic Research*, 42(4):390–398.
- James, C. S., Goldbeck, U. K., Patini, A., and Jordanova, A. A. (2008). Influence of foliage on flow resistance of emergent vegetation. *Journal of Hydraulic Research*, 46(4):536–542.
- Jang, C. and Shimizu, Y. (2007). Vegetation effects on the morphological behavior of alluvial channels. *Journal of Hydraulic Research*, 45(6):763–772.
- Jang, C.-L. and Shimizu, Y. (2005). Numerical simulations of the behavior of alternate bars with different bank strengths. *Journal of Hydraulic Research*, 43(6):596–612.
- Jankowska, E., Włodarska-Kowalczyk, M., Kotwicki, L., Balazy, P., and Kuliński, K. (2014). Seasonality in vegetation biometrics and its effects on sediment characteristics and meiofauna in baltic seagrass meadows. *Estuarine, Coastal and Shelf Science*, 139:159–170.
- Järvelä, J. (2002). Flow resistance of flexible and stiff vegetation: a flume study with natural plants. *Journal of Hydrology*, 269(1-2):44–54.
- Järvelä, J. (2003). Influence of vegetation on flow structure in floodplains and wetlands. In A. Sánchez-Arcilla & A. Bateman (Eds.), *River, coastal and estuarine morphodynamics 2003 (Vol. Vol II, p. 845-856)*. Barcelona, Spain: IAHR.
- Järvelä, J. (2004). Determination of flow resistance caused by non-submerged woody vegetation. *International Journal of River Basin Management*, 2(1):61–70.
- Jeffries, R., Darby, S. E., and Sear, D. A. (2003). The influence of vegetation and organic debris on flood-plain sediment dynamics: case study of a low-order stream in the New Forest, England. *Geomorphology*, 51(1-3):61–80.
- Jin, D. and Schumm, S. (1987). *A new technique for modeling river morphology*, chapter International Geomorphology, pages 681–690. Chichester: Wiley.
- Johansson, M. E., Nilsson, C., and Nilsson, E. (1996). Do rivers function as corridors for plant dispersal? *Journal of Vegetation Science*, 7(4):593–598.
- Johnson, E. A. and Miyanishi, K. (2008). Testing the assumptions of chronosequences in succession. *Ecology Letters*, 11(5):419–431.
- Johnson, W. C. (1994). Woodland expansions in the Platte River, Nebraska: Patterns and causes. *Ecological Monographs*, 64(1):45–84.
- Johnson, W. C. (2000). Tree recruitment and survival in rivers: influence of hydrological processes. *Hydrological Processes*, 14(16-17):3051–3074.

- Jones, C. G., Lawton, J. H., and Shachak, M. (1994). Organisms as ecosystem engineers. *Oikos*, 69(3):373–386.
- Jordanova, A. A. and James, C. S. (2003). Experimental study of bed load transport through emergent vegetation. *Journal of Hydraulic Engineering*, 129(6):474–478.
- Jordanova, A. A., James, C. S., and Birkhead, A. L. (2006). Practical resistance estimation for flow through emergent vegetation. In *Proceedings of the Institution of Civil Engineers, Water Management, Vol. 159, No. WM3*, pp 173–181.
- Jørgensen, S. E. and Fath, B. D. (2011). *Fundamentals of Ecological Modelling*, volume 23 of *Developments in Environmental Modelling*. Elsevier.
- Junk, W., Bayley, P., and Sparks, R. (1989). The flood pulse concept in river-floodplain systems. In Dodge, D., editor, *Proceedings of the International Large River Symposium (LARS). Canadian Special Publication of Fisheries and Aquatic Sciences 106*, pages 110–127.
- Kalliola, R., Salo, J., Puhakka, M., and Rajasilta, M. (1991). New site formation and colonizing vegetation in primary succession on the western amazon floodplains. *Journal of Ecology*, 79(4):877–901.
- Khan, O., Mwelwa-Mutekenya, E., Crosato, A., and Zhou, Y. (2014). Effects of dam operation on downstream river morphology: the case of the middle Zambezi River. *Proceedings of the Institution of Civil Engineers - Water Management*, pages 1–16(15).
- Kim, H. S., Kimura, I., and Shimizu, Y. (2015). Bed morphological changes around a finite patch of vegetation. *Earth Surface Processes and Landforms*, 40(3):375–388.
- Kim, S., Toda, Y., and Tsujimoto, T. (2014). Effects of a low-head dam removal on river morphology and riparian vegetation: A case study of Gongreung River. *Journal of Water Resource and Protection*, 6(18):1682–1690.
- King, A. T., Tinoco, R. O., and Cowen, E. A. (2012). A k-e turbulence model based on the scales of vertical shear and stem wakes valid for emergent and submerged vegetated flows. *Journal of Fluid Mechanics*, 701:1–39.
- Klasz, G., Reckendorfer, W., Gabriel, H., Baumgartner, C., Schmalfluss, R., and Gutknecht, D. (2014). Natural levee formation along a large and regulated river: The Danube in the National Park Donau-Auen, Austria. *Geomorphology*, 215:20–33.
- Klein Tank, A. M. G., Wijngaard, J. B., Können, G. P., Böhm, R., Demarée, G., Gocheva, A., Mileta, M., Pashiardis, S., Hejkrlik, L., Kern-Hansen, C., Heino, R., Bessemoulin, P., Müller-Westermeier, G., Tzanakou, M., Szalai, S., Pálsdóttir, T., Fitzgerald, D., Rubin, S., Capaldo, M., Maugeri, M., Leitass, A., Bukantis, A., Aberfeld, R., van Engelen, A. F. V., Forland, E., Miletus, M., Coelho, F., Mares, C., Razuvaev, V., Nieplova, E., Cegnar, T., Antonio López, J., Dahlström, B., Moberg, A., Kirchhofer, W., Ceylan, A., Pachaliuk, O., Alexander, L. V., and Petrovic, P. (2002). Daily dataset of 20th-century surface air temperature and precipitation series for the European climate assessment. *International Journal of Climatology*, 22(12):1441–1453.

- Kleinhans, M. G. (2010). Sorting out river channel patterns. *Progress in Physical Geography*, 34(3):287–326.
- Kleinhans, M. G., van Dijk, W. M., van de Lageweg, W. I., Hoyal, D. C. J. D., Markies, H., van Maarseveen, M., Roosendaal, C., van Weesep, W., van Breemen, D., Hoendervoogt, R., and Cheshier, N. (2014). Quantifiable effectiveness of experimental scaling of river- and delta morphodynamics and stratigraphy. *Earth-Science Reviews*, 133:43–61.
- Klopstra, D., Barneveld, H. J., Van Noortwijk, J., and Van Velzen, E. (1997). Analytical model for hydraulic roughness of submerged vegetation. In *Conference proceedings of the 27th IAHR Conference, San Francisco. HKV publication*, pages 775–780.
- Koch, F. G. and Flokstra, C. (1980). Bed level computations for curved alluvial channels. In *Proceedings of the XIXth congress of the International Association for Hydraulic Research, 2-7 Feb. 1981, New Delhi, India, vol. 2*, pages 357–364.
- Kondolf, G. M. (2006). River restoration and meanders. *Ecology and Society*, 11(2):42.
- Kondolf, G. M. (2011). *Stream Restoration in Dynamic Fluvial Systems: Scientific Approaches, Analyses, and Tools*, chapter Setting Goals in River Restoration: When and Where Can the River ‘Heal Itself’?, pages 29–43. Geophysical Monograph Series, Vol.194, American Geophysical Union, Washington DC.
- Kondolf, G. M. and Micheli, E. R. (1995). Evaluating stream restoration projects. *Environmental Management*, 19(1):1–15.
- Kondolf, G. M., Podolak, K., and Grantham, T. E. (2013). Restoring mediterranean-climate rivers. *Hydrobiologia*, 719(1):527–545.
- Kondolf, G. M., Smeltzer, M. W., and Railsback, S. F. (2001). Design and performance of a channel reconstruction project in a coastal California gravel-bed stream. *Environmental Management*, 28(6):761–776.
- Kothyari, U. C., Hashimoto, H., and Hayashi, K. (2009a). Effect of tall vegetation on sediment transport by channel flows. *Journal of Hydraulic Research*, 47(6):700–710.
- Kothyari, U. C., Hayashi, K., and Hashimoto, H. (2009b). Drag coefficient of submerged rigid vegetation stems in open channel flows. *Journal of Hydraulic Research*, 47(6):691–699.
- Kouwen, N., Unny, T. E., and Hill, H. M. (1969). Flow retardance in vegetated channels. *Journal of the Irrigation and Drainage Division*, 95(IR2):329–357.
- Kozlowski, T. T. (2002). Physiological-ecological impacts of flooding on riparian forest ecosystems. *Wetlands*, 22(3):550–561.
- Kubrak, E., Kubrak, J., and Rowiński, P. M. (2008). Vertical velocity distributions through and above submerged, flexible vegetation. *Hydrological Sciences Journal*, 53(4):905–920.

- Kummu, M., Lu, X. X., Rasphone, A., Sarkkula, J., and Koponen, J. (2008). Riverbank changes along the Mekong River: Remote sensing detection in the Vientiane–Nong Khai area. *Quaternary International*, 186(1):100–112.
- Labbe, J. M., Hadley, K. S., Schipper, A. M., Leuven, R. S. E. W., and Perala Gardiner, C. (2011). Influence of bank materials, bed sediment, and riparian vegetation on channel form along a gravel-to-sand transition reach of the Upper Tualatin River, Oregon, USA. *Geomorphology*, 125(3):374–382.
- Lane, S. N., Richards, K. S., and Chandler, J. H. (1996). Discharge and sediment supply controls on erosion and deposition in a dynamic alluvial channel. *Geomorphology*, 15(1):1–15.
- Lane, S. N., Westaway, R. M., and Hicks, D. M. (2003). Estimation of erosion and deposition volumes in a large, gravel-bed, braided river using synoptic remote sensing. *Earth Surface Processes and Landforms*, 28(3):249–271.
- Large, A. R. and Prach, K. (1999). *Eco-hydrology: plants and water in terrestrial and aquatic environments*, chapter Plants and water in streams and rivers, pages 223–252. London: Routledge.
- Larsen, L. G., Harvey, J. W., and Crimaldi, J. P. (2009). Predicting bed shear stress and its role in sediment dynamics and restoration potential of the everglades and other vegetated flow systems. *Ecological Engineering*, 35(12):1773–1785.
- Latrubesse, E. M. (2008). Patterns of anabranching channels: The ultimate end-member adjustment of mega rivers. *Geomorphology*, 101(1-2):130–145.
- Lece, S. A. (1997). Spatial patterns of historical overbank sedimentation and floodplain evolution, blue river, wisconsin. *Geomorphology*, 18(3-4):265–277.
- Lesser, G., Roelvink, J., van Kester, J., and Stelling, G. (2004). Development and validation of a three-dimensional morphological model. *Coastal Engineering*, 51(8-9):883–915.
- Levine, J. M. (2003). A patch modeling approach to the community-level consequences of directional dispersal. *Ecology*, 84(5):1215–1224.
- Lewin, J. and Ashworth, P. J. (2014). Defining large river channel patterns: Alluvial exchange and plurality. *Geomorphology*, 215:83–98.
- Li, L., Lu, X., and Chen, Z. (2007). River channel change during the last 50 years in the middle Yangtze River, the Jianli reach. *Geomorphology*, 85(3-4):185–196.
- Li, P. and Li, Z. (2011). Soil reinforcement by a root system and its effects on sediment yield in response to concentrated flow in the loess plateau. *Agricultural Sciences*, 2(2):86–93.
- Li, R. and Shen, H. (1973). Effect of tall vegetations on flow and sediment. *Journal of the Hydraulics Division ASCE*, 99(5):793–813.

- Li, S., Hao, Q., Swift, E., Bourque, C.-A., and Meng, F.-R. (2011). A stand dynamic model for red pine plantations with different initial densities. *New Forests*, 41(1):41–53.
- Lightbody, A. F. and Nepf, H. M. (2006). Prediction of velocity profiles and longitudinal dispersion in salt marsh vegetation. *Limnology and Oceanography*, 51(1):218–228.
- Liu, D., Diplas, P., Fairbanks, J. D., and Hodges, C. C. (2008). An experimental study of flow through rigid vegetation. *Journal of Geophysical Research: Earth Surface*, 113(F4):F04015.
- López, F. and García, M. (1998). Open-channel flow through simulated vegetation: Suspended sediment transport modeling. *Water Resources Research*, 34(9):2341–2352.
- Lotka, A. J. (1956). *Elements of mathematical biology*. New York: Dover.
- Luhar, M. and Nepf, H. M. (2011). Flow-induced reconfiguration of buoyant and flexible aquatic vegetation. *Limnology and Oceanography*, 56(6):2003–2017.
- Luhar, M. and Nepf, H. M. (2013). From the blade scale to the reach scale: A characterization of aquatic vegetative drag. *Advances in Water Resources*, 51:305–316.
- Lytle, D. A. and Merritt, D. M. (2004). Hydrologic regimes and riparian forests: a structured population model for cottonwood. *Ecology*, 85(9):2493–2503.
- Ma, G., Kirby, J. T., Su, S.-F., Figlus, J., and Shi, F. (2013). Numerical study of turbulence and wave damping induced by vegetation canopies. *Coastal Engineering*, 80:68–78.
- Maas, G. J., Wolfert, H. P., Schoor, M. M., and Middelkoop, H. (1997). Classificatie van riviertrajecten en kansrijkdom voor ecotopen. Technical report, Report 552, DLO-Staring Centrum, Wageningen, the Netherlands (in Dutch).
- Madsen, J. D., Chambers, P. A., James, W. E., Koch, E. W., and Westlake, D. F. (2001). The interaction between water movement, sediment dynamics and submersed macrophytes. *Hydrobiologia*, 444(1-3):71–84.
- Madsen, S. and Debois, P. (2006). River restoration in Denmark - 24 examples. Technical report, Storstrom County, Technical and Environmental Division.
- Mahoney, J. M. and Rood, S. B. (1998). Streamflow requirements for cottonwood seedling recruitment - an integrative model. *Wetlands*, 18(4):634–645.
- Marjoribanks, T. I., Hardy, R. J., and Lane, S. N. (2014). The hydraulic description of vegetated river channels: the weaknesses of existing formulations and emerging alternatives. *WIREs Water*, 1(6):549–560.
- Massel, S., Furukawa, K., and Brinkman, R. (1999). Surface wave propagation in mangrove forests. *Fluid Dynamics Research*, 24(4):219–249.
- McBride, J. R. and Strahan, J. (1984). Establishment and survival of woody riparian species on gravel bars of an intermittent stream. *American Midland Naturalist*, 112(2):235–245.

- McBride, M., Hession, W. C., Rizzo, D. M., and Thompson, D. M. (2007). The influence of riparian vegetation on near-bank turbulence: a flume experiment. *Earth Surface Processes and Landforms*, 32(13):2019–2037.
- McDowell, N., Pockman, W. T., Allen, C. D., Breshears, D. D., Cobb, N., Kolb, T., Plaut, J., Sperry, J., West, A., Williams, D. G., and Yezpe, E. A. (2008). Mechanisms of plant survival and mortality during drought: why do some plants survive while others succumb to drought? *New Phytologist*, 178(4):719–739.
- Meier, C. I., Reid, B. L., and Sandoval, O. (2013). Effects of the invasive plant *Lupinus polyphyllus* on vertical accretion of fine sediment and nutrient availability in bars of the gravel-bed Paloma river. *Limnologica - Ecology and Management of Inland Waters*, 43(5):381–387.
- Meijer, D. (1998a). Modelproeven overstroomd riet. Technical report, HKV Consultants, Technical report PR177, Lelystad, The Netherlands. (in Dutch).
- Meijer, D. (1998b). Modelproeven overstroomde vegetatie. Technical report, HKV Consultants, Technical report PR121, Lelystad, The Netherlands. (in Dutch).
- Meijer, D. G. and van Velzen, E. H. (1999). Prototype-scale flume experiments on hydraulic roughness of submerged vegetation. In *XXVIII IAHR Conference, Technical University of Graz, Graz, Austria*.
- Meng, F.-R., Meng, C. H., Tang, S., and Arp, P. A. (1997). A new height growth model for dominant and codominant trees. *Forest Science*, 43(3):348–354.
- Merritt, D. M. and Wohl, E. E. (2002). Processes governing hydrochory along rivers: Hydraulics, hydrology, and dispersal phenology. *Ecological Applications*, 12(4):1071–1087.
- Meyer-Peter, E. and Müller, R. (1948). Formulas for bed load transport. In *Proceedings of the 2nd IAHR Congress, Stockholm, Sweden, 2: 39-64*.
- Middelkoop, H. (2002). Reconstructing floodplain sedimentation rates from heavy metal profiles by inverse modelling. *Hydrological Processes*, 16(1):47–64.
- Milan, D. J., Heritage, G. L., Large, A. R. G., and Fuller, I. C. (2011). Filtering spatial error from DEMs: Implications for morphological change estimation. *Geomorphology*, 125(1):160–171.
- Miles, J. (1979). *Vegetation dynamics*. Chapman and Hall, London.
- Millar, R. and Quick, M. (1993). Effect of bank stability on geometry of gravel rivers. *Journal of Hydraulic Engineering*, 119(12):1343–1363.
- Millar, R. and Quick, M. (1998). Stable width and depth of gravel-bed rivers with cohesive banks. *Journal of Hydraulic Engineering*, 124(10):1005–1013.
- Millar, R. G. (2000). Influence of bank vegetation on alluvial channel patterns. *Water Resources Research*, 36(4):1109–1118.

- Millar, R. G. and Eaton, B. C. (2013). *Bank Vegetation, Bank Strength, and Application of the University of British Columbia Regime Model to Stream Restoration*, chapter Stream Restoration in Dynamic Fluvial Systems, pages 475–485. American Geophysical Union.
- Mladenoff, D. J. (2004). LANDIS and forest landscape models. *Ecological Modelling*, 180(1):7–19.
- Mohl, A. (2004). Life river restoration projects in Austria. In *3rd European Conference on River Restoration, River Restoration 2004. Zagreb, Croatia, 17-21 May 2004*, pages 201–209.
- Mohler, C. L., Marks, P. L., and Sprugel, D. G. (1978). Stand structure and allometry of trees during self-thinning of pure stands. *Journal of Ecology*, 66(2):599–614.
- Montes Arboleda, A., Crosato, A., and Middelkoop, H. (2010). Reconstructing the early 19th-century Waal River by means of a 2d physics-based numerical model. *Hydrological Processes*, 24(25):3661–3675.
- Mooney, H., Larigauderie, A., Cesario, M., Elmquist, T., Hoegh-Guldberg, O., Lavorel, S., Mace, G. M., Palmer, M., Scholes, R., and Yahara, T. (2009). Biodiversity, climate change, and ecosystem services. *Current Opinion in Environmental Sustainability*, 1(1):46–54.
- Mosselman, E. (1992). *Mathematical modelling of morphological processes in rivers with erodible cohesive banks*. PhD thesis, Delft University of Technology.
- Mosselman, E., Shishikura, T., and Klaassen, G. (2000). Effect of bank stabilization on bend scour in anabranches of braided rivers. *Physics and Chemistry of the Earth, Part B: Hydrology, Oceans and Atmosphere*, 25(7-8):699–704.
- Murota, A., Fakahara, T., and Sato, M. (1984). Turbulence structure in vegetated open channel flow. *Journal of Hydroscience and Hydraulic Engineering*, 2:47–61.
- Murphy, E., Ghisalberti, M., and Nepf, H. (2007). Model and laboratory study of dispersion in flows with submerged vegetation. *Water Resources Research*, 43(5):W05438.
- Murray, A. B. and Paola, C. (1994). A cellular model of braided rivers. *Nature*, 371(6492):54–57.
- Murray, A. B. and Paola, C. (1997). Properties of a cellular braided-stream model. *Earth Surface Processes and Landforms*, 22(11):1001–1025.
- Murray, A. B. and Paola, C. (2003). Modelling the effect of vegetation on channel pattern in bedload rivers. *Earth Surface Processes and Landforms*, 28(2):131–143.
- Nadler, C. T. and Schumm, S. A. (1981). Metamorphosis of South Platte and Arkansas rivers, eastern Colorado. *Physical Geography*, 2(2):95–115.
- Nanson, G. and Croke, J. (1992). A genetic classification of floodplains. *Geomorphology*, 4(6):459–486.

- Nanson, G. C. (1980). Point bar and floodplain formation of the meandering Beatton River, northeastern British Columbia, Canada. *Sedimentology*, 27(1):3–29.
- Neary, V., Constantinescu, S., Bennett, S., and Diplas, P. (2012). Effects of vegetation on turbulence, sediment transport, and stream morphology. *Journal of Hydraulic Engineering*, 138(9):765–776.
- Nepf, H. M. (1999). Drag, turbulence, and diffusion in flow through emergent vegetation. *Water Resources Research*, 35(2):479–489.
- Nepf, H. M. (2012a). Flow and transport in regions with aquatic vegetation. *Annual Review of Fluid Mechanics*, 44(1):123–142.
- Nepf, H. M. (2012b). Hydrodynamics of vegetated channels. *Journal of Hydraulic Research*, 50(3):262–279.
- Nepf, H. M. and Vivoni, E. R. (2000). Flow structure in depth-limited, vegetated flow. *Journal of Geophysical Research*, 105(C12):28,547–28,557.
- Newton, P. F. (1997). Stand density management diagrams: Review of their development and utility in stand-level management planning. *Forest Ecology and Management*, 98(3):251–265.
- Newton, P. F. and Smith, V. G. (1990). Reformulated self-thinning exponents as applied to black spruce. *Canadian Journal of Forest Research*, 20(7):887–893.
- Nezu, I. and Sanjou, M. (2008). Turbulence structure and coherent motion in vegetated canopy open-channel flows. *Journal of Hydro-environment Research*, 2(2):62–90.
- Nicholas, A. P. (2013). Modelling the continuum of river channel patterns. *Earth Surface Processes and Landforms*, 38(10):1187–1196.
- Nicolle, A. and Eames, I. (2011). Numerical study of flow through and around a circular array of cylinders. *Journal of Fluid Mechanics*, 679:1–31.
- Nienhuis, P. and Leuven, R. (2001). River restoration and flood protection: controversy or synergism? *Hydrobiologia*, 444(1):85–99.
- Niklas, K. J., Midgley, J. J., and Enquist, B. J. (2003). A general model for mass-growth-density relations across tree-dominated communities. *Evolutionary Ecology Research*, 5(3):459–468.
- Nikora, V., Larned, S., Nikora, N., Debnath, K., Cooper, G., and Reid, M. (2008). Hydraulic resistance due to aquatic vegetation in small streams: Field study. *Journal of Hydraulic Engineering*, 134(9):1326–1332.
- Nikuradse, J. (1933). Strömungsgesetze in rauhen rohren. Technical report, Forschungsheft 361. Ausgabe B. Band 4 (in German).

- Nilsson, C. and Svedmark, M. (2002). Basic principles and ecological consequences of changing water regimes: Riparian plant communities. *Environmental Management*, 30(4):468–480.
- O'Connor, J. E., Jones, M. A., and Haluska, T. L. (2003). Flood plain and channel dynamics of the Quinault and Queets Rivers, Washington, USA. *Geomorphology*, 51(1-3):31–59.
- Odgaard, A. J. (1989a). River-meander model. I: Development. *Journal of Hydraulic Engineering*, 115(11):1433–1450.
- Odgaard, A. J. (1989b). River-meander model. II: Applications. *Journal of Hydraulic Engineering*, 115(11):1451–1464.
- Odum, H. T. (1983). *System Ecology: An Introduction*. John Wiley, New York.
- Ogawa, K. (2005). Time-trajectory of mean phytomass and density during a course of self-thinning in a sugi (*Cryptomeria japonica* d. don) plantation. *Forest Ecology and Management*, 214(1-3):104–110.
- Ogawa, K. (2009). Theoretical analysis of the interrelationships between self-thinning, biomass density, and plant form in dense populations of hinoki cypress (*Chamaecyparis obtusa*) seedlings. *European Journal of Forest Research*, 128(5):447–453.
- O'Hare, M. T., Hutchinson, K. A., and Clarke, R. T. (2007). The drag and reconfiguration experienced by five macrophytes from a lowland river. *Aquatic Botany*, 86(3):253–259.
- Okabe, T., Yuuki, T., and M., K. (1997). Bed-load rate on movable beds covered by vegetation. In *Environmental and Coastal Hydraulics: Protecting the Aquatic Habitat*, pages 1396–1401.
- Okamoto, T. and Nezu, I. (2010a). Resistance and turbulence structure in open-channel flows with flexible vegetations. In Christodolou, G. C. and Stamou, A. I., editors, *Proceedings of the 6th International symposium on Environmental Hydraulics, Athens, Greece, 23-25 June 2010*, pages 215–220. CRC Press.
- Okamoto, T.-A. and Nezu, I. (2010b). Flow resistance law in open-channel flows with rigid and flexible vegetation. In Dittrich, A., Koll, K., Aberle, J., and Geisenhainer, P., editors, *River Flow 2010, Proceedings of the International Conference on Fluvial Hydraulics, Braunschweig, Germany September 8-10, 2010*, pages 261–268.
- Oldham, C. E. and Sturman, J. J. (2001). The effect of emergent vegetation on convective flushing in shallow wetlands: Scaling and experiments. *Limnology and Oceanography*, 46(6):1486–1493.
- Olesen, K. W. (1984). Alternate bars in and meandering of alluvial rivers. In *in River Meandering, Proceedings of the Conference on Rivers'83*, edited by C. M. Elliott, pp. 873-884. American Society of Civil Engineers, New York.
- Omanga, P. A., Summerfield, R. J., and Qi, A. (1995). Flowering of pigeonpea (*Cajanus cajan*) in Kenya: Responses of early-maturing genotypes to location and date of sowing. *Field Crops Research*, 41(1):25–34.

- Omanga, P. A., Summerfield, R. J., and Qi, A. (1996). Flowering in pigeonpea (*Cajanus cajan*) in Kenya: Responses of medium- and late-maturing genotypes to location and date of sowing. *Experimental Agriculture*, 32:111–128.
- Osman, A. M. and Thorne, C. R. (1988). Riverbank stability analysis. I: Theory. *Journal of Hydraulic Engineering*, 114(2):134–150.
- Osterkamp, W. and Hupp, C. (2010). Fluvial processes and vegetation - glimpses of the past, the present, and perhaps the future. *Geomorphology*, 116(3-4):274–285.
- Ott, R. (2000). Factors affecting stream bank and river banks stability, with an emphasis on vegetation influences. an annotated bibliography. In *Tanana Chiefs Conference*. Inc. Forestry Program, Fairbanks, Alaska.
- Owens, P. N., Batalla, R. J., Collins, A. J., Gomez, B., Hicks, D. M., Horowitz, A. J., Kondolf, G. M., Marden, M., Page, M. J., Peacock, D. H., Petticrew, E. L., Salomons, W., and Trustrum, N. A. (2005). Fine-grained sediment in river systems: environmental significance and management issues. *River Research and Applications*, 21(7):693–717.
- Owens, P. N., Walling, D. E., and Leeks, G. J. L. (1999). Deposition and storage of fine-grained sediment within the main channel system of the river Tweed, Scotland. *Earth Surface Processes and Landforms*, 24(12):1061–1076.
- Page, K., Nanson, G., and Frazier, P. (2003). Floodplain formation and sediment stratigraphy resulting from oblique accretion on the Murrumbidgee River, Australia. *Journal of Sedimentary Research*, 73(1):5–14.
- Palmer, M. a., Bernhardt, E. s., Allan, J. D., Lake, P. s., Alexander, G., Brooks, S., Carr, J., Clayton, S., Dahm, C. N., Follstad Shah, J., Galat, D. L., Loss, S. G., Goodwin, P., Hart, D. d., Hassett, B., Jenkinson, R., Kondolf, G. m., Lave, R., Meyer, J. l., O'donnell, T. k., Pagano, L., and Sudduth, E. (2005). Standards for ecologically successful river restoration. *Journal of Applied Ecology*, 42(2):208–217.
- Paola, C., Straub, K., Mohrig, D., and Reinhardt, L. (2009). The "unreasonable effectiveness" of stratigraphic and geomorphic experiments. *Earth-Science Reviews*, 97(1-4):1–43.
- Parker, G. (1976). On the cause and characteristic scales of meandering and braiding in rivers. *Journal of Fluid Mechanics*, 76(03):457–480.
- Parker, G. (1978a). Self-formed straight rivers with equilibrium banks and mobile bed. part 1. the sand-silt river. *Journal of Fluid Mechanics*, 89(1):109–125.
- Parker, G. (1978b). Self-formed straight rivers with equilibrium banks and mobile bed. part 2. the gravel river. *Journal of Fluid Mechanics*, 89(1):127–146.
- Parker, G. (2004). The uses of sediment transport and morphodynamic modeling in stream restoration. In *Proceedings, ASCE World Water and Environmental Resources 2004 Congress, Salt Lake City, June 27-July 1, 10 p.*, pages 1–10.

- Parker, G. and Johanneson, H. (1989). Observations on several recent theories of resonance and overdeepening in meandering channels. In *in River Meandering, edited by S. Ikeda and G. Parker, Water Resources Monograph, Vol. 12, pp. 379-415, ISBN 0-87590-316-9.* AGU, Washington, D.C.
- Parker, G., Shimizu, Y., Wilkerson, G. V., Eke, E. C., Abad, J. D., Lauer, J. W., Paola, C., Dietrich, W. E., and Voller, V. R. (2011). A new framework for modeling the migration of meandering rivers. *Earth Surface Processes and Landforms*, 36(1):70–86.
- Parnet, B., Kwadijk, J., and Raak, M. (1995). Impact of climate change on the discharge of the river rhine. In Zwerver, S., Rompaey, R. S. A. R., van, Kok, M. T. J., and Berk, M. M., editors, *Climate change research: evaluation and policy implications; proceedings of the International Climate Change Research Conference, Maastricht, The Netherlands, 6-9 December 1994. Vol. B*, volume 65 of *Studies in Environmental Science*, pages 911–918. Elsevier.
- Parolin, P. (2009). Submerged in darkness: adaptations to prolonged submergence by woody species of the amazonian floodplains. *Annals of Botany*, 103(2):359–376.
- Pasche, E. and Rouvé, G. (1985). Overbank flow with vegetatively roughened flood plains. *Journal of Hydraulic Engineering*, 111(9):1262–1278.
- Peakall, J., Ashworth, P. J., and Best, J. L. (2007). Meander-bend evolution, alluvial architecture, and the role of cohesion in sinuous river channels: A flume study. *Journal of Sedimentary Research*, 77(3):197–212.
- Pearlstone, L., Friedman, S., and Supernaw, M. (2011). Everglades Landscape Vegetation Succession Model (ELVeS). Technical report, Ecological Design Document: Freshwater Marsh & Prairie Component Version 1.1 South Florida Natural Resources Center. Everglades National Park, National Park Service, Homestead, Florida. 128 pages.
- Pearlstone, L., McKellar, H., and Kitchens, W. (1985). Modelling the impacts of a river diversion on bottomland forest communities in the Santee River floodplain, South Carolina. *Ecological Modelling*, 29(1-4):283–302.
- Peel, M. C., Finlayson, B. L., and McMahon, T. A. (2007). Updated world map of the köppen-geiger climate classification. *Hydrology and Earth System Sciences*, 11(5):1633–1644.
- Perona, P., Camporeale, C., Perucca, E., Savina, M., Molnar, P., Burlando, P., and Ridolfi, L. (2009). Modelling river and riparian vegetation interactions and related importance for sustainable ecosystem management. *Aquatic Sciences*, 71(3):266–278.
- Perona, P., Crouzy, B., McLelland, S., Molnar, P., and Camporeale, C. (2014). Ecomorphodynamics of rivers with converging boundaries. *Earth Surface Processes and Landforms*, 39(12):1651–1662.
- Perry, G. L. W. and Enright, N. J. (2007). Contrasting outcomes of spatially implicit and spatially explicit models of vegetation dynamics in a forest-shrubland mosaic. *Ecological Modelling*, 207(2-4):327–338.

- Perucca, E., Camporeale, C., and Ridolfi, L. (2006). Influence of river meandering dynamics on riparian vegetation pattern formation. *Journal of Geophysical Research*, 111. G01001.
- Perucca, E., Camporeale, C., and Ridolfi, L. (2007). Significance of the riparian vegetation dynamics on meandering river morphodynamics. *Water Resources Research*, 43. W03430.
- Petryk, S. and Bosmajian, G. (1975). Analysis of flow through vegetation. *Journal of the Hydraulics Division ASCE*, 101(7):871–884.
- Phillips, J. D. (1995). Biogeomorphology and landscape evolution: The problem of scale. *Geomorphology*, 13(1-4):337–347.
- Phillips, O. L., Aragão, L. E. O. C., Lewis, S. L., Fisher, J. B., Lloyd, J., López-González, G., Malhi, Y., Monteagudo, A., Peacock, J., Quesada, C. A., van der Heijden, G., Almeida, S., Amaral, I., Arroyo, L., Aymard, G., Baker, T. R., Bánki, O., Blanc, L., Bonal, D., Brando, P., Chave, J., de Oliveira, A. C. A., Cardozo, N. D., Czimczik, C. I., Feldpausch, T. R., Freitas, M. A., Gloor, E., Higuchi, N., Jiménez, E., Lloyd, G., Meir, P., Mendoza, C., Morel, A., Neill, D. A., Nepstad, D., Patiño, S., Peñuela, M. C., Prieto, A., Ramírez, E., Schwarz, M., Silva, J., Silveira, M., Thomas, A. S., Steege, H. t., Stropp, J., Vásquez, R., Zelazowski, P., Dávila, E. A., Andelman, S., Andrade, A., Chao, K.-J., Erwin, T., Di Fiore, A., C., E. H., Keeling, H., Killeen, T. J., Laurance, W. F., Cruz, A. P., Pitman, N. C. A., Núñez Vargas, P., Ramírez-Angulo, H., Rudas, A., Salamão, R., Silva, N., Terborgh, J., and Torres-Lezama, A. (2009). Drought sensitivity of the amazon rainforest. *Science*, 323(5919):1344–1347.
- Pidwirny, M. (2006). "Plant Succession". Fundamentals of Physical Geography. Technical report, Retrieved on May 2016, <http://www.physicalgeography.net/fundamentals/9i.html>.
- Piégay, H., Darby, S. E., Mosselman, E., and Surian, N. (2005). A review of techniques available for delimiting the erodible river corridor: a sustainable approach to managing bank erosion. *River Research and Applications*, 21(7):773–789.
- Pizzuto, J. (1987). Sediment diffusion during overbank flows. *Sedimentology*, 34(2):301–317.
- Poff, N. L., Allan, J. D., Bain, M. B., Karr, J. R., Prestegard, K. L., Richter, B. D., Sparks, R. E., and Stromberg, J. C. (1997). The natural flow regime. *BioScience*, 47(11):769–784.
- Poggi, D., Krug, C., and Katul, G. G. (2009). Hydraulic resistance of submerged rigid vegetation derived from first-order closure models. *Water Resources Research*, 45(10):W10442.
- Pollen, N. and Simon, A. (2005). Estimating the mechanical effects of riparian vegetation on stream bank stability using a fiber bundle model. *Water Resources Research*, 41(7). W07025.

- Pollen-Bankhead, N. and Simon, A. (2010). Hydrologic and hydraulic effects of riparian root networks on streambank stability: Is mechanical root-reinforcement the whole story? *Geomorphology*, 116(3-4):353–362.
- Prosser, I. P., Dietrich, W. E., and Stevenson, J. (1995). Flow resistance and sediment transport by concentrated overland flow in a grassland valley. *Geomorphology*, 13(1-4):71–86.
- Provansal, M., Villiet, J., Eyrolle, F., Raccasi, G., Gurriaran, R., and Antonelli, C. (2010). High-resolution evaluation of recent bank accretion rate of the managed Rhone: A case study by multi-proxy approach. *Geomorphology*, 117(3-4):287–297.
- PUB (2014). Active beautiful clean waters design guidelines, third edition, retrieved on may 26 2016 from http://www.pub.gov.sg/abcwaters/abcwatersdesignguidelines/Documents/ABC_DG_2014.pdf. Technical report, Singapore's National Water Agency.
- Puckridge, J. T., Sheldon, F., Walker, K. F., and Boulton, A. J. (1998). Flow variability and the ecology of large rivers. *Marine and Freshwater Research*, 49(1):55–72.
- Puhakka, M., Kalliola, R., Rajasilta, M., and Salo, J. (1992). River types, site evolution and successional vegetation patterns in peruvian amazonia. *Journal of Biogeography*, 19(6):651–665.
- Raupach, M. (1992). Drag and drag partition on rough surfaces. *Boundary-Layer Meteorology*, 60(4):375–395.
- Ree, W. and Crow, F. (1977). Friction factors for vegetated waterways of small slope. Technical report, Technical Report Publication S-151, US Department of Agriculture, Agricultural Research Service.
- Reineke, L. (1933). Perfecting a stand-density index for even-aged forest. *Journal of Agricultural Research*, 46:627–638.
- Reynolds, J. H. and Ford, E. D. (2005). Improving competition representation in theoretical models of self-thinning: a critical review. *Journal of Ecology*, 93(2):362–372.
- Richardson, D. M., Holmes, P. M., Esler, K. J., Galatowitsch, S. M., Stromberg, J. C., Kirkman, S. P., Pyšek, P., and Hobbs, R. J. (2007). Riparian vegetation: degradation, alien plant invasions, and restoration prospects. *Diversity and Distributions*, 13(1):126–139.
- Richter, B. D. and Richter, H. E. (2000). Prescribing flood regimes to sustain riparian ecosystems along meandering rivers. *Conservation Biology*, 14(5):1467–1478.
- Righetti, M. (2008). Flow analysis in a channel with flexible vegetation using double-averaging method. *Acta Geophysica*, 56(3):801–823.
- Rijke, J., van Herk, S., Zevenbergen, C., and Ashley, R. (2012). Room for the River: delivering integrated river basin management in the Netherlands. *International Journal of River Basin Management*, 10(4):369–382.

- Rinaldi, M. and Darby, S. E. (2007). Modelling river-bank erosion processes and mass failure mechanisms: progress towards fully coupled simulations. In Habersack, H., Piegay, H., and Rinaldi, M., editors, *Gravel-Bed Rivers VI: From Process Understanding to River Restoration*, pages 213–239. Elsevier.
- Rominger, J. T., Lightbody, A. F., and Nepf, H. M. (2010). Effects of added vegetation on sand bar stability and stream hydrodynamics. *Journal of Hydraulic Engineering*, 136(12):994–1002.
- Rood, S. B., Braatne, J. H., and Hughes, F. M. R. (2003). Ecophysiology of riparian cottonwoods: stream flow dependency, water relations and restoration. *Tree Physiology*, 23(16):1113–1124.
- Rouse, H. (1965). Critical analysis of open-channel resistance. *Journal of the Hydraulics Division*, 91(4):1–23.
- Sand-Jensen, K. (2003). Drag and reconfiguration of freshwater macrophytes. *Freshwater Biology*, 48(2):271–283.
- Sand-Jensen, K., Andersen, K., and Andersen, T. (1999). Dynamic properties of recruitment, expansion and mortality of macrophyte patches in streams. *International Review of Hydrobiology*, 84(5):497–508.
- Sand-Jensen, K., Jeppesen, E., Nielsen, K., Van Der Bijl, L., Hjermand, L., Nielsen, L. W., and Ivlrsln, T. M. (1989). Growth of macrophytes and ecosystem consequences in a lowland Danish stream. *Freshwater Biology*, 22(1):15–32.
- Sand-Jensen, K. and Mebus, J. R. (1996). Fine-scale patterns of water velocity within macrophyte patches in streams. *Oikos*, 76(1):169–180.
- Sandercock, P., Hooke, J., and Mant, J. (2007). Vegetation in dryland river channels and its interaction with fluvial processes. *Progress in Physical Geography*, 31(2):107–129.
- Sanjou, M., Nezu, I., Suzuki, S., and Itai, K. (2010). Turbulence structure of compound open-channel flows with one-line emergent vegetation. *Journal of Hydrodynamics, Ser. B*, 22(5, Supplement 1):577–581.
- Schirmer, M., Luster, J., Linde, N., Perona, P., Mitchell, E. A. D., Barry, D. A., Hollender, J., Cirpka, O. A., Schneider, P., Vogt, T., Radny, D., and Durisch-Kaiser, E. (2014). Morphological, hydrological, biogeochemical and ecological changes and challenges in river restoration – the thur river case study. *Hydrology and Earth System Sciences*, 18(6):2449–2462.
- Schlichting, H. (1936). Experimental investigations of the problem of surface roughness. Technical report, NASA technical memorandum 823, Washington, DC.
- Schneider, R. L. and Sharitz, R. R. (1988). Hydrochory and regeneration in a Bald Cypress-Water Tupelo Swamp Forest. *Ecology*, 69(4):1055–1063.

- Schulz, M., Kozerski, H., Pluntke, T., and Rinke, K. (2003). The influence of macrophytes on sedimentation and nutrient retention in the lower River Spree (Germany). *Water Research*, 37(3):569–578.
- Schumm, S. and Khan, H. (1972). Experimental study of channel patterns. *Geological Society of America Bulletin*, 83(6):1755–1770.
- Schuurman, F., Shimizu, Y., Iwasaki, T., and Kleinhans, M. G. (2016). Dynamic meandering in response to upstream perturbations and floodplain formation. *Geomorphology*, 253:94–109.
- Sharpe, R. G. and James, C. S. (2007). Deposition of sediment from suspension in emergent vegetation. *Water SA*, 32(2):211–218.
- Shaw, J. B., Mohrig, D., and Whitman, S. K. (2013). The morphology and evolution of channels on the Wax Lake Delta, Louisiana, USA. *Journal of Geophysical Research: Earth Surface*, 118(3):1562–1584.
- Shimizu, Y., Tsujimoto, T., Nakagawa, H., and Kitamura, T. (1991). Experimental study on flow over rigid vegetation simulated by cylindrical with equi-spacing (in Japanese). In *Proc. Jpn Soc. Civ. Eng.*, 438/II-17, pages 31–40.
- Shucksmith, J. D., Boxall, J. B., and Guymer, I. (2011). Determining longitudinal dispersion coefficients for submerged vegetated flow. *Water Resources Research*, 47(10):W10516.
- Simon, A., Bennett, S. J., and Neary, V. S. (2004). *Riparian Vegetation and Fluvial Geomorphology*, chapter Riparian Vegetation and Fluvial Geomorphology: Problems and Opportunities, pages 1–10. American Geophysical Union, Washington, D. C.
- Simon, A. and Collison, A. J. C. (2002). Quantifying the mechanical and hydrologic effects of riparian vegetation on streambank stability. *Earth Surface Processes and Landforms*, 27(5):527–546.
- Simon, A., Curini, A., Darby, S. E., and Langendoen, E. J. (2000). Bank and near-bank processes in an incised channel. *Geomorphology*, 35(3-4):193–217.
- Simon, A., Doyle, M., Kondolf, M., Shields, F., Rhoads, B., and McPhillips, M. (2007). Critical evaluation of how the rosgen classification and associated "natural channel design" methods fail to integrate and quantify fluvial processes and channel response. *JAWRA Journal of the American Water Resources Association*, 43(5):1117–1131.
- Siniscalchi, F. and Nikora, V. (2013). Dynamic reconfiguration of aquatic plants and its interrelations with upstream turbulence and drag forces. *Journal of Hydraulic Research*, 51(1):46–55.
- Smith, C. E. (1998). Modeling high sinuosity meanders in a small flume. *Geomorphology*, 25(1-2):19–30.

- Smith, N. J. and Hann, D. W. (1986). A growth model based on the self-thinning rule. *Canadian Journal of Forest Research*, 16(2):330–334.
- Solari, L., van Oorschot, M., Belletti, B., Hendriks, D., Rinaldi, M., and Vargas-Luna, A. (2015). Advances on modelling riparian vegetation-hydromorphology interactions. *River Research and Applications*, 32(2):164–178.
- Song, X., Xu, G., Bai, Y., and Xu, D. (2016). Experiments on the short-term development of sine-generated meandering rivers. *Journal of Hydro-environment Research*, 11:42–58.
- Spruyt, A., Mosselman, E., and Jagers, B. (2011). A new approach to river bank retreat and advance in 2D numerical models of fluvial morphodynamics. In *RCEM 2011: Proceedings of the 7th IAHR Symposium of River, Coastal and Estuarine Morphodynamics, Beijing, China, 6-8 September 2011*. Tsinghua University Press.
- Statzner, B., Lamouroux, N., Nikora, V., and Sagnes, P. (2006). The debate about drag and reconfiguration of freshwater macrophytes: comparing results obtained by three recently discussed approaches. *Freshwater Biology*, 51(11):2173–2183.
- Steiger, J., Tabacchi, E., Dufour, S., Corenblit, D., and Peiry, J.-L. (2005). Hydrogeomorphic processes affecting riparian habitat within alluvial channel-floodplain river systems: a review for the temperate zone. *River Research and Applications*, 21(7):719–737.
- Stoesser, T., Kim, S., and Diplas, P. (2010). Turbulent flow through idealized emergent vegetation. *Journal of Hydraulic Engineering*, 136(12):1003–1017.
- Stoesser, T., Salvador, G., Rodi, W., and Diplas, P. (2009). Large eddy simulation of turbulent flow through submerged vegetation. *Transport in Porous Media*, 78(3):347–365.
- Stoesser, T., Wilson, C. A. M. E., Bates, P. D., and Dittrich, A. (2003). Application of a 3D numerical model to a river with vegetated floodplains. *Journal of Hydroinformatics*, 5:99–112.
- Stone, B. M. and Shen, H. T. (2002). Hydraulic resistance of flow in channels with cylindrical roughness. *Journal of Hydraulic Engineering*, 128(5):500–506.
- Struiksmma, N. and Crosato, A. (1989). Analysis of a 2-D bed topography model for rivers. In *in River Meandering, AGU, Water Resources Monograph, Vol. 12, Ikeda S. and Parker G. Editors, 153-180. ISBN 0-87590-316-9*. AGU, Washington, D.C.
- Struiksmma, N., Olesen, K. W., Flokstra, C., and De Vriend, H. J. (1985). Bed deformation in curved alluvial channels. *Journal of Hydraulic Research*, 23(1):57–79.
- Tabacchi, E., Correll, D. L., Hauer, R., Pinay, G., Planty-Tabacchi, A.-M., and Wissmar, R. C. (1998). Development, maintenance and role of riparian vegetation in the river landscape. *Freshwater Biology*, 40(3):497–516.
- Takebayashi, H., Teraoka, M., Okabe, T., and Egashira, S. (2006). Effect of vegetation growth and unsteady characteristics of water supply on formative condition of mesoscale channel configuration. In Alves, E. C. T. L., Cardoso, A. H., Leal, J. G. A. B.,

- and Ferreira, R. M. L., editors, *River Flow 2006, Proceedings of the International Conference on Fluvial Hydraulics, Lisbon, Portugal, 6-8 September 2006*, pages 1086–1096. Taylor & Francis.
- Takemura, T. and Tanaka, N. (2007). Flow structures and drag characteristics of a colony-type emergent roughness model mounted on a flat plate in uniform flow. *Fluid Dynamics Research*, 39(9-10):694–710.
- Tal, M. and Paola, C. (2007). Dynamic single-thread channels maintained by the interaction of flow and vegetation. *Geology*, 35(4):347–350.
- Tal, M. and Paola, C. (2010). Effects of vegetation on channel morphodynamics: results and insights from laboratory experiments. *Earth Surface Processes and Landforms*, 35(9):1014–1028.
- Talmon, A. M., Struiksma, N., and Van Mierlo, M. C. L. M. (1995). Laboratory measurements of the direction of sediment transport on transverse alluvial-bed slopes. *Journal of Hydraulic Research*, 33(4):495–517.
- Tanaka, N. and Yagisawa, J. (2009). Effects of tree characteristics and substrate condition on critical breaking moment of trees due to heavy flooding. *Landscape and Ecological Engineering*, 5(1):59–70.
- Tang, H., Tian, Z., Yan, J., and Yuan, S. (2014). Determining drag coefficients and their application in modelling of turbulent flow with submerged vegetation. *Advances in Water Resources*, 69:134–145.
- Tang, S., Meng, C. H., Meng, F.-R., and Wang, Y. H. (1994). A growth and self-thinning model for pure even-age stands: theory and applications. *Forest Ecology and Management*, 70(1-3):67–73.
- Tanino, Y. and Nepf, H. (2008). Laboratory investigation of mean drag in a random array of rigid, emergent cylinders. *Journal of Hydraulic Engineering*, 134(1):34–41.
- Tealdi, S., Camporeale, C., Perucca, E., and Ridolfi, L. (2010). Longitudinal dispersion in vegetated rivers with stochastic flows. *Advances in Water Resources*, 33(5):562–571.
- Tealdi, S., Camporeale, C., and Ridolfi, L. (2013). Inter-species competition-facilitation in stochastic riparian vegetation dynamics. *Journal of Theoretical Biology*, 318:13–21.
- Temmerman, S., Bouma, T., Van de Koppel, J., Van der Wal, D., De Vries, M., and Herman, P. (2007). Vegetation causes channel erosion in a tidal landscape. *Geology*, 35(7):631–634.
- Temmerman, S., Bouma, T. J., Govers, G., Wang, Z. B., De Vries, M. B., and Herman, P. M. J. (2005). Impact of vegetation on flow routing and sedimentation patterns: Three-dimensional modeling for a tidal marsh. *Journal of Geophysical Research: Earth Surface*, 110(F4):F04019.

- Temmerman, S., Govers, G., Wartel, S., and Meire, P. (2003). Spatial and temporal factors controlling short-term sedimentation in a salt and freshwater tidal marsh, Scheldt estuary, Belgium, SW Netherlands. *Earth Surface Processes and Landforms*, 28(7):739–755.
- Terwilliger, V. J. (1990). Effects of vegetation on soil slippage by pore pressure modification. *Earth Surface Processes and Landforms*, 15(6):553–570.
- Thompson, A., Wilson, B., and Hansen, B. (2004). Shear stress partitioning for idealized vegetated surfaces. *Transactions of the ASAE*, 47(3):701–709.
- Thorne, C. R. (1982). Processes and mechanisms of river bank erosion. In Hey, R. D., Bathurst, J. C., and Thorne, C. R., editors, *Gravel-bed Rivers*, pages 227–271. Wiley, Chichester.
- Thorne, C. R. (1990). *Vegetation and Erosion: Processes and Environments*, chapter Effects of vegetation on riverbank erosion and stability, pages 125–144. Chichester, England: John Wiley & Sons.
- Thornton, C., Abt, S., Morris, C., and Fischenich, J. (2000). Calculating shear stress at channel-overbank interfaces in straight channels with vegetated floodplains. *Journal of Hydraulic Engineering*, 126(12):929–936.
- Tinoco Lopez, R. O. (2011). *An experimental investigation of drag and the turbulent flow structure in simulated and real aquatic vegetation*. PhD thesis, Cornell University.
- Tollner, E. W., Barfield, B. J., Vachirakomwatana, C., and Haan, C. T. (1977). Sediment deposition patterns in simulated grass filters. *Transactions of the ASAE*, 20(5):940–944.
- Tritton, D. J. (1959). Experiments on the flow past a circular cylinder at low Reynolds numbers. *Journal of Fluid Mechanics*, 6:547–567.
- Tsujimoto, T. (1999). Fluvial processes in streams with vegetation. *Journal of Hydraulic Research*, 37(6):789–803.
- Tsujimoto, T., Okada, T., and Kitamura, T. (1991). Turbulent flow over flexible vegetation covered bed in open channels. Technical report, KHL progressive report 1, Kanazawa University, Kanazawa, Japan.
- Tsujimoto, T., Okada, T., and Kontani, K. (1993). Turbulent structure of open channel flow over flexible vegetation. Technical report, KHL progressive report 4, Kanazawa University, Kanazawa, Japan.
- Tubino, M. and Seminara, G. (1990). Free-forced interactions in developing meanders and suppression of free bars. *Journal of Fluid Mechanics*, 214:131–159.
- Turner, A. and Chanmeesri, N. (1984). Shallow flow of water through non-submerged vegetation. *Agricultural Water Management*, 8(4):375–385.
- Uijtewaal, W. S. (2014). Hydrodynamics of shallow flows: application to rivers. *Journal of Hydraulic Research*, 52(2):157–172.

- van Breen, L. E., Jesse, P., and Havinga, H. (2003). River restoration from a river manager's point of view. *Archiv für Hydrobiologie Supplement 155/1-4, Large Rivers*, 15(1-4):359–371.
- van de Koppel, J., Herman, P. M. J., Thoolen, P., and Heip, C. H. R. (2001). Do alternate stable states occur in natural ecosystems? Evidence from a tidal flat. *Ecology*, 82(12):3449–3461.
- van de Koppel, J., Rietkerk, M., Dankers, N., and Herman, P. M. J. (2005). Scale-dependent feedback and regular spatial patterns in young mussel beds. *The American Naturalist*, 165(3):E66–77.
- van de Lageweg, W. I., van Dijk, W. M., Baar, A. W., Rutten, J., and Kleinhans, M. G. (2014). Bank pull or bar push: What drives scroll-bar formation in meandering rivers? *Geology*.
- van der Drift, J. W. M. (1995). The effect of temperature change on soil structure stability. In Zwerver, S., Rompaey, R. S. A. R., van, Kok, M. T. J., and Berk, M. M., editors, *Climate change research: evaluation and policy implications; proceedings of the International Climate Change Research Conference, Maastricht, The Netherlands, 6-9 December 1994. Vol. B*, volume 65 of *Studies in Environmental Science*, pages 923–930. Elsevier.
- van der Heide, T., Roijackers, R. M., van Nes, E. H., and Peeters, E. T. (2006). A simple equation for describing the temperature dependent growth of free-floating macrophytes. *Aquatic Botany*, 84(2):171–175.
- van der Maarel, E. (1981). Fluctuations in a coastal dune grassland due to fluctuations in rainfall: Experimental evidence. *Vegetatio*, 46(1):259–265.
- van der Maarel, E. (1988). Vegetation dynamics: patterns in time and space. *Vegetatio*, 77(1):7–19.
- van der Maarel, E., Boot, R., van Dorp, D., and Rijntjes, J. (1985). Vegetation succession on the dunes near Oostvoorne, The Netherlands; a comparison of the vegetation in 1959 and 1980. *Vegetatio*, 58(3):137–187.
- Van der Wal, D., Wielemaker-Van den Dool, A., and Herman, P. M. (2008). Spatial patterns, rates and mechanisms of saltmarsh cycles (Westerschelde, The Netherlands). *Estuarine, Coastal and Shelf Science*, 76(2):357–368.
- van der Wegen, M. and Roelvink, J. A. (2008). Long-term morphodynamic evolution of a tidal embayment using a two-dimensional, process-based model. *Journal of Geophysical Research: Oceans*, 113(C03016):1–23.
- van Dijk, W. M., Teske, R., van de Lageweg, W. I., and Kleinhans, M. G. (2013). Effects of vegetation distribution on experimental river channel dynamics. *Water Resources Research*, 49(11):7558–7574.

- van Dijk, W. M., van de Lageweg, W. I., and Kleinhans, M. G. (2012). Experimental meandering river with chute cutoffs. *Journal of Geophysical Research*, 117(F3):F03023.
- van Mantgem, P. J., Stephenson, N. L., Byrne, J. C., Daniels, L. D., Franklin, J. F., Fulé, P. Z., Harmon, M. E., Larson, A. J., Smith, J. M., Taylor, A. H., and Veblen, T. T. (2009). Widespread increase of tree mortality rates in the Western United States. *Science*, 323(5913):521–524.
- van Oorschot, M., Kleinhans, M., Geerling, G., and Middelkoop, H. (2016). Distinct patterns of interaction between vegetation and morphodynamics. *Earth Surface Processes and Landforms*, 41(6):791–808.
- van Rijn, L. (1984a). Sediment transport, part I: Bed load transport. *Journal of Hydraulic Engineering*, 110(10):1431–1456.
- van Rijn, L. (1984b). Sediment transport, part II: Suspended load transport. *Journal of Hydraulic Engineering*, 110(11):1613–1641.
- van Ruijven, J. and Berendse, F. (2005). Diversity-productivity relationships: Initial effects, long-term patterns, and underlying mechanisms. *Proceedings of the National Academy of Sciences of the United States of America*, 102(3):695–700.
- van Ruijven, J., De Deyn, G. B., and Berendse, F. (2003). Diversity reduces invasibility in experimental plant communities: the role of plant species. *Ecology Letters*, 6(10):910–918.
- Van Velzen, E., Jesse, P., Cornelissen, P., and Coops, H. (2003). Stromingsweerstand vegetatie in uiterwaarden; handboek. part 1 and 2. Technical report, RIZA Reports, 2003.028 and 2003.029, Arnhem, The Netherlands (in Dutch).
- van Vuuren, W. (2005). Verdeling zomer- en winterhoogwaters voor de rijntakken in de periode 1770-2004. Technical report, In: Memo WRR 2005-012, to: E. Van Velzen (in Dutch).
- Vanclay, J. K. (2009). Tree diameter, height and stocking in even-aged forests. *Annals of Forest Science*, 66(7):702–702.
- Vanoni, V. A. and Brooks, N. H. (1957). Laboratory studies of the roughness and suspended load of alluvial streams. Report no. E-68, Sedimentation Laboratory, California Institute of Technology, Pasadena, California.
- Vargas-Luna, A., Angel Escobar, J., Stierman, E., Gorte, B., and Uijttewaal, W. (2016a). Measuring bathymetric evolution in mobile-bed laboratory flumes. In Constantinescu, G., Garcia, M., and Hanes, D., editors, *8th International Conference on Fluvial Hydraulics, River Flow 2016, St. Louis, USA, July 12-15, 2016, ISBN 978-1-138-02913-2*, pages 411–416.
- Vargas-Luna, A., Crosato, A., Calvani, G., and Uijttewaal, W. S. J. (2016b). Representing plants as rigid cylinders in experiments and models. *Advances in Water Resources*, 93, Part B:205–222.

- Vargas-Luna, A., Crosato, A., Collot, L., and Uijttewaal, W. S. J. (2015a). Laboratory investigation on the hydrodynamic characterization of artificial grass. In *E-proceedings of the 36th IAHR World Congress 28 June-3 July, 2015, The Hague, the Netherlands*. ISBN: 978-90-824846-0-1., pages 728–734.
- Vargas-Luna, A., Crosato, A., and Uijttewaal, W. S. J. (2015b). Effects of vegetation on flow and sediment transport: comparative analyses and validation of predicting models. *Earth Surface Processes and Landforms*, 40(2):157–176.
- Västilä, K., Järvelä, J., and Aberle, J. (2013). Characteristic reference areas for estimating flow resistance of natural foliated vegetation. *Journal of Hydrology*, 492(1):49–60.
- Västilä, K., Järvelä, J., and Koivusalo, H. (2016). Flow-vegetation-sediment interaction in a cohesive compound channel. *Journal of Hydraulic Engineering*, 142(1):04015034–1–04015034–11.
- Velasco, D., Bateman, A., and Medina, V. (2008). A new integrated, hydro-mechanical model applied to flexible vegetation in riverbeds. *Journal of Hydraulic Research*, 46(5):579–597.
- Villada Arroyave, J. and Crosato, A. (2010). Effects of river floodplain lowering and vegetation cover. *Proceedings of the ICE - Water Management*, 163(9):457–467.
- Volterra, V. (1926). Fluctuations in the abundance of a species considered mathematically. *Nature*, 118:558–560.
- Waldron, L. J. and Dakessian, S. (1981). Soil reinforcement by roots: calculation of increased soil shear resistance from root properties. *Soil Science*, 132(6):427–435.
- Walker, L. R., Walker, J., and del Moral, R. (2007). Forging a new alliance between succession and restoration. In Walker, L. R., Walker, J., and Hobbs, R. J., editors, *Linking Restoration and Ecological Succession*, pages 1–18. Springer New York.
- Walker, L. R., Wardle, D. A., Bardgett, R. D., and Clarkson, B. D. (2010). The use of chronosequences in studies of ecological succession and soil development. *Journal of Ecology*, 98(4):725–736.
- Walling, D. and He, Q. (1997). Investigating spatial patterns of overbank sedimentation on river floodplains. In Evans, R. D., Wisniewski, J., and Wisniewski, J. R., editors, *The Interactions Between Sediments and Water, Proceedings of the 7th International Symposium, Baveno, Italy 22-25 September 1996*, pages 9–20. Springer Netherlands.
- Wang, C., Wang, Q., Meire, D., Ma, W., Wu, C., Meng, Z., Van de Koppel, J., Troch, P., Verhoeven, R., De Mulder, T., and Temmerman, S. (2016). Biogeomorphic feedback between plant growth and flooding causes alternative stable states in an experimental floodplain. *Advances in Water Resources*, 93, Part B:223–235.
- Ward, J. V. (1989). The four-dimensional nature of lotic ecosystems. *Journal of the North American Benthological Society*, 8(1):2–8.

- Ward, J. V., Malard, F., and Tockner, K. (2002). Landscape ecology: a framework for integrating pattern and process in river corridors. *Landscape Ecology*, 17(1):35–45.
- Ward, P. D., Montgomery, D. R., and Smith, R. (2000). Altered river morphology in south africa related to the permian-triassic extinction. *Science*, 289(5485):1740–1743.
- Watanabe, K., Nagy, H. M., and Noguchi, H. (2002). Flow structure and bed-load transport in vegetation flow. In *Advances in Hydraulics and Water Engineering: Proceedings of the 13th IAHR-APD Congress, Singapore*, pages 214–218.
- Weller, D. E. (1987a). A reevaluation of the $-3/2$ power rule of plant self-thinning. *Ecological Monographs*, 57(1):23–43.
- Weller, D. E. (1987b). Self-thinning exponent correlated with allometric measures of plant geometry. *Ecology*, 68(4):813–821.
- Westoby, M., Brasington, J., Glasser, N., Hambrey, M., and Reynolds, J. (2012). 'Structure-from-Motion' photogrammetry: A low-cost, effective tool for geoscience applications. *Geomorphology*, 179:300 – 314.
- White, B. L. and Nepf, H. M. (2008). A vortex-based model of velocity and shear stress in a partially vegetated shallow channel. *Water Resources Research*, 44(1):W01412.
- White, J. (1981). The allometric interpretation of the self-thinning rule. *Journal of Theoretical Biology*, 89(3):475–500.
- Wilson, C. (2007). Flow resistance models for flexible submerged vegetation. *Journal of Hydrology*, 342(3-4):213–222.
- Wilson, C., Hoyt, J., and Schnauder, I. (2008). Impact of foliage on the drag force of vegetation in aquatic flows. *Journal of Hydraulic Engineering*, 134(7):885–891.
- Wilson, C. a. M. E. and Horritt, M. S. (2002). Measuring the flow resistance of submerged grass. *Hydrological Processes*, 16(13):2589–2598.
- Wilson, C. A. M. E., Stoesser, T., Bates, P. D., and Pinzen, A. B. (2003). Open channel flow through different forms of submerged flexible vegetation. *Journal of Hydraulic Engineering*, 129(11):847–853.
- Wintenberger, C. L., Rodrigues, S., Br  h  ret, J.-G., and Villar, M. (2015). Fluvial islands: First stage of development from nonmigrating (forced) bars and woody-vegetation interactions. *Geomorphology*, 246:305–320.
- Wolman, M. G. and Leopold, L. B. (1957). River flood plains: Some observations on their formation. Technical report, USGS Professional paper 282-C.
- Wright, N. and Crosato, A. (2011). The hydrodynamics and morphodynamics of rivers. In Wilderer, P., editor, *Treatise on Water Science*, volume 2, chapter 2.07, pages 135–156 (2102). Elsevier Science Ltd, Oxford.

- Wu, F. C., Shen, H. W., and Chou, Y. J. (1999). Variation of roughness coefficients for un-submerged and submerged vegetation. *Journal of Hydraulic Engineering*, 125(9):934–942.
- Wu, T. H., McKinnell III, W. P., and Swanston, D. N. (1979). Strength of tree roots and landslides on Prince of Wales Island, Alaska. *Canadian Geotechnical Journal*, 16(1):19–33.
- Wu, W. and He, Z. (2009). Effects of vegetation on flow conveyance and sediment transport capacity. *International Journal of Sediment Research*, 24(3):247–259.
- Wu, W., Jr, F. D. S., Bennett, S. J., and Wang, S. S. Y. (2005). A depth-averaged two-dimensional model for flow, sediment transport, and bed topography in curved channels with riparian vegetation. *Water Resources Research*, 41(3):W03015.
- Wu, Y., Falconer, R., and Struve, J. (2001). Mathematical modelling of tidal currents in mangrove forests. *Environmental Modelling & Software*, 16(1):19–29.
- Wunder, S., Lehmann, B., and Nestmann, F. (2011). Determination of the drag coefficients of emergent and just submerged willows. *International Journal of River Basin Management*, 9(3-4):231–236.
- Wynn, T. and Mostaghimi, S. (2006). The effects of vegetation and soil type on stream-bank erosion, southwestern virginia, usa. *JAWRA Journal of the American Water Resources Association*, 42(1):69–82.
- Yager, E. M. and Schmeeckle, M. W. (2013). The influence of vegetation on turbulence and bed load transport. *Journal of Geophysical Research: Earth Surface*, 118(3):1585–1601.
- Yan, J. (2008). *Experimental study of flow resistance and turbulence characteristics of open channel flow with vegetation*. PhD thesis, Hohai University, Hohai, China.
- Yan, W. and Hunt, L. A. (1999). An equation for modelling the temperature response of plants using only the cardinal temperatures. *Annals of Botany*, 84(5):607–614.
- Yan, W. and Wallace, D. H. (1998). Simulation and prediction of plant phenology for five crops based on photoperiod x temperature interaction. *Annals of Botany*, 81(6):705–716.
- Yan, W., Wallace, D. H., and Ross, J. (1996). A model of photoperiod x temperature interaction effects on plant development. *Critical Reviews in Plant Sciences*, 15(1):63–96.
- Yang, W. (2008). *Experimental study of turbulent open-channel flows with submerged vegetation*. PhD thesis, Yonsei University, Korea.
- Yang, W. and Choi, S. U. (2010). A two-layer approach for depth-limited open-channel flows with submerged vegetation. *Journal of Hydraulic Research*, 48(4):466–475.

- Yao, Z., Ta, W., Jia, X., and Xiao, J. (2011). Bank erosion and accretion along the Ningxia–Inner Mongolia reaches of the Yellow River from 1958 to 2008. *Geomorphology*, 127(1-2):99–106.
- Ye, F., Chen, Q., Blanckaert, K., and Ma, J. (2013). Riparian vegetation dynamics: insight provided by a process-based model, a statistical model and field data. *Ecohydrology*, 6(4):567–585.
- Ye, Q. (2012). *An approach towards generic coastal geomorphological modelling with applications*. PhD thesis, Delft University of Technology, CRC press.
- Yen, B. C. (2002). Open channel flow resistance. *Journal of Hydraulic Engineering*, 128(1):20–39.
- Yin, X. and Kropff, M. J. (1996). The effect of temperature on leaf appearance in rice. *Annals of Botany*, 77(3):215–221.
- Yin, X., Kropff, M. J., and Ellis, R. H. (1996). Rice flowering in response to diurnal temperature amplitude. *Field Crops Research*, 48(1):1–9.
- Yin, X., Kropff, M. J., McLaren, G., and Visperas, R. M. (1995). A nonlinear model for crop development as a function of temperature. *Agricultural and Forest Meteorology*, 77(1-2):1–16.
- Yoda, K., Kira, T., Ogawa, H., and Hozumi, K. (1963). Self-thinning in overcrowded pure stands under cultivated and natural conditions. *Journal of Biology, Osaka City University*, 14:107–129.
- Zen, S., Zolezzi, G., Toffolon, M., and Gurnell, A. M. (2016). Biomorphodynamic modelling of inner bank advance in migrating meander bends. *Advances in Water Resources*, 93, Part B:166–181.
- Zevenbergen, C., Rijke, J., van Herk, S., and Bloemen, P. (2015). Room for the river: a stepping stone in adaptive delta management. *International Journal of Water Governance*, 3:121–140.
- Zevenbergen, C., Rijke, J., Van Herk, S., Ludy, J., and Ashley, R. (2013). Room for the river: International relevance. *Water Governance*, 3(2):24–31.
- Zimmerman, R., Goodlett, J., and Comer, G. (1967). The influence of vegetation on channel form of small streams. In *Symposium on River Morphology, International Association of Hydrological Sciences, Wallingford*, pages 255–275.
- Zong, L. and Nepf, H. (2011). Spatial distribution of deposition within a patch of vegetation. *Water Resources Research*, 47. W03516.
- Zong, L. and Nepf, H. (2012). Vortex development behind a finite porous obstruction in a channel. *Journal of Fluid Mechanics*, 691:368–391.

LIST OF MAIN SYMBOLS

Symbol	Unit ^a	Description
a	[L ⁻¹]	Projected plant area per unit volume = mD
B	[L]	Channel width
Be	[L]	Equilibrium channel width
C	[L ^{1/2} T ⁻¹]	Chézy coefficient obtained from the measurements
C_f	[-]	Friction coefficient obtained from the measurements = g/C^2
C_b	[L ^{1/2} T ⁻¹]	Chézy coefficient of the bare soil for vegetated beds
C_b'	[L ^{1/2} T ⁻¹]	Chézy coefficient of the bed for submerged plants
C_r	[L ^{1/2} T ⁻¹]	Chézy coefficient for the global resistance of emergent plants
C_r'	[L ^{1/2} T ⁻¹]	Chézy coefficient for the global resistance of submerged plants
C_D	[-]	Mean drag coefficient of the vegetation
D	[L]	Plants characteristic diameter
D_{50}	[L]	Mean sediment diameter
g	[LT ⁻²]	gravity acceleration
h	[L]	Water depth
h_v	[L]	Vegetation height
I	[-]	Sorting index
I_S	[-]	Channel sinuosity
m	[L ⁻²]	Number of stems per unit bed surface
Q	[L ³ T ⁻¹]	Flow discharge
R_h	[L]	Hydraulic radius = A/P_m
A	[L ²]	Cross-sectional area
P_m	[L]	Wet perimeter
Re_D	[-]	Element Reynolds number
S	[L]	Diagonal separation between vegetation elements
s_1	[L]	Separation between elements in parallel direction to the flow
s_2	[L]	Separation between elements in perpendicular direction to the flow
$u(z)$	[LT ⁻¹]	Vertical velocity profile
u	[LT ⁻¹]	Mean flow velocity
u_c	[LT ⁻¹]	Mean flow velocity in the vegetation layer
i_b	[-]	Channel slope
λ	[-]	Surface density of stems = $m\pi D^2/4$
ξ	[-]	Degree of discontinuity
μ	[L ² T ⁻¹]	Cinematic viscosity of the fluid
ρ	[ML ⁻³]	Mass density of water
ρ_s	[ML ⁻³]	Mass density of sediment
κ	[-]	Von Kármán's constant = 0.41
τ	[ML ⁻¹ T ⁻²]	Total bed shear stress
τ_{bv}	[ML ⁻¹ T ⁻²]	Bed shear stress in a vegetated bed
τ_v	[ML ⁻¹ T ⁻²]	Shear stress caused by vegetation

^a M = mass; L = length; T = time; - = dimensionless

ACKNOWLEDGEMENTS

COMPLETING a five-year life-project such as a PhD requires the collaboration of many people who at different stages and in varied ways contribute to maintain the researcher's motivation. This doctoral research is a perfect example of this, so my most humble and sincere thanks go to:

My supervisors, Wim Uijttewaal and Alessandra Crosato, for challenging me to become an expert on my research field since the very first day and for all the support and guidance through this process. Wim, I admire your dedication and commitment, having always time for a quick question. For delivering your broaden-view and to-the-point feedback on time I am very grateful. This seems simple, but unfortunately not too many PhD students can say the same about their promotors. Alessandra, I have much to say, it has been great to work with you during this time. I feel blessed of having the opportunity to meet an exceptional woman that cares about people and that has so much knowledge to share. The combination of a charming sense of humour, a sharp point of view and a positive- and critical-thinking was a very enjoyable way of discussing everything. I will really miss our meetings that covered interesting aspects of river morphodynamics, but also so many other topics. I just hope to be able to trigger in my students the same enthusiasm and interest that you inspired in me.

COLCIENCIAS (Colombian Administrative Department of Science, Technology and Innovation) and Pontificia Universidad Javeriana, for the financial support of my studies in the Netherlands. It made me very proud to be selected from many candidates to represent my country and my University during these years.

The doctoral committee selected for my defence, for reading this dissertation and for the questions formulated during the ceremony. I also want to acknowledge Prof. Frans Klijn for the thorough reading of the document and for the interesting comments.

The group of technicians of the Waterlab, DEMO and the carpentry of Delft University of Technology that were somehow involved in my project, for helping me in building my "*original*" structures, setting up the experiments, or driving/working to/on the field. Sander, Jaap, Frank, Ruben, Rob and Arno. Special thanks to Rob van Dijk for all the experiences shared inside and outside the laboratory.

The students that worked with me during these years, for the direct or indirect contribution to this thesis and all the hard work. BSc. students: Antoine, Harmen, Eva, Lonis, Timo and Jeffrey. MSc. students: Riccardo, Protogene, Giulio, Jairo Alejandro and Daisy. I'll always remember the pleasant time working with Giulio and Protogene in the old lab's office, synergy that significantly changed the course of this research.

The group of friends from UNESCO-IHE, for helping me out on adapting to the Dutch environment, especially during the first year, while conditions were adverse at TUD. Angie, Joa, Juan Carlos, Gonza, Carito, Juanca, Neiler, Ferchita, Aky, Pato, Jessy, Mauri,

Maribel, Guy, Yared, Juliette, Juancho, Verito and so many others. Benno Groosman, my favourite Dutchy, deserves my gratitude for all the good moments and for the support as paranymp.

The entire “*gang*” of the Hydraulic Engineering Department, for making of every day an enjoyable occasion with the company of a *bakkie pleur* or just having an improvised last-minute dinner/beer. Cynthia, La Tía, Marco, Lodewijk, Yorick, Gonzalo, Anne, Erik, Liselot, Irene, Dirk, Saulo, Nils, Xuexue and Soti. I will definitely miss you guys and the good vibe of our group.

Other members of the staff of our department, for the entertaining and inspiring talks, Marion, Sierd, Matthieu, Bram and Astrid. Special thanks to Matthieu for the kind help in setting up the equipment for the field campaigns and to Astrid for sharing more than the delicious chocolate accompanying a regular coffee.

Dr. Ben Gorte, from the Remote Sensing group, for all the time invested in helping me and my students to measure the bed-level evolution in our laboratory flumes.

The people from the Water Management Department working at the laboratory, for cheering me up and stopping by just to ask how were the experiments going?, Juan Pablo, Julián, César, Mohammed, and Victor.

The colleagues of Deltares that crossed my path, for the willingness to collaborate or to share a nice experience, with special thanks to Erik (not only for having the nicest stories, but also for playing so many roles during my stay in the Netherlands), Aukje, Ton, Bert, Qinghua and Kees.

Gabriel, my Colombian friend, for being always there during these five years; and to Iván Dávila, for designing the cover of this dissertation.

Nici and Vittorio, my fantastic roomies, for the nice chats and all the funny moments we shared; and to Clarita, *la mia Amica Sarda*, for letting me be more than a colleague and for taking me to discover the most beautiful island. I’ll keep you guys in my hearth forever.

My wonderful family, the responsible ones of forging the person who I am. *Porque gracias a su amor y ejemplo he logrado alcanzar tantas metas. Gracias también por nuestras charlas interactivas y/o correos electrónicos que a pesar de la distancia me hicieron sentirlos a mi lado en cada paso, los amo.*

The exceptional woman that decided to join me in this adventure, *Pao*, my partner, my friend, my love, my imagineer, my paranymp. Thanks for taking care of me during this period, for the support in the difficult times and for the unmeasurable patience. It was amazing to share this experience with you, reinforcing our relationship as well. You helped me to discover the meaning and the value of a good company and that together we are stronger, almost invincible now. I honestly cannot express with words all my gratitude, *Amo-te mi Bonita*.

Finally, I’d like to apologize because I’m sure I’ve failed to mention all the persons that contributed to this project in some way or another. I’m taking the best memories of these years in Delft to Colombia, *thank you all!!*

Andrés VARGAS LUNA
Delft, September 2016

LIST OF PUBLICATIONS

JOURNAL PAPERS

6. **Vargas-Luna A.**, Duró G., Crosato A., and Uijttewaal W.S.J. Effects of plant colonization on river morphology: a laboratory study. *In preparation for future publication in the Journal of Geophysical Research: Biogeosciences*.
5. **Vargas-Luna A.**, Byishimo, P., Crosato A., and Uijttewaal W.S.J. Impact of flow variability and sediment characteristics on channel width in laboratory streams and their implications for rivers. Submitted to *Earth Surface Processes and Landforms*.
4. **Vargas-Luna A.**, Crosato A., Anders N., Hoitink A.J.F., Keesstra S.D., and Uijttewaal W.S.J. Morphodynamic effects of riparian vegetation growth after stream restoration. Submitted to *Earth Surface Processes and Landforms*, [Chapter 7].
3. **Vargas-Luna A.**, Crosato A., and Uijttewaal W.S.J. (2016). Representing plants as rigid cylinders in experiments and models. *Advances in Water Resources* 93, Part B: 205-222. Published in the *special issue: Ecogeomorphological feedbacks of water fluxes, sediment transport and vegetation dynamics in rivers and estuaries*. <http://dx.doi.org/10.1016/j.advwatres.2015.10.004>, [Chapter 6].
2. **Vargas-Luna A.**, Crosato A., and Uijttewaal W.S.J. (2015). Effects of vegetation on flow and sediment transport: comparative analyses and validation of predicting models. *Earth Surface Processes and Landforms* 40(2): 157-176. Published as a *State of Science paper*. <http://dx.doi.org/10.1002/esp.3633>, [Chapter 5].
1. Solari L., van Oorschot M., Belletti B., Hendricks D., Rinaldi M., and **Vargas-Luna A.** (2015). Advances on Modelling Riparian Vegetation-Hydromorphology Interactions, *River Research and Applications* 32(2): 164-178. Published in the *special issue: Hydrogeomorphology-Ecology Interactions in River Systems*. <http://dx.doi.org/10.1002/rra.2910>, [partly presented in Chapter 2 and 4].

CONFERENCE PROCEEDINGS

14. **Vargas-Luna A.** Crosato A., Hoitink A.J.F., Groot J., and Uijttewaal W.S.J. (2016). Effects of riparian vegetation development in a restored lowland stream. In: Constantinescu, G.; Garcia, M. and Hanes, D. (Eds.), 8th International Conference on Fluvial Hydraulics, River Flow 2016, St. Louis, USA, July 12-15, 2016, ISBN 978-1-138-02913-2. pp. 2197-2200.
13. **Vargas-Luna A.** Angel Escobar J.A, Stierman E.M.J., Gorte, B.G.H. and Uijttewaal, W.S.J. (2016). Measuring bathymetric evolution in mobile-bed laboratory flumes. In: Constantinescu, G.; Garcia, M. and Hanes, D. (Eds.), 8th International Conference on Fluvial Hydraulics, River Flow 2016, St. Louis, USA, July 12-15, 2016, ISBN 978-1-138-02913-2. pp. 411-416.

12. **Vargas-Luna A.**, Crosato A., Collot L. and Uijttewaal W.S.J. (2015). Laboratory investigation on the hydrodynamic characterization of artificial grass. E-proceedings of the 36th IAHR World Congress 28 June - 3 July, 2015, The Hague, the Netherlands. ISBN: 978-90-824846-0-1. pp. 728-734.
11. Benifei R., Solari L., **Vargas-Luna A.**, Geerling G., and van Oorschot M. (2015). Effect of vegetation on floods: the case of the river Magra. E-proceedings of the 36th IAHR World Congress 28 June – 3 July, 2015, The Hague, the Netherlands. ISBN: 978-90-824846-0-1. pp. 719-727.
10. **Vargas-Luna A.**, Collot, L., Crosato A., and Uijttewaal W.S.J. (2014). Laboratory investigation on the hydrodynamic characterization of artificial grass. In: D.C.M. Augustijn and J.J. Warminck, (eds.), NCR-Days 2014, Book of Abstracts, NCR Publication 38-2014, Nederlands Centrum voor Rivierkunde, 2, 3 October 2014, Enschede, The Netherlands. ISSN: 1568 – 234X, pp. 17-18.
9. Angel J.A., Gorte B.G.H., **Vargas-Luna A.**, and Uijttewaal W.S.J. (2014), Mapping bed-level evolution in laboratory flumes by means of structured light. In: D.C.M. Augustijn and J.J. Warminck, (eds.), NCR-Days 2014, Book of Abstracts, NCR Publication 38-2014, Nederlands Centrum voor Rivierkunde, 2, 3 October 2014, Enschede, The Netherlands. ISSN: 1568 – 234X, pp. 57-58.
8. Byishimo P, **Vargas-Luna A.**, and Crosato A. (2014). Effects of variable discharge on the river channel width variation. In: D.C.M. Augustijn and J.J. Warminck, (eds.), NCR-Days 2014, Book of Abstracts, NCR Publication 38-2014, Nederlands Centrum voor Rivierkunde, 2, 3 October 2014, Enschede, The Netherlands. ISSN: 1568 – 234X, pp. 31-32.
7. **Vargas-Luna A.**, Crosato A., Calvani G., and Uijttewaal W.S.J. (2014). Mimicking the effects of vegetation in laboratory setups. In: Proceedings of the 10th International Symposium on Ecohydraulics, Paper No. 288, Vegetation and fluvial processes. Norwegian University of Technology, Trondheim, Norway, June 23rd-27th 2014.
6. Gorte B.G.H., **Vargas-Luna A.**, and Sirmacek B. (2013). Camera-Projector 3D Scanning of a Semi-Submerged Terrain in a Flume. ISPRS Annals of Photogrammetry, Remote Sensing and Spatial Information Sciences II-4/W1, pp. 13-18.
5. Basset A., Blom A., Crosato A., and **Vargas-Luna A.** (2013). A comparison of existing models for particle velocity. In: A. Crosato (ed.), NCR-Days 2013, Book of Abstracts, NCR Publication 37-2013. Nederlands Centrum voor Rivierkunde, 3, 4 October 2013, Delft The Netherlands, pp. 3-21 - 3-22.
4. Benifei R., Solari L., van Oorschot M., Geerling G., and **Vargas-Luna A.** (2013). Effects of vegetation on flooding: the study case of the Magra river. In: A. Crosato (ed.), NCR-Days 2013, Book of Abstracts, NCR Publication 37-2013. Nederlands Centrum voor Rivierkunde, 3, 4 October 2013, Delft The Netherlands, pp. 2-5 - 2-6.
3. Byishimo, P, **Vargas-Luna A.**, and Crosato, A. (2013). Effects of variable discharge on width formation and cross-sectional shape of sinuous rivers with riparian vegetation. In A. Crosato (ed.), NCR-Days 2013, Book of Abstracts, NCR Publication 37-2013, Nederlands Centrum voor Rivierkunde, 3, 4 October 2013, Delft The Netherlands, pp. 3-33 - 3-34.

2. **Vargas-Luna A.**, Uijttewaal W.S.J., Crosato A., Tanczos I., and De Vries M. (2013). Effects of vegetation on sediment transport, experience from laboratory measurements. In RCEM 2013: 8th Symposium on River, Coastal and Estuarine Morphodynamics, Santander, Spain, 9-13 June 2013. ISBN: 978-7-89444-548-3. pp 156.
1. **Vargas-Luna A.**, Crosato A., and Uijttewaal W.S.J. (2012). Research on river bank accretion. In: R. Schielen (ed.), NCR-days 2012, Book of abstracts, NCR Publication 36-2012, Netherlands Centrum voor Rivierkunde. 4, 5 October 2012, Arnhem, The Netherlands, pp. 70-72.

TECHNICAL REPORTS, MAGAZINES AND OTHERS

5. **Vargas-Luna A.** (2016). 10,000 plastic plantjes in het waterlab (In Dutch). Contact Magazine, Uitgave van de faculteit Civiele Techniek en Geowetenschappen, July 2016.
4. **Vargas-Luna A.** (2016). Development of Riverbanks by TU Delft. Dredging Today on-line magazine, May 2016. <http://www.dredgingtoday.com/2016/06/10/video-development-of-riverbanks-by-tu-delft/>
3. **Vargas-Luna A.** (2016). 10,000 plastic plants in the waterlab. Stories of Science, Hydraulic Engineering Department, Civil Engineering and Geosciences Faculty, Delft University of Technology, March 2016. <http://www.citg.tudelft.nl/en/research/stories-of-science/hydraulic-engineering/10000-plastic-plants-in-the-waterlab/>
2. **Vargas-Luna A.** (2015). Understanding the formation of new river-banks. ExtraCT Magazine, Verenigingsperiodiek van het gezelschap "Practische studie", Jaargang 18, No. 3, Oct. 2015.
1. Gurnell A., González Del Tánago M., O'Hare M., van Oorschot M., Belletti B., García De Jalón D., Grabowski R., Hendricks D., Mountford, O., Rinaldi M., Solari L., Szweczyk M., **Vargas-Luna A.** (2014). Influence of Natural Hydromorphological Dynamics on Biota and Ecosystem Function, Part 1 (Chapters 1 to 3 of 6), Deliverable 2.2 of the Work Package 2: Hydromorphological and ecological processes and interactions, Technical report, REFORM (REstoring rivers FOR effective catchment Management) Project, funded by the European Commission within the 7th Framework Programme (2007–2013) under Grant Agreement No. 282656. <http://reformrivers.eu/deliverables/d2-2>

CURRICULUM VITÆ

ANDRÉS VARGAS LUNA was born in Bogotá (Colombia) on November 24th, 1978. He received his degree in Civil Engineering at the *Universidad Nacional de Colombia* in 2002 but he started working in the Hydrology Department of a consultancy company few months before getting graduated. One year later he started his Master studies in the same University and simultaneously he had the opportunity to teach there *Hydrology* for bachelor students, thanks to a Lecturer's formation program granted by the same institution. It was during this period that he discovered his passion for teaching and research and soon, after obtaining his Master degree in Water Resources in 2006, he decided to combine his consultancy activities with part-time teaching positions at the *Universidad Nacional de Colombia*, the *Universidad Distrital "Francisco José de Caldas"*, and the *Universidad Tecnológica del Chocó*.

In 2007, Mr. Vargas Luna continued his academic career at the *Pontificia Universidad Javeriana*, institution in which he was appointed to a full-time position, dedicated to teach and supervise bachelor and master students. In 2011, Andrés was awarded with the funding of the program "*Generación del Bicentenario*", granted by COLCIENCIAS and co-financed by the *Pontificia Universidad Javeriana*, fellowship that allowed him to conduct his PhD studies in the *Delft University of Technology*. During his stay in the Netherlands, Mr. Vargas Luna participated actively in the establishment of the Delft-YPN (Young professional Network) of the IAHR. He has also played the role of reviewer for the Scientific Committee of the Latin American Congress on Hydraulics (*LADHI 2016*) and for several scientific Journals, such as the *Journal of Fluids Engineering "Transactions of the ASME"*; the *Journal of Hydro-Environment Research*; *Earth Surface Processes and Landforms*; and the *International Journal of Sediment Research*.

After defending his PhD Thesis, Andrés will return to Colombia for continuing his academic career at the *Pontificia Universidad Javeriana* in Bogotá.



